frontiers | Research Topics

Epigenetics in cancer: Mechanisms and drug development, volume II

Edited by
Xiao Zhu, Zhenhua Xu and Biaoru Li

Published in
Frontiers in Cell and Developmental Biology
Frontiers in Genetics

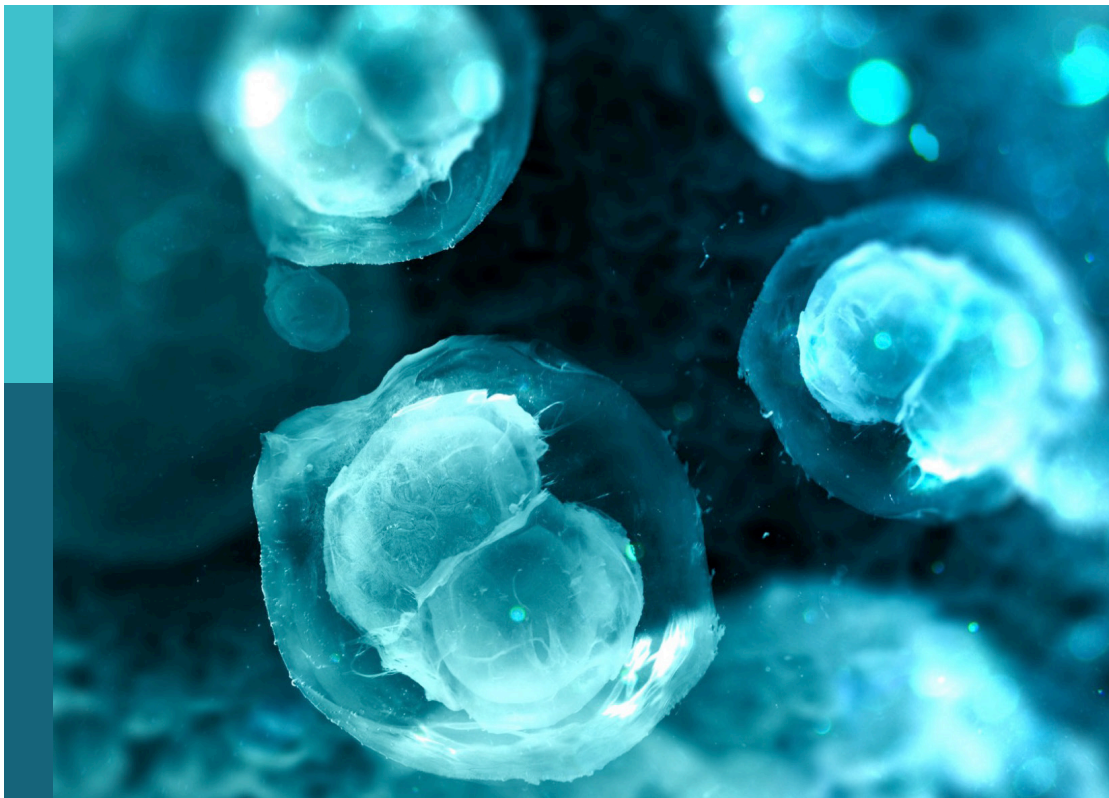

ISSN 1664-8714
ISBN 978-2-8325-3041-2
DOI 10.3389/978-2-8325-3041-2

About Frontiers

Frontiers is more than just an open access publisher of scholarly articles: it is a pioneering approach to the world of academia, radically improving the way scholarly research is managed. The grand vision of Frontiers is a world where all people have an equal opportunity to seek, share and generate knowledge. Frontiers provides immediate and permanent online open access to all its publications, but this alone is not enough to realize our grand goals.

Frontiers journal series

The Frontiers journal series is a multi-tier and interdisciplinary set of open-access, online journals, promising a paradigm shift from the current review, selection and dissemination processes in academic publishing. All Frontiers journals are driven by researchers for researchers; therefore, they constitute a service to the scholarly community. At the same time, the *Frontiers journal series* operates on a revolutionary invention, the tiered publishing system, initially addressing specific communities of scholars, and gradually climbing up to broader public understanding, thus serving the interests of the lay society, too.

Dedication to quality

Each Frontiers article is a landmark of the highest quality, thanks to genuinely collaborative interactions between authors and review editors, who include some of the world's best academicians. Research must be certified by peers before entering a stream of knowledge that may eventually reach the public - and shape society; therefore, Frontiers only applies the most rigorous and unbiased reviews. Frontiers revolutionizes research publishing by freely delivering the most outstanding research, evaluated with no bias from both the academic and social point of view. By applying the most advanced information technologies, Frontiers is catapulting scholarly publishing into a new generation.

What are Frontiers Research Topics?

Frontiers Research Topics are very popular trademarks of the *Frontiers journals series*: they are collections of at least ten articles, all centered on a particular subject. With their unique mix of varied contributions from Original Research to Review Articles, Frontiers Research Topics unify the most influential researchers, the latest key findings and historical advances in a hot research area.

Find out more on how to host your own Frontiers Research Topic or contribute to one as an author by contacting the Frontiers editorial office: frontiersin.org/about/contact

Epigenetics in cancer: Mechanisms and drug development - volume II

Topic editors

Xiao Zhu — Guangdong Medical University, China

Zhenhua Xu — Children's National Hospital, United States

Biaoru Li — Augusta University, United States

Citation

Zhu, X., Xu, Z., Li, B., eds. (2023). *Epigenetics in cancer: Mechanisms and drug development - volume II*. Lausanne: Frontiers Media SA.

doi: 10.3389/978-2-8325-3041-2

Table of contents

frontiers | Frontiers in Genetics

TYPE Editorial
PUBLISHED 05 July 2023
DOI 10.3389/fgene.2023.1242960

OPEN ACCESS

EDITED AND REVIEWED BY
Michael E. Symonds,
University of Nottingham,
United Kingdom

*CORRESPONDENCE
Zhenhua Xu,
zxu@childrensnational.org
Biaoru Li,
bli@augusta.edu

RECEIVED 20 June 2023
ACCEPTED 21 June 2023
PUBLISHED 05 July 2023

CITATION
Zhu X, Xu Z and Li B (2023), Editorial: Epigenetics in cancer: mechanisms and drug development-volume II.
Front. Genet. 14:1242960.
doi: 10.3389/fgene.2023.1242960

Editorial: Epigenetics in cancer: mechanisms and drug development-volume II

Xiao Zhu[1,2], Zhenhua Xu[3]* and Biaoru Li[4]*

[1]Southern Marine Science and Engineering Guangdong Laboratory (Zhanjiang), Guangdong Medical University, Zhanjiang, China, [2]Zhejiang Provincial People's Hospital, People's Hospital of Hangzhou Medical College, Hangzhou Medical College, Hangzhou, China, [3]Center for Cancer and Immunology, Children's National Health System, Washington, DC, United States, [4]Cancer Center, Medical College of Georgia, Augusta University, Augusta, GA, United States

KEYWORDS

editorial, epigenetics, cancer, DNA methylation, RNA methylation

Editorial on the Research Topic
Epigenetics in cancer: mechanisms and drug development-volume II

Cancer remains the leading cause of death in affluent nations, underscoring the urgent need for innovative approaches to combat this devastating disease (Siegel et al., 2023). Epigenetics, a field of study focusing on the modulation of gene expression and function without altering the DNA sequence, holds tremendous promise in understanding and addressing cancer development and progression.

The Research Topic titled "*Epigenetics in Cancer: Mechanisms and Drug Development-volume II*" presents a compilation of ten articles contributed by over sixty esteemed authors in the fields of cancer epigenetics and therapeutics. This comprehensive collection encompasses diverse research directions, including the roles of transcription and chromatin in gene regulation, DNA modifications, RNA epigenetics, non-coding RNA, and epigenomic methods. Alongside shedding light on the latest discoveries regarding epigenetic mechanisms, these articles also emphasize novel and promising therapeutic drugs aimed at reversing specific epigenetic alterations.

DNA methylation, a key epigenetic modification, has been extensively studied due to its involvement in transcriptional inhibition and gene silencing (Liang et al., 2021). Recent investigations have elucidated the downstream mechanisms of gene silencing mediated by DNA methylation, uncovering the remarkable contribution of molecular domain proteins (Wurster et al., 2021). In hepatocellular carcinoma (HCC), the understanding of epigenetic abnormalities linked to aberrant enhancers provides novel insights into drug therapy for this malignancy. It has been observed that DNA methylation can finely tune gene expression by balancing the effects of transcriptional inhibition and activation, highlighting its role in gene repression (Goncharova et al., 2023).

For instance, Yang et al. demonstrated the involvement of promoter methylation and miR-454-3p in the dysregulation of 4.1N/EPB41L1 at the transcriptional and posttranscriptional levels, respectively. These findings support the potential therapeutic use of targeting DNA methylation and miR-454-3p for NSCLC treatment. Additionally, Huang et al. analyzed epigenomic and transcriptomic data, proposing a prognostic signature based on six AE-DEGs that outperforms previous models in predicting long-term and short-term overall survival in HCC patients. Their discovery of the unique role of epigenetic

aberration-induced aberrant enhancers in HCC progression offers new insights for drug therapy.

RNA methylation, another significant epigenetic modification, has emerged as a major focus of research. With over 100 chemical modification methods identified, N6-methyladenine (m6A) stands out as a predominant RNA modification (Zhou et al., 2020). Studies have highlighted the reversible nature of m6A modification, controlled by writers, readers, and demethylases. M6A plays a critical role in regulating gene expression, splicing, RNA editing, RNA stability, and controlling mRNA lifetime and degradation (Li et al., 2023; Xiong et al., 2023). Notably, the clinical and prognostic value of m6A-related features has been elucidated in glioblastoma multiforme (GBM), laying a foundation for future research in glioma (Liu et al.). Furthermore, researchers have emphasized the potential of ncRNA m6A modification and m6A regulators as promising diagnostic and prognostic biomarkers across various cancers, aiding in recurrence and survival prediction, and serving as potential therapeutic targets in cancer treatment (Chen et al. and Mobet et al.). However, while these advancements offer significant promise, further exploration is necessary to unravel more specific mechanisms and develop theories closer to practical applications in clinical diagnosis and treatment.

Another crucial post-transcriptional modification, 5-methylcytosine (m5C), has demonstrated a pivotal role in gene expression and RNA stability. In hepatocellular HCC, the characterization of m5C-related regulators has enhanced our understanding of the tumor immune landscape and provides a practical tool for predicting prognosis (Liu et al.). This valuable insight has the potential to improve patient outcomes and guide effective interventions for this challenging disease.

Although epigenetic modifiers have shown promise as targets for cancer treatment, their efficacy as standalone therapies remain limited. Combinatorial approaches that integrate epigenetic therapies with other anti-tumor treatments offer a more comprehensive strategy for maximizing therapeutic outcomes (Ye et al., 2021; Li et al., 2022; Lin et al., 2023).

In conclusion, the study of epigenetics in cancer has unveiled intricate mechanisms and opened new avenues for drug development. This collection of articles provides a snapshot of the latest research, encompassing diverse aspects of epigenetic regulation in cancer. As scientists delve deeper into these mechanisms and translate their findings into clinical practice, we anticipate further breakthroughs that will transform the landscape of cancer treatment and improve patient outcomes.

Author contributions

XZ, ZX, and BL conceived the work. XZ wrote and drafted the manuscript. All authors contributed to the article and approved the submitted version.

Acknowledgments

Thanks to all authors who contributed to our Research Topic.

Conflict of interest

The authors declare that the research was conducted in the absence of any commercial or financial relationships that could be construed as a potential conflict of interest.

Publisher's note

References

Goncharova, I. A., Zarubin, A. A., Babushkina, N. P., Koroleva, I. A., and Nazarenko, M. S. (2023). Changes in DNA methylation profile in liver tissue during progression of HCV-induced fibrosis to hepatocellular carcinoma. *Vavilovskii Zhurnal Genet. Sel.* 27, 72–82. doi:10.18699/VJGB-23-10

Li, X., Li, M., Huang, M., Lin, Q., Fang, Q., Liu, J., et al. (2022). The multi-molecular mechanisms of tumor-targeted drug resistance in precision medicine. *Biomed. Pharmacother.* 150, 113064. doi:10.1016/j.biopha.2022.113064

Li, Y., Yi, Y., Lv, J., Gao, X., Yu, Y., Babu, S. S., et al. (2023). Low RNA stability signifies increased post-transcriptional regulation of cell identity genes. *Nucleic Acids Res.*, gkad300. Online ahead of print. doi:10.1093/nar/gkad300

Liang, R., Li, X., Li, W., Zhu, X., and Li, C. (2021). DNA methylation in lung cancer patients: Opening a "window of life" under precision medicine. *Biomed. Pharmacother.* 144, 112202. doi:10.1016/j.biopha.2021.112202

Lin, Q., Zhang, M., Kong, Y., Huang, Z., Zou, Z., Xiong, Z., et al. (2023). Risk score = LncRNAs associated with doxorubicin metabolism can be used as molecular markers for immune microenvironment and immunotherapy in non-small cell lung cancer. *Heliyon* 9, e13811. doi:10.1016/j.heliyon.2023.e13811

Siegel, R. L., Miller, K. D., Wagle, N. S., and Jemal, A. (2023). Cancer statistics, 2023. *CA Cancer J. Clin.* 73, 17–48. doi:10.3322/caac.21763

Wurster, K. D., Costanza, M., Kreher, S., Glaser, S., Lamprecht, B., Schleussner, N., et al. (2021). Aberrant expression of and cell death induction by engagement of the MHC-II chaperone CD74 in anaplastic large cell lymphoma (ALCL). *Cancers (Basel)* 13, 5012. doi:10.3390/cancers13195012

Xiong, Z., Han, Z., Pan, W., Zhu, X., and Liu, C. (2023). Correlation between chromatin epigenetic-related lncRNA signature (CELncSig) and prognosis, immune microenvironment, and immunotherapy in non-small cell lung cancer. *PLoS One* 18, 0286122. doi:10.1371/journal.pone.0286122

Ye, Z., Huang, Y., Ke, J., Zhu, X., Leng, S., and Luo, H. (2021). Breakthrough in targeted therapy for non-small cell lung cancer. *Biomed. Pharmacother.* 133, 111079. doi:10.1016/j.biopha.2020.111079

Zhou, Y., Kong, Y., Fan, W., Tao, T., Xiao, Q., Li, N., et al. (2020). Principles of RNA methylation and their implications for biology and medicine. *Biomed. Pharmacother.* 131, 110731. doi:10.1016/j.biopha.2020.110731

frontiers in Cell and Developmental Biology

REVIEW
published: 22 December 2021
doi: 10.3389/fcell.2021.778582

Non-Coding RNA m6A Modification in Cancer: Mechanisms and Therapeutic Targets

Da-Hong Chen[1†], Ji-Gang Zhang[2†], Chuan-Xing Wu[3] and Qin Li[1]**

[1]Department of Clinical Pharmacy, Shanghai General Hospital, Shanghai Jiao Tong University School of Medicine, Shanghai, China, [2]Clinical Research Center, Shanghai General Hospital, Shanghai Jiao Tong University School of Medicine, Shanghai, China, [3]Department of General Surgery, Shanghai General Hospital, Shanghai Jiao Tong University School of Medicine, Shanghai, China*

Recently, N6-methyl-adenosine (m6A) ribonucleic acid (RNA) modification, a critical and common internal RNA modification in higher eukaryotes, has generated considerable research interests. Extensive studies have revealed that non-coding RNA m6A modifications (e.g. microRNAs, long non-coding RNAs, and circular RNAs) are associated with tumorigenesis, metastasis, and other tumour characteristics; in addition, they are crucial molecular regulators of cancer progression. In this review, we discuss the relationship between non-coding RNA m6A modification and cancer progression from the perspective of various cancers. In particular, we focus on important mechanisms in tumour progression such as proliferation, apoptosis, invasion and metastasis, tumour angiogenesis. In addition, we introduce clinical applications to illustrate more vividly that non-coding RNA m6A modification has broad research prospects. With this review, we aim to summarize the latest insights and ideas into non-coding RNA m6A modification in cancer progression and targeted therapy, facilitating further research.

Keywords: m6A RNA modification, non-coding RNA, tumorigenesis mechanism, cancer therapy, epigenetics

OPEN ACCESS

Edited by:
Xiao Zhu,
Guangdong Medical University, China

Reviewed by:
Apiwat Mutirangura,
Chulalongkorn University, Thailand
Antonino Zito,
Massachusetts General Hospital and Harvard Medical School, United States

****Correspondence:***
Chuan-Xing Wu
doc_zf@163.com
Qin Li
liqin0626@hotmail.com

†These authors have contributed equally to this work

Specialty section:
This article was submitted to Epigenomics and Epigenetics, a section of the journal Frontiers in Cell and Developmental Biology

Received: *17 September 2021*
Accepted: *06 December 2021*
Published: *22 December 2021*

Citation:
Chen D-H, Zhang J-G, Wu C-X and Li Q (2021) Non-Coding RNA m6A Modification in Cancer: Mechanisms and Therapeutic Targets. Front. Cell Dev. Biol. 9:778582. doi: 10.3389/fcell.2021.778582

1 INTRODUCTION

In eukaryotic cells, some non-coding ribonucleic acids (ncRNAs), such as microRNAs (miRNAs), long non-coding RNAs (lncRNAs), and circular RNAs (circRNAs), usually do not encode proteins but perform their respective biological functions at the RNA level. Generally, ncRNAs have long been thought to be post-transcriptional regulators of gene expression, but RNA modifications have rendered it possible for ncRNAs to generate new regulatory effects on gene expression. N6-methyl-adenosine (m6A), methylated at the N6 position of adenosine, is a reversible epigenetic RNA modification that modulates splicing, degradation, and other biological processes of RNAs (Fazi and Fatica 2019; Zhou et al., 2020). During the process from DNA to RNA, adenylate undergoes

Abbreviations: CRC, colorectal cancer; ccRCC, clear cell renal cell carcinoma; ceRNA, endogenous ribonucleic acid; circRNA, circular ribonucleic acid; EMT, epithelial-mesenchymal transition; ESCC, esophageal squamous cell carcinoma; GC, gastric cancer; HCC, hepatocellular carcinoma; HNSCC, head and neck squamous cell carcinoma; lncRNA, long non-coding ribonucleic acid; miRNA, micro ribonucleic acid; m6A, N6-methyl-adenosine; ncRNA, non-coding ribonucleic acid; NM, nafamostat mesilate; NSCLC, non-small cell lung cancer; RBRP, RNA-binding regulatory peptide; 3′-UTR, 3′-untranslated region.

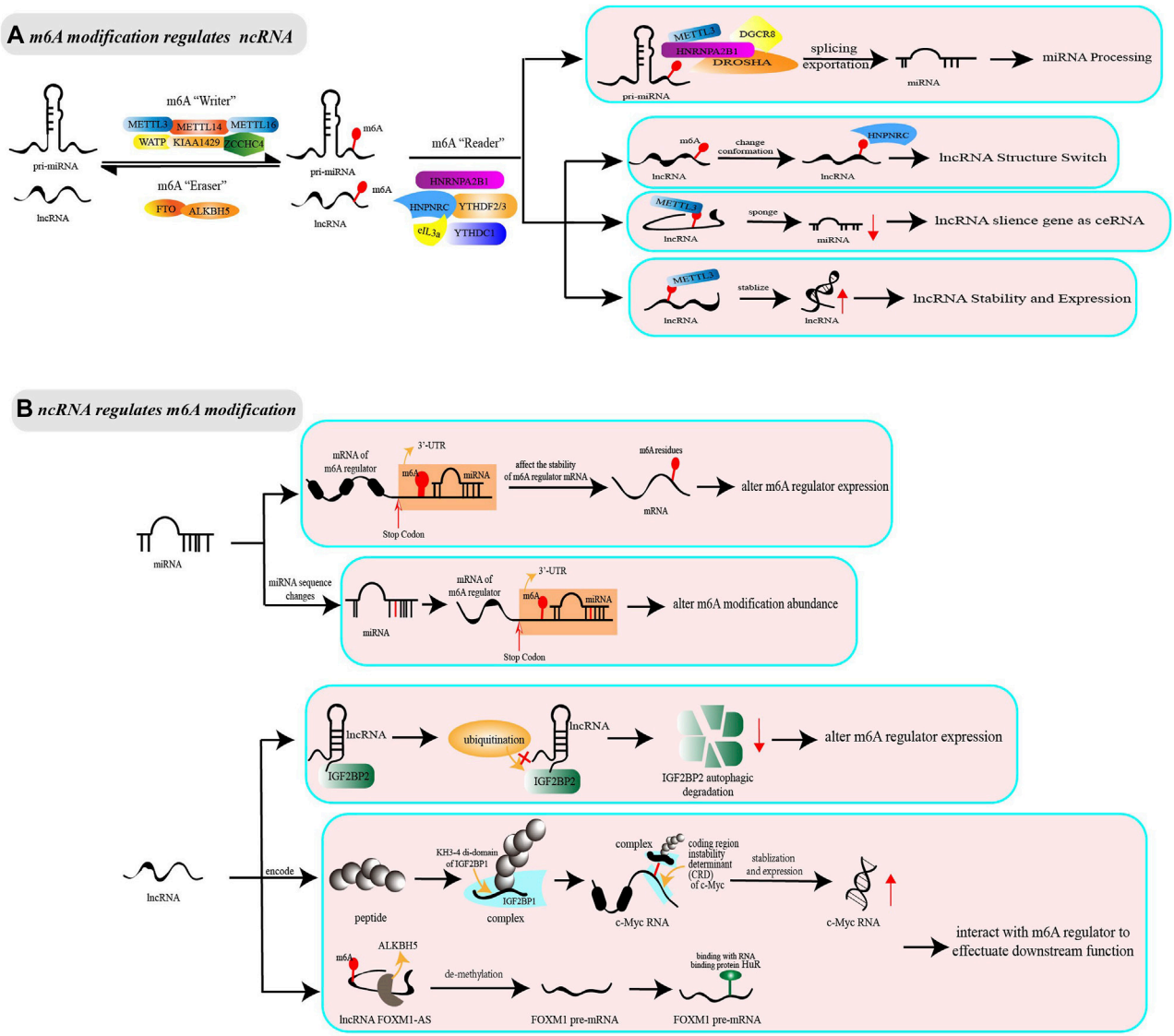

FIGURE 1 | The interaction between non-coding RNA and m6A modification. The adenosine(A) bases reside in non-coding RNA could be methylated by methyltransferase complex ("Writer") comprised of METTL3/METTL14/WATP and other regulator cofactors. The non-coding RNA with m6A modification resides could by recognized by m6A binding proteins ("Reader," e.g. NRNPA2B1, HNRNPC, YTHDF) to effectuate downstream functions, or be reversibly erased by demethyltransferase ("Eraser," e.g. FTO, ALKBH5). **(A)** m6A modification regulates ncRNA. During the processing from pri-miRNA to miRNA, the presence of m6A modification can regulate the splicing and exportation, facilitating the maturation of miRNA. Besides, m6A modification can play extraordinary complex and diversity roles in lncRNA. The lncRNA marked m6A writer proteins could change conformation to bind to proteins, leading to that m6A modification is regarded as lncRNA structure switch and facilitate the RNA-protein interaction. Secondly, the lncRNA which is methylated by m6A writer proteins have the effect on sponging miRNA as ceRNA, greatly augmenting the RNA-RNA interaction. For lncRNA itself, m6A modification could regulate transcript stabilization and expression level to activate or participate in subsequent functions. **(B)** ncRNA regulates m6A modification. Non-coding RNA could regulate m6A modification from the perspective of expression level and function. MiRNA integrate into the mRNA 3′-UTR region of m6A regulator cofactors, which alters the expression level of m6A regulators and indirectly influences on the abundance of m6A modification. Differently, lncRNA can alter the expression level of m6A regulators by affecting the stability and degradation of mRNA. Notably, lncRNA or RNA-binding regulatory peptide that is encoded by lncRNA (e.g. LncRNA LINC00266-1) has the capability to bind with m6A regulator to strengthen m6A recognition, therefore affecting the stabilization and expression of the downstream target mRNA. Anti-sense lncRNA could recruit m6A eraser proteins to decrease m6A abundance on the sense mRNA to active downstream effects (e.g. lncRNA FOXM1-AS and m6A eraser ALKBH5).

methylation modification at the sixth position under the action of methyltransferase ("writer") METTL3/14, WTAP, KIAA1429, RBM15, and ZC3H13. Next, the bases are demethylated by demethyltransferase ("eraser") FTO and ALKBH. Finally, these methylated RNA base sites require specific enzymes ("readers") to accomplish the purpose of embellishing ncRNAs (Sun et al., 2019). The molecular mechanisms of m6A modification involved in the regulation of ncRNA gene expression have been reported previously (Erson-Bensan and Begik 2017; Fazi and Fatica 2019; He et al., 2020; Zhang et al., 2020d), and more interestingly, the

abundance of m6A modification and the expression of m6A regulators are also regulated by ncRNAs.

The genes encoding miRNA are transcribed as long transcripts, called primary miRNA (pri-miRNA) in the nucleus. Pri-miRNA undergoes nuclear cleavage mediated by Drosha-DGCR8 complex, to form precursor miRNA (pre-miRNA), which is then transported to cytoplasm via Exportin-5 and sheared by RNase III endonuclease Dicer to short RNA fragments, namely miRNA (Vishnoi and Rani 2017). Studies have shown that pri-miRNAs methylated by m6A are more likely to be identified by molecules that are responsible for miRNA maturation, thus accelerating the initiation, splicing, transportation and other processes of miRNA biogenesis (Alarcón et al., 2015a; Alarcón et al., 2015b; Chen et al., 2020c) (see **Figure 1A**). For example, the m6A "writer" METTL3, marked in pri-miRNA, has been reported to interact with DGCR8 and to positively promote the splicing and maturation of miR-25 (Alarcón et al., 2015b), miR-143-3p (Wang et al., 2019a), pri-miR-221/miR-222 (Han et al., 2019a), pri-miR-1246 (Peng et al., 2019), and miR-25-3p (Zhang et al., 2019a). Further, the m6A "reader" HNRNPC can directly bind pri-miR-21 to increase miR-21 expression (Park et al., 2012), whereas HNRNPA2B1 interacts with lncRNA LINC01234 to indirectly modulate miR-106b-5p maturation (Chen et al., 2020d). Inconsistent with the above findings, a study has shown that HNRNPA2B1 overexpression downregulates miR-29a-3p, miR-29b-3p, miR-222, and inversely upregulates miR-1266-5p, miR-1268a, and miR-671-3p (Klinge et al., 2019). Notably, the methyltransferase NSun2 blocks the splicing of pri-miR-125b2 and interferes with miR-125b cleavage, which is in contrast to the action of methyltransferase METTL3/14 (Yang et al., 2015; Yuan et al., 2014). These data suggest the extraordinary complexity and diversity of m6A modification in miRNA biosynthesis.

LncRNA is a kind of ncRNA with a length of more than 200 nucleotides, but was initially considered as "transcriptional noise" because its biological functions were unknown (Yang et al., 2020b). With further research, increasing associated machineries of lncRNA have been found. The current studies indicate that m6A modification can act as a structural "switch" to change the conformation of lncRNA, participate in the ceRNA model for silencing miRNA or affect the stability and expression of lncRNA (see **Figure 1A**). Specifically, m6A-modified lncRNA is demonstrated to have hairpins that are more suitable for conformation in the RNA-HNRNPC complex, suggesting that m6A modification acts as a "switch" to trigger the combination of lncRNA and HNRNPC (Liu et al., 2015; Zhou et al., 2016). In addition, m6A modification can facilitate lncRNA to act as endogenous RNAs (ceRNAs) and then sponge downstream miRNA by improving the stability of lncRNA transcript or reducing RNA degradation (Jin et al., 2019; Wang et al., 2020a). Notably, m6A modification contributes to the function of lncRNAs, as well as affects their expression level. It is reported that YTHDF1 knockdown downregulates LINC00278-sORF1 translation without changing the m6A modification level. METTL3, METTL14, and WTAP knockdown reduces the m6A modification level and LINC00278-sORF1 translation, while ALKBH5 increases them (Wu et al., 2020).

The interaction between m6A modification and ncRNAs is reciprocal, which means that ncRNAs can also regulate m6A modification in biological processes. Some miRNAs can target the mRNA of m6A regulators and integrate into the 3′-UTR region of mRNA to alter their stability and expression, thus indirectly affecting m6A modification abundance. Further, lncRNA can affect the stability and degradation of m6A-related enzymes or combine with them to form complexes, thus facilitating a regulatory effect on the downstream target mRNA of m6A regulators (see **Figure 1B**). For example, miR-33a, miR-600, miRNA let-7g, miR-744-5p, and miRNA-145 are shown to decrease the expression of METTL3, HNRNPC or YTHDF2 at both the mRNA and protein levels (Cai et al., 2018; Du et al., 2017; Kleemann et al., 2018; Wei et al., 2019; Yang et al., 2017). Furthermore, the IGF2BP2 mRNA is regulated by lncRNA LINRIS, which is not only responsible for maintaining IGF2BP2 mRNA stability but also prevents its degradation (Wang et al., 2019b). Except for changing the expression level of m6A regulators, ncRNA can change m6A abundance via a sequence-dependent manner. For example, the decrease of endonuclease Dicer leads to aberrant miRNA expression, and modulates the binding of m6A-related enzymes to mRNAs that contain miRNA binding sites, thus downregulating the abundance of m6A modification without affecting the expression of m6A regulators, METTL3, FTO, and ALKBH5 (Chen et al., 2015).

So far, several studies have enriched our understanding of the interactions between ncRNA and m6A modification, and indicated that aberrant expression of m6A regulators and m6A modification on ncRNAs can alter normal biological processes. Notably, this abnormal biological change caused by m6A modification makes ncRNAs involved in tumorigenesis and cancer progression, associating with cell proliferation and apoptosis, invasion and metastasis, cell stemness, drug resistance and other mechanisms that enhance the malignancy of cells and the difficulty of cancer therapies. Therefore, the role of ncRNA m6A modification in various cancers is worthy of further study to better understand the related mechanisms, contributing to provide insights for early cancer diagnosis, outcome prediction and cancer treatment strategies. In this review, we discuss the relationship between ncRNA m6A modification and cancer progression from the perspective of various cancers. In particular, we focus on important mechanisms in tumour progression and introduce potential clinical applications to illustrate more vividly that ncRNA m6A modification has broad research prospects in cancer. We aim to summarize the latest insights into ncRNA m6A modification in cancer progression and targeted therapy, facilitating further research.

2 Functions of ncRNA m6A Modification in Different Types of Cancer

2.1 Lung Cancer and ncRNA m6A Modification

Lung cancer, also known as primary bronchial lung cancer, refers to malignant tumour originating in bronchial mucous epithelium or alveolar epithelium, and is mainly classified into adenocarcinoma, squamous cell carcinoma, large cell

carcinoma and small-cell lung cancer. Due to the huge difference between small cell carcinoma and other types in biological behaviour, treatment prognosis and other aspects, lung cancer other than small cell lung cancer is collectively referred to as non-small-cell lung cancer (NSCLC) (Yousef and Tsiani 2017; Inamura 2018). During the progression of NSCLC, LINC01234 is reported to be an oncogenic lncRNA that interacts with m6A "reader" HNRNPA2B1. Overexpression of LINC01234 combined with HNRNPA2B1 recruits DGCR8 and facilitates the processing of several miRNA precursors, including pri-miR-106b. Interestingly, activated c-Myc by miR-106b-5p can bind to the LINC01234 promoter to create a positive feedback loop (Chen et al., 2020d). Contrast to interaction, METTL3 accelerates the splicing of the precursor and generates mature miR-143-3p, regulating the expression of oncogene miR-143-3p (Wang et al., 2019a). Similarly, the miR-107/LAST2 axis is regulated by the m6A "eraser" ALKBH5 in an HuR-dependent manner to decrease YAP activity and inhibit tumour growth (Jin et al., 2020); lncRNA MALAT1 is stabilized by the METTL3/YTHDF1 complex and its RNA level is increased with high levels of m6A modification (Jin et al., 2019). METTL3 has been shown to promote the expression of some crucial oncoproteins and facilitate tumour proliferation, apoptosis, and invasion in human lung cancer (Du et al., 2017). However, miR-600 and miR-33a inhibit the expression of METTL3, reversing its positive effects on NSCLC progression and playing the role of tumour suppressor genes (Du et al., 2017; Wei et al., 2019). In summary, the effect of m6A modification on cancers may be completely opposite under the regulation of ncRNAs, suggesting the relationship between ncRNA and m6A modification is complex and variable in cancer progression.

2.2 Liver Cancer and ncRNA m6A Modification

Primary carcinoma of the liver has multifactorial pathogenesis and is a malignant tumour occurring in hepatocytes or intrahepatic bile duct epithelial cells, including hepatocellular carcinoma (HCC), hepatobiliary carcinoma and hepatic sarcoma (Gao et al., 2020). HCC occurs in liver cells and is the main histological subtype of the hepatic malignancy (accounting for more than 90% cases of primary carcinoma of the liver). Overwhelming evidence has proved the regulatory roles of ncRNAs related to liver carcinogenesis, and their relationship can be summed up as "frenemy" which is means a kind of love-hate relationship (Wong et al., 2018). The miR-186, which plays the role of anti-hepatoblastoma, is weakly expressed in HCC tissues, and its overexpression inhibits cell aggressive characteristics; however, the increase of its direct target METTL3 reverses the inhibitory effect (Cui et al., 2020). In addition, another study has shown that METTL3 can improve the expression of c-Myc by increasing m6A modification, whereas miR-338-5p inhibit the expression of METTL3 to interfere with the lung cancer progression (Wu et al., 2021). The m6A "writer" METTL14 positively modulate pri-miRNA-126 maturation by interacting with DGCR8 to suppress the metastatic potential of HCC cells. Similar to the interaction of miR-186 and METTL3, the overexpression of pri-miRNA-126 inversely inhibits the repressing effect of METTL14 (Ma et al., 2017).

Thus, hostility alters their normal biological functions, while the friendship represents a positive correlation between ncRNAs and m6A regulators. With the help of m6A modification mediated by METTL3/METTL14, lncRNA LINC00958 (Zuo et al., 2020)and circ-SORE (Xu et al., 2020a)are upregulated because of enhancement of transcript stability. The m6A "reader" IGF2BP1 plays an oncogenic role in HCC progression, but the decrease of lncRNA LIN28B-AS can deplete the expression of IGF2BP1-dependent mRNAs, such as IGF2 and Myc, thereby inhibiting HCC cell proliferation, migration, and invasion (Zhang et al., 2020c). In addition to influencing the expression of molecules, m6A modification and ncRNA also affect their binding to downstream molecules. KIAA1429 is a member of m6A methyltransferases, and GATA3 mRNA is a direct downstream target of KIAA1429-methylation, facilitating the degradation of GATA3. Strikingly, KIAA1429 preferentially induces GATA3 pre-mRNA in a targeted manner under the guidance of the antisense gene lncRNA GATA3-AS to maintain their roles in cancer progression (Lan et al., 2019). In addition, m6A modification targets the 3′-UTR of YAP, which induces the repression effect of miR-582-3p, although whether the m6A regulator is primarily responsible for this essential part of the interaction is unclear until now (Zhang et al., 2018). The complexity of m6A modification and ncRNAs suggest that it is necessary to further study the mechanisms and effects of their crosstalk in liver cancer, thus using the stable and significant indicators to assist early diagnosis and treatment.

2.3 Gastric Cancer and ncRNA m6A Modification

Gastric cancer (GC) is a malignant tumour of digestive system occurring from gastric mucosal epithelium and glandular epithelium (Karimi et al., 2014), accounting for the second largest malignant tumour in China. In GC tissues, it is found that MEETL3 promotes the maturation of pri-miR-17-92 (Sun et al., 2020b), and m6A-modified motif-assisted miR-660 to reduce oncogene E2F3 activity (He and Shu 2019). Besides, METTL3 can upregulate the expression of target mRNA SEC62 by facilitating the stabilizing effect of IGF2BP1 on SEC62, but this positive regulation could be inhibited by miR-4429 (He et al., 2019). In contrast, lncRNA ARHGAP5-AS1 is responsible for recruiting METTLE3 to stabilise ARHGAP5 mRNA in the cytoplasm (Zhu et al., 2019). Unlike enhancing downstream target mRNA stability, METTL3 has been reported to combine with the m6A "reader" YTHDF2 to promote the degradation of PTEN mRNA and increase tumour malignancy, and subtly, the oncogenic lncRNA LINC00470 serves as an accelerator in this process (Yan et al., 2020). Many studies have reported that aberrant expressions of lncRNA (Sun et al., 2016), miRNA (Shin and Chu 2014), and circRNA (Shan et al., 2019) play important roles in GC progression and could be regarded as diagnostic/prognostic markers and chemotherapeutic tools. Compared with the complex change

of m6A modification in liver cancer, most ncRNAs and protein genes related to m6A are upregulated in GC tissues, suggesting that the m6A-related risk score might be informative for risk assessment and prognostic stratification (Guan et al., 2020).

2.4 Bladder Cancer and ncRNA m6A Modification

Bladder cancer is a morbid malignancy of the urinary tract, and 95% of bladder tumors originate from epithelial tissue. Notably, the symptoms of bladder cancer mimic those of a urinary tract infection, increasing the diagnosis difficulty and delaying timely therapy (Li et al., 2019c). Accumulating evidence implies that the abnormal m6A modification of ncRNA is related to tumorigenicity and poor prognosis in bladder cancer. Oncogenic METTL3 facilitates DGCR8 to recognise pri-miRNA and accelerate the maturation of pri-miR221/222, which is targeted to PTEN (Han et al., 2019a). Differently from the direct regulation, the m6A "eraser" FTO regulates the expression of MALAT/miR-384/MAL2 axis by catalysing MALAT1 demethylation in an m6A-dependent manner, indicating the potential of FTO as a diagnostic and prognostic biomarker (Tao et al., 2021). Low expression of METTL14 and decreased global m6A abundance in bladder cancer tissue are also associated with the clinical severity and outcomes of bladder cancer. METTL14 knockout promotes the proliferation, self-renewal, metastasis, and initiation of tumour cells, while overexpression plays an adverse role (Gu et al., 2019). These m6A-related molecules may play important roles in the clinical diagnosis and treatment of bladder cancer in the future.

2.5 Breast Cancer and ncRNA m6A Modification

Breast cancer is an epithelial malignant tumour originating from the terminal ductal lobule unit of the breast. The breast epithelial cells have unlimited replicative potential and other malignant characteristics because of various carcinogenic factors (Nagini 2017). The hostile hypoxic microenvironment is a major reason for the rapid expansion of cancer cells. It has been reported that the lncRNA KB-1980E6.3 that is associated with hypoxia can recruit m6A "reader" IGF2BP1 to stabilize c-Myc mRNA and enhance the malignant characteristics (Zhu et al., 2021). In endocrine-resistant LCC9 breast cancer cells, HNRNPA2B1 expression is higher than that in parental and tamoxifen-sensitive cells, and this increase alters the transcriptome and expression of miRNAs, because HNRNPA2B1 is a "reader" of the m6A mark in pri-miRNAs and is responsible for promoting DROSHA processing of pre-miRNAs (Klinge et al., 2019). Similarly, m6A methyltransferase METTL14 has been demonstrated to be significantly increased in breast cancer tissues with the function of reshaping miRNA profile of cancer cell lines. It has been verified that hsa-miR-146a-5p is a differentially expressed miRNA, modulated by METTL14-induced m6A modification, and thus affects the migration and invasion of breast cancer cells (Yi et al., 2020). In addition, METTL14 is regulated by the oncogenic lncRNA LNC942 to facilitate cell growth and cancer progression. Mechanistically, LNC942 recruits the METTL14 protein and elevated post-transcriptional METTL14-mediated m6A modification levels, thereby stabilising the expression of downstream targets (Sun et al., 2020a). In human epidermal growth factor receptor 2 (HER2)-positive breast cancer, it is reported that m6A "eraser" FTO inhibits miR-181b-3p and upregulates the expression of oncogenic ARL5B (Xu et al., 2020b). Overall, more extensive and in-depth researches on the aberrant m6A modification of ncRNA for the carcinogenesis and development of breast cancer are required.

2.6 Colorectal Cancer and ncRNA m6A Modification

Carcinoma of large intestine is a malignant gastrointestinal tract tumour that originates from large intestine mucous membrane epithelium and gland with a high metastasis and reoccurrence rate, including colon cancer and carcinoma of the rectum (Muller et al., 2016). Most researchers focus on the relationship between ncRNA m6A modification and metastasis of colorectal cancer (CRC). A novel lncRNA RP11-138 J23.1 (RP11) is demonstrated to positively regulate epithelial-mesenchymal transition (EMT) in CRC cells. Mechanistically, the expression of RP11 is upregulated in an m6A modification-dependent manner; then, the complex composed by RP11 and HNRNPA2B1 prevents Zeb1 degradation, triggering the dissemination of cancer cells (Wu et al., 2019). LncRNA GAS5 promotes YAP ubiquitin-mediated degradation, but YTHDF3 alleviates this effect via lncRNA GAS5 decay, confirming that YTHDF3 is not only a novel target of YAP but also a significant player in YAP signalling by facilitating lncRNA GAS5 degradation (Ni et al., 2019). Overexpression of METTL14 is also reported to correlate with the YAP pathway and can suppress CRC cell growth and metastasis via the miR-375/YAP1 pathway (Chen et al., 2020b). Besides, the expression of oncogene lncRNA XIST negatively correlates with YTHDF2 and METTL14 in CRC tissues because of the m6A modification (Yang et al., 2020c). In contrast, YTHDC1 recognises circNSUN2 and export it to the cytoplasm, eventually participating in cancer progression by forming the cir-cNSun2/IGF2BP2/HMGA2 complex (Chen et al., 2019a). In addition, the oncogene lncRNA LINC00460 combines with IGF2BP2 and upregulates the expression of HMGA1 mRNA and increase its stability, participating in cancer development (Hou et al., 2021). The m6A "reader" YTH protein family and IGF2BP2 have been widely reported in colorectal cancer, and therefore it is reasonable to speculate that the m6A "reader" may play an important role in the progression of colorectal cancer, which deserves deeply study.

2.7 Other Cancers and ncRNA m6A Modification

Abnormal m6A modification of ncRNAs is also associated with the progression of other cancers. In clear cell renal cell carcinoma, Gu et al. find a novel DNA methylation-deregulated and RNA m6A reader-cooperating lncRNA (DMDRMR), which interacts

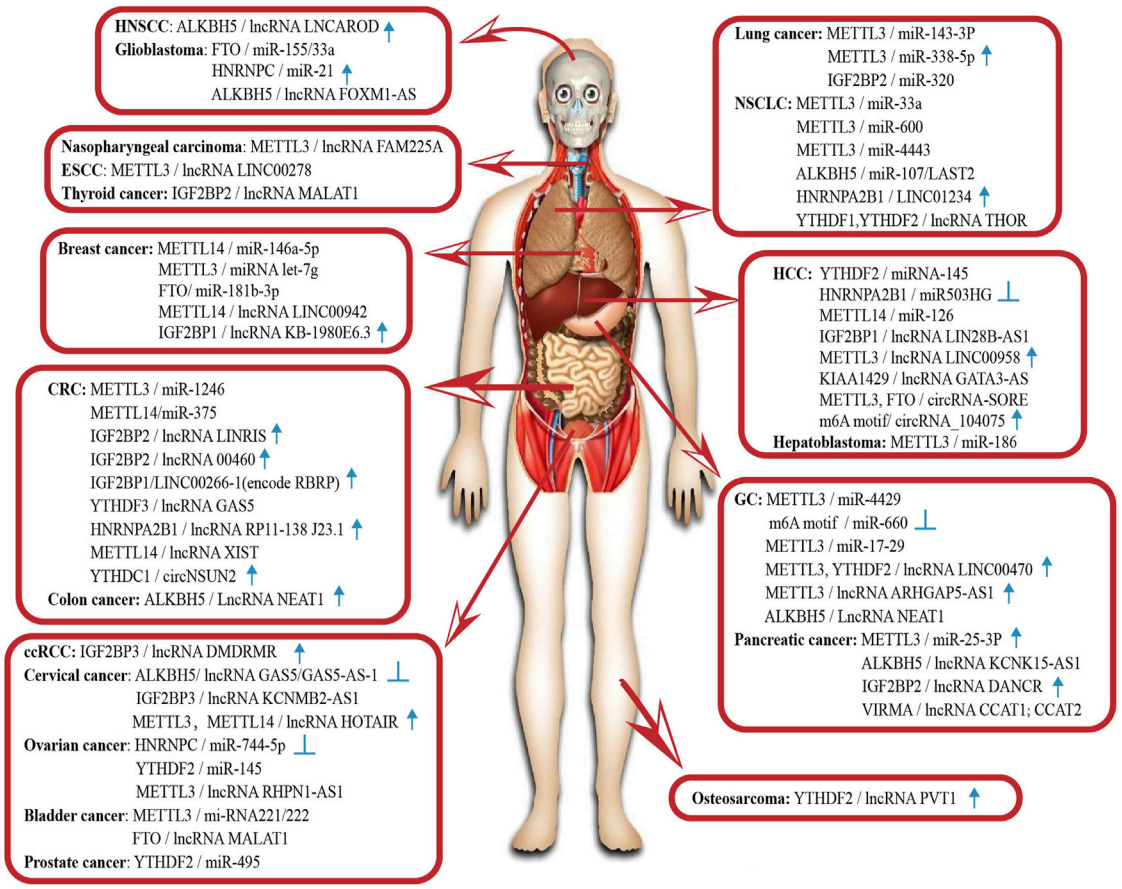

FIGURE 2 | Abnormal m6A modification of non-coding RNA in human cancers. HNSCC, head and neck squamous cell carcinoma; ESCC, esophageal squamous cell carcinoma; HCC, hepatocellular carcinoma; CRC, colorectal cancer; NSCLC, non-small-cell lung carcinoma; GC, gastric cancer; ccRCC, clear cell renal cell carcinoma. The icons represent the ncRNAs that can be regarded as potential diagnostic and prognostic biomarkers. ↑ High expression is positively associated with poor prognosis. High expression is negatively associated with poor prognosis.

with IGF2BP3 to stabilize target genes and plays a carcinogenic role (Gu et al., 2021). In thyroid cancer, lncRNA MALAT1 competitively binds to miR-204, upregulates IGF2BP2 and enhances MYC expression in m6A-dependent manner, conferring a stimulatory effect on cancer progression (Ye et al., 2021). In osteosarcoma, ALKBH5 inhibits the degradation of lncRNA PVT1 and leads to the overexpression of lncRNA PVT1. Overexpressed PVT1 can suppress the binding of YTHDF2 with PVT1 to promote cancer cell proliferation (Chen et al., 2020a). This combination of the m6A "reader" and lncRNA, which affects cancer cell proliferation, also occurs in pancreatic cancer. IGF2BP2 and lncRNA DANCR have been reported to interact and promote the cancer stemness-like properties of pancreatic cancer. The adenosine at 664 of DANCR is modified by N6-methyladenosine, and IGF2BP2 serves as a reader for this structural change to stabilise DANCR RNA and promote cell proliferation (Hu et al., 2020). In pancreatic duct epithelial cells, oncogenic miR-25-3p is correlated with poor prognosis in patients with pancreatic cancer. One study has found that NF-κB-associated protein induced by m6A modification facilitates excessive pri-miR-25 maturation under the environment of cigarette smoke condensate; then it activates the oncogenic AKT-p70S6K signalling and provokes malignancy of pancreatic cancer (Zhang et al., 2019a). In head and neck squamous cell carcinoma, oncogenic LNCAROD affects the degree of tumour malignancy. METTL3-and METTL14-induced dysregulated m6A modification could account for the aberrant expression of LNCAROD and lead to the malignant behaviour of tumour cells (Ban et al., 2020). Moreover, Zheng et al. propose that m6A is highly enriched in oncogenic lncRNA FAM225A and enhances RNA stability, contributing to cell proliferation, migration, invasion, and metastasis (Zheng et al., 2019). Similarly, m6A modification improves the transcript stability of lncRNA RHPN1-AS1 and upregulates its expression in epithelial ovarian cancer tissues, facilitating RHPN1-AS1 to act as an oncogene (Wang et al., 2020a). In glioblastoma, it has been found that 13 central m6A methylation regulators are associated with the clinical and molecular phenotype, suggesting that m6A regulators are important participants in malignant progression (Du et al., 2020b). A more specific example is HNRNPC, which directly binds to pri-miR-21 and

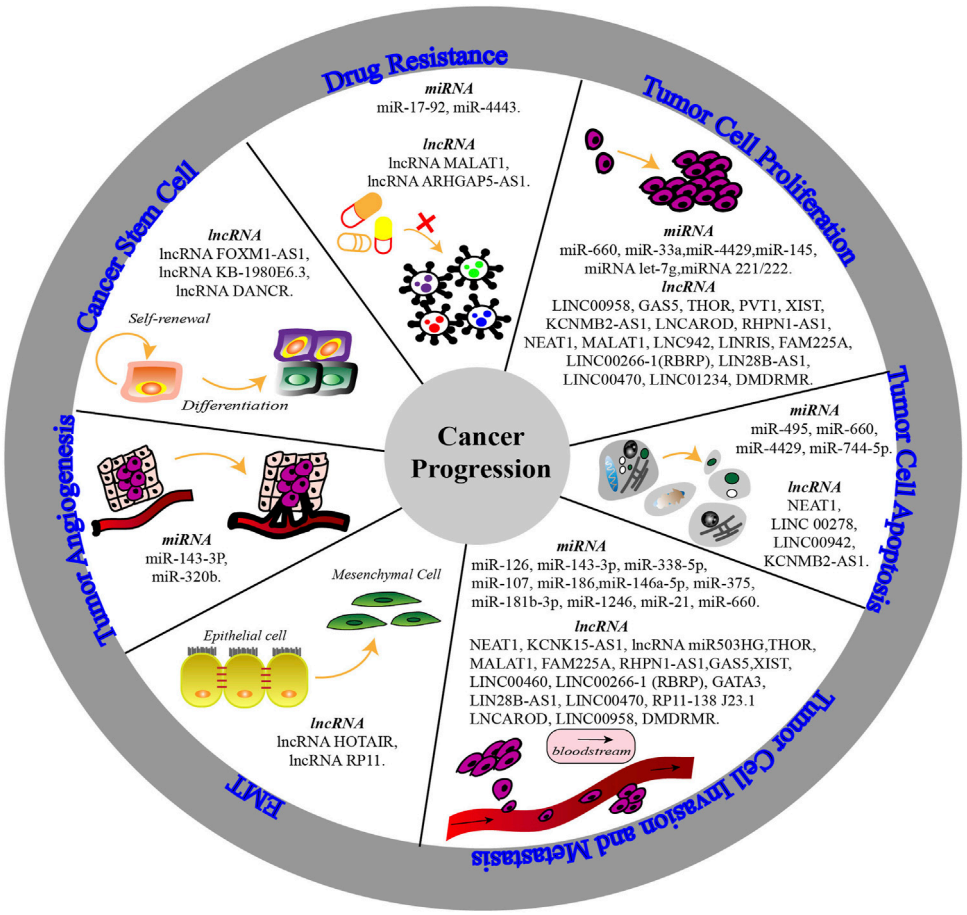

FIGURE 3 | The mechanisms of non-coding RNA (miRNA & lncRNA) m6A modification involved in cancer progression. The biological functions of non-coding RNAs are altered by abnormal m6A modification and the interaction with m6A regulators. Thereby, non-coding RNAs participate in tumor cell proliferation, apoptosis, invasion and metastasis, epithelial-mesenchymal transition (EMT), tumor angiogenesis, cancer stemness and drug resistance to affect cell characteristics and cancer progression.

promotes its expression, playing a role in the metastatic potential of the glioblastoma cell lines. The experimental results show that the expression levels of HNRNPC are higher in highly aggressive cancer cells and are elevated along with the brain tumour grade (Park et al., 2012). In the cancers listed above, the abundance of m6A modification and the enzymes involved in it can affect ncRNA maturation and activation and change their biological functions, which in turn can impact the progression of various cancers (see **Figure 2**).

3 MECHANISMS OF NCRNA M6A MODIFICATION IN CANCER PROGRESSION

The ncRNA and m6A regulators show significant changes in different cancers owing to their interactions, which cause abnormal biological functions and thereby affect cancer progression (see **Figure 3**). Among urological cancers (Wang et al., 2020c), METTL3 is overexpressed in bladder cancer (Xie et al., 2020)and prostate cancer (Yuan et al., 2020), but shows low expression in kidney cancer (Tao et al., 2020). METTL14 is downregulated in kidney and bladder cancers, playing a tumour suppressive role. Surprisingly, even though METTL3 and METTL14 show different expression levels and functions in urological cancers, they both participate in cancer progression through cell growth- and cell death-related pathways (Tao et al., 2020). Therefore, understanding ncRNA m6A modification from the perspective of cancer progression mechanisms will provide more promising ideas and methods to interfere with cancer progression (see **Table 1**).

3.1 Tumour Cell Proliferation

Many studies have reported that m6A modification of ncRNAs influences tumorigenesis and cell proliferation; for example, ectopic expression of miR-660 directly binds to oncogene E2F3 to affect cell proliferation owing to the m6A motif in the region of E2F3 3′-UTR (He and Shu 2019). The stabilisation of oncogene SEC62 mRNA could be enhanced by the m6A

TABLE 1 | The biological function and mechanism of ncRNAs and m6A modification involved in cancer progression.

Non-coding RNA	Cancer	Biological function and mechanism	References
miR-143-3P	lung cancer	Methylation facilitates miR-143-3p biogenesis and promotes brain metastasis *via* miR-143-3p/VASH1 axis	Wang et al. (2019a)
miR-338-5p	lung cancer	MiR-338-5p inhibits cell growth and migration *via* inhibition METTL3/c-Myc pathway	Wu et al. (2021)
miR-320b	lung cancer	miR-320b suppresses HNF4G and IGF2BP2 expression to inhibit angiogenesis and tumor growth	Ma et al. (2021)
miR-33a	NSCLC	MiR-33a attenuates cell proliferation by reducing the expression of METTL3	Du et al. (2017)
miR-107	NSCLC	ALKBH5 regulates miR-107/LATS2 axis to inhibit YAP, thus inhibiting tumor growth and metastasis	Jin et al. (2020)
miR-600	NSCLC	MiR-600 downregulates METTL3 expression to induce migration, proliferation and apoptosis	Wei et al. (2019)
miR-4443	NSCLC	Exosomal miR-4443 facilitates tumor growth and promotes cisplatin resistance *via* METTL3	Song et al. (2021)
lncRNA THOR	NSCLC	YTHDF1/2 regulate the stability of lncRNA THOR, strengthening cell proliferation and metastasis	Liu et al. (2020a)
lncRNA MALAT1	NSCLC	MALAT1 is stabilized by METTL3/YTHDF3 complex and sponges miR-1914-3p to promote invasion, metastasis and resistance	Jin et al. (2019)
lncRNA LINC01234	NSCLC	LINC01234 interacts with HNRNPA2B1 to enhance cell growth *via* miR-106b/CRY2/c-Myc axis	Chen et al. (2020d)
miR-186	hepatoblastoma	METTL3/miR-186 axis contributes to migration and invasion *via* the Wnt/β-catenin signaling pathway	Cui et al. (2020)
miR503HG	HCC	MiR503HG promotes HNRNPA2B1 degradation and inhibits migration *via* NF-κB signaling pathway	Wang et al. (2018)
miR-126	HCC	Methylation facilitates miR-126 maturation and alters cell metastatic capacity	Ma et al. (2017)
lncRNA LIN28B-AS1	HCC	LIN28B-AS1 downregulates IGF2BP1-dependent mRNAs, inhibiting proliferation, migration and invasion	Zhang et al. (2020c)
lncRNA LINC00958	HCC	Methylated LINC00958 sponges miR-3619-5p to upregulate HDGF, facilitating cell proliferation, motility and lipogenesis	Zuo et al. (2020)
lncRNA GATA3	HCC	GATA3-AS participates in the binding of KIAA1429 and GATA3, relating with tumor growth and metastasis	Lan et al. (2019)
circRNA-SORE	HCC	CircRNA-SORE induces sorafenib resistance *via* miR-103a-2-5p/miR-660-3p and Wnt/β-catenin pathway	Xu et al. (2020a)
circRNA_104075	HCC	CircRNA_104075 stimulates YAP-dependent tumorigenesis and cell proliferation through m6A modification	Zhang et al. (2018)
miR-4429	GC	MiR-4429 inhibits METTL3 to repress SEC62, preventing proliferation and facilitating apoptosis	He et al. (2019)
miR-660	GC	Ectopic expressed miR-660 directly binds to E2F3 and realizes anti-proliferation effect via the m6A motif	He and Shu (2019)
miR-17-92	GC	METTL3 facilitates the maturation of miR-17-92, decreases the resistance to mTOR inhibitor everolimus	Sun et al. (2020b)
lncRNA ARHGAP5-AS1	GC	lncRNA ARHGAP5-AS1 facilitates ARHGAP5 methylation, accelerating the chemotherapeutic resistance	Zhu et al. (2019)
lncRNA LINC00470	GC	LINC00470 decrease PTEN expression via m6A regulators, promoting proliferation, migration and invasion	Yan et al. (2020)
lncRNA NEAT1	GC	ALKBH5 and NEAT1 influences the expression of EZH2 and thus affects invasion and metastasis	Zhang et al. (2019b)
miR-146a-5p	breast cancer	METTL14 modulates hsa-miR-146a-5p expression, affecting migration and invasion of cancer cells	Yi et al. (2020)
miR-181b-3p	breast cancer	The FTO/miR-181b-3p/ARL5B signaling pathway regulates cell migration and invasion	Xu et al. (2020b)
miRNA let-7g	breast cancer	The loop of HBXIP/let-7g/METTL3/HBXIP related with cell proliferation	Cai et al. (2018)
lncRNA LINC00942	breast cancer	LNC942 increases methylation level, elevates cell proliferation and inhibits cell apoptosis	Sun et al. (2020a)
lncRNA KB-1980E6.3	breast cancer	LncRNA KB-1980E6.3 maintains CSC stemness via interacting with IGF2BP1 to facilitate c-Myc stability	Zhu et al. (2021)
miR-1246	CRC	Upregulated METTL3 facilitates migration and invasion via miR-1246/SPRED2/MAPK signaling pathway	Peng et al. (2019)
miR-375	CRC	METTL14 suppresses cell growth via the miR-375/YAP1, inhibits cell migration and invasion through the miR-375/SP1 pathway	Chen et al. (2020b)
lncRNA LINRIS	CRC	LINRIS stabilizes IGF2BP2 and prevents its degradation, promoting the aerobic glycolysis and proliferation	Wang et al. (2019b)
lncRNA GAS5	CRC	LncRNA GAS5 promotes YAP degradation, but YTHDF3 alleviates this effect via lncRNA GAS5 decay	Ni et al. (2019)
lncRNA LINC00460	CRC	LncRNA LINC00460 combines with IGF2BP2 to increase HMGA1, facilitating invasion and metastasis	Hou et al. (2021)
lncRNA RP11-138 J23.1	CRC	The m6A modification upregulates RP11 to promote EMT, migration, invasion and enhance liver metastasis	Wu et al. (2019)

(Continued on following page)

TABLE 1 | (*Continued*) The biological function and mechanism of ncRNAs and m6A modification involved in cancer progression.

Non-coding RNA	Cancer	Biological function and mechanism	References
lncRNA XIST	CRC	Methylation decrease enhances the expression of XIST, increasing tumorigenicity and metastasis	Yang et al. (2020c)
LINC00266-1 (RBRP)	CRC	The LINC00266-1-encoded RBRP peptide promotes tumorigenesis and metastasis via IGF2BP1/c-Myc	Zhu et al. (2020a)
Circ-NSUN2	CRC	YTHDC1 recognizes cir-cNSun2 and facilitates invasion by forming the cir-cNSun2/IGF2BP2/HMGA2 complex	Chen et al. (2019a)
lncRNA NEAT1	colon cancer	ALKBH5 upregulates NEAT1 expression by demethylation, which leads to inhibit apoptosis and induce cell proliferation and migration	Guo et al. (2020)
miR-25-3p	pancreatic cancer	Methylation facilitates pri-miR-25 maturation to provoke malignant phenotypes via AKT-p70S6K pathway	Zhang et al. (2019a)
lncRNA KCNK15-AS1	pancreatic cancer	Demethylation KCNK15-AS1is related with cell motility	He et al. (2018)
lncRNA DANCR	pancreatic cancer	DANCR is stabilized by IGF2BP2. IGF2BP2 and DANCR promote cancer stemness-like properties	Hu et al. (2020)
lncRNA GAS5/GAS5-AS-1	cervical cancer	GAS5-AS1 regulates m6A modification of GAS5 to inhibit proliferation and metastasis	Peng et al. (2016)
lncRNA KCNMB2-AS1	cervical cancer	KCNMB2-AS1 sponges miR-130b-5p/miR-4294 to upregulate IGF2BP3, inhibiting apoptosis of cancer cells and inducing proliferation	Zhang et al. (2020d)
lncRNA HOTAIR	cervical cancer	LncRNA HOTAIR methylated by m6A upregulate EMT related-genes and increase aggressiveness	Peng et al. (2016)
lncRNA RHPN1-AS1	epithelial ovarian cancer	RHPN1-AS1 is stabilized by methylation, promotes cell proliferation and metastasis *via* miR-596/LETM1 and activates FAK/PI3K/Akt pathway	Wang et al. (2020a)
miR-744-5p	ovarian cancer	The overexpression of miR-744-5p decreases HNRNPC, relating with cell apoptosis	Kleemann et al. (2018)
miR-145	ovarian cancer	MiR-145 downregulates YTHDF2 expression and increase m6A levels, suppressing cell proliferation	Li et al. (2020a)
miRNA221/222	bladder cancer	METTL3 overexpressed cells, miRNA221/222 promotes tumor proliferation by regulating PTEN.	Han et al. (2019a)
lncRNA DMDRMR	clear cell renal cell carcinoma	LncRNA DMDRMR-mediated regulation of m6A-modified CDK4 by IGF2BP3 promotes cell proliferation and metastasis	Gu et al. (2021)
lncRNA FOXM1-AS	Glioblastoma	FOXM1-AS regulates FOXM1 expression to maintain tumorigenicity of glioblastoma stemness-like cells	Zhang et al. (2017)
miR-21	glioblastoma multiforme	HNRNPC controls the metastatic potential by regulating the expression of miR-21 and PDCD4	Park et al. (2012)
lncRNA PVT1	Osteosarcoma	ALKBH5 upregulates PVT1 to suppress its binding with YTHDF2, promoting tumor proliferation	Chen et al. (2020a)
miR-495	prostate cancer	KDM5A/miRNA-495/YTHDF2/m6A-MOB3B axis is associated with cancer cell apoptosis	Du et al. (2020a)
lncRNA CCAT1/CCAT2	prostate cancer	M6A "reader" VIRMA downregulation attenuates the aggressive phenotype by overall reduction of m6A-levels decreasing stability and abundance of oncogenic lncRNA CCAT1 and lncRNA CCAT2	Barros-Silva et al. (2020)
lncRNA FAM225A	nasopharyngeal carcinoma	FAM225A with highly enriched m6A modification promotes tumorigenesis and metastasis *via* miR-590-3p/miR-1275/ITGB3	Zheng et al. (2019)
lncRNA LNCAROD	HNSCC	Methylation stabilizes LNCAROD and promotes cancer progression via HSPA1A/YBX1, associating with cell proliferation and mobility	Ban et al. (2020)
lncRNA LINC00278	ESCC	LINC00278 modified by m6A encodes a micropeptide YY1BM, whose downregulation upregulates eEF2K expression, disrupts negative regulation of the AR signaling pathway and inhibits cell apoptosis	Wu et al. (2020)
lncRNA MALAT1	thyroid cancer	MALAT1 upregulates IGF2BP2 and enhances Myc expression by competitively binding to miR-204, conferring a stimulatory effect on proliferation, migration, invasion and cell apoptosis	Ye et al. (2021)

modification of METTL3 and IGF2BP1; however, it was demonstrated that miR-4429 targets and suppresses METTL3 to repress SEC62 and realise an anti-proliferative effect (He et al., 2019). In addition, the overexpression of miR-145 inhibits cancer cell proliferation, while this suppression is impaired by the overexpression of YTHDF2, resulting in a crucial crosstalk between miR-145 and YTHDF2 by forming a double-negative feedback loop (Li et al., 2020a). Carcinogenic lncRNA THOR has been reported to be related to m6A modification for the first time. YTHDF1 and YTHDF2 can regulate the stability of THOR by reading the m6A motifs, thereby strengthening cell proliferation and helping THOR to realise its oncogenic function (Liu et al., 2020a). In terms of the m6A "reader," METTL3-induced m6A methylation reduces lncRNA RHPN1-AS1 degradation to help it serve as a ceRNA and activate the PI3K/AKT pathway (Wang et al., 2020a). Similarly, LNC942, lncRNA XIST and lncRNA FAM225A can affect cell proliferation and cancer progression under the m6A "writer"-mediated m6A modification (Sun et al., 2020a; Yang et al., 2020c; Zheng et al., 2019).

With the participation of m6A modification, both lncRNA THOR and lncRNA RHPN1-AS1, regarded as oncogenes, can promote tumorigenesis and cell proliferation, while it is worth noting that LINC00266-1 itself cannot promote tumorigenesis but RBRP encoded by it is a potential oncogene in colorectal cancer. LncRNA LINC00266-1 encodes a 71-amino acid peptide named "RNA-binding regulatory peptide" (RBRP), which binds to the RNA-binding proteins, including the m6A "reader" IGF2BP1. The existence and expression of natural endogenous RBRP has been verified in colorectal, breast, and ovarian cancers and nasopharyngeal carcinoma. RBRP, considered as a regulatory subunit of a m6A "reader," strengthens m6A recognition by IGF2BP1 on targeted RNAs through the essential G19 residue and promotes tumorigenesis (Zhu et al., 2020a).

3.2 Tumour Cell Apoptosis

To investigate the function of miRNA m6A modification in cell apoptosis, regions upstream and downstream of miRNA 675 m6A modification sites in the H19 locus are mutated with a system of adenine base editors, showing that mutation facilitates cell apoptosis by downregulating the expression of H19 (Hao et al., 2020). Gu et al. (2018) also believed that m6A-modified miRNAs regulated the pathway closely related to cell apoptosis, as verified in arsenite-transformed cells. In prostate cancer, YTHDF2 is regarded as a target of miR-495 to recognise MOB3B m6A modification and inhibit its expression. At the same time, the miR-495 promoter interacts with overexpressed oncogenic KDM5A and restrains the expression of miR-495. It has been reported that the progression of prostate cancer can be motivated by the activation of the KDM5A/miRNA-495/YTHDF2/m6A-MOB3B axis by influencing the apoptosis of cancer cells (Du et al., 2020a). YTHDF2 is also considered as a direct target gene of miR-145 in epithelial ovarian cancer, and its overexpression enhances cell apoptosis (Li et al., 2020a). Besides, cigarette smoke decreases the m6A modification of LINC00278 and the translation of YY1BM encoded by LINC00278, and these dysregulations inhibit the apoptosis of cancer cells (Wu et al., 2020). In addition, overexpressed lncRNA KCNMB2-AS1 plays the role of ceRNA and upregulates the oncogene IGF2BP3 by sponging miR-130b-5p and miR-4294. IGF2BP3 binds to KCNMB2-AS1 m6A sites, forming a positive regulatory loop composed of KCNMB2-AS1 and IGF2BP3 to inhibit cell apoptosis and induce proliferation (Zhang et al., 2020e).

3.3 Tumour Cell Invasion and Metastasis

Some researchers have proposed a correlation between m6A and invasion, metastasis, such as the overexpression of FTO, which promotes the migration and invasion of GC cell lines (Xu et al., 2017). ALKBH5 is involved in mediating methylation reversal, and it is reported that ALKBH5-demethylated lncRNA NEAT1 is overexpressed in GC and colon cancer cells, promoting invasion and metastasis (Guo et al., 2020; Zhang et al., 2019b). Yang et al. also determined that the downregulation of ALKBH5 in colon cancer is associated with tumour inhibition. Overexpression of ALKBH5 restrains the invasion and metastasis of colon cancer cells (Yang et al., 2020a). In addition, ALKBH5 demethylates lncRNA KCNK15-AS1 and downregulates its expression in pancreatic cancer tissues, inhibiting cell motility and invasion (He et al., 2018). These interesting roles of ALKBH5 in different cancers warrant further study. The m6A modification level is significantly reduced in HCC tissue, especially in metastatic tissues. It was confirmed that the main factor is the downregulation of METTL14, which mediates miRNA maturation and alters the metastatic capacity of HCC (Ma et al., 2017). LncRNA miR503HG is also reduced in HCC tissues. Further investigation suggested that HNRNPA2B1 degradation is promoted by miR503HG, suppressing the NF-κB pathway and facilitating the invasion and metastasis of HCC cells (Wang et al., 2018). In other tumours, METTL3-methylated regulates the MALAT1-miR-1914-3p-YAP axis and increases YAP activity to enhance drug resistance and metastasis (Jin et al., 2019). METTL3-mediated methylation can also enhance the stability of lncRNA FAM225A, which regulates the expression of ITGB3 by binding to miR-590-3p and miR-1275 as ceRNA, and thus activates the FAK/PI3K/AKT signalling pathway and promotes the invasion and migration of cancer cells (Zheng et al., 2019). Moreover, the carcinogenic lncRNA RHPN1-AS1 and lncRNA THOR have also been found to be associated with cell viability and mobility by ectopic m6A modification, thereby affecting cancer cell invasion and metastasis (Liu et al., 2020a; Wang et al., 2020a).

3.4 Epithelial-Mesenchymal Transition

During epithelial-mesenchymal transition (EMT) progression, the loss of E-cadherin causes cells to acquire mobility and the capacity (Castosa et al., 2018; Ribatti et al., 2020). It has previously been reported that the decrease of METTL3 inhibited the lung cancer cell morphological conversion induced by TGF-β, and augmented the expression changes of EMT-related marker genes, indicating the importance of m6A modification in EMT (Wanna-Udom et al., 2020). As for ncRNA m6A modification, it has been proposed that m6A-methylated lncRNA HOTAIR could upregulate EMT genes and increase the aggressiveness of tumour cells (Peng et al., 2016). In addition, lncRNA RP11 was reported to positively regulate the migration, invasion, and EMT of colorectal cancer cells. It is believed that m6A methylation increases nuclear accumulation and participates in the upregulation of RP11, triggering the spread of colorectal cancer cells (Wu et al., 2019). By analysing the cancer cells and clinical samples, Kandimalla et al. established the RNAMethyPro-a gene expression signature, which is correlated with EMT-related prognosis genes (Kandimalla et al., 2019). The specific mechanisms between ncRNA m6A modification and EMT deserve further study.

3.5 Tumour Angiogenesis

Angiogenesis is regarded as a significant step in tumour development, and some of the genes associated with EMT and tumour angiogenesis are m6A target genes involved in tumorigenesis; they are very sensitive to m6A modification. Previously, RNA functional analysis confirm that METTL14 and ALKBH5 can regulate the expression of each other, inhibit the demethylation activity of YTHDF3, and induce

aberrant m6A modification to play roles in tumour angiogenesis and metastasis (Panneerdoss et al., 2018). In lung cancer, the anti-cancer gene miR-320b downregulates the expression of IGF2BP2 and thymidine kinase 1 (TK1), thus suppressing angiogenesis and lung cancer growth (Ma et al., 2021). During the process of lung cancer brain metastasis, upregulated miR-143-3p promoted by METTL3-methylation facilitates miRNA splicing and biogenesis, interacts with VASH1 and increases invasion capability and angiogenesis (Wang et al., 2019a). In brain metastasis of breast cancer, transcripts associated with brain metastasis are enriched by YTHDF3 and promote cancer cells to interact with cells in the tumour microenvironment, benefiting angiogenesis and metastasis (Chang et al., 2020).

3.6 Cancer Stem Cells

Cancer stem cells maintain the vitality of the cellular population through self-renewal and infinite proliferation, which are essential for cancer initiation and metastasis. Experimental analysis has shown that ALKBH5 facilitates the proliferation and tumorigenicity of cancer stem cells by interacting with lncRNA FOXM1-AS (Zhang et al., 2017). Moreover, the identified m6A "reader" YTHDF2 can reduce the half-life of diverse m6A transcripts, including the tumour necrosis factor receptor (Tnfrsf2), leading to negative effects on the overall integrity of leukemic stem cell function. Under YTHDF2 depletion, Tnfrsf2 is upregulated to facilitate cell apoptosis in leukemic stem cells (Paris et al., 2019). In addition to leukemic stem cells, YTHDF2 is associated with the liver cancer stem cell phenotype (Zhang et al., 2020b). In breast cancer, a recent study showed that lncRNA KB-1980E6.3 can augment cancer cell self-renewal and maintain the stemness of cancer cells under a hypoxic microenvironment, indicating that targeting the lncRNA KB-1980E6.3/IGF2BP1/c-Myc axis may be a promising therapy for refractory hypoxic tumours (Zhu et al., 2021).

3.7 Drug Resistance

Drug resistance that develops during conventional drug therapy is one of the significant reasons for chemotherapy failure in cancer. As the main component of methylase involved in m6A modification, METTL3 has been widely reported to be associated with drug resistance. In NSCLC, the METTL3/YTHDF3 complex enhances the stability of lncRNA MALAT1, regulating the MALAT1-miR-1914-3p-YAP axis to increase YAP expression and induce drug resistance (Jin et al., 2019); METTL3, as a direct target gene of miR-4443 in tumour exosomes, is involved in regulating FSP1 expression and interferes with the ferroptosis induced by cisplatin, resulting in drug resistance (Song et al., 2021). Furthermore, in GC cells, METTL3 is recruited by lncRNA ARHGAP5-AS1 to stabilize ARHGAP5 mRNA and promotes chemoresistance (Zhu et al., 2019), and consistent with this study, Sun et al. find that elevated METTL3 and levels of m6A modification facilitate the maturation of pri-miR-17-92 to the miR-17-92 cluster, which activates the AKT/mTOR pathway. High levels of METTL3 and the miR-17-92 cluster then enhance the sensitivity of cancer cells to the mTOR inhibitor, everolimus (Sun et al., 2020b).

In tamoxifen-resistant LCC9 breast cancer cells, studies have determined that overexpressed m6A "reader" HNRNPA2B1 can upregulate and downregulate different miRNAs simultaneously and affect the downstream signalling pathways of these miRNAs. Transient overexpression of HNRNPA2B1 reduces the sensitivity of cancer cells to 4-hydroxytamoxifen and fulvestrant, suggesting the potential role of HNRNPA2B1 in endocrine-resistance (Klinge et al., 2019). Oncogene circRNA-SORE is upregulated in sorafenib-resistant HCC cells, acting as ceRNA to sponge miR-103a-2-5p and miR-660-3p, competitively activate the Wnt/β-catenin pathway, and induce sorafenib resistance (Xu et al., 2020a). However, further study shows that interfering the expression of circRNA-SORE has effects on improving sorafenib efficacy, which represents a promising pharmaceutical intervention targeted circRNA-SORE in sorafenib-treated HCC patients. Besides, recent studies have shown that depletion or inhibition of FTO suppresses the expression of immune checkpoint genes and attenuates the self-renewal ability of cancer stem cells, thus overcoming their immune escape (Su et al., 2020). Another study indicated that the m6A modification induced by 'eraser' FTO augments melanoma growth, whereas FTO inhibition increases the sensitivity of cancer cells to anti-PD-1 immunotherapy, suggesting that the immune checkpoint molecular inhibitors represented by PD-1/PD-L1 can play an important role with the help of FTO inhibitors (Yang et al., 2019). Although these two studies were based on the demethylation effect of FTO on mRNAs, it is reasonable to believe that FTO inhibitors can also inhibit ncRNA-related targets or signal pathways with the deepening of studies on the crosstalk of FTO and ncRNAs. These findings provide in-depth insights into chemoresistance and support the therapeutic potential of ncRNA m6A modification, especially in combination with existing drugs to target refractory malignant tumours.

4 CLINICAL APPLICATION OF NCRNA M6A MODIFICATION IN CANCERS

4.1 m6A Regulators and Abnormally Modified ncRNAs as Potential Diagnostic and Prognostic Biomarkers

The interaction between ncRNAs and m6A modification suggests that they may provide new ideas for the clinical treatment of cancer and even become prognostic biomarkers or therapeutic targets for cancer therapy. Zhang et al. constructed an m6A-score model to quantify m6A modification patterns in cancers. By analysing tumour microenvironment phenotypes and 5-year survival rates in patients with low and high m6A-score subgroups, it was found that patients with low m6A-scores show significant therapeutic advantages, suggesting a crosstalk between m6A modification and tumour microenvironment diversity and complexity (Zhang et al., 2020a). In HCC tissues, m6A methyltransferases WATP and KIAA1429 are related to prognosis (Chen et al., 2019b; Liu et al., 2020b), and METTL3, YTHDF2, ZC3H13 and ALKBH5 are considered independent prognostic factors for overall survival; of these, only METTL3 is an independent prognostic factor for recurrence-free

survival (Li et al., 2019b; Liu et al., 2021). In CRC, depletion of METTL14 is associated with poor prognosis (Chen et al., 2020b; Yang et al., 2020c), which is different from the methylated enzymes METTTL3 and KIAA1429 in liver cancer. Notably, m6A "reader" ALKBH5 is associated with TNM stage, tumour size, lymph node metastasis (Tang et al., 2020), and can be regarded as a prognostic indicator in colon cancer (Guo et al., 2020). ALKBH5 is also believed to be a novel biomarker and independent prognostic factor in pancreatic cancer and NSCLC (Tang et al., 2020; Zhu et al., 2020b). Further, studies have revealed that FTO expression is closely correlated with low differentiation, peritumoral lymphovascular invasion, lymph node metastasis and is positively correlated with TNM stage in HCC, GC, HER2-positive breast cancer and bladder cancer, which makes FTO a possible biomarker for diagnostic and prognostic purposes (Cui et al., 2020; Tao et al., 2021; Xu et al., 2017; Xu et al., 2020b). Notably, high expression of HNRNPC in glioblastoma enhances cell invasiveness by regulating the miR-21/PDCD4 axis, and the level of HNRNPC is reported to increase with the increasing grade of brain tumour (Park et al., 2012). Bioinformatics analysis and validation experiments further confirmed the value of high expression HNRNPC in the prognosis of GBM patients at the expression level (Wang et al., 2020b). Interestingly, Ying et al. have identified m6A "reader" HNRNPC genes in the Chinese population and discussed the relationship between single nucleotide polymorphisms and susceptibility to pancreatic cancer, providing a completely novel idea on studying the role of m6A modification in tumorigenesis (Ying et al., 2021). Besides, several studies have analyzed the m6A regulators expression differences and their correlations in normal tissue and tumour tissue based on the clinical data of TCGA and GTEx databases, and it is found that the differential expression of some m6A regulators are closely associated with the risk factors of prognosis in hematologic system tumours and endocrine-system-related tumours (Li et al., 2020b; Zhang et al., 2021). Based on TCGA, GTEx and GEO, a novel risk signature has been constructed to evaluate the relationship between m6A regulators and survival rate of patients in uterine corpus endometrial carcinoma and uterine carcinosarcoma, further inspiring us to combine the bioinformatics with the study of m6A modification (Zou et al., 2021). Taken together, focusing on the expression of m6A regulators and their prognostic value provides us with a potential experimental avenue. It will have good clinical significance to directly or indirectly measure the expression level of m6A, the degree of tumours malignancy and the prognosis of patients by using tumour samples of patients.

ncRNAs modified by abnormal m6A modification could also be regarded as biomarkers, but these ncRNAs show a high degree of specificity and difference in various cancers. A m6A-lncRNA co-expression network has been constructed in primary glioblastoma to identify four m6A-related prognostic lncRNAs: MIR9-3HG, LINC00900, MIR155HG, and LINC00515 (Wang et al., 2021). Using a similar approach, LINC00152, LINC00265, and nine other lncRNAs are documented as biomarkers for predicting the overall survival of lower-grade glioma patients (Tu et al., 2020). In HCC, high expressed circRNA_104075 acts as a ceRNA to sponge miR-582-3p and upregulate YAP expression. The significant changes in downstream pathways caused by circRNA_104075 render it possible to be a new diagnostic marker (Zhang et al., 2018). LncRNA00266-1-encoded peptides RBRP bind to m6A "reader" IGF2BP1 to facilitate tumorigenesis, and the patients with high level of RBRP display an unfavourable prognosis (Zhu et al., 2020a); high expression of LINC00958 also can independently predict poor overall survival in patients with HCC. The good news is to take advantage of the role of LINC00958 as a biomarker, Zuo et al. constructed a novel drug delivery system, a PLGA-based nanoplatform filled with si-LINC00958, with the advantages of controlled release, tumour targeting, and better safety and effectiveness (Zuo et al., 2020). Differently, as a prognostic indicator, lncRNA miR503HG is significantly decreased in HCC tissues, and is positively associated with overall survival and time to recurrence (Wang et al., 2018).

The same phenomenon occurs in GC and cervical cancer. High expression of lncRNA ARHGAP5-AS1 (Zhu et al., 2019)and lncRNA LINC00470 (Yan et al., 2020) is related to the poor prognosis of patients with GC, whereas low expression of miR-660 is strongly linked with a large tumour size, severe lymph node metastasis, advanced TNM stage, and poor outcome (He and Shu 2019). In cervical cancer, lncRNA HOTAIR and lncRNA GAS5 show opposite effects on forecasting the clinical states of patients, high expression of HOTAIR indicates a high degree of malignancy, whereas lncRNA GAS5 is downregulated in cancer tissues, indicating that low GAS5 expression suggests poor prognosis (Peng et al., 2016). The above examples show that under m6A modification, multiple ncRNAs with significant changes may appear in the same cancer, which makes them have great potential for future prognostic diagnosis. However, accuracy cannot be determined solely using existing studies, and is worth further experimental exploration.

Surprisingly, lncRNA LINRIS (Wang et al., 2019b), lncRNA RP11 (Wu et al., 2019), lncRNA LINC00460 (Hou et al., 2021), lncRNA NEAT1 (Guo et al., 2020), and circRNA NSUN2 (Chen et al., 2019a) are all upregulated in patients with CRC and poor overall survival, indicating their promising role as critical prognostic markers and therapeutic targets. In prostate cancer, lncRNA CCAT1 and lncRNA CCAT2 can be regarded as a group variable to independently predict the prognosis of patients (Barros-Silva et al., 2020). Further, evidence confirms that potential prognostic markers also exist in other cancers, such as LINC01234 in NSCLC (Chen et al., 2020d), miR-744-5p in ovarian cancer (Kleemann et al., 2018), lncRNA LNCAROD in head and neck squamous cell carcinoma (Ban et al., 2020), lncRNA PVT1 in osteosarcoma (Chen et al., 2020a), miR-25-3p (Zhang et al., 2019a)and lncRNA DANCR (Hu et al., 2020)in pancreatic cancer (see **Figure 2**). Notably, several recent studies have used data models to analyse differentially expressed ncRNAs in some cancers to identify potential prognostic or diagnostic markers, such as in ovarian cancer (Li et al., 2021), adrenocortical carcinoma (Jin et al., 2021), kidney renal clear cell carcinoma (Yu et al., 2021), and colorectal cancer (Zuo et al., 2021). This new approach can explore the relationship between ncRNAs and different cancers on a large scale, as well as provide ideas and directions for further molecular mechanism research. To effectuate the role of ncRNAs and m6A regulators as biomarkers, the remarkable relationship between the expression level of m6A and prognosis needs to be explored

more specifically. Demonstrating or testing the changes in m6A levels based on existing data in various cancers to evaluate clinical significance maybe more convincing.

4.2 m6A Regulators as Drug Targets to Participate in Cancer Therapy

Increasing attention has been focused on m6A regulators in hope of finding new treatments. For instance, a study shows that the new sodium channel blocker MV1035 can disturb migration and invasion characteristics by targeting ALKBH5 in glioblastoma (Malacrida et al., 2020). The potential of ALKBH as a drug target has been demonstrated by screening ALKBH blockers from newly synthesised anthraquinone derivatives (Huang et al., 2015). As an important demethylase, FTO has been identified to play an oncogenic role in NSCLC, ovarian cancer, and acute myeloid leukemia, associating with cancer cell proliferation, cancer stem cell maintenance and other malignant characteristics (Huang et al., 2020a; Huang et al., 2019; Li et al., 2019a). In recent years, researchers have used FTO as a target to develop FTO inhibitors, hoping to make new breakthroughs in cancer treatment. It is well known that meclofenamic acid, R-2-hydroxyglutarate, and MO-I-500 inhibit the activity of FTO and display anti-cancer activity (Huang et al., 2015; Singh et al., 2016; Su et al., 2018). Huang et al. find that artificially developed FTO inhibitors FB23 and FB23-2 can directly bind to FTO, selectively inhibit the m6A demethylase activity of FTO, and significantly inhibit cell proliferation in human acute myeloid leukaemia (Huang et al., 2019). Su et al. screen out two small-molecule FTO inhibitors, CS1 and CS2, and showed strong anti-cancer effects in multiple types of cancers. According to a previous study, the self-renewal of leukaemia stem cells can be attenuated and the immune response can be reprogrammed by CS1/2 (Su et al., 2020). A recent trial of FTO inhibitors shows that the ethylester form of meclofenamic acid (MA2) can negatively regulate Myc-miR-155/23a cluster-MXI1 feedback circuit and augment the efficacy of the chemotherapy drug temozolomide (TMZ) on inhibiting proliferation of malignant glioma cells (Xiao et al., 2020). In addition, the protease inhibitor nafamostat mesilate (NM) has been shown to inhibit the growth and metastasis of colorectal cancer and has anti-cancer effects in pancreatic cancer and lung cancer (Han et al., 2019b). Han et al. find that the activity of FTO can be inhibited by NM, indicating that NM might play a role in interfering with cancer progression as an FTO inhibitor. In addition, some biotech or pharmaceutic companies get down to developing high-efficiency small-molecule inhibitors, targeting the m6A regulators, in particular molecules like METTL3 and FTO that vary significantly in many cancers (Huang et al., 2020b). Undoubtedly, it provides a new choice for the effective management of a variety of cancers whether used alone or in combination with anti-tumour drugs, especially under the circumstance of chemotherapy drug resistance.

5 CONCLUSION AND PROSPECTS

Multiple regulation of various "writers" and "erasers" allows m6A modification in a dynamic and reversible manner, and significantly interacts with ncRNAs. Numerous studies have focused on the role of abnormal ncRNA m6A modifications in cancer progression. Aberrant m6A-modified ncRNAs and alteration of m6A regulators are closely related to cellular proliferation, apoptosis, invasion and metastasis, as well as other key steps of tumorigenesis and cancer progression. Undoubtedly, the cancers listed in this review form only a small part of the disease, and mainly include mainstream cancers and ncRNAs from recent years. Therefore, from the perspective of m6A modification, further research is needed to understand whether ncRNAs can participate in tumorigenesis and progression in other cancers, whether the same ncRNA plays the same role in different cancers (e.g. lncRNA MALAT1 and RBRP encoded by lncRNA LINC00266-1), and how different ncRNAs come into effect when they are involved in the same cancer; more research are also needed to explore the underlying mechanisms, especially in the field of stemness, reprogramming of tumour immune microenvironment and angiogenesis, and to illustrate the effects of ncRNA and m6A modification on cancer initiation, promotion and progression. Accordingly, the overall abundance of m6A modification may not be of vital significance; instead, some specific transcripts or genes play significant roles in biological function and cancer progression (most of them play the role in promoting cancer). Therefore, increased attention should be given to the significant changes in specific molecules, improving their clinical value as diagnostic/prognostic biomarkers. Further, studies now mainly focus on the cellular level, whereas fewer studies have been conducted *in vivo*. In clinical applications, several studies have elucidated the effect of ncRNAs in cancer prognosis based on m6A-Seq, m6A score, and designing data models, which has revealed molecules that could serve as biomarkers or therapeutic targets, and have greatly enriched the research in this field. However, applying these molecules in developing pharmaceutical preparations and in clinical diagnosis is still challenging. Overall, given the importance of ncRNA m6A modification and m6A regulators in various cancers, we consider that they are promising diagnostic and prognostic biomarkers contributing to the prediction of recurrence and survival, even serving as potential drug targets for therapeutic interventions in cancer treatment. Nevertheless, more specific mechanisms, more in-depth theories, and closer to practical applications of clinical diagnosis and treatment require further exploration.

AUTHOR CONTRIBUTIONS

D-HC and J-GZ drafted the manuscript. C-XW participated in interpretation. QL participated in the design of the manuscript and helped modifying the manuscript.

FUNDING

This work was supported by the subject of the National Key R&D Program of China (No. 2017YFC0909900) and the Clinical Research Plan of SHDC (No. SHDC2020CR4076).

REFERENCES

Alarcón, C. R., Goodarzi, H., Lee, H., Liu, X., Tavazoie, S., and Tavazoie, S. F. (2015a). HNRNPA2B1 Is a Mediator of m6A-dependent Nuclear RNA Processing Events. *Cell* 162, 1299–1308. doi:10.1016/j.cell.2015.08.011

Alarcón, C. R., Lee, H., Goodarzi, H., Halberg, N., and Tavazoie, S. F. (2015b). N6-methyladenosine marks Primary microRNAs for Processing. *Nature* 519, 482–485. doi:10.1038/nature14281

Ban, Y., Tan, P., Cai, J., Li, J., Hu, M., Zhou, Y., et al. (2020). LNCAROD Is Stabilized by m6A Methylation and Promotes Cancer Progression via Forming a Ternary Complex with HSPA1A and YBX1 in Head and Neck Squamous Cell Carcinoma. *Mol. Oncol.* 14, 1282–1296. doi:10.1002/1878-0261.12676

Barros-Silva, D., Lobo, J., Guimarães-Teixeira, C., Carneiro, I., Oliveira, J., Martens-Uzunova, E. S., et al. (2020). VIRMA-dependent N6-Methyladenosine Modifications Regulate the Expression of Long Non-coding RNAs CCAT1 and CCAT2 in Prostate Cancer. *Cancers* 12, 771. doi:10.3390/cancers12040771

Cai, X., Wang, X., Cao, C., Gao, Y., Zhang, S., Yang, Z., et al. (2018). HBXIP-elevated Methyltransferase METTL3 Promotes the Progression of Breast Cancer via Inhibiting Tumor Suppressor Let-7g. *Cancer Lett.* 415, 11–19. doi:10.1016/j.canlet.2017.11.018

Castosa, R., Martinez-Iglesias, O., Roca-Lema, D., Casas-Pais, A., Díaz-Díaz, A., Iglesias, P., et al. (2018). Hakai Overexpression Effectively Induces Tumour Progression and Metastasis *In Vivo*. *Sci. Rep.* 8, 3466. doi:10.1038/s41598-018-21808-w

Chang, G., Shi, L., Ye, Y., Shi, H., Zeng, L., Tiwary, S., et al. (2020). YTHDF3 Induces the Translation of m6A-Enriched Gene Transcripts to Promote Breast Cancer Brain Metastasis. *Cancer Cell* 38, 857–871. e7. doi:10.1016/j.ccell.2020.10.004

Chen, R.-X., Chen, X., Xia, L.-P., Zhang, J.-X., Pan, Z.-Z., Ma, X.-D., et al. (2019a). N6-methyladenosine Modification of circNSUN2 Facilitates Cytoplasmic export and Stabilizes HMGA2 to Promote Colorectal Liver Metastasis. *Nat. Commun.* 10, 4695. doi:10.1038/s41467-019-12651-2

Chen, S., Zhou, L., and Wang, Y. (2020a). ALKBH5-mediated m6A Demethylation of lncRNA PVT1 Plays an Oncogenic Role in Osteosarcoma. *Cancer Cell Int* 20, 34. doi:10.1186/s12935-020-1105-6

Chen, T., Hao, Y.-J., Zhang, Y., Li, M.-M., Wang, M., Han, W., et al. (2015). m6A RNA Methylation Is Regulated by MicroRNAs and Promotes Reprogramming to Pluripotency. *Cell Stem Cell* 16, 289–301. doi:10.1016/j.stem.2015.01.016

Chen, X., Xu, M., Xu, X., Zeng, K., Liu, X., Sun, L., et al. (2020b). METTL14 Suppresses CRC Progression via Regulating N6-methyladenosine-dependent Primary miR-375 Processing. *Mol. Ther.* 28, 599–612. doi:10.1016/j.ymthe.2019.11.016

Chen, Y., Lin, Y., Shu, Y., He, J., and Gao, W. (2020c). Interaction between N6-Methyladenosine (m6A) Modification and Noncoding RNAs in Cancer. *Mol. Cancer* 19, 94. doi:10.1186/s12943-020-01207-4

Chen, Y., Peng, C., Chen, J., Chen, D., Yang, B., He, B., et al. (2019b). WTAP Facilitates Progression of Hepatocellular Carcinoma via m6A-HuR-dependent Epigenetic Silencing of ETS1. *Mol. Cancer* 18, 127. doi:10.1186/s12943-019-1053-8

Chen, Z., Chen, X., Lei, T., Gu, Y., Gu, J., Huang, J., et al. (2020d). Integrative Analysis of NSCLC Identifies LINC01234 as an Oncogenic lncRNA that Interacts with HNRNPA2B1 and Regulates miR-106b Biogenesis. *Mol. Ther.* 28, 1479–1493. doi:10.1016/j.ymthe.2020.03.010

Cui, X., Wang, Z., Li, J., Zhu, J., Ren, Z., Zhang, D., et al. (2020). Cross Talk between RNA N6-methyladenosine Methyltransferase-like 3 and miR-186 Regulates Hepatoblastoma Progression through Wnt/β-catenin Signalling Pathway. *Cell Prolif* 53, e12768. doi:10.1111/cpr.12768

Du, C., Lv, C., Feng, Y., and Yu, S. (2020a). Activation of the KDM5A/miRNA-495/YTHDF2/m6A-MOB3B axis Facilitates Prostate Cancer Progression. *J. Exp. Clin. Cancer Res.* 39, 223. doi:10.1186/s13046-020-01735-3

Du, J., Hou, K., Mi, S., Ji, H., Ma, S., Ba, Y., et al. (2020b). Malignant Evaluation and Clinical Prognostic Values of m6A RNA Methylation Regulators in Glioblastoma. *Front. Oncol.* 10, 208. doi:10.3389/fonc.2020.00208

Du, M., Zhang, Y., Mao, Y., Mou, J., Zhao, J., Xue, Q., et al. (2017). MiR-33a Suppresses Proliferation of NSCLC Cells via Targeting METTL3 mRNA. *Biochem. Biophysical Res. Commun.* 482, 582–589. doi:10.1016/j.bbrc.2016.11.077

Erson-Bensan, A. E., and Begik, O. (2017). m6A Modification and Implications for microRNAs. *Mirna* 6, 97–101. doi:10.2174/2211536606666170511102219

Fazi, F., and Fatica, A. (2019). Interplay Between N6-Methyladenosine (m6A) and Non-coding RNAs in Cell Development and Cancer. *Front. Cell Dev. Biol.* 7, 116. doi:10.3389/fcell.2019.00116

Gao, Y. X., Yang, T. W., Yin, J. M., Yang, P. X., Kou, B. X., Chai, M. Y., et al. (2020). Progress and Prospects of Biomarkers In Primary Liver Cancer (Review). *Int. J. Oncol.* 57, 54–66. doi:10.3892/ijo.2020.5035

Gu, C., Wang, Z., Zhou, N., Li, G., Kou, Y., Luo, Y., et al. (2019). Mettl14 Inhibits Bladder TIC Self-Renewal and Bladder Tumorigenesis through N6-Methyladenosine of Notch1. *Mol. Cancer* 18, 168. doi:10.1186/s12943-019-1084-1

Gu, S., Sun, D., Dai, H., and Zhang, Z. (2018). N6-methyladenosine Mediates the Cellular Proliferation and Apoptosis via microRNAs in Arsenite-Transformed Cells. *Toxicol. Lett.* 292, 1–11. doi:10.1016/j.toxlet.2018.04.018

Gu, Y., Niu, S., Wang, Y., Duan, L., Pan, Y., Tong, Z., et al. (2021). DMDRMR-mediated Regulation of m6A-Modified CDK4 by m6A Reader IGF2BP3 Drives ccRCC Progression. *Cancer Res.* 81, 923–934. doi:10.1158/0008-5472.CAN-20-1619

Guan, K., Liu, X., Li, J., Ding, Y., Li, J., Cui, G., et al. (2020). Expression Status And Prognostic Value of M6A-Associated Genes in Gastric Cancer. *J. Cancer* 11, 3027–3040. doi:10.7150/jca.40866

Guo, T., Liu, D. F., Peng, S. H., and Xu, A. M. (2020). ALKBH5 Promotes colon Cancer Progression by Decreasing Methylation of the lncRNA NEAT1. *Am. J. Transl Res.* 12, 4542–4549.

Han, J., Wang, J.-z., Yang, X., Yu, H., Zhou, R., Lu, H.-C., et al. (2019a). METTL3 Promote Tumor Proliferation of Bladder Cancer by Accelerating Pri-miR221/222 Maturation in m6A-dependent Manner. *Mol. Cancer* 18, 110. doi:10.1186/s12943-019-1036-9

Han, X., Wang, N., Li, J., Wang, Y., Wang, R., and Chang, J. (2019b). Identification of Nafamostat Mesilate as an Inhibitor of the Fat Mass and Obesity-Associated Protein (FTO) Demethylase Activity. *Chemico-Biological Interactions* 297, 80–84. doi:10.1016/j.cbi.2018.10.023

Hao, J., Li, C., Lin, C., Hao, Y., Yu, X., Xia, Y., et al. (2020). Targeted point Mutations of the m6A Modification in miR675 Using RNA-Guided Base Editing Induce Cell Apoptosis. *Biosci. Rep.* 40. doi:10.1042/bsr20192933

He, H., Wu, W., Sun, Z., and Chai, L. (2019). MiR-4429 Prevented Gastric Cancer Progression through Targeting METTL3 to Inhibit m6A-Caused Stabilization of SEC62. *Biochem. Biophysical Res. Commun.* 517, 581–587. doi:10.1016/j.bbrc.2019.07.058

He, R.-Z., Jiang, J., and Luo, D.-X. (2020). The Functions of N6-Methyladenosine Modification in lncRNAs. *Genes Dis.* 7, 598–605. doi:10.1016/j.gendis.2020.03.005

He, X., and Shu, Y. (2019). RNA N6-Methyladenosine Modification Participates in miR-660/E2F3 axis-mediated Inhibition of Cell Proliferation in Gastric Cancer. *Pathol. - Res. Pract.* 215, 152393. doi:10.1016/j.prp.2019.03.021

He, Y., Hu, H., Wang, Y., Yuan, H., Lu, Z., Wu, P., et al. (2018). ALKBH5 Inhibits Pancreatic Cancer Motility by Decreasing Long Non-coding RNA KCNK15-AS1 Methylation. *Cell Physiol Biochem* 48, 838–846. doi:10.1159/000491915

Hou, P., Meng, S., Li, M., Lin, T., Chu, S., Li, Z., et al. (2021). LINC00460/DHX9/IGF2BP2 Complex Promotes Colorectal Cancer Proliferation and Metastasis by Mediating HMGA1 mRNA Stability Depending on m6A Modification. *J. Exp. Clin. Cancer Res.* 40, 52. doi:10.1186/s13046-021-01857-2

Hu, X., Peng, W.-X., Zhou, H., Jiang, J., Zhou, X., Huang, D., et al. (2020). IGF2BP2 Regulates DANCR by Serving as an N6-Methyladenosine Reader. *Cell Death Differ* 27, 1782–1794. doi:10.1038/s41418-019-0461-z

Huang, H., Wang, Y., Kandpal, M., Zhao, G., Cardenas, H., Ji, Y., et al. (2020a). FTO-dependent N6-Methyladenosine Modifications Inhibit Ovarian Cancer Stem Cell Self-Renewal by Blocking cAMP Signaling. *Cancer Res.* 80, 3200–3214. doi:10.1158/0008-5472.Can-19-4044

Huang, H., Weng, H., and Chen, J. (2020b). m6A Modification in Coding and Non-coding RNAs: Roles and Therapeutic Implications in Cancer. *Cancer Cell* 37, 270–288. doi:10.1016/j.ccell.2020.02.004

Huang, Y., Su, R., Sheng, Y., Dong, L., Dong, Z., Xu, H., et al. (2019). Small-Molecule Targeting of Oncogenic FTO Demethylase in Acute Myeloid Leukemia. *Cancer Cell* 35, 677–691. e10. doi:10.1016/j.ccell.2019.03.006

Huang, Y., Yan, J., Li, Q., Li, J., Gong, S., Zhou, H., et al. (2015). Meclofenamic Acid Selectively Inhibits FTO Demethylation of m6A over ALKBH5. *Nucleic Acids Res.* 43, 373–384. doi:10.1093/nar/gku1276

Inamura, K. (2018). Update on Immunohistochemistry for the Diagnosis of Lung Cancer. *Cancers* 10, 72. doi:10.3390/cancers10030072

Jin, D., Guo, J., Wu, Y., Du, J., Yang, L., Wang, X., et al. (2019). m6A mRNA Methylation Initiated by METTL3 Directly Promotes YAP Translation and Increases YAP Activity by Regulating the MALAT1-miR-1914-3p-YAP axis to Induce NSCLC Drug Resistance and Metastasis. *J. Hematol. Oncol.* 12, 135. doi:10.1186/s13045-019-0830-6

Jin, D., Guo, J., Wu, Y., Yang, L., Wang, X., Du, J., et al. (2020). m6A Demethylase ALKBH5 Inhibits Tumor Growth and Metastasis by Reducing YTHDFs-Mediated YAP Expression and Inhibiting miR-107/LATS2-Mediated YAP Activity in NSCLC. *Mol. Cancer* 19, 40. doi:10.1186/s12943-020-01161-1

Jin, Y., Wang, Z., He, D., Zhu, Y., Hu, X., Gong, L., et al. (2021). Analysis of m6A-Related Signatures in the Tumor Immune Microenvironment and Identification of Clinical Prognostic Regulators in Adrenocortical Carcinoma. *Front. Immunol.* 12, 637933. doi:10.3389/fimmu.2021.637933

Kandimalla, R., Gao, F., Li, Y., Huang, H., Ke, J., Deng, X., et al. (2019). RNAMethyPro: a Biologically Conserved Signature of N6-Methyladenosine Regulators for Predicting Survival at Pan-Cancer Level. *Npj Precis. Onc.* 3, 13. doi:10.1038/s41698-019-0085-2

Karimi, P., Islami, F., Anandasabapathy, S., Freedman, N. D., and Kamangar, F. (2014). Gastric Cancer: Descriptive Epidemiology, Risk Factors, Screening, and Prevention. *Cancer Epidemiol. Biomarkers Prev.* 23, 700–713. doi:10.1158/1055-9965.EPI-13-1057

Kleemann, M., Schneider, H., Unger, K., Sander, P., Schneider, E. M., Fischer-Posovszky, P., et al. (2018). MiR-744-5p Inducing Cell Death by Directly Targeting HNRNPC and NFIX in Ovarian Cancer Cells. *Sci. Rep.* 8, 9020. doi:10.1038/s41598-018-27438-6

Klinge, C. M., Piell, K. M., Tooley, C. S., and Rouchka, E. C. (2019). HNRNPA2/B1 Is Upregulated in Endocrine-Resistant LCC9 Breast Cancer Cells and Alters the miRNA Transcriptome when Overexpressed in MCF-7 Cells. *Sci. Rep.* 9, 9430. doi:10.1038/s41598-019-45636-8

Lan, T., Li, H., Zhang, D., Xu, L., Liu, H., Hao, X., et al. (2019). KIAA1429 Contributes to Liver Cancer Progression through N6-methyladenosine-dependent post-transcriptional Modification of GATA3. *Mol. Cancer* 18, 186. doi:10.1186/s12943-019-1106-z

Li, J., Zhu, L., Shi, Y., Liu, J., Lin, L., and Chen, X. (2019b). m6A Demethylase FTO Promotes Hepatocellular Carcinoma Tumorigenesis via Mediating PKM2 Demethylation. *Am. J. Transl Res.* 11, 6084–6092.

Li, J., Han, Y., Zhang, H., Qian, Z., Jia, W., Gao, Y., et al. (2019a). The m6A Demethylase FTO Promotes the Growth of Lung Cancer Cells by Regulating the m6A Level of USP7 mRNA. *Biochem. Biophysical Res. Commun.* 512, 479–485. doi:10.1016/j.bbrc.2019.03.093

Li, J., Wu, L., Pei, M., and Zhang, Y. (2020a). YTHDF2, a Protein Repressed by miR-145, Regulates Proliferation, Apoptosis, and Migration in Ovarian Cancer Cells. *J. Ovarian Res.* 13, 111. doi:10.1186/s13048-020-00717-5

Li, K., Luo, H., Luo, H., and Zhu, X. (2020b). Clinical and Prognostic Pan-Cancer Analysis of m6A RNA Methylation Regulators in Four Types of Endocrine System Tumors. *Aging* 12, 23931–23944. doi:10.18632/aging.104064

Li, Q., Ren, C.-C., Chen, Y.-N., Yang, L., Zhang, F., Wang, B.-J., et al. (2021). A Risk Score Model Incorporating Three m6A RNA Methylation Regulators and a Related Network of miRNAs-m6A Regulators-m6A Target Genes to Predict the Prognosis of Patients with Ovarian Cancer. *Front. Cell Dev. Biol.* 9, 703969. doi:10.3389/fcell.2021.703969

Li, Q., Wang, H., Peng, H., Huang, Q., Huyan, T., Huang, Q., et al. (2019c). MicroRNAs: Key Players in Bladder Cancer. *Mol. Diagn. Ther.* 23, 579–601. doi:10.1007/s40291-019-00410-4

Liu, G.-M., Zeng, H.-D., Zhang, C.-Y., and Xu, J.-W. (2021). Identification of METTL3 as an Adverse Prognostic Biomarker in Hepatocellular Carcinoma. *Dig. Dis. Sci.* 66, 1110–1126. doi:10.1007/s10620-020-06260-z

Liu, H., Xu, Y., Yao, B., Sui, T., Lai, L., and Li, Z. (2020a). A Novel N6-Methyladenosine (m6A)-dependent Fate Decision for the lncRNA THOR. *Cell Death Dis* 11, 613. doi:10.1038/s41419-020-02833-y

Liu, J., Sun, G., Pan, S., Qin, M., Ouyang, R., Li, Z., et al. (2020b). The Cancer Genome Atlas (TCGA) Based m6A Methylation-Related Genes Predict Prognosis in Hepatocellular Carcinoma. *Bioengineered* 11, 759–768. doi:10.1080/21655979.2020.1787764

Liu, N., Dai, Q., Zheng, G., He, C., Parisien, M., and Pan, T. (2015). N6-methyladenosine-dependent RNA Structural Switches Regulate RNA-Protein Interactions. *Nature* 518, 560–564. doi:10.1038/nature14234

Ma, J. Z., Yang, F., Zhou, C. C., Liu, F., Yuan, J. H., Wang, F., et al. (2017). METTL14 Suppresses the Metastatic Potential of Hepatocellular Carcinoma by Modulating N 6 -methyladenosine-dependent Primary MicroRNA Processing. *Hepatology* 65, 529–543. doi:10.1002/hep.28885

Ma, Y.-S., Shi, B.-W., Guo, J.-H., Liu, J.-B., Yang, X.-L., Xin, R., et al. (2021). microRNA-320b Suppresses HNF4G and IGF2BP2 Expression to Inhibit Angiogenesis and Tumor Growth of Lung Cancer. *Carcinogenesis* 42, 762–771. doi:10.1093/carcin/bgab023

Malacrida, A., Rivara, M., Di Domizio, A., Cislaghi, G., Miloso, M., Zuliani, V., et al. (2020). 3D Proteome-wide Scale Screening and Activity Evaluation of a New ALKBH5 Inhibitor in U87 Glioblastoma Cell Line. *Bioorg. Med. Chem.* 28, 115300. doi:10.1016/j.bmc.2019.115300

Müller, M. F., Ibrahim, A. E. K., and Arends, M. J. (2016). Molecular Pathological Classification of Colorectal Cancer. *Virchows Arch.* 469, 125–134. doi:10.1007/s00428-016-1956-3

Nagini, S. (2017). Breast Cancer: Current Molecular Therapeutic Targets and New Players. *Acamc* 17, 152–163. doi:10.2174/1871520616666160502122724

Ni, W., Yao, S., Zhou, Y., Liu, Y., Huang, P., Zhou, A., et al. (2019). Long Noncoding RNA GAS5 Inhibits Progression of Colorectal Cancer by Interacting with and Triggering YAP Phosphorylation and Degradation and Is Negatively Regulated by the m6A Reader YTHDF3. *Mol. Cancer* 18, 143. doi:10.1186/s12943-019-1079-y

Panneerdoss, S., Eedunuri, V. K., Yadav, P., Timilsina, S., Rajamanickam, S., Viswanadhapalli, S., et al. (2018). Cross-talk Among Writers, Readers, and Erasers of m6A Regulates Cancer Growth and Progression. *Sci. Adv.* 4, eaar8263. doi:10.1126/sciadv.aar8263

Paris, J., Morgan, M., Campos, J., Spencer, G. J., Shmakova, A., Ivanova, I., et al. (2019). Targeting the RNA m6A Reader YTHDF2 Selectively Compromises Cancer Stem Cells in Acute Myeloid Leukemia. *Cell Stem Cell* 25, 137–148. e6. doi:10.1016/j.stem.2019.03.021

Park, Y. M., Hwang, S. J., Masuda, K., Choi, K.-M., Jeong, M.-R., Nam, D.-H., et al. (2012). Heterogeneous Nuclear Ribonucleoprotein C1/C2 Controls the Metastatic Potential of Glioblastoma by Regulating PDCD4. *Mol. Cell Biol* 32, 4237–4244. doi:10.1128/mcb.00443-12

Peng, L., Yuan, X., Jiang, B., Tang, Z., and Li, G.-C. (2016). LncRNAs: Key Players and Novel Insights into Cervical Cancer. *Tumor Biol.* 37, 2779–2788. doi:10.1007/s13277-015-4663-9

Peng, W., Li, J., Chen, R., Gu, Q., Yang, P., Qian, W., et al. (2019). Upregulated METTL3 Promotes Metastasis of Colorectal Cancer via miR-1246/SPRED2/MAPK Signaling Pathway. *J. Exp. Clin. Cancer Res.* 38, 393. doi:10.1186/s13046-019-1408-4

Ribatti, D., Tamma, R., and Annese, T. (2020). Epithelial-Mesenchymal Transition in Cancer: A Historical Overview. *Translational Oncol.* 13, 100773. doi:10.1016/j.tranon.2020.100773

Shan, C., Zhang, Y., Hao, X., Gao, J., Chen, X., and Wang, K. (2019). Biogenesis, Functions and Clinical Significance of circRNAs in Gastric Cancer. *Mol. Cancer* 18, 136. doi:10.1186/s12943-019-1069-0

Shin, V. Y., and Chu, K. M. (2014). MiRNA as Potential Biomarkers and Therapeutic Targets for Gastric Cancer. *Wjg* 20, 10432–10439. doi:10.3748/wjg.v20.i30.10432

Singh, B., Kinne, H. E., Milligan, R. D., Washburn, L. J., Olsen, M., and Lucci, A. (2016). Important Role of FTO in the Survival of Rare Panresistant Triple-Negative Inflammatory Breast Cancer Cells Facing a Severe Metabolic Challenge. *PLoS One* 11, e0159072. doi:10.1371/journal.pone.0159072

Song, Z., Jia, G., Ma, P., and Cang, S. (2021). Exosomal miR-4443 Promotes Cisplatin Resistance in Non-small Cell Lung Carcinoma by Regulating FSP1 m6A Modification-Mediated Ferroptosis. *Life Sci.* 276, 119399. doi:10.1016/j.lfs.2021.119399

Su, R., Dong, L., Li, C., Nachtergaele, S., Wunderlich, M., Qing, Y., et al. (2018). R-2HG Exhibits Anti-tumor Activity by Targeting FTO/m6A/MYC/CEBPA Signaling. *Cell* 172, 90–105. doi:10.1016/j.cell.2017.11.031

Su, R., Dong, L., Li, Y., Gao, M., Han, L., Wunderlich, M., et al. (2020). Targeting FTO Suppresses Cancer Stem Cell Maintenance and Immune Evasion. *Cancer Cell* 38, 79–96. e11. doi:10.1016/j.ccell.2020.04.017

Sun, T., Wu, R., and Ming, L. (2019). The Role of m6A RNA Methylation in Cancer. *Biomed. Pharmacother.* 112, 108613. doi:10.1016/j.biopha.2019.108613

Sun, T., Wu, Z., Wang, X., Wang, Y., Hu, X., Qin, W., et al. (2020a). LNC942 Promoting METTL14-Mediated m6A Methylation in Breast Cancer Cell Proliferation and Progression. *Oncogene* 39, 5358–5372. doi:10.1038/s41388-020-1338-9

Sun, W., Yang, Y., Xu, C., Xie, Y., and Guo, J. (2016). Roles of Long Noncoding RNAs in Gastric Cancer and Their Clinical Applications. *J. Cancer Res. Clin. Oncol.* 142, 2231–2237. doi:10.1007/s00432-016-2183-7

Sun, Y., Li, S., Yu, W., Zhao, Z., Gao, J., Chen, C., et al. (2020b). N6-methyladenosine-dependent Pri-miR-17-92 Maturation Suppresses PTEN/TMEM127 and Promotes Sensitivity to Everolimus in Gastric Cancer. *Cell Death Dis* 11, 836. doi:10.1038/s41419-020-03049-w

Tang, B., Yang, Y., Kang, M., Wang, Y., Wang, Y., Bi, Y., et al. (2020). m6A Demethylase ALKBH5 Inhibits Pancreatic Cancer Tumorigenesis by Decreasing WIF-1 RNA Methylation and Mediating Wnt Signaling. *Mol. Cancer* 19, 3. doi:10.1186/s12943-019-1128-6

Tao, L., Mu, X., Chen, H., Jin, D., Zhang, R., Zhao, Y., et al. (2021). FTO Modifies the m6A Level of MALAT and Promotes Bladder Cancer Progression. *Clin. Translational Med.* 11, e310. doi:10.1002/ctm2.310

Tao, Z., Zhao, Y., and Chen, X. (2020). Role of Methyltransferase-like Enzyme 3 and Methyltransferase-like Enzyme 14 in Urological Cancers. *PeerJ* 8, e9589. doi:10.7717/peerj.9589

Tu, Z., Wu, L., Wang, P., Hu, Q., Tao, C., Li, K., et al. (2020). N6-Methylandenosine-Related lncRNAs Are Potential Biomarkers for Predicting the Overall Survival of Lower-Grade Glioma Patients. *Front. Cell Dev. Biol.* 8, 642. doi:10.3389/fcell.2020.00642

Vishnoi, A., and Rani, S. (2017). MiRNA Biogenesis and Regulation of Diseases: An Overview. *Methods Mol. Biol.* 1509, 1–10. doi:10.1007/978-1-4939-6524-3_1

Wang, H., Deng, Q., Lv, Z., Ling, Y., Hou, X., Chen, Z., et al. (2019a). N6-methyladenosine Induced miR-143-3p Promotes the Brain Metastasis of Lung Cancer via Regulation of VASH1. *Mol. Cancer* 18, 181. doi:10.1186/s12943-019-1108-x

Wang, H., Liang, L., Dong, Q., Huan, L., He, J., Li, B., et al. (2018). Long Noncoding RNA miR503HG, a Prognostic Indicator, Inhibits Tumor Metastasis by Regulating the HNRNPA2B1/NF-κB Pathway in Hepatocellular Carcinoma. *Theranostics* 8, 2814–2829. doi:10.7150/thno.23012

Wang, J., Ding, W., Xu, Y., Tao, E., Mo, M., Xu, W., et al. (2020a). Long Non-coding RNA RHPN1-AS1 Promotes Tumorigenesis and Metastasis of Ovarian Cancer by Acting as a ceRNA against miR-596 and Upregulating LETM1. *Aging* 12, 4558–4572. doi:10.18632/aging.102911

Wang, L.-c., Chen, S.-h., Shen, X.-l., Li, D.-c., Liu, H.-y., Ji, Y.-l., et al. (2020b). M6A RNA Methylation Regulator HNRNPC Contributes to Tumorigenesis and Predicts Prognosis in Glioblastoma Multiforme. *Front. Oncol.* 10, 536875. doi:10.3389/fonc.2020.536875

Wang, W., Li, J., Lin, F., Guo, J., and Zhao, J. (2021). Identification of N6-Methyladenosine-Related lncRNAs for Patients with Primary Glioblastoma. *Neurosurg. Rev.* 44, 463–470. doi:10.1007/s10143-020-01238-x

Wang, X., Xie, H., Ying, Y., Chen, D., and Li, J. (2020c). Roles of N 6 -methyladenosine (M 6 A) RNA Modifications in Urological Cancers. *J. Cell Mol Med* 24, 10302–10310. doi:10.1111/jcmm.15750

Wang, Y., Lu, J.-H., Wu, Q.-N., Jin, Y., Wang, D.-S., Chen, Y.-X., et al. (2019b). LncRNA LINRIS Stabilizes IGF2BP2 and Promotes the Aerobic Glycolysis in Colorectal Cancer. *Mol. Cancer* 18, 174. doi:10.1186/s12943-019-1105-0

Wanna-Udom, S., Terashima, M., Lyu, H., Ishimura, A., Takino, T., Sakari, M., et al. (2020). The m6A Methyltransferase METTL3 Contributes to Transforming Growth Factor-Beta-Induced Epithelial-Mesenchymal Transition of Lung Cancer Cells through the Regulation of JUNB. *Biochem. Biophysical Res. Commun.* 524, 150–155. doi:10.1016/j.bbrc.2020.01.042

Wei, W., Huo, B., and Shi, X. (2019). miR-600 Inhibits Lung Cancer via Downregulating the Expression of METTL3. *Cmar* Vol. 11, 1177–1187. doi:10.2147/cmar.S181058

Wong, C.-M., Tsang, F. H.-C., and Ng, I. O.-L. (2018). Non-coding RNAs in Hepatocellular Carcinoma: Molecular Functions and Pathological Implications. *Nat. Rev. Gastroenterol. Hepatol.* 15, 137–151. doi:10.1038/nrgastro.2017.169

Wu, H., Li, F., and Zhu, R. (2021). miR-338-5p Inhibits Cell Growth and Migration via Inhibition of the METTL3/m6A/c-Myc Pathway in Lung Cancer. *Acta Biochim. Biophys. Sin (Shanghai)* 53, 304–316. doi:10.1093/abbs/gmaa170

Wu, S., Zhang, L., Deng, J., Guo, B., Li, F., Wang, Y., et al. (2020). A Novel Micropeptide Encoded by Y-Linked LINC00278 Links Cigarette Smoking and AR Signaling in Male Esophageal Squamous Cell Carcinoma. *Cancer Res.* 80, 2790–2803. doi:10.1158/0008-5472.Can-19-3440

Wu, Y., Yang, X., Chen, Z., Tian, L., Jiang, G., Chen, F., et al. (2019). m^6A-induced lncRNA RP11 Triggers the Dissemination of Colorectal Cancer Cells via Upregulation of Zeb1. *Mol. Cancer* 18, 87. doi:10.1186/s12943-019-1014-2

Xiao, L., Li, X., Mu, Z., Zhou, J., Zhou, P., Xie, C., et al. (2020). FTO Inhibition Enhances the Antitumor Effect of Temozolomide by Targeting MYC-miR-155/23a Cluster-MXI1 Feedback Circuit in Glioma. *Cancer Res.* 80, 3945–3958. doi:10.1158/0008-5472.CAN-20-0132

Xie, H., Li, J., Ying, Y., Yan, H., Jin, K., Ma, X., et al. (2020). $METTL_3$/$YTHDF_2$ M^6A axis Promotes Tumorigenesis by Degrading $SETD_7$ and KLF_4 mRNAs in Bladder Cancer. *J. Cell Mol Med* 24, 4092–4104. doi:10.1111/jcmm.15063

Xu, D., Shao, W., Jiang, Y., Wang, X., Liu, Y., and Liu, X. (2017). FTO Expression Is Associated with the Occurrence of Gastric Cancer and Prognosis. *Oncol. Rep.* 38, 2285–2292. doi:10.3892/or.2017.5904

Xu, J., Wan, Z., Tang, M., Lin, Z., Jiang, S., Ji, L., et al. (2020a). N6-methyladenosine-modified CircRNA-SORE Sustains Sorafenib Resistance in Hepatocellular Carcinoma by Regulating β-catenin Signaling. *Mol. Cancer* 19, 163. doi:10.1186/s12943-020-01281-8

Xu, Y., Ye, S., Zhang, N., Zheng, S., Liu, H., Zhou, K., et al. (2020b). The FTO/miR-181b-3p/ARL5B Signaling Pathway Regulates Cell Migration and Invasion in Breast Cancer. *Cancer Commun.* 40, 484–500. doi:10.1002/cac2.12075

Yan, J., Huang, X., Zhang, X., Chen, Z., Ye, C., Xiang, W., et al. (2020). LncRNA LINC00470 Promotes the Degradation of PTEN mRNA to Facilitate Malignant Behavior in Gastric Cancer Cells. *Biochem. Biophysical Res. Commun.* 521, 887–893. doi:10.1016/j.bbrc.2019.11.016

Yang, L., Ma, Y., Han, W., Li, W., Cui, L., Zhao, X., et al. (2015). Proteinase-activated Receptor 2 Promotes Cancer Cell Migration through RNA Methylation-Mediated Repression of miR-125b. *J. Biol. Chem.* 290, 26627–26637. doi:10.1074/jbc.M115.667717

Yang, P., Wang, Q., Liu, A., Zhu, J., and Feng, J. (2020a). ALKBH5 Holds Prognostic Values and Inhibits the Metastasis of Colon Cancer. *Pathol. Oncol. Res.* 26, 1615–1623. doi:10.1007/s12253-019-00737-7

Yang, S., Wei, J., Cui, Y.-H., Park, G., Shah, P., Deng, Y., et al. (2019). m6A mRNA Demethylase FTO Regulates Melanoma Tumorigenicity and Response to Anti-PD-1 Blockade. *Nat. Commun.* 10, 2782. doi:10.1038/s41467-019-10669-0

Yang, X., Liu, M., Li, M., Zhang, S., Hiju, H., Sun, J., et al. (2020b). Epigenetic Modulations of Noncoding RNA: a Novel Dimension of Cancer Biology. *Mol. Cancer* 19, 64. doi:10.1186/s12943-020-01159-9

Yang, X., Zhang, S., He, C., Xue, P., Zhang, L., He, Z., et al. (2020c). METTL14 Suppresses Proliferation and Metastasis of Colorectal Cancer by Down-Regulating Oncogenic Long Non-coding RNA XIST. *Mol. Cancer* 19, 46. doi:10.1186/s12943-020-1146-4

Yang, Z., Li, J., Feng, G., Gao, S., Wang, Y., Zhang, S., et al. (2017). MicroRNA-145 Modulates N6-Methyladenosine Levels by Targeting the 3′-Untranslated mRNA Region of the N6-Methyladenosine Binding YTH Domain Family 2 Protein. *J. Biol. Chem.* 292, 3614–3623. doi:10.1074/jbc.M116.749689

Ye, M., Dong, S., Hou, H., Zhang, T., and Shen, M. (2021). Oncogenic Role of Long Noncoding RNAMALAT1 in Thyroid Cancer Progression through Regulation of the miR-204/IGF2BP2/m6A-MYC Signaling. *Mol. Ther. - Nucleic Acids* 23, 1–12. doi:10.1016/j.omtn.2020.09.023

Yi, D., Wang, R., Shi, X., Xu, L., Yilihamu, Y. e., and Sang, J. (2020). METTL14 Promotes the Migration and Invasion of Breast Cancer Cells by Modulating N6-methyladenosine and hsa-miR-146a-5p E-xpression. *Oncol. Rep.* 43, 1375–1386. doi:10.3892/or.2020.7515

Ying, P., Li, Y., Yang, N., Wang, X., Wang, H., He, H., et al. (2021). Identification of Genetic Variants in m6A Modification Genes Associated with Pancreatic

Cancer Risk in the Chinese Population. *Arch. Toxicol.* 95, 1117–1128. doi:10.1007/s00204-021-02978-5

Yousef, M., and Tsiani, E. (2017). Metformin in Lung Cancer: Review of *in Vitro* and *in Vivo* Animal Studies, *Cancers* 9, 45. doi:10.3390/cancers9050045

Yu, J., Mao, W., Sun, S., Hu, Q., Wang, C., Xu, Z., et al. (2021). Identification of an m6A-Related lncRNA Signature for Predicting the Prognosis in Patients with Kidney Renal Clear Cell Carcinoma. *Front. Oncol.* 11, 663263. doi:10.3389/fonc.2021.663263

Yuan, S., Tang, H., Xing, J., Fan, X., Cai, X., Li, Q., et al. (2014). Methylation by NSun2 Represses the Levels and Function of microRNA 125b. *Mol. Cell Biol.* 34, 3630–3641. doi:10.1128/MCB.00243-14

Yuan, Y., Du, Y., Wang, L., and Liu, X. (2020). The M6A Methyltransferase METTL3 Promotes the Development and Progression of Prostate Carcinoma via Mediating MYC Methylation. *J. Cancer* 11, 3588–3595. doi:10.7150/jca.42338

Zhang, B., Wu, Q., Li, B., Wang, D., Wang, L., and Zhou, Y. L. (2020a). m6A Regulator-Mediated Methylation Modification Patterns and Tumor Microenvironment Infiltration Characterization in Gastric Cancer. *Mol. Cancer* 19, 53. doi:10.1186/s12943-020-01170-0

Zhang, C., Huang, S., Zhuang, H., Ruan, S., Zhou, Z., Huang, K., et al. (2020b). YTHDF2 Promotes the Liver Cancer Stem Cell Phenotype and Cancer Metastasis by Regulating OCT4 Expression via m6A RNA Methylation. *Oncogene* 39, 4507–4518. doi:10.1038/s41388-020-1303-7

Zhang, J., Bai, R., Li, M., Ye, H., Wu, C., Wang, C., et al. (2019a). Excessive miR-25-3p Maturation via N6-Methyladenosine Stimulated by Cigarette Smoke Promotes Pancreatic Cancer Progression. *Nat. Commun.* 10, 1858. doi:10.1038/s41467-019-09712-x

Zhang, J., Guo, S., Piao, H.-y., Wang, Y., Wu, Y., Meng, X.-y., et al. (2019b). ALKBH5 Promotes Invasion and Metastasis of Gastric Cancer by Decreasing Methylation of the lncRNA NEAT1. *J. Physiol. Biochem.* 75, 379–389. doi:10.1007/s13105-019-00690-8

Zhang, J., Hu, K., Yang, Y.-q., Wang, Y., Zheng, Y.-f., Jin, Y., et al. (2020c). LIN28B-AS1-IGF2BP1 Binding Promotes Hepatocellular Carcinoma Cell Progression. *Cell Death Dis* 11, 741. doi:10.1038/s41419-020-02967-z

Zhang, L., Hou, C., Chen, C., Guo, Y., Yuan, W., Yin, D., et al. (2020d). The Role of N6-Methyladenosine (m6A) Modification in the Regulation of circRNAs. *Mol. Cancer* 19, 105. doi:10.1186/s12943-020-01224-3

Zhang, S., Zhao, B. S., Zhou, A., Lin, K., Zheng, S., Lu, Z., et al. (2017). m 6 A Demethylase ALKBH5 Maintains Tumorigenicity of Glioblastoma Stem-like Cells by Sustaining FOXM1 Expression and Cell Proliferation Program. *Cancer Cell* 31, 591–606. e6. doi:10.1016/j.ccell.2017.02.013

Zhang, X., Xu, Y., Qian, Z., Zheng, W., Wu, Q., Chen, Y., et al. (2018). circRNA_104075 Stimulates YAP-dependent Tumorigenesis through the Regulation of HNF4a and May Serve as a Diagnostic Marker in Hepatocellular Carcinoma. *Cell Death Dis* 9, 1091. doi:10.1038/s41419-018-1132-6

Zhang, X., Zhong, L., Zou, Z., Liang, G., Tang, Z., Li, K., et al. (2021). Clinical and Prognostic Pan-Cancer Analysis of N6-Methyladenosine Regulators in Two Types of Hematological Malignancies: A Retrospective Study Based on TCGA and GTEx Databases. *Front. Oncol.* 11, 623170. doi:10.3389/fonc.2021.623170

Zhang, Y., Wang, D., Wu, D., Zhang, D., and Sun, M. (2020e). Long Noncoding RNA KCNMB2-AS1 Stabilized by N6-Methyladenosine Modification Promotes Cervical Cancer Growth through Acting as a Competing Endogenous RNA. *Cell Transpl.* 29, 096368972096438. doi:10.1177/0963689720964382

Zheng, Z.-Q., Li, Z.-X., Zhou, G.-Q., Lin, L., Zhang, L.-L., Lv, J.-W., et al. (2019). Long Noncoding RNA FAM225A Promotes Nasopharyngeal Carcinoma Tumorigenesis and Metastasis by Acting as ceRNA to Sponge miR-590-3p/miR-1275 and Upregulate ITGB3. *Cancer Res.* 79, 4612–4626. doi:10.1158/0008-5472.Can-19-0799

Zhou, K. I., Parisien, M., Dai, Q., Liu, N., Diatchenko, L., Sachleben, J. R., et al. (2016). N6-Methyladenosine Modification in a Long Noncoding RNA Hairpin Predisposes its Conformation to Protein Binding. *J. Mol. Biol.* 428, 822–833. doi:10.1016/j.jmb.2015.08.021

Zhou, Y., Kong, Y., Fan, W., Tao, T., Xiao, Q., Li, N., et al. (2020). Principles of RNA Methylation and Their Implications for Biology and Medicine. *Biomed. Pharmacother.* 131, 110731. doi:10.1016/j.biopha.2020.110731

Zhu, L., Zhu, Y., Han, S., Chen, M., Song, P., Dai, D., et al. (2019). Impaired Autophagic Degradation of lncRNA ARHGAP5-AS1 Promotes Chemoresistance in Gastric Cancer. *Cell Death Dis* 10, 383. doi:10.1038/s41419-019-1585-2

Zhu, P., He, F., Hou, Y., Tu, G., Li, Q., Jin, T., et al. (2021). A Novel Hypoxic Long Noncoding RNA KB-1980E6.3 Maintains Breast Cancer Stem Cell Stemness via Interacting with IGF2BP1 to Facilitate C-Myc mRNA Stability. *Oncogene* 40, 1609–1627. doi:10.1038/s41388-020-01638-9

Zhu, S., Wang, J.-Z., Chen, D., He, Y.-T., Meng, N., Chen, M., et al. (2020a). An Oncopeptide Regulates m6A Recognition by the m6A Reader IGF2BP1 and Tumorigenesis. *Nat. Commun.* 11, 1685. doi:10.1038/s41467-020-15403-9

Zhu, Z., Qian, Q., Zhao, X., Ma, L., and Chen, P. (2020b). N6-methyladenosine ALKBH5 Promotes Non-small Cell Lung Cancer Progress by Regulating TIMP3 Stability. *Gene* 731, 144348. doi:10.1016/j.gene.2020.144348

Zou, Z., Zhou, S., Liang, G., Tang, Z., Li, K., Tan, S., et al. (2021). The Pan-Cancer Analysis of the Two Types of Uterine Cancer Uncovered Clinical and Prognostic Associations with m6A RNA Methylation Regulators. *Mol. Omics* 17, 438–453. doi:10.1039/d0mo00113a

Zuo, L., Su, H., Zhang, Q., Wu, W.-y., Zeng, Y., Li, X.-m., et al. (2021). Comprehensive Analysis of lncRNAs N6-Methyladenosine Modification in Colorectal Cancer. *Aging* 13, 4182–4198. doi:10.18632/aging.202383

Zuo, X., Chen, Z., Gao, W., Zhang, Y., Wang, J., Wang, J., et al. (2020). M6A-mediated Upregulation of LINC00958 Increases Lipogenesis and Acts as a Nanotherapeutic Target in Hepatocellular Carcinoma. *J. Hematol. Oncol.* 13, 5. doi:10.1186/s13045-019-0839-x

Conflict of Interest: The authors declare that the research was conducted in the absence of any commercial or financial relationships that could be construed as a potential conflict of interest.

Publisher's Note: All claims expressed in this article are solely those of the authors and do not necessarily represent those of their affiliated organizations, or those of the publisher, the editors and the reviewers. Any product that may be evaluated in this article, or claim that may be made by its manufacturer, is not guaranteed or endorsed by the publisher.

frontiers in Cell and Developmental Biology

REVIEW
published: 03 February 2022
doi: 10.3389/fcell.2022.813581

Interplay Between m^{6}A RNA Methylation and Regulation of Metabolism in Cancer

Youchaou Mobet[1,2], Xiaoyi Liu[1], Tao Liu[1], Jianhua Yu[3,4,5]* and Ping Yi[1]**

[1]Department of Obstetrics and Gynecology, The Third Affiliated Hospital of Chongqing Medical University, Chongqing, China, [2]Laboratory of Biochemistry, Faculty of Science, University of Douala, Douala, Cameroon, [3]Department of Hematology and Hematopoietic Cell Transplantation, City of Hope National Medical Center, Los Angeles, CA, United States, [4]Hematologic Malignancies and Stem Cell Transplantation Institute, City of Hope National Medical Center, Los Angeles, CA, United States, [5]Comprehensive Cancer Center, City of Hope, Los Angeles, CA, United States

Methylation of adenosine in RNA to N6-methyladenosine (m^{6}A) is widespread in eukaryotic cells with his integral RNA regulation. This dynamic process is regulated by methylases (editors/writers), demethylases (remover/erasers), and proteins that recognize methylation (effectors/readers). It is now evident that m^{6}A is involved in the proliferation and metastasis of cancer cells, for instance, altering cancer cell metabolism. Thus, determining how m^{6}A dysregulates metabolic pathways could provide potential targets for cancer therapy or early diagnosis. This review focuses on the link between the m^{6}A modification and the reprogramming of metabolism in cancer. We hypothesize that m^{6}A modification could dysregulate the expression of glucose, lipid, amino acid metabolism, and other metabolites or building blocks of cells by adaptation to the hypoxic tumor microenvironment, an increase in glycolysis, mitochondrial dysfunction, and abnormal expression of metabolic enzymes, metabolic receptors, transcription factors as well as oncogenic signaling pathways in both hematological malignancies and solid tumors. These metabolism abnormalities caused by m^{6}A's modification may affect the metabolic reprogramming of cancer cells and then increase cell proliferation, tumor initiation, and metastasis. We conclude that focusing on m^{6}A could provide new directions in searching for novel therapeutic and diagnostic targets for the early detection and treatment of many cancers.

Keywords: M^{6}A, methylation, reprogramming, metabolism, metabolite, oncogenic, cancer

OPEN ACCESS

Edited by:
Huilin Huang,
Sun Yat-sen University Cancer Center (SYSUCC), China

Reviewed by:
Jiangbo Wei,
University of Chicago, United States
Eswar Shankar,
The Ohio State University, United States
Bo Wen,
Fudan University, China

****Correspondence:***
Tao Liu
anti1988@163.com
Jianhua Yu
jiayu@coh.org
Ping Yi
yiping@cqmu.edu.cn

Specialty section:
This article was submitted to Epigenomics and Epigenetics, a section of the journal Frontiers in Cell and Developmental Biology

Received: *12 November 2021*
Accepted: *17 January 2022*
Published: *03 February 2022*

Citation:
Mobet Y, Liu X, Liu T, Yu J and Yi P (2022) Interplay Between m^{6}A RNA Methylation and Regulation of Metabolism in Cancer. Front. Cell Dev. Biol. 10:813581. doi: 10.3389/fcell.2022.813581

INTRODUCTION

Adenosine methylation is the most common modification of RNA in eukaryotes. The methyl group is attached to the nitrogen-6 position of adenosine, creating N6-methyladenosine or m^{6}A (Wang et al., 2017). This modification is highly dynamic and reversible, as it involves enzymes that methylate adenosine (writers), remove methylation (erasers), or recognize it (readers) (Chen et al., 2019b). Moreover, the m^{6}A modification is integral to the regulation of RNA, as it affects mRNA processing, mRNA translation, mRNA decay, mRNA export to the cytoplasm, and miRNA maturation (Roundtree et al., 2017a). In the past several years, compelling evidence has witnessed the implication of m^{6}A in RNA modification. Recent work has uncovered that m^{6}A plays an important role in gene expression regulation emerged as critical post-transcriptional modifications. Currently, Shi et al., (2019) review advances progress in understanding the mechanisms which specific cellular contexts and molecular function of N6-methyladenosine and

highlight the importance of RNA modification regulation, including mRNA, tRNA, rRNA, and other non-coding RNA. They conclude that the recent biological outcome of m^{6}A methylation could be promising for translational medicine. Previously, the roles of m^{6}A modifications in modulating gene expression throughout cell differentiation and animal development were reviewed by Frye et al., (2018). Their study illustrates that m^{6}A methylation plays a critical role by regulating various aspects of RNA metabolism, physiological processes, and stress response (Frye et al., 2018). More interestingly, others recent evidence indicates that the modification of m^{6}A also regulates physiology and metabolism in tumors (Faubert et al., 2017; Choe et al., 2018).

Metabolic reprogramming in cancer cells was discovered to promote tumorigenesis (Frezza, 2020). Biochemical and molecular studies have suggested several possible mechanisms for its evolution during cancer development (Hanahan and Weinberg, 2011). Recently, m^{6}A's function in oncology and its involvement in the regulation of cancer metabolism has received growing attention. As a result, our understanding of the metabolic mechanisms regulated by the m^{6}A's modification in carcinogenesis and their potential therapeutic implications have progressed significantly.

Interestingly, m^{6}A can act as a suppressor or promoter in the proliferation (Liu et al., 2018; Shen, 2020), differentiation (Chen et al., 2019a), and metastasis of tumor cells (Ma et al., 2017) in various cancers. It also appears to reprogram cancer cell metabolism (Shen et al., 2020), as it can regulate metabolic enzymes, transporters, pathways, and transcription factors that promote cancer progression (Li et al., 2020c; Chen et al., 2021a). Here, we discuss the current understanding of how the m^{6}A modification affects cancer metabolism and the potential for regulating it to provide new targets for cancer therapy.

M^{6}A REGULATION

Modification of m^{6}A is regulated by: methyltransferases that catalyze methylation (writers), demethylases that remove (erasers) the methyl group from m^{6}A, then m^{6}A recognition proteins (readers) recognize the modification (Lewis et al., 2017). Interestingly, m^{6}A methyltransferase, m^{6}A demethylases, and m^{6}A recognition proteins play essential roles in gene regulation.

m^{6}A Methyltransferase

Methyltransferase-like3 (METTL3) and Methyltransferase-like14 (METTL14) are the critical components of the m^{6}A methyltransferase complex (MTC). These two methyltransferases colocalize in the nucleus (Liu et al., 2014), forming a heterodimer. METTL3 transfers the methyl of the S-adenosyl methionine (SAM) to produce S-adenosyl homocysteine (SAH) and leads to global miRNA downregulation. By binding with eIF3h in the cytoplasm, METTL3 can also promote oncogenic mRNAs translation (Choe et al., 2018). METTL3 could be modulated through post-transcriptional modifications, affecting protein stability, localization, writer complex formation, and writer catalytic activity (Shi et al., 2019). In comparison, METTL14 identifies specific RNA sequences as a target and stabilizes the structure of MTC (Liu et al., 2014; Lin et al., 2016; Sledz and Jinek, 2016). For example, METTL14 can methylate target miRNA by cooperating with HNRNPA2B1 and DGCR8, promoting miRNA maturation (Alarcon et al., 2015).

Wilms' tumor associating protein (WTAP), another writer protein, plays a role in localizing the methylase complex in the nucleus by interaction with heterodimer (Ping et al., 2014; Knuckles et al., 2018). Recently, other components, such as HAKAI, ZC3H13, and VIRMA/KIAA1429, have been identified to interact with other parts of the MTC (Yue et al., 2018), while ZCCHC4 is a ribosomal RNA-28S methyltransferase (Ma et al., 2019). Other methyltransferase components like METTL5 have been found to be independent m^{6}A writers. It catalyzes the attachment of m^{6}A onto specific structure RNAs, including U6-small nuclear RNA (snRNA), 18S rRNA, and 28S rRNA (Wang et al., 2017; Ignatova et al., 2020). METTL16 catalyzes m^{6}A of the U6- spliceosomal small nuclear RNA and MAT2A 3′-UTR mRNA (Pendleton et al., 2017).

m^{6}A Demethylases

The m^{6}A remover proteins erase the m^{6}A modification by increasing the level of iron ferrous (Fe^{2+}) (co-factor) and α-ketoglutarate (co-substrate) dependent oxygenase family (Fedeles et al., 2015). Two erasers that catalyze m^{6}A demethylation ALKB homolog 5 (ALKBH5) and fat mass and obesity-associated protein (FTO) can recognize adenine and cytosine methylation in RNA (Fu et al., 2013). ALKBH5 and FTO are members of the Fe^{2+}/α-ketoglutarate-dependent dioxygenases family. The first RNA demethylase identified FTO was reported to remove the methyl group of N6 - methyladenosine (m^{6}A) in RNA. m^{6}A erasers may exhibit different expression levels, post-translational modifications, and cellular localization, depending on cell types. For instance, m^{6}A demethylase FTO is predominantly nucleus localized and regulates 5–10% of total mRNA m^{6}A demethylation (Wei et al., 2018). In contrast, FTO is also highly abundant in the cell cytoplasm and can mediate up to 40% m^{6}A demethylation of total mRNA in certain leukemia cells (Shi et al., 2019). Additionally, FTO regulates alternative splicing via m6A by interacting with Serine-rich splicing factor 2(SRSF2) (Bartosovic et al., 2017). Interestingly, FTO may control metabolic disorders. ALKBH5 another m^{6}A demethylase, affects mRNA export and processing factors (Zheng et al., 2013). ALKB homolog 3 (ALKBH3) was found to demethylate only tRNAs (Ueda et al., 2017; Yang et al., 2020).

m^{6}A Recognition

The m^{6}A recognition proteins (readers) control the destiny of RNAs that have been modified. Readers/effectors are distributed in the nucleus and cytoplasm, indicating their functional diversity. While writers and erasers carry out methylation and demethylation, the readers determine the functional consequences of modification. m^{6}A recognition proteins characterization has provided valuable insights into the molecular mechanisms of the m^{6}A-mediated post-transcriptional gene regulation (Shi et al., 2019). Furthermore,

RNA binding proteins (RBPs) could regulate the interactions between m^{6}A effectors and RNA substrates.

YTHDF1/2/3 and YTHDC1 recognize the m^{6}A change and alter mRNA's splicing, translation, and decay (Xu et al., 2014; Wu et al., 2017a). Intriguingly, these proteins also play crucial roles in mRNA metabolism (Wang et al., 2015). For instance, YTHDF1 binds to mRNA, including eukaryotic translation initiation factor 3 (eIF3) and poly-A- binding protein (PABP) complex to promote RNA translation (Wang et al., 2015). YTHDF2 recognizes mRNAs not destined for translation, accelerating their destruction. Interestingly, it identifies specific m^{6}A -modified binds to CCR4-NOT transcription complex subunit 1 (CNOT1). However, it recruits the CCR4-NOT complex of the m^{6}A -tagged RNA P-body to promote its destruction (Du et al., 2016). YTHDF3 by interaction with YTHDF1 accelerates mRNA translation, affecting YTHDF2-mediated degradation of mRNAs labeled with m^{6}A (Li et al., 2017a).

YTHDC1 mediates mRNA export marked with m^{6}A by interaction with the nuclear export adaptor protein SRSF3 (Roundtree et al., 2017b). Importantly, YTHDC1 regulates splicing events by inhibiting SRSF10 or activating splicing factor SRSF3. In conjunction with nuclear RNA export factor 1 (NXF1), YTHDC1 can also mediate mRNA export to the cytoplasm. Unlike the rest of the family, YTHDC2, an RNA helicase. Its helicase domain contributes to RNA binding (Hsu et al., 2017). Significantly, YTHDC2 and YTHDF3 can facilitate RNA degradation or enhance RNA translation depending on the context (Shi et al., 2017).

hnRNPs, another m^{6}A recognition family, is localized in the nucleus where heterogeneous nuclear ribonucleoprotein C (hnRNPC) can bind with nascent RNA transcripts and control their processing (Alarcon et al., 2015). For instance, the lncRNA MALAT1 facilitates a change in the m^{6}A site for recognition and binding by hnRNPC (Liu et al., 2015). Interestingly, m^{6}A regulates RNA binding motifs (RBMs) accessibility by altering mRNA and long noncoding RNA (lncRNA) structure to promote hnRNPC interaction. These changes influence RNA-protein interactions in human cells. This mechanism is called the "m^{6}A -switch" (Liu et al., 2015). hnRNPC-binding regulated by the m^{6}A -switch regulates RNA alternative splicing, indicating that the switch helps regulate gene expression and RNA maturation (Liu et al., 2015).

Another component of the m^{6}A recognition family, Heterogeneous nuclear ribonucleoprotein A2B1 (hnRNPA2B1), regulates RNA alternative splicing and microRNA processing (Alarcon et al., 2015; Liu et al., 2015). Further, it interacts with DiGeorge syndrome critical region gene 8 (DGCR8) for miRNA maturation and recognizes the m^{6}A signals of microRNA (Zhao et al., 2017). Eukaryotic initiation factor 3 (eIF3), another effector/reader, could initiate protein translation in a cap on its 5′-UTR (Meyer et al., 2015). In conjunction with Hu antigen R (HuR), these proteins recognize m^{6}A's modification and stabilize their RNA transcripts (Meyer et al., 2015).

Insulin growth factor-2 binding proteins 1, 2, and 3 (IGF2BP 1/2/3) were identified as another m^{6}A recognition. After co-localizing with HuR, these proteins protect mRNA decay and enhance mRNA translation (Huang et al., 2018). These findings demonstrated that m^{6}A methyltransferases (editors/writers) and m^{6}A demethylases (remover/erasers) cooperate to modulate the distribution of m^{6}A on RNA by adding (writer) or removing (erasers) the methyl. While the m^{6}A recognition (effectors/readers) proteins recognize the m^{6}A modified transcripts and determine their fate regulate functions (**Figure 1**).

M^{6}A REGULATES CANCER METABOLISM

Cancer cells need abundant energy and raw materials to grow and divide; therefore, they substantially alter their metabolic pathways (Hanahan and Weinberg, 2011; Li and Zhang, 2016). Importantly, biochemical and molecular studies suggest several possible mechanisms for the evolution of aberrant metabolism during cancer development (Hanahan and Weinberg, 2011). For example, proliferating cancer cells can enhance the synthesis of glucose of carbohydrates, lipids, and proteins to obtain an ample and uninterrupted supply of molecules needed for biosynthesis (Khan et al., 2020). Moreover, most cancer cells depend on aerobic glycolysis rather than the TCA cycle (Vander Heiden et al., 2009). The preference for glycolysis over mitochondrial oxidative phosphorylation seems to be a hallmark of cancer cells (Garber, 2006).

However, aerobic glycolysis transports chemical generates ATP. This ATP and its breakdown product adenosine are widespread throughout the body, and both have been shown to regulate cell proliferation and differentiation. Therefore, metabolic reprogramming is widely utilized during oncogenesis, and the m^{6}A modification can regulate metabolism in cancer progression (**Figure 2**).

m^{6}A Regulates Glucose Metabolism

Glucose, an essential nutrient in blood, is the main energy source for cells (Shaw, 2006). However, several studies have found that hyperglycemia increases the overall risk of cancer (Stattin et al., 2007). Cancer cells enhanced glucose uptake has also been implicated in metastasis and poor prognosis (Macheda et al., 2005). Aerobic glycolysis in cancer can increase the m^{6}A modification genes associated with glycolysis (Fry et al., 2017).

Recent evidence demonstrated that cancer reprograms glucose metabolism (Li et al., 2020c); thus, aerobic glycolysis exemplifies an evolutionary change in cancer cells. Not surprisingly, glycolytic transporters like glucose transporter (GLUT), glycolytic enzymes such as pyruvate kinase isozyme M1/2 (PKM1/2), pyruvate dehydrogenase kinase (PDK), lactate dehydrogenase (LDH), and hexokinase (HK) is important targets to understand cancer metabolism (Doherty and Cleveland, 2013; Viale et al., 2014). The relationship between m^{6}A and glucose metabolism is crucial for understanding cancer progression because glucose is the most important metabolite associated with many enzymes and transporters. Additionally, glycolysis is an essential pathway involved in cancer progression, metastasis, and chemotherapy resistance (Ganapathy-Kanniappan and Geschwind, 2013).

In Colorectal Cancer (CRC), the METTL3-HK2/GLUT1-MYC-IGF2BP is involved in cells proliferation and metastasis

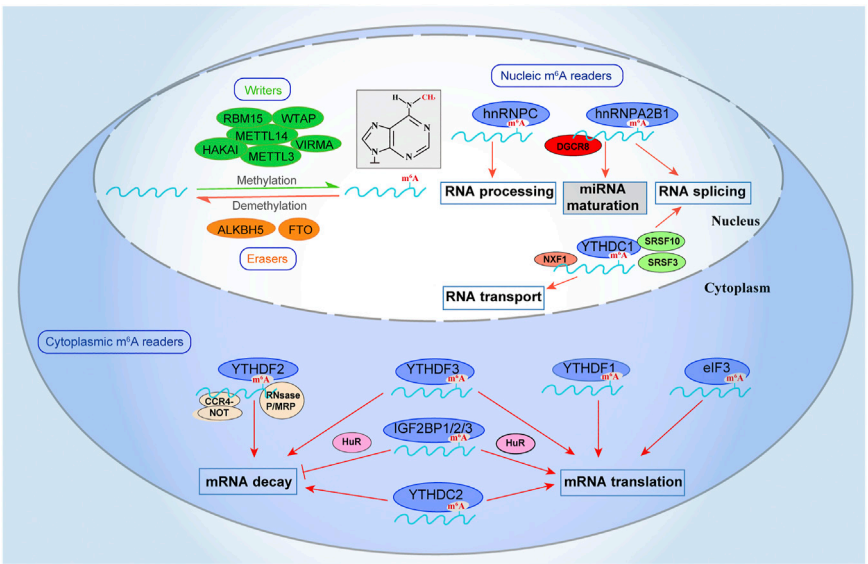

FIGURE 1 | m^{6}A-mediated RNA regulation. The m^{6}A modification is integral to the regulation of RNA. m^{6}A can be installed by "writers" (METTL3/14, WTAP, RBM15, VIRMA, and HAKAI), removed by "erasers" (FTO and ALKBH5), and recognized by "readers" (YTHDF1/2/3, YTHDC1/2, IGF2BP1/2/3, eIF3, and HNRNPC/A2B1). m^{6}A methyltransferases (writers) catalyze methylation while the m^{6}A demethylases (erasers) remove the methyl in m^{6}A. The m^{6}A recognition (readers) proteins bind the m^{6}A modified transcripts and determine their fate. The modification of "writers," "erasers," and "readers" proteins affect RNA processing, including RNA splicing, mRNA translation, mRNA decay, mRNA export to the cytoplasm, and miRNA maturation.

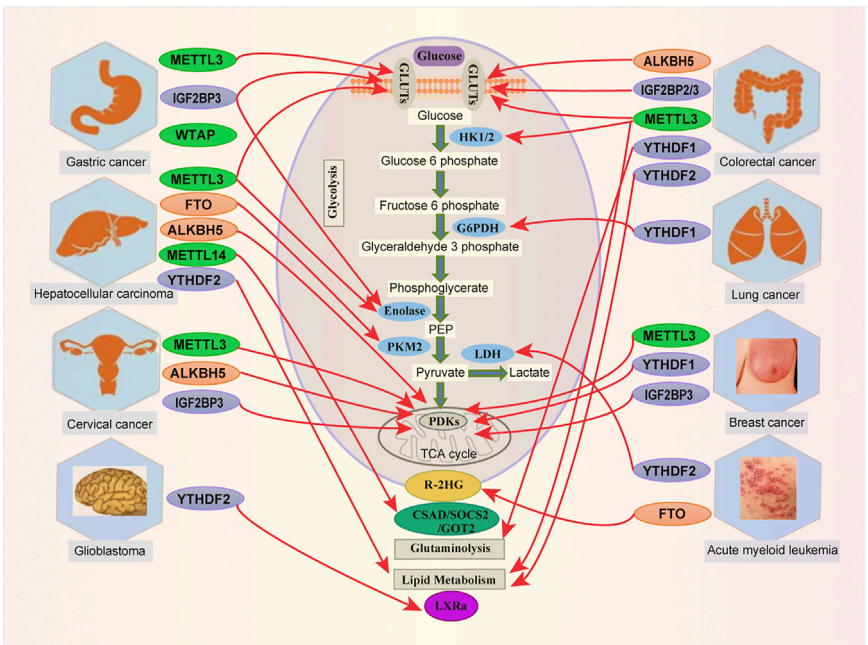

FIGURE 2 | Links between m^{6}A modification and metabolites in human cancer. m^{6}A RNA modification by targeting metabolic pathways is involved in various tumorigenesis, including Acute Myeloid Leukemia (AML), Breast Cancer (BC), Cervical Cancer (CC), Colorectal Cancer (CRC), Glioblastoma (GBM), Hepatocellular Carcinoma (HCC), Gastric Cancer (GC) and Lung Cancer (LC).

(Shen et al., 2020; Xiang et al., 2020; Chen et al., 2021a). Hexokinase (HK) catalyzed the first step of anaerobic glycolysis and oxidative phosphorylation, which converts glucose to glucose 6-phosphate (G6P) (Wilson, 2003). Many investigations reveal the implication of HK in cancers. For instance, HK2 bound to mitochondria enable cancer cells to

become more glycolytic (Chen et al., 2014; Wu et al., 2017b). GLUT1, a glucose transporter, mediates the first step of glucose inside cells (Cheeseman, 2008). Overexpression of GLUTs facilitates glucose consumption in cancer progression (Ancey et al., 2018). METTL3 stabilizes GLUT1 and HK2 mRNA in colorectal cancer by directly interacting with the 3′ UTR mRNA of GLUT1 and the 5'/3′-UTRs mRNA of HK2. This enhanced HK2 and GLUT1 expression, promoting CRC progression (Shen et al., 2020). One recent study established that METTL3 enhanced CRC growth and identified GLUT1-mTORC1 as the primary target of METTL3 in that disease (Chen et al., 2021a). More interestingly, METTL3 induced GLUT1 translation in m^{6}A to promote glucose uptake and lactate production, leading to mTORC1 activation. These findings indicate that METTL3 promotes CRC *via* the m^{6}A-mediated GLUT1-mTORC1 signaling activation.

In Cervical Cancer, (Li et al., 2020c) demonstrated that m^{6}A regulates glycolysis in cancer cells through pyruvate dehydrogenase kinase 4 (PDK4). PDKs are the gatekeeper enzymes involved in altered glucose metabolism in tumors (Patel and Korotchkina, 2006; Devedjiev et al., 2007). They are remarkably overexpressed in multiple human tumor samples. Among them, PDK4 was noticed as one critical metabolic factor of metabolism control because it can divert carbon flux from oxidative phosphorylation into glycolysis (OXPHOS) (Stacpoole, 2017). According to Li and collaborators, the extracellular acidification rate (ECAR) was decreased in Mettl3$^{Mut/-}$ HeLa cells, While the oxygen consumption rate (OCR) was increased (Li et al., 2020c), demonstrating that METTL3 promotes glycolysis. Additionally, PDK4 can reverse lactate production level, glucose consumption, and ATP rate in Mettl3-depleted cells. More importantly, overexpression of PDK4 to an endogenous level attenuated the metabolic phenotypes of SiHa cells that had lost METTL3. Also, overexpression of ALKBH5 suppressed PDK4 expression in HeLa cells (Li et al., 2020c). Moreover, compared with negative control samples, IGF2BP3 and YTHDF1 were significantly higher in cervical cancer samples (Li et al., 2020c). Li et al. (2020b) further determined whether the m^{6}A modification can regulate PDK4 expression in addition to affecting the stability of the kinase's mRNA. Modifying the PDK4 mRNA at its 5′-UTR by m^{6}A positively regulated its elongation during translation and the stability of its mRNA because m^{6}A is bound to the YTHDF1 and IGF2BP3 (Li et al., 2020c). In HeLa cells, IGF2BP3 inhibition can suppress PDK4 expression and alter the suppressive effect of METTL3 on PDK4 expression (Li et al., 2020c). More interestingly, YTHDF1 and IGF2BP3-targeting PDK4 with d m^{6}A CRISPR significantly downregulated PDK4 mRNA and protein levels (Li et al., 2020c). Thus, targeting m^{6}A on PDK4 mRNA with dm6ACRISPR appears to regulate glycolysis and ATP generation in cancer (Li et al., 2020c). These studies suggest that PDK4 is a critical metabolic agent of glycolysis and ATP generation regulated by m^{6}A in cervical cancer progression.

In Hepatocellular Carcinoma (HCC), hepatic FTO helps regulate the expression of the gluconeogenic gene. Recent evidence indicates that demethylation of m^{6}A by FTO affects glucose metabolism *via* hepatic gluconeogenesis (Shen et al., 2015). On the other hand, the FTO level may be affected by insulin in HCC (Mizuno et al., 2017). Pyruvate kinase isozymes M1 (PKM1) and M2 (PKM2) are glycolytic enzymes (Doherty and Cleveland, 2013). They mediate the final steps of glycolysis by dephosphorylation of phosphoenolpyruvate (PEP), producing pyruvate and ATP. According to (Li et al., 2019a), FTO promotes HCC tumorigenesis by demethylating m^{6}A on PKM2 mRNA. This demethylation accelerates translation, leading to tumorigenesis in HCC (Li et al., 2019a). The demethylation of PKM2 mRNA by FTO suggests that FTO also regulates the expression of PKM2. Knocking down FTO repressed HCC progression (Li et al., 2019a). This finding revealed that FTO could demethylate PKM2 mRNA, thereby upregulating the kinase's expression. Upregulated PDK4 was found to reduce hepatic chemotherapy-induced colorectal liver metastasis (Strowitzki et al., 2019). PDK4 collaborates with METTL3 to induce proliferation and hepatic chemosensitivity cancer cells (Li et al., 2020c). Regarding the link between PDK4 and m^{6}A, Li and collaborators found that m^{6}A -PDK4 plays an essential role in liver cancer progression. Consistent with this finding, knocking down METTL3 inhibited PDK4 antibodies in Huh7 cells. Moreover, overexpression of the demethylase ALKBH5 (another m^{6}A eraser) decreased glucose, lactate, and ATP abundance in Huh7 HCC cells (Li et al., 2020c). Li and collaborators also provided evidence that METTL3 regulates glycolytic activity in HCC. Downregulation of METTL3 cooperates with the 2-deoxyglucose (2-DG) to inhibit HCC proliferation, suggesting that suppressing glycolysis by inhibiting METTL3 might be a potential strategy for treating HCC (Lin et al., 2020).

In Acute Myeloid Leukemia (AML), α-ketoglutarate, produced by isocitrate dehydrogenase in the TCA cycle, interacts with m^{6}A demethylase proteins (Losman et al., 2020). R-2HG (R-2-hydroxyglutarate) inhibited FTO activity by stimulating the modification of m^{6}A -RNA in cells. Moreover, through targeting the FTO/MYC/CEBPA axis, R-2HG inhibited the proliferation of leukemia cells (Su et al., 2018). It was reported that knocking down FTO or LDHB (lactate dehydrogenase B) inhibits R-2HG in leukemia cells (Qing et al., 2021). Additionally, R-2HG abrogated FTO/m^{6}A/YTHDF2-mediated upregulation of LDHB, suppressing aerobic glycolysis (Qing et al., 2021). These findings show that R-2HG attenuates aerobic glycolysis by inhibiting FTO in leukemia cells. Lactate dehydrogenase (LDH) converts pyruvate to lactate, and this enzyme is frequently upregulated in multiple cancers (Wang et al., 2012). Lactate, ketone, and pyruvate are monocarboxylates that play essential roles in cancer metabolism (Halestrap, 2013).

In Gastric Cancer (GC), overexpression of METTL3 (a writer) promoted metastasis to the liver *in vitro* and *in vivo,* and it also stimulated the modification of adenosine to m^{6}A, enhancing mRNA stability (Wang et al., 2020c). Tumor angiogenesis was promoted by Hepatoma-derived growth factor (HDGF) upregulation, while nuclear HDGF activated GLUT4 and ENO2 expression and increased metastasis in GC cells (Wang et al., 2020c). WTAP (a writer) promoted GC cell proliferation and glycolytic capacity and enhanced HK2 expression through

interacting with the m^{6}A modified 3′-UTR of HK2 mRNA (Yu et al., 2021).

In Glioblastoma (GBM), Li et al. recently showed that long noncoding RNA just proximal to X-inactive specific transcript (JPX) interacted with N6-methyladenosine (m^{6}A) demethylase FTO and enhanced FTO-mediated PDK1 mRNA demethylation. Additionally, JPX exerted its GBM-promotion effects through the FTO/PDK1 axis (Li et al., 2021). These outcomes reveal the critical role of JPX in promoting GBM aerobic glycolysis-m^{6}A demethylase FTO.

In Lung Cancer (LC), YTHDF2 expression is increased in tumor tissues, promoted proliferation, and bound to 3′-UTR of 6-phosphogluconate dehydrogenase (G6PD) mRNA (Sheng et al., 2020). This binding facilitates G6PD mRNA translation in LC and promotes tumorigenesis. Recently, Yang and collaborators showed that FTO is declined in lung adenocarcinoma, which correlates with poor patient overall survival. Moreover, downregulated FTO expression enhanced m^{6}A levels in mRNAs of genes involved in metabolic pathways such as MYC (Yang et al., 2021). Interestingly, the enhanced levels recruited the binding of YTHDF1, which promoted the translation of MYC mRNA and increased glycolysis and cancer progression (Yang et al., 2021).

In Breast Cancer (BC), METTL3 overexpression enhanced the PDK4 protein expression in breast cancer cells (Li et al., 2020c). Interestingly, the m^{6}A -modified 5′-UTR of PDK4 regulated the kinase's elongation during translation and the stability of its mRNA through interaction with YTHDF1 and IGF2BP3. Further, clinical data confirm that m6A/PDK4 is implicated in breast cancer progression (Li et al., 2020c). These findings suggest that proteins associated with m^{6}A regulate glycolysis in breast cancer cells.

m^{6}A Regulates Lipid Metabolism

Recently, elevated lipid levels were recognized as an important aberration of cancer metabolism (Swierczynski et al., 2014). Moreover, previous studies have noticed that lipid metabolism is reprogrammed in tumors (Schulze and Harris, 2012; Nath and Chan, 2016). Dysregulation of lipid metabolism is an essential feature of cancer cells (Murai, 2015; Gaida et al., 2016).

There is also a link between m^{6}A proteins and lipid metabolism in cancer. After observing that knocking down METTL3 and YTHDF2 decreased lipid accumulation in hepatocellular carcinoma cells, Zhong et al. (2018) proposed that the presence of m^{6}A in mRNA mediates crosstalk between the circadian clock and lipid metabolism (Zhong et al., 2018). Kang et al. (2018) showed that FTO increased triglyceride (TG) deposition and decreased mitochondrial content. FTO regulates lipid metabolism in hepatocytes by modulating RNA m^{6}A levels (Kang et al., 2018). These studies revealed that FTO's demethylating is an important actor in the lipid metabolism of hepatocytes. By linking the epigenetic modification of RNA with fat deposition, they suggested a new m^{6}A target for regulating hepatic fat metabolism (Kang et al., 2018). FTO overexpression in HepG2 cells also reduced m^{6}A levels, enhancing stearoyl CoA desaturase (SCD), monoacylglycerol O acyltransferase 1 (MOGAT1), and fatty acid synthase (FAS), which contribute to cell growth (Kang et al., 2018). Numerous studies demonstrated that METTL3-mediated m^{6}A modification and inhibition of mRNA decay promoted the miR-3619-5p/HDGF axis, enhancing lipogenesis in Hepatocellular Carcinoma (Zhong et al., 2019; Zuo et al., 2020).

In GBM, Fang et al. (2021) recently showed that YTHDF2 facilitates m^{6}A -dependent mRNA decay, impacting glioma patients' survival. Moreover, YTHDF2 inhibited cholesterol homeostasis in GBM cells. These outcomes highlight the critical function of YTHDF2 regulated cholesterol homeostasis in GBM (Fang et al., 2021). Other reported studies showed that YTHDF2 could also regulate lipogenic genes, including acetyl CoA carboxylase 1 (ACC1), fatty acid synthase (FAS), and stearoyl-CoA desaturase 1(SCD1), to decrease their mRNA stability (Zhou et al., 2021).

As a lipid, sphingolipids also regulate cancer proliferation, migration, invasion, and metastasis. Among this class of lipid, delta 4 desaturase sphingolipid 2 (DEGS2) catalyzes the conversion of dhCers to phytoceramides (Casasampere et al., 2016). Recently, Guo and collaborators found the role of m^{6}A modification on DEGS2 in colorectal cancer and suggested that inhibited m^{6}A promotes DEGS2 expression and dysregulated lipid metabolites, contributing to colorectal cancer (Guo et al., 2021). Furthermore, overexpression of DEGS2 promoted cell growth, while depletion of DEGS2 inhibited cell growth (Casasampere et al., 2016). Regarding the molecular mechanism, Guo and collaborators found that METTL3 depletion promoted the DEGS2 mRNA, increased DEGS2 expression in HCT116 cells, suggesting that METTL3 is essential for the stability and translation of DEGS2. YTHDF2 knockdown induced the level of DEGS2 mRNA expression, meaning that YTHDF2 contributes to the DEGS2 mRNA decay (Guo et al., 2021). Collectively, this recent evidence suggests that m^{6}A regulates lipid metabolism in cancer.

m^{6}A Regulates Amino Acid Metabolism

To proliferate, cancer cells need large amounts of amino acids (Sivanand and Vander Heiden, 2020), which are essential building blocks of proteins (Murugan, 2019; Vettore et al., 2020). Moreover, there is much evidence for specific degradation in amino acid metabolism in cancers (Li and Zhang, 2016). Glutamine, which regulates the expression of many genes related to metabolism (Curi et al., 2005), is carried into cancer cells by multiple transporters, such as Na + -coupled neutral amino acid transporters (SNATs) and Na + -dependent transporters (Kandasamy et al., 2018).

To renew the TCA cycle, many tumor cells highly need glutamine (Matés et al., 2013). Glutamate dehydrogenase (GLUD1) and transaminases can transform glutamine to α-KG to reconstruct the TCA cycle (Vander Heiden et al., 2009). FTO and ALKBH5 were identified as α-KG-dependent dioxygenases (Zhu et al., 2020). METTL14 may promote HCC progression by modulating m^{6}A -regulated genes, including glutamic oxaloacetic transaminase 2 (GOT2), cysteine sulfonic acid decarboxylase (CSAD), and suppressor of cytokine signaling 2 (SOCS2) (Li et al., 2020b). In colon cancer, Chen and

TABLE 1 | Regulation of metabolites by m^{6}A associated proteins in cancer.

Metabolic pathways	Metabolites/Enzymes/Signaling pathways	m^{6}A associated proteins	Cancer type	Role in cancer	References
Glycolysis	GLUT1-mTORC1	METTL3	CRC	Oncogene	Chen et al. (2021a)
	GLUT1	METTL3/IGF2BP2/3	CRC	Oncogene	Shen et al. (2020)
	PDK4	METTL3	Breast cancer	Oncogene	Li et al. (2020c)
	HK2	METTL3	CRC	Oncogene	Shen et al. (2020)
	GLUT4/Enolase	METTL3	Liver cancer	Oncogene	Wang et al. (2020c)
	GLUT4/HDGF/ENO2	METTL3/IGF2BP3	Gastric cancer	Oncogene	Wang et al. (2020c)
	PDK4	METTL3/IGF2BP3/ALKBH5	Cervical cancer	Oncogene	Li et al. (2020c)
	MYC	FTO/YTHDF1	Lung cancer	Oncogene	Yang et al. (2021)
	PDK4	METTL3	Liver cancer	Oncogene	Li et al. (2020c)
	HK2	WTAP	Gastric cancer	Oncogene	Yu et al. (2021)
	PDK4	YTHDF1/IGF2BP3	Breast cancer	Oncogene	Li et al. (2020c)
	PKM2	FTO	HCC	Oncogene	Li et al. (2019a)
	PDK4	ALKBH5	Cervical cancer	Oncogene	Li et al. (2020c)
	PDK4	ALKBH5	HCC	Oncogene	Li et al. (2020c)
	GLUT1	ALKBH5	CRC	Oncogene	Shen et al. (2020)
	G6PD	YTHDF2	Lung cancer	Oncogene	Sheng et al. (2020)
	2-deoxyglucose	METTL3	HCC	Oncogene	Lin et al. (2020)
	MYC	METTL3	CRC	Oncogene	Lin et al. (2020)
	LDHB	YTHDF2	AML	Oncogene	Qing et al. (2021)
Lipid metabolism	Lipid	METTL3/YTHDF2	Liver cancer	Oncogene	Zhong et al. (2018)
	Cholesterol	YTHDF2	Glioblastoma cancer	Oncogene	Fang et al. (2021)
	Triglyceride	METTL3	Liver cancer	Oncogene	Kang et al. (2018)
	Sphingolipid (DEGS2)	METTL3/YTHDF2	CRC	Oncogene	Guo et al. (2021)
Glutaminolysis	R-2HG-MYC	FTO	Leukemia	Oncogene	Su et al. (2018)
	CSAD/GOT2/SOCS2	METTL14	HCC	Oncogene	Li et al. (2020b)
	R-2HG	FTO	AML	Oncogene	Qing et al. (2021)
	Glutamine	YTHDF1	Colon cancer	Oncogene	Chen et al. (2021b)
Other metabolic	Iron and ferritin metabolism	YTHDF1	HPSCC	Oncogene	Ye et al. (2020)

collaborators demonstrated YTHDF1-mediated as a positive association between glutamine metabolism and cisplatin resistance (Chen et al., 2021b).

Recently, reports have indicated that AMP-activated protein kinase (AMPK) could act as a beneficial target for treating cancer patients (Wang et al., 2016b). AMPK can act to inhibit tumorigenesis through the regulation of cell proliferation. AMP-activated protein kinase-alpha2 (AMPKα2) was inversely correlated with FTO (Wang et al., 2016a). FTO is upregulated in colorectal cancer and interacts with MYC to accelerate cell proliferation and migration (Zou et al., 2019). In colorectal cancer, Yue and collaborators reveal that AMPKα2 inhibits CRC cell growth and promotes apoptosis through altering FTO (Yue et al., 2020). More interestingly, miR-96 could retard cancerogenesis by inactivating the FTO-mediated MYC AMPKα2-dependent manner in CRC cells (Yue et al., 2020). Together, these findings elucidate links between m^{6}A and metabolic changes in cancers (**Table 1** and **Figure 2**).

Other Metabolic Processes Regulated by m^{6}A in Cancer

Emerging evidence demonstrates that m^{6}A can also regulate metabolic processes in carcinogenesis that do not involve glucose, lipids, or amino acids. For example, iron metabolism plays a key role in tumorigenesis (Jung et al., 2019). Therefore, pathways that acquire, export, or store iron are often perturbed in cancer (Jung et al., 2019). The tumor microenvironment exerts selective pressure that renders the cancer cells adopt altered metabolism, supporting these cells' energy and metabolic demands, thereby facilitating tumor growth. Recent evidence showed that tumor-associated macrophages (TAMs) could provide iron to impact metabolism within the tumor microenvironment. When Ye and collaborators evaluated the correlation between the m^{6}A modification and iron metabolism, they found that YTHDF1 regulates growth and iron metabolism in hypopharyngeal squamous cell carcinoma (HPSCC) (Ye et al., 2020). YTHDF1 was also associated with intratumoral iron and ferritin levels in hypopharyngeal squamous cell carcinoma (HPSCC) patients. They further demonstrated that HPSCC tumorigenesis induced by YTHDF1 is dependent on iron metabolism and regulates transferrin receptor protein (TFRC) expression in this cancer (Ye et al., 2020). Regarding the molecular mechanism, YTHDF1 binds to the UTR of TFRC mRNA to regulate mRNA translation of TFRC (Ye et al., 2020). Targeting TFRC-mediated iron metabolism and YTHDF1 could become potential candidates for early diagnosis or treatment for HPSCC patients (Ye et al., 2020).

CONTROL OF M^{6}A BY METABOLITES IN CANCER

In cancer, metabolism is often regulated by the m^{6}A modification. But could certain metabolites regulate m^{6}A? This controversial

TABLE 2 | Control of m^{6}A by metabolites in cancer.

m^{6}A implicated proteins	Metabolites	Effects	References
FTO	NADP	NADP decreases m^{6}A methylation in RNA and promotes adipogenesis	Wang et al. (2020b)
FTO	R-2HG	R-2HG attenuates aerobic glycolysis and downregulates the expression of FTO in leukemia cells	Qing et al. (2021)
FTO	R-2HG	R-2HG increases m^{6}A modification of RNA by inhibiting FTO activity, destabilizing MYC transcripts in leukemia cells	Su et al. (2018)
FTO	Isocitrate	Isocitrate increases m^{6}A levels of RNA by inhibiting FTO's activity in leukemia cells	Li et al. (2017b)

idea is supported by the finding that proteins that regulate m^{6}A associate highly with many types of cancer. Also, Wang et al. (2020b) showed that nicotinamide adenine dinucleotide phosphate (NADP) binds to FTO, decreases m^{6}A methylation in RNA, and promotes adipogenesis. Furthermore, NADP regulated mRNA m6A *via* FTO *in vivo*, and deletion of FTO blocked adipogenesis caused by enhanced NADP in 3T3-L1 pre-adipocytes.

Succinate prevents α-ketoglutarate-dependent dioxygenase from regulating critical factors of tumorigenesis, including hypoxia responses and histone demethylation. Additionally, hypoxia in tumors broadly increases levels of m^{6}A in GLUT1 and MYC mRNAs (Priolo et al., 2014). ALKBH5 and FTO m^{6}A demethylases require α-KG, Fe(II), and O_2 for total enzymatic activity (Zhang et al., 2019; Xu and Bochtler, 2020; Losman et al., 2020). The TCA cycle produces other metabolites that regulate m^{6}A demethylation. Interestingly, citrate, another critical metabolite in the TCA, was noticed with an α-KG-binding site in ALKBH5 (Feng et al., 2014). Citrate by binding to α-KG/FTO complex can inhibit the enzyme's activity (Aik et al., 2013).

In AML cells, the FTO's enzymatic activity is inhibited, carrying the IDH (isocitrate dehydrogenase) mutation, which correlates with significantly increased m^{6}A levels (Li et al., 2017b). IDHs are critical enzymes that catalyze isocitrate to α-ketoglutarate (α-KG) and CO_2 in the TCA cycle. They also epigenetically control gene expression through effects on α-KG-dependent dioxygenases. R-2HG was recently reported to exhibit antitumor activity. It attenuates aerobic glycolysis and downregulates the expression of FTO/LDHB/PFKP in leukemia cells (Qing et al., 2021). Moreover, it increases m^{6}A modification of RNA by inhibiting FTO activity, destabilizing CEBPA/MYC transcripts in leukemia cells (Su et al., 2018). These findings, therefore, indicate that certain metabolites can drive the m^{6}A modification of RNA in cancer (**Table 2**).

Potential Clinical Applications of M^{6}A and Targeting the Modification in Cancer

As proteins that create, erase and recognize m^{6}A play a role in cancer metabolism, targeting altered metabolic pathways by focusing on m^{6}A modification has become a promising anticancer strategy. Survival analysis of patients showed that METTL3 (a writer) is a prognostic factor for poor outcomes in HCC (Lin et al., 2020), thyroid carcinoma (Wang et al., 2020a), pancreatic cancer (Xia et al., 2019), CRC (Li et al., 2019b), gastric cancer (Wang et al., 2020c), and colorectal cancer (Chen et al., 2021a). WTAP (another writer) predicts the survival of patients with high-grade serous ovarian carcinoma (Yu et al., 2019), HCC (Chen et al., 2019c), RCC, and GC (Li et al., 2020a). As METTL3 depletion can decline oncogenes' expression and reduce CRC proliferation (Shen et al., 2020), breast cancer (Li et al., 2020c), cervical cancer (Li et al., 2020c), and liver cancer (Wang et al., 2020c), METTL3 offers an alternative therapeutic target in colorectal cancer patients with high glucose levels (Shen et al., 2020). It also could promote colorectal tumorigenesis *via* the m^{6}A-GLUT1-mTORC1 axis. Combined targeting of METTL3 and mTORC1 showed promise for suppressing CRC proliferation, suggesting that METTL3 could also be an alternative therapeutic target in that disease (Chen et al., 2021a). Deleting METTL3 from HeLa cells also decreased PDK4 expression and increased the cells' sensitivity to doxorubicin (DOX) treatment (Li et al., 2020c). However, ectopic overexpression of PDK4 attenuated this effect and reduced DOX sensitivity in cervical cancer cells. This suggests that PDK4 is involved in the proliferation and chemosensitivity of METTL3-cells (Li et al., 2020c). Moreover, METTL3-silenced pancreatic cancer cells and glioma stem cells (GSCs) showed enhanced irradiation sensitivity (Visvanathan et al., 2018) (Taketo et al., 2018). High level of R-2HG expressed by mutant isocitrate dehydrogenase, was demonstrated to play important antitumor effect in glioma and leukemia cells by inhibiting FTO activity (Su et al., 2018).

Recently, Yankova et al. (2021) showed that STM2457, the small-molecule inhibitor targeting METTL3, might be a strategy for treating myeloid leukemia. Pharmacological METTL3 inhibition prolonged survival in AML mouse models (Yankova et al., 2021). Intriguingly, treating tumors with STM2457 increased apoptosis and reduced AML growth (Yankova et al., 2021). These results identified METTL3 inhibition as a promising therapeutic strategy for AML treatment and demonstrated that targeting enzymes that modify RNA is a new approach promising anticancer therapy (Yankova et al., 2021). Depleting METTL3 from cells induced resistance to cisplatin, gemcitabine, and 5-fluorouracil in pancreatic cancer and non-small cell lung cancer (Jin et al., 2019). Also, FTO inhibitors (FB23 and FB23-2) provide a therapeutic strategy for treating leukemia. Targeting regulators of RNA methylation have also shown promise in preclinical models, which are effective against AML, as exemplified by FB23 and FB23-2 (small-molecule inhibitors) of the m^{6}A eraser FTO (Huang et al., 2019).

By pharmacological approaches, FTO is broadly viewed as an attractive biological target. Peng et al. (2019) found a small

TABLE 3 | Non-exhaustive list of Potential alternative therapeutic agents offers by m^{6}A targeting modifications in cancer.

m^{6}A proteins involved	Drugs/Therapeutic agents	Metabolites Pathways/Immune system	Underlying mechanism and Key results	References
METTL3	Doxorubicin (DOX)	Glycolytic metabolism/ Antitumor	METTL3 depletion decreased PDK4 expression and increased sensitivity to doxorubicin treatment in cervical cancer cells	Li et al. (2020c)
METTL3	STM2457	Antitumor	STM2457 by targeting METTL3 increased apoptosis and reduced AML growth treating myeloid leukemia	Yankova et al. (2021)
METTL3	Cisplatin, Gemcitabine, 5-fluorouracil	Antitumor	Depleting METTL3 from cells induced resistance to cisplatin, gemcitabine, and 5-fluorouracil in pancreatic cancer and non-small cell lung cancer	Jin et al. (2019)
METTL3	Gamma-irradiation	Antitumor	METTL3-silenced pancreatic cancer cells and glioma stem cells showed enhanced irradiation sensitivity	Visvanathan et al. (2018)
FTO	R-2HG	Metabolic regulation/ Antitumor	R-2HG, highly expressed by isocitrate dehydrogenase, inhibit FTO and act an antitumor in glioma and leukemisa cells	Su et al. (2018)
FTO	Entacapone	Metabolic regulation/ Antitumor	Entacapone bound to FTO and inhibited FTO activity involved in the regulation of metabolic homeostasis and amino acid metabolism	Peng et al. (2019)
FTO	FB23 and FB23-2	Antitumor	Targeting FTO, FB23 and FB23-2 are effective promise in preclinical models against acute myeloid leukemia	Huang et al. (2019)
FTO	Tyrosine kinase inhibitor (TKI)	Immunity control	Disregulated FTO help tumor cells to escape TKI-mediated killing and broad defense mechanism by which leukemia cells develop resistance mechanism to TKI	Yan et al. (2018)
FTO	Dac51	Antitumor/Immunity control	Small molecule Dac51 can block FTO-mediated immune evasion and control immunity against cancer cells	Liu et al. (2021)
FTO	Glycolytic agents	Immunity control	Disregulated complex FTO - glycolytic agents help tumor cells to escape immune surveillance	Liu et al. (2021)
FTO	Anti-PD-1 blockade	Antitumor immunity	Knockdown of FTO sensitizes melanoma cells to interferon-gamma (IFNγ) and sensitizes melanoma to anti-PD-1 treatment in mice	Yang et al. (2019)
FTO	Temozolomide (TMZ)	Glycolytic metabolism/ Antitumor	JPX/FTO/PDK1 axis facilitate aerobic glycolysis in GBM cells, and correlated with GBM cells' sensitivity to temozolomide	Li et al. (2021)
YTHDF1	Cisplatin	Amino acid metabolism/ Antitumor	YTHDF1 is associated with cisplatin resistance in colon cancer.Inhibition of GLS1 synergized with cisplatin to induce cell death of colon cancer cells	Chen et al. (2021b)
YTHDF1	PD-L1 inhibitor	Antitumor immunity	YTHDF1 regulate antitumor immunity and have synergetic effect on immunotherapy by improving the therapeutic effect of PD-L1 inhibitor	Han et al. (2019)
YTHDF2	STAT5	Immune response	Upon activation by cytokines, YTHDF2 is upregulated in NK Cells. YTHDF2 promoted NK Cell effector function by inhibiting a STAT5-YTHDF2-positive feedback loop involved in tumor progression	Ma et al. (2021)

molecular inhibitor of FTO and selected m6A demethylase FTO as a potential target by developing a new strategy. By studying the molecular function of FTO in metabolism, they identified entacapone (FDA-approved drug) as a selective inhibitor of FTO activity involved in the regulation of metabolic homeostasis (Peng et al., 2019). Entacapone bound to FTO and inhibited FTO activity. They conclude that the FTO-entacapone complex may be promising for designing new drug-like FTO inhibitors as translational medicine (Peng et al., 2019). Furthermore, they discovered that the transcription factor forkhead box protein O1 (FOXO1) mRNA as a substrate of FTO, which Knockdown of FOXO1 through the inhibition of FTO could be used to treat metabolic dysregulation (Peng et al., 2019).

Targeting YTHDF1 (a reader) might be another promising therapeutic approach, as (Liu et al., 2020) identified the YTHDF1-EIF3C axis as a critical translational factor involved in ovarian cancer progression (Liu et al., 2020). Chen and collaborators (2021) recently reported that YTHDF1 is associated positively with cisplatin resistance in colon cancer (Chen et al., 2021a; Chen et al., 2021b). Furthermore, inhibition of GLS1 synergized with cisplatin to induce cell death of colon cancer cells (Chen et al., 2021b). Recently, Kumar et al., 2021 reviewed how components of EEE (Editor/Eraser/Effector) could become potential candidates for treating leukemia (Kumar et al., 2021).

Regarding immunotherapy against cancer cells, FTO was identified as an essential regulator of glycolytic metabolism that tumors could use to escape immune surveillance (Liu et al., 2021). Consistent with this idea, depleting FTO impaired the glycolytic activity of tumor cells to restore the $CD8^+$ T cell function needed to inhibit tumor growth (Liu et al., 2021). Moreover, Dac51 (a small molecule) can block FTO-mediated immune evasion and control immunity, suggesting that RNA epitranscriptome could promise a new strategy for immunotherapy against cancer cells (Liu et al., 2021).

On the other hand, Yang et al. (2019) demonstrate that the effect of FTO knockdown on melanoma response to anti-PD-1 (a novel immunotherapies for the patient with melanomas) immunotherapy is dependent on the immune system. The combination of m^{6}A demethylase FTO inhibition with anti-PD-1 blockade may reduce the resistance to immunotherapy in melanoma (Yang et al., 2019). Additionally, FTO depletion sensitizes melanoma cells to interferon-gamma (IFNγ) and sensitizes melanoma to anti-PD-1 treatment (Yang et al., 2019). Their findings suggest a crucial role of FTO, which

increases FTO's level, decreases response to anti-PD-1 blockade immunotherapy, and enhances tumor growth in melanoma (Yang et al., 2019). One other recent study demonstrates that the YTHDF1 reader regulated antitumor immunity, a synergetic effect on immunotherapy by improving the therapeutic effect of PD-L1 inhibitors (Han et al., 2019). Yan and collaborators demonstrate that FTO-m^{6}A axis deregulation induces response to tyrosine kinase inhibitor (TKI) treatment in leukemia cells (Yan et al., 2018). Cells with FTO upregulation have more TKI tolerance and higher growth rates in mice (Yan et al., 2018). Currently, Li and collaborators demonstrated that the JPX/FTO/PDK1 axis could facilitate aerobic glycolysis in GBM cells, which was correlated with GBM cells' sensitivity to temozolomide (TMZ). These findings provide valuable information for understanding that blocking the JPX/FTO/PDK1 axis may serve as a promising strategy for mitigating the efficacy of TMZ in GBM(Li et al., 2021).

By elucidating the biological roles of m^{6}A's modification in natural killer (NK) cells, Ma and collaborators uncovered a new direction for harnessing NK Cell antitumor immunity. YTHDF2 deficiency in NK Cells impaired NK Cells' antitumor and antiviral activity *in vivo*. Upon activation by cytokines, YTHDF2 is upregulated in NK Cells. More interestingly, YTHDF2 promoted NK Cell effector function by inhibiting a STAT5-YTHDF2-positive feedback loop involved in tumor progression (Ma et al., 2021). These findings suggested that m^{6}A and its regulatory or associated proteins are involved in cancer progression. The development of new applicable inhibitors or the translation of existing inhibitors into clinical practice may provide innovative and effective therapeutic strategies for treatment (**Table 3**).

CONCLUSION AND PERSPECTIVES

The connection between metabolism and tumorigenesis is attracting attention, and many gratifying results have revealed the link between the m^{6}A modification and oncometabolite in cancer progression. The data demonstrates that the m^{6}A modification regulators could act as promising candidates for diagnosis, prognosis, or treatment against cancer. Thus, designing a diagnostic profile for cancer is possible based on oncometabolite regulated by m^{6}A. In this review, the potential crosstalk between m^{6}A RNA methylation and metabolic control in tumorigenesis was described. These findings build a link between metabolic reprogramming and the m^{6}A modification. As investigators have focused mostly on glucose metabolism and performed *in vitro* studies with cell lines, their investigations need to be validated in animal models and clinical studies.

As integrated regulation of metabolism in cancers, the network of several major anabolic and catabolic pathways are important co-factors or substrates of the critical enzymes for RNA modifications. Since many of the metabolic alterations and consequently aberrated RNA regulation are common to a wide range of cancer types, they can serve as promising targets for anti-cancer therapies. Considering current efforts to target both cancer metabolism and regulation of the epigenome, it is still elusive to fully clarify the critical downstream factors functions mediated by some oncometabolite in cancer cells. Understanding the integrated metabolism in cancer cells may open new avenues for anti-cancer strategies. Therefore, determining metabolic differences between normal proliferating and cancer cells will be of great interest. Nevertheless, heterogeneity of tumors is yet another challenge, which is multiples phenotypes metabolic in multi-cellular systems. In addition, more researches should be conducted to better understand the molecular mechanisms among metabolic enzymes, transporters, transcription factors, and their pathways regulated by the m^{6}A modification in cancer metabolism.

By pharmacological approach, evidence has shown that characterization of m^{6}A writers and erasers proteins have provided valuable insights promising anti-cancer drugs targeting modification in cancer. While several small-molecule inhibitors targeting writers or erasers are either approved drugs or are currently being evaluated in clinical trials, the targeting m^{6}A recognition proteins have lagged behind. After writers and erasers carry out methylation and demethylation, the readers determine the functional consequences of modification. Thus, more investigations and pharmacological research needs to target m^{6}A readers in cancer progression to yield meaningful results.

Most importantly, attempts to target m^{6}A pathways and their associated metabolic pathways need to consider immune cells, as m^{6}A was recently reported to play roles in antitumor immunity, immune responses, and immunotherapy in cancers (Liu et al., 2021; Ma et al., 2021). Such an approach will help us better understand and fully clarify how the dysregulation of metabolism by m^{6}A in tumorigenesis jeopardizes immune surveillance. As well as regulating glucose, amino acids, and lipids, m^{6}A can regulate other metabolites, such as SAM, SAH, IDH, R-2HG, vitamin C, and iron. It will be interesting to understand how the m^{6}A modification affects those compounds and how that knowledge could enhance cancer treatment. As m^{6}A often alters metabolism, some metabolites might also regulate the production, editing, and recognition of m^{6}A to affect cancer progression. Due to this controversial idea, it will also be interesting to discover how metabolite signaling networks regulate m^{6}A in cancer and how they, in turn, could be regulated.

AUTHOR CONTRIBUTIONS

PY, JY and TL conceived the review. YM and XL wrote the manuscript. PY, JY and TL. revised the manuscript with feedback from YM and XL All authors approved the manuscript for publication.

REFERENCES

Aik, W., Demetriades, M., Hamdan, M. K. K., Bagg, E. A. L., Yeoh, K. K., Lejeune, C., et al. (2013). Structural Basis for Inhibition of the Fat Mass and Obesity Associated Protein (FTO). *J. Med. Chem.* 56, 3680–3688. doi:10.1021/jm400193d

Alarcón, C. R., Goodarzi, H., Lee, H., Liu, X., Tavazoie, S., and Tavazoie, S. F. (2015). HNRNPA2B1 Is a Mediator of m6A-dependent Nuclear RNA Processing Events. *Cell* 162, 1299–1308. doi:10.1016/j.cell.2015.08.011

Ancey, P. B., Contat, C., and Meylan, E. (2018). Glucose Transporters in Cancer - from Tumor Cells to the Tumor Microenvironment. *Febs J.* 285, 2926–2943. doi:10.1111/febs.14577

Bartosovic, M., Molares, H. C., Gregorova, P., Hrossova, D., Kudla, G., and Vanacova, S. (2017). N6-methyladenosine Demethylase FTO Targets Pre-mRNAs and Regulates Alternative Splicing and 3′-end Processing. *Nucleic Acids Res.* 45, 11356–11370. doi:10.1093/nar/gkx778

Casasampere, M., Ordoñez, Y. F., Pou, A., and Casas, J. (2016). Inhibitors of Dihydroceramide Desaturase 1: Therapeutic Agents and Pharmacological Tools to Decipher the Role of Dihydroceramides in Cell Biology. *Chem. Phys. Lipids* 197, 33–44. doi:10.1016/j.chemphyslip.2015.07.025

Cheeseman, C. (2008). GLUT7: a New Intestinal Facilitated Hexose Transporter. *Am. J. Physiology-Endocrinology Metab.* 295, E238–E241. doi:10.1152/ajpendo.90394.2008

Chen, H., Gao, S., Liu, W., Wong, C.-C., Wu, J., Wu, J., et al. (2021a). RNA N6-Methyladenosine Methyltransferase METTL3 Facilitates Colorectal Cancer by Activating the m6A-GLUT1-mTORC1 Axis and Is a Therapeutic Target. *Gastroenterology* 160, 1284–1300. e1216. doi:10.1053/j.gastro.2020.11.013

Chen, J., Zhang, S., Li, Y., Tang, Z., and Kong, W. (2014). Hexokinase 2 Overexpression Promotes the Proliferation and Survival of Laryngeal Squamous Cell Carcinoma. *Tumor Biol.* 35, 3743–3753. doi:10.1007/s13277-013-1496-2

Chen, J., Zhang, Y.-C., Huang, C., Shen, H., Sun, B., Cheng, X., et al. (2019a). m6A Regulates Neurogenesis and Neuronal Development by Modulating Histone Methyltransferase Ezh2. *Genomics, Proteomics & Bioinformatics* 17, 154–168. doi:10.1016/j.gpb.2018.12.007

Chen, P., Liu, X.-q., Lin, X., Gao, L.-y., Zhang, S., and Huang, X. (2021b). Targeting YTHDF1 Effectively Re-sensitizes Cisplatin-Resistant colon Cancer Cells by Modulating GLS-Mediated Glutamine Metabolism. *Mol. Ther. - Oncolytics* 20, 228–239. doi:10.1016/j.omto.2021.01.001

Chen, X.-Y., Zhang, J., and Zhu, J.-S. (2019b). The Role of m6A RNA Methylation in Human Cancer. *Mol. Cancer* 18, 103. doi:10.1186/s12943-019-1033-z

Chen, Y., Peng, C., Chen, J., Chen, D., Yang, B., He, B., et al. (2019c). WTAP Facilitates Progression of Hepatocellular Carcinoma via m6A-HuR-dependent Epigenetic Silencing of ETS1. *Mol. Cancer* 18, 127. doi:10.1186/s12943-019-1053-8

Choe, J., Lin, S., Zhang, W., Liu, Q., Wang, L., Ramirez-Moya, J., et al. (2018). mRNA Circularization by METTL3-eIF3h Enhances Translation and Promotes Oncogenesis. *Nature* 561, 556–560. doi:10.1038/s41586-018-0538-8

Curi, R., Lagranha, C. J., Doi, S. Q., Sellitti, D. F., Procopio, J., Pithon-Curi, T. C., et al. (2005). Molecular Mechanisms of Glutamine Action. *J. Cel. Physiol.* 204, 392–401. doi:10.1002/jcp.20339

Devedjiev, Y., Steussy, C. N., and Vassylyev, D. G. (2007). Crystal Structure of an Asymmetric Complex of Pyruvate Dehydrogenase Kinase 3 with Lipoyl Domain 2 and its Biological Implications. *J. Mol. Biol.* 370, 407–416. doi:10.1016/j.jmb.2007.04.083

Doherty, J. R., and Cleveland, J. L. (2013). Targeting Lactate Metabolism for Cancer Therapeutics. *J. Clin. Invest.* 123, 3685–3692. doi:10.1172/jci69741

Du, H., Zhao, Y., He, J., Zhang, Y., Xi, H., Liu, M., et al. (2016). YTHDF2 Destabilizes m(6)A-Containing RNA Through Direct Recruitment of the CCR4-NOT Deadenylase Complex. *Nat. Commun.* 7, 12626. doi:10.1038/ncomms12626

Fang, R., Chen, X., Zhang, S., Shi, H., Ye, Y., Shi, H., et al. (2021). EGFR/SRC/ERK-stabilized YTHDF2 Promotes Cholesterol Dysregulation and Invasive Growth of Glioblastoma. *Nat. Commun.* 12, 177. doi:10.1038/s41467-020-20379-7

Faubert, B., Li, K. Y., Cai, L., Hensley, C. T., Kim, J., Zacharias, L. G., et al. (2017). Lactate Metabolism in Human Lung Tumors. *Cell* 171, 358–371. doi:10.1016/j.cell.2017.09.019

Fedeles, B. I., Singh, V., Delaney, J. C., Li, D., and Essigmann, J. M. (2015). The AlkB Family of Fe(II)/α-Ketoglutarate-dependent Dioxygenases: Repairing Nucleic Acid Alkylation Damage and beyond. *J. Biol. Chem.* 290, 20734–20742. doi:10.1074/jbc.r115.656462

Feng, C., Liu, Y., Wang, G., Deng, Z., Zhang, Q., Wu, W., et al. (2014). Crystal Structures of the Human RNA Demethylase Alkbh5 Reveal Basis for Substrate Recognition. *J. Biol. Chem.* 289, 11571–11583. doi:10.1074/jbc.m113.546168

Frezza, C. (2020). Metabolism and Cancer: the Future Is Now. *Br. J. Cancer* 122, 133–135. doi:10.1038/s41416-019-0667-3

Fry, N. J., Law, B. A., Ilkayeva, O. R., Holley, C. L., and Mansfield, K. D. (2017). N6-methyladenosine Is Required for the Hypoxic Stabilization of Specific mRNAs. *Rna* 23, 1444–1455. doi:10.1261/rna.061044.117

Frye, M., Harada, B. T., Behm, M., and He, C. (2018). RNA Modifications Modulate Gene Expression during Development. *Science* 361, 1346–1349. doi:10.1126/science.aau1646

Fu, Y., Jia, G., Pang, X., Wang, R. N., Wang, X., Li, C. J., et al. (2013). FTO-mediated Formation of N6-Hydroxymethyladenosine and N6-Formyladenosine in Mammalian RNA. *Nat. Commun.* 4, 1798. doi:10.1038/ncomms2822

Gaida, M. M., Mayer, C., Dapunt, U., Stegmaier, S., Schirmacher, P., Wabnitz, G. H., et al. (2016). Expression of the Bitter Receptor T2R38 in Pancreatic Cancer: Localization in Lipid Droplets and Activation by a Bacteria-Derived Quorum-sensing Molecule. *Oncotarget* 7, 12623–12632. doi:10.18632/oncotarget.7206

Ganapathy-Kanniappan, S., and Geschwind, J.-F. H. (2013). Tumor Glycolysis as a Target for Cancer Therapy: Progress and Prospects. *Mol. Cancer* 12, 152. doi:10.1186/1476-4598-12-152

Garber, K. (2006). Energy Deregulation: Licensing Tumors to Grow. *Science* 312, 1158–1159. doi:10.1126/science.312.5777.1158

Guo, W., Zhang, C., Feng, P., Li, M., Wang, X., Xia, Y., et al. (2021). M6A Methylation of DEGS2, a Key Ceramide-Synthesizing Enzyme, Is Involved in Colorectal Cancer Progression through Ceramide Synthesis. *Oncogene*. doi:10.1038/s41388-021-01987-z

Halestrap, A. P. (2013). Monocarboxylic Acid Transport. *Compr. Physiol.* 3, 1611–1643. doi:10.1002/cphy.c130008

Han, D., Liu, J., Chen, C., Dong, L., Liu, Y., Chang, R., et al. (2019). Anti-tumour Immunity Controlled through mRNA m6A Methylation and YTHDF1 in Dendritic Cells. *Nature* 566, 270–274. doi:10.1038/s41586-019-0916-x

Hanahan, D., and Weinberg, R. A. (2011). Hallmarks of Cancer: the Next Generation. *Cell* 144, 646–674. doi:10.1016/j.cell.2011.02.013

Hsu, P. J., Zhu, Y., Ma, H., Guo, Y., Shi, X., Liu, Y., et al. (2017). Ythdc2 Is an N6-Methyladenosine Binding Protein that Regulates Mammalian Spermatogenesis. *Cell Res* 27, 1115–1127. doi:10.1038/cr.2017.99

Huang, H., Weng, H., Sun, W., Qin, X., Shi, H., Wu, H., et al. (2018). Recognition of RNA N6-Methyladenosine by IGF2BP Proteins Enhances mRNA Stability and Translation. *Nat. Cel Biol* 20, 285–295. doi:10.1038/s41556-018-0045-z

Huang, Y., Su, R., Sheng, Y., Dong, L., Dong, Z., Xu, H., et al. (2019). Small-Molecule Targeting of Oncogenic FTO Demethylase in Acute Myeloid Leukemia. *Cancer Cell* 35, 677–691. e610. doi:10.1016/j.ccell.2019.03.006

Ignatova, V. V., Stolz, P., Kaiser, S., Gustafsson, T. H., Lastres, P. R., Sanz-Moreno, A., et al. (2020). The rRNA m6A Methyltransferase METTL5 Is Involved in Pluripotency and Developmental Programs. *Genes Dev.* 34, 715–729. doi:10.1101/gad.333369.119

Jin, D., Guo, J., Wu, Y., Du, J., Yang, L., Wang, X., et al. (2019). m6A mRNA Methylation Initiated by METTL3 Directly Promotes YAP Translation and Increases YAP Activity by Regulating the MALAT1-miR-1914-3p-YAP axis to Induce NSCLC Drug Resistance and Metastasis. *J. Hematol. Oncol.* 12, 135. doi:10.1186/s13045-019-0830-6

Jung, M., Mertens, C., Tomat, E., and Brüne, B. (2019). Iron as a Central Player and Promising Target in Cancer Progression. *Int. J. Mol. Sci.* 20. doi:10.3390/ijms20020273

Kandasamy, P., Gyimesi, G., Kanai, Y., and Hediger, M. A. (2018). Amino Acid Transporters Revisited: New Views in Health and Disease. *Trends Biochemical Sciences* 43, 752–789. doi:10.1016/j.tibs.2018.05.003

Kang, H., Zhang, Z., Yu, L., Li, Y., Liang, M., and Zhou, L. (2018). FTO Reduces Mitochondria and Promotes Hepatic Fat Accumulation through RNA Demethylation. *J. Cel. Biochem.* 119, 5676–5685. doi:10.1002/jcb.26746

Khan, M. A., Zubair, H., Anand, S., Srivastava, S. K., Singh, S., and Singh, A. P. (2020). Dysregulation of Metabolic Enzymes in Tumor and Stromal Cells: Role

in Oncogenesis and Therapeutic Opportunities. *Cancer Lett.* 473, 176–185. doi:10.1016/j.canlet.2020.01.003

Knuckles, P., Lence, T., Haussmann, I. U., Jacob, D., Kreim, N., Carl, S. H., et al. (2018). Zc3h13/Flacc Is Required for Adenosine Methylation by Bridging the mRNA-Binding Factor Rbm15/Spenito to the m6A Machinery Component Wtap/Fl(2)d. *Genes Dev.* 32, 415–429. doi:10.1101/gad.309146.117

Kumar, S., Nagpal, R., Kumar, A., Ashraf, M. U., and Bae, Y. S. (2021). Immunotherapeutic Potential of m6A-Modifiers and MicroRNAs in Controlling Acute Myeloid Leukaemia. *Biomedicines* 9. doi:10.3390/biomedicines9060690

Lewis, C. J. T., Pan, T., and Kalsotra, A. (2017). RNA Modifications and Structures Cooperate to Guide RNA-Protein Interactions. *Nat. Rev. Mol. Cel Biol* 18, 202–210. doi:10.1038/nrm.2016.163

Li, A., Chen, Y.-S., Ping, X.-L., Yang, X., Xiao, W., Yang, Y., et al. (2017a). Cytoplasmic m6A Reader YTHDF3 Promotes mRNA Translation. *Cel Res* 27, 444–447. doi:10.1038/cr.2017.10

Li, H., Su, Q., Li, B., Lan, L., Wang, C., Li, W., et al. (2020a). High Expression of WTAP Leads to Poor Prognosis of Gastric Cancer by Influencing Tumour-associated T Lymphocyte Infiltration. *J. Cel Mol Med* 24, 4452–4465. doi:10.1111/jcmm.15104

Li, J., Zhu, L., Shi, Y., Liu, J., Lin, L., and Chen, X. (2019a). m6A Demethylase FTO Promotes Hepatocellular Carcinoma Tumorigenesis via Mediating PKM2 Demethylation. *Am. J. Transl Res.* 11, 6084–6092.

Li, T., Hu, P.-S., Zuo, Z., Lin, J.-F., Li, X., Wu, Q.-N., et al. (2019b). METTL3 Facilitates Tumor Progression via an m6A-igf2bp2-dependent Mechanism in Colorectal Carcinoma. *Mol. Cancer* 18, 112. doi:10.1186/s12943-019-1038-7

Li, X. D., Wang, M. J., Zheng, J. L., Wu, Y. H., Wang, X., and Jiang, X. B. (2021). Long Noncoding RNA Just Proximal to X-inactive Specific Transcript Facilitates Aerobic Glycolysis and Temozolomide Chemoresistance by Promoting Stability of PDK1 mRNA in an m6A-dependent Manner in Glioblastoma Multiforme Cells. *Cancer Sci.* 112, 4543–4552. doi:10.1111/cas.15072

Li, Z., Li, F., Peng, Y., Fang, J., and Zhou, J. (2020b). Identification of Three m6A-related mRNAs Signature and Risk Score for the Prognostication of Hepatocellular Carcinoma. *Cancer Med.* 9, 1877–1889. doi:10.1002/cam4.2833

Li, Z., Peng, Y., Li, J., Chen, Z., Chen, F., Tu, J., et al. (2020c). N6-methyladenosine Regulates Glycolysis of Cancer Cells through PDK4. *Nat. Commun.* 11, 2578. doi:10.1038/s41467-020-16306-5

Li, Z., Weng, H., Su, R., Weng, X., Zuo, Z., Li, C., et al. (2017b). FTO Plays an Oncogenic Role in Acute Myeloid Leukemia as a N 6 -Methyladenosine RNA Demethylase. *Cancer Cell* 31, 127–141. doi:10.1016/j.ccell.2016.11.017

Li, Z., and Zhang, H. (2016). Reprogramming of Glucose, Fatty Acid and Amino Acid Metabolism for Cancer Progression. *Cell. Mol. Life Sci.* 73, 377–392. doi:10.1007/s00018-015-2070-4

Lin, S., Choe, J., Du, P., Triboulet, R., and Gregory, R. I. (2016). The M 6 A Methyltransferase METTL3 Promotes Translation in Human Cancer Cells. *Mol. Cel* 62, 335–345. doi:10.1016/j.molcel.2016.03.021

Lin, Y., Wei, X., Jian, Z., and Zhang, X. (2020). METTL3 Expression Is Associated with Glycolysis Metabolism and Sensitivity to Glycolytic Stress in Hepatocellular Carcinoma. *Cancer Med.* 9, 2859–2867. doi:10.1002/cam4.2918

Liu, J., Eckert, M. A., Harada, B. T., Liu, S.-M., Lu, Z., Yu, K., et al. (2018). m6A mRNA Methylation Regulates AKT Activity to Promote the Proliferation and Tumorigenicity of Endometrial Cancer. *Nat. Cel Biol* 20, 1074–1083. doi:10.1038/s41556-018-0174-4

Liu, J., Yue, Y., Han, D., Wang, X., Fu, Y., Zhang, L., et al. (2014). A METTL3-METTL14 Complex Mediates Mammalian Nuclear RNA N6-Adenosine Methylation. *Nat. Chem. Biol.* 10, 93–95. doi:10.1038/nchembio.1432

Liu, N., Dai, Q., Zheng, G., He, C., Parisien, M., and Pan, T. (2015). N6-methyladenosine-dependent RNA Structural Switches Regulate RNA-Protein Interactions. *Nature* 518, 560–564. doi:10.1038/nature14234

Liu, T., Wei, Q., Jin, J., Luo, Q., Liu, Y., Yang, Y., et al. (2020). The m6A Reader YTHDF1 Promotes Ovarian Cancer Progression via Augmenting EIF3C Translation. *Nucleic Acids Res.* 48, 3816–3831. doi:10.1093/nar/gkaa048

Liu, Y., Liang, G., Xu, H., Dong, W., Dong, Z., Qiu, Z., et al. (2021). Tumors Exploit FTO-Mediated Regulation of Glycolytic Metabolism to Evade Immune Surveillance. *Cell Metab.* doi:10.1016/j.cmet.2021.04.001

Losman, J.-A., Koivunen, P., and Kaelin, W. G., Jr. (2020). 2-Oxoglutarate-dependent Dioxygenases in Cancer. *Nat. Rev. Cancer* 20, 710–726. doi:10.1038/s41568-020-00303-3

Ma, H., Wang, X., Cai, J., Dai, Q., Natchiar, S. K., Lv, R., et al. (2019). N6-Methyladenosine Methyltransferase ZCCHC4 Mediates Ribosomal RNA Methylation. *Nat. Chem. Biol.* 15, 88–94. doi:10.1038/s41589-018-0184-3

Ma, J. z., Yang, F., Zhou, C. c., Liu, F., Yuan, J. h., Wang, F., et al. (2017). METTL14 Suppresses the Metastatic Potential of Hepatocellular Carcinoma by Modulating N 6 -methyladenosine-dependent Primary MicroRNA Processing. *Hepatology* 65, 529–543. doi:10.1002/hep.28885

Ma, S., Yan, J., Barr, T., Zhang, J., Chen, Z., Wang, L. S., et al. (2021). The RNA m6A Reader YTHDF2 Controls NK Cell Antitumor and Antiviral Immunity. *J. Exp. Med.* 218. doi:10.1084/jem.20210279

Macheda, M. L., Rogers, S., and Best, J. D. (2005). Molecular and Cellular Regulation of Glucose Transporter (GLUT) Proteins in Cancer. *J. Cel. Physiol.* 202, 654–662. doi:10.1002/jcp.20166

Matés, J. M., Segura, J. A., Martín-Rufián, M., Campos-Sandoval, J. A., Alonso, F. J., and Márquez, J. (2013). Glutaminase Isoenzymes as Key Regulators in Metabolic and Oxidative Stress against Cancer. *Curr. Mol. Med.* 13, 514–534.

Meyer, K. D., Patil, D. P., Zhou, J., Zinoviev, A., Skabkin, M. A., Elemento, O., et al. (2015). 5′ UTR m6A Promotes Cap-independent Translation. *Cell* 163, 999–1010. doi:10.1016/j.cell.2015.10.012

Mizuno, T. M., Lew, P. S., Luo, Y., and Leckstrom, A. (2017). Negative Regulation of Hepatic Fat Mass and Obesity Associated (Fto) Gene Expression by Insulin. *Life Sci.* 170, 50–55. doi:10.1016/j.lfs.2016.11.027

Murai, T. (2015). Lipid Raft-Mediated Regulation of Hyaluronan-CD44 Interactions in Inflammation and Cancer. *Front. Immunol.* 6, 420. doi:10.3389/fimmu.2015.00420

Murugan, A. K. (2019). mTOR: Role in Cancer, Metastasis and Drug Resistance. *Semin. Cancer Biol.* 59, 92–111. doi:10.1016/j.semcancer.2019.07.003

Nath, A., and Chan, C. (2016). Genetic Alterations in Fatty Acid Transport and Metabolism Genes Are Associated with Metastatic Progression and Poor Prognosis of Human Cancers. *Sci. Rep.* 6, 18669. doi:10.1038/srep18669

Patel, M. S., and Korotchkina, L. G. (2006). Regulation of the Pyruvate Dehydrogenase Complex. *Biochem. Soc. Trans.* 34, 217–222. doi:10.1042/bst0340217

Pendleton, K. E., Chen, B., Liu, K., Hunter, O. V., Xie, Y., Tu, B. P., et al. (2017). The U6 snRNA M 6 A Methyltransferase METTL16 Regulates SAM Synthetase Intron Retention. *Cell* 169, 824–835. e814. doi:10.1016/j.cell.2017.05.003

Peng, S., Xiao, W., Ju, D., Sun, B., Hou, N., Liu, Q., et al. (2019). Identification of Entacapone as a Chemical Inhibitor of FTO Mediating Metabolic Regulation through FOXO1. *Sci. Transl Med.* 11. doi:10.1126/scitranslmed.aau7116

Ping, X.-L., Sun, B.-F., Wang, L., Xiao, W., Yang, X., Wang, W.-J., et al. (2014). Mammalian WTAP Is a Regulatory Subunit of the RNA N6-Methyladenosine Methyltransferase. *Cel Res* 24, 177–189. doi:10.1038/cr.2014.3

Priolo, C., Pyne, S., Rose, J., Regan, E. R., Zadra, G., Photopoulos, C., et al. (2014). AKT1 and MYC Induce Distinctive Metabolic Fingerprints in Human Prostate Cancer. *Cancer Res.* 74, 7198–7204. doi:10.1158/0008-5472.can-14-1490

Qing, Y., Dong, L., Gao, L., Li, C., Li, Y., Han, L., et al. (2021). R-2-hydroxyglutarate Attenuates Aerobic Glycolysis in Leukemia by Targeting the FTO/m6A/PFKP/LDHB axis. *Mol. Cel* 81, 922–939. e929. doi:10.1016/j.molcel.2020.12.026

Roundtree, I. A., Luo, G. Z., Zhang, Z., Wang, X., Zhou, T., Cui, Y., et al. (2017b). YTHDC1 Mediates Nuclear export of N6-Methyladenosine Methylated mRNAs. *Elife* 6. doi:10.7554/eLife.31311

Roundtree, I. A., Evans, M. E., Pan, T., and He, C. (2017a). Dynamic RNA Modifications in Gene Expression Regulation. *Cell* 169, 1187–1200. doi:10.1016/j.cell.2017.05.045

Schulze, A., and Harris, A. L. (2012). How Cancer Metabolism Is Tuned for Proliferation and Vulnerable to Disruption. *Nature* 491, 364–373. doi:10.1038/nature11706

Shaw, R. J. (2006). Glucose Metabolism and Cancer. *Curr. Opin. Cel. Biol.* 18, 598–608. doi:10.1016/j.ceb.2006.10.005

Shen, C., Xuan, B., Yan, T., Ma, Y., Xu, P., Tian, X., et al. (2020). m6A-dependent Glycolysis Enhances Colorectal Cancer Progression. *Mol. Cancer* 19, 72. doi:10.1186/s12943-020-01190-w

Shen, F., Huang, W., Huang, J.-T., Xiong, J., Yang, Y., Wu, K., et al. (2015). DecreasedN6-Methyladenosine in Peripheral Blood RNA from Diabetic

Patients Is Associated WithFTOExpression rather ThanALKBH5. *J. Clin. Endocrinol. Metab.* 100, E148–E154. doi:10.1210/jc.2014-1893

Shen, R. (2020). Commentary on 'Metabolic Reprogramming-associated Genes Predict Overall Survival for Rectal Cancer'. *J. Cel. Mol. Med.* 24, 12862–12863. doi:10.1111/jcmm.15938

Sheng, H., Li, Z., Su, S., Sun, W., Zhang, X., Li, L., et al. (2020). YTH Domain Family 2 Promotes Lung Cancer Cell Growth by Facilitating 6-phosphogluconate Dehydrogenase mRNA Translation. *Carcinogenesis* 41, 541–550. doi:10.1093/carcin/bgz152

Shi, H., Wang, X., Lu, Z., Zhao, B. S., Ma, H., Hsu, P. J., et al. (2017). YTHDF3 Facilitates Translation and Decay of N6-Methyladenosine-Modified RNA. *Cel Res* 27, 315–328. doi:10.1038/cr.2017.15

Shi, H., Wei, J., and He, C. (2019). Where, when, and How: Context-dependent Functions of RNA Methylation Writers, Readers, and Erasers. *Mol. Cel* 74, 640–650. doi:10.1016/j.molcel.2019.04.025

Sivanand, S., and Vander Heiden, M. G. (2020). Emerging Roles for Branched-Chain Amino Acid Metabolism in Cancer. *Cancer Cell* 37, 147–156. doi:10.1016/j.ccell.2019.12.011

Sledz, P., and Jinek, M. (2016). Structural Insights into the Molecular Mechanism of the M(6)A Writer Complex. Elife *5*.

Stacpoole, P. W. (2017). Therapeutic Targeting of the Pyruvate Dehydrogenase Complex/Pyruvate Dehydrogenase Kinase (PDC/PDK) Axis in Cancer. *J. Natl. Cancer Inst.* 109. doi:10.1093/jnci/djx071

Stattin, P., Björ, O., Ferrari, P., Lukanova, A., Lenner, P., Lindahl, B., et al. (2007). Prospective Study of Hyperglycemia and Cancer Risk. *Diabetes care* 30, 561–567. doi:10.2337/dc06-0922

Strowitzki, M. J., Radhakrishnan, P., Pavicevic, S., Scheer, J., Kimmer, G., Ritter, A. S., et al. (2019). High Hepatic Expression of PDK4 Improves Survival upon Multimodal Treatment of Colorectal Liver Metastases. *Br. J. Cancer* 120, 675–688. doi:10.1038/s41416-019-0406-9

Su, R., Dong, L., Li, C., Nachtergaele, S., Wunderlich, M., Qing, Y., et al. (2018). R-2HG Exhibits Anti-tumor Activity by Targeting FTO/m6A/MYC/CEBPA Signaling. *Cell* 172, 90–105. e123. doi:10.1016/j.cell.2017.11.031

Swierczynski, J., Hebanowska, A., and Sledzinski, T. (2014). Role of Abnormal Lipid Metabolism in Development, Progression, Diagnosis and Therapy of Pancreatic Cancer. *Wjg* 20, 2279–2303. doi:10.3748/wjg.v20.i9.2279

Taketo, K., Konno, M., Asai, A., Koseki, J., Toratani, M., Satoh, T., et al. (2018). The Epitranscriptome m6A Writer METTL3 Promotes Chemo- and Radioresistance in Pancreatic Cancer Cells. *Int. J. Oncol.* 52, 621–629. doi:10.3892/ijo.2017.4219

Ueda, Y., Ooshio, I., Fusamae, Y., Kitae, K., Kawaguchi, M., Jingushi, K., et al. (2017). AlkB Homolog 3-mediated tRNA Demethylation Promotes Protein Synthesis in Cancer Cells. *Sci. Rep.* 7, 42271. doi:10.1038/srep42271

Vander Heiden, M. G., Cantley, L. C., and Thompson, C. B. (2009). Understanding the Warburg Effect: the Metabolic Requirements of Cell Proliferation. *Science* 324, 1029–1033. doi:10.1126/science.1160809

Vettore, L., Westbrook, R. L., and Tennant, D. A. (2020). New Aspects of Amino Acid Metabolism in Cancer. *Br. J. Cancer* 122, 150–156. doi:10.1038/s41416-019-0620-5

Viale, A., Pettazzoni, P., Lyssiotis, C. A., Ying, H., Sánchez, N., Marchesini, M., et al. (2014). Oncogene Ablation-Resistant Pancreatic Cancer Cells Depend on Mitochondrial Function. *Nature* 514, 628–632. doi:10.1038/nature13611

Visvanathan, A., Patil, V., Arora, A., Hegde, A. S., Arivazhagan, A., Santosh, V., et al. (2018). Essential Role of METTL3-Mediated m6A Modification in Glioma Stem-like Cells Maintenance and Radioresistance. *Oncogene* 37, 522–533. doi:10.1038/onc.2017.351

Wang, K., Jiang, L., Zhang, Y., and Chen, C. (2020a). Progression of Thyroid Carcinoma Is Promoted by the m6A Methyltransferase METTL3 through Regulating m6A Methylation on TCF1. *Ott* 13, 1605–1612. doi:10.2147/ott.s234751

Wang, L., Song, C., Wang, N., Li, S., Liu, Q., Sun, Z., et al. (2020b). NADP Modulates RNA m6A Methylation and Adipogenesis via Enhancing FTO Activity. *Nat. Chem. Biol.* 16, 1394–1402. doi:10.1038/s41589-020-0601-2

Wang, Q., Chen, C., Ding, Q., Zhao, Y., Wang, Z., Chen, J., et al. (2020c). METTL3-mediated m6A Modification of HDGF mRNA Promotes Gastric Cancer Progression and Has Prognostic Significance. *Gut* 69, 1193–1205. doi:10.1136/gutjnl-2019-319639

Wang, S., Sun, C., Li, J., Zhang, E., Ma, Z., Xu, W., et al. (2017). Roles of RNA Methylation by Means of N6-Methyladenosine (m6A) in Human Cancers. *Cancer Lett.* 408, 112–120. doi:10.1016/j.canlet.2017.08.030

Wang, X., Zhao, B. S., Roundtree, I. A., Lu, Z., Han, D., Ma, H., et al. (2015). N6-methyladenosine Modulates Messenger RNA Translation Efficiency. *Cell* 161, 1388–1399. doi:10.1016/j.cell.2015.05.014

Wang, Y., Buyse, J., Song, Z., Decuypere, E., and Everaert, N. (2016a). AMPK Is Involved in the Differential Neonatal Performance of Chicks Hatching at Different Time. *Gen. Comp. Endocrinol.* 228, 53–59. doi:10.1016/j.ygcen.2016.02.008

Wang, Z.-Y., Loo, T. Y., Shen, J.-G., Wang, N., Wang, D.-M., Yang, D.-P., et al. (2012). LDH-A Silencing Suppresses Breast Cancer Tumorigenicity through Induction of Oxidative Stress Mediated Mitochondrial Pathway Apoptosis. *Breast Cancer Res. Treat.* 131, 791–800. doi:10.1007/s10549-011-1466-6

Wang, Z., Wang, N., Liu, P., and Xie, X. (2016b2012). AMPK and Cancer. *Experientia supplementum* 107, 203–226. doi:10.1007/978-3-319-43589-3_9

Wei, J., Liu, F., Lu, Z., Fei, Q., Ai, Y., He, P. C., et al. (2018). Differential m6A, m6Am, and m1A Demethylation Mediated by FTO in the Cell Nucleus and Cytoplasm. *Mol. Cel* 71, 973–985. doi:10.1016/j.molcel.2018.08.011

Wilson, J. E. (2003). Isozymes of Mammalian Hexokinase: Structure, Subcellular Localization and Metabolic Function. *J. Exp. Biol.* 206, 2049–2057. doi:10.1242/jeb.00241

Wu, B., Li, L., Huang, Y., Ma, J., and Min, J. (2017a). Readers, Writers and Erasers of N6-Methylated Adenosine Modification. *Curr. Opin. Struct. Biol.* 47, 67–76. doi:10.1016/j.sbi.2017.05.011

Wu, J., Hu, L., Wu, F., Zou, L., and He, T. (2017b). Poor Prognosis of Hexokinase 2 Overexpression in Solid Tumors of Digestive System: a Meta-Analysis. *Oncotarget* 8, 32332–32344. doi:10.18632/oncotarget.15974

Xia, T., Wu, X., Cao, M., Zhang, P., Shi, G., Zhang, J., et al. (2019). The RNA m6A Methyltransferase METTL3 Promotes Pancreatic Cancer Cell Proliferation and Invasion. *Pathol. - Res. Pract.* 215, 152666. doi:10.1016/j.prp.2019.152666

Xiang, S., Liang, X., Yin, S., Liu, J., and Xiang, Z. (2020). N6-methyladenosine Methyltransferase METTL3 Promotes Colorectal Cancer Cell Proliferation through Enhancing MYC Expression. *Am. J. Transl Res.* 12, 1789–1806.

Xu, C., Wang, X., Liu, K., Roundtree, I. A., Tempel, W., Li, Y., et al. (2014). Structural Basis for Selective Binding of m6A RNA by the YTHDC1 YTH Domain. *Nat. Chem. Biol.* 10, 927–929. doi:10.1038/nchembio.1654

Xu, G.-L., and Bochtler, M. (2020). Reversal of Nucleobase Methylation by Dioxygenases. *Nat. Chem. Biol.* 16, 1160–1169. doi:10.1038/s41589-020-00675-5

Yan, F., Al-Kali, A., Zhang, Z., Liu, J., Pang, J., Zhao, N., et al. (2018). A Dynamic N6-Methyladenosine Methylome Regulates Intrinsic and Acquired Resistance to Tyrosine Kinase Inhibitors. *Cel Res* 28, 1062–1076. doi:10.1038/s41422-018-0097-4

Yang, G., Sun, Z., and Zhang, N. (2020). Reshaping the Role of m6A Modification in Cancer Transcriptome: a Review. *Cancer Cel Int* 20, 353. doi:10.1186/s12935-020-01445-y

Yang, S., Wei, J., Cui, Y.-H., Park, G., Shah, P., Deng, Y., et al. (2019). m6A mRNA Demethylase FTO Regulates Melanoma Tumorigenicity and Response to Anti-PD-1 Blockade. *Nat. Commun.* 10, 2782. doi:10.1038/s41467-019-10669-0

Yang, X., Shao, F., Guo, D., Wang, W., Wang, J., Zhu, R., et al. (2021). WNT/β-catenin-suppressed FTO Expression Increases m6A of C-Myc mRNA to Promote Tumor Cell Glycolysis and Tumorigenesis. *Cell Death Dis* 12, 462. doi:10.1038/s41419-021-03739-z

Yankova, E., Blackaby, W., Albertella, M., Rak, J., De Braekeleer, E., Tsagkogeorga, G., et al. (2021). Small Molecule Inhibition of METTL3 as a Strategy against Myeloid Leukaemia. *Nature*. doi:10.1038/s41586-021-03536-w

Ye, J., Wang, Z., Chen, X., Jiang, X., Dong, Z., Hu, S., et al. (2020). YTHDF1-enhanced Iron Metabolism Depends on TFRC m6A Methylation. *Theranostics* 10, 12072–12089. doi:10.7150/thno.51231

Yu, H.-L., Ma, X.-D., Tong, J.-F., Li, J.-Q., Guan, X.-J., and Yang, J. (2019). WTAP Is a Prognostic Marker of High-Grade Serous Ovarian Cancer and Regulates the Progression of Ovarian Cancer Cells. *Ott* 12, 6191–6201. doi:10.2147/ott.s205730

Yu, H., Zhao, K., Zeng, H., Li, Z., Chen, K., Zhang, Z., et al. (2021). N6-methyladenosine (m6A) Methyltransferase WTAP Accelerates the Warburg Effect of Gastric Cancer through Regulating HK2 Stability. *Biomed. Pharmacother.* 133, 111075. doi:10.1016/j.biopha.2020.111075

Yue, C., Chen, J., Li, Z., Li, L., Chen, J., and Guo, Y. (2020). microRNA-96 Promotes Occurrence and Progression of Colorectal Cancer via Regulation of the AMPKα2-FTO-m6A/MYC axis. *J. Exp. Clin. Cancer Res.* 39, 240. doi:10.1186/s13046-020-01731-7

Yue, Y., Liu, J., Cui, X., Cao, J., Luo, G., Zhang, Z., et al. (2018). VIRMA Mediates Preferential m6A mRNA Methylation in 3′UTR and Near Stop Codon and Associates with Alternative Polyadenylation. *Cell Discov* 4, 10. doi:10.1038/s41421-018-0019-0

Zhang, X., Wei, L.-H., Wang, Y., Xiao, Y., Liu, J., Zhang, W., et al. (2019). Structural Insights into FTO's Catalytic Mechanism for the Demethylation of Multiple RNA Substrates. *Proc. Natl. Acad. Sci. USA* 116, 2919–2924. doi:10.1073/pnas.1820574116

Zhao, B. S., Roundtree, I. A., and He, C. (2017). Post-transcriptional Gene Regulation by mRNA Modifications. *Nat. Rev. Mol. Cel Biol* 18, 31–42. doi:10.1038/nrm.2016.132

Zheng, G., Dahl, J. A., Niu, Y., Fedorcsak, P., Huang, C.-M., Li, C. J., et al. (2013). ALKBH5 Is a Mammalian RNA Demethylase that Impacts RNA Metabolism and Mouse Fertility. *Mol. Cel* 49, 18–29. doi:10.1016/j.molcel.2012.10.015

Zhong, L., Liao, D., Zhang, M., Zeng, C., Li, X., Zhang, R., et al. (2019). YTHDF2 Suppresses Cell Proliferation and Growth via Destabilizing the EGFR mRNA in Hepatocellular Carcinoma. *Cancer Lett.* 442, 252–261. doi:10.1016/j.canlet.2018.11.006

Zhong, X., Yu, J., Frazier, K., Weng, X., Li, Y., Cham, C. M., et al. (2018). Circadian Clock Regulation of Hepatic Lipid Metabolism by Modulation of m6A mRNA Methylation. *Cel Rep.* 25, 1816–1828. e1814. doi:10.1016/j.celrep.2018.10.068

Zhou, B., Liu, C., Xu, L., Yuan, Y., Zhao, J., Zhao, W., et al. (2021). N 6 - Methyladenosine Reader Protein YT521-B Homology Domain-Containing 2 Suppresses Liver Steatosis by Regulation of mRNA Stability of Lipogenic Genes. *Hepatology* 73, 91–103. doi:10.1002/hep.31220

Zhu, S., Wang, J.-Z., Chen, D., He, Y.-T., Meng, N., Chen, M., et al. (2020). An Oncopeptide Regulates m6A Recognition by the m6A Reader IGF2BP1 and Tumorigenesis. *Nat. Commun.* 11, 1685. doi:10.1038/s41467-020-15403-9

Zou, D., Dong, L., Li, C., Yin, Z., Rao, S., and Zhou, Q. (2019). The m6A Eraser FTO Facilitates Proliferation and Migration of Human Cervical Cancer Cells. *Cancer Cel Int* 19, 321. doi:10.1186/s12935-019-1045-1

Zuo, X., Chen, Z., Gao, W., Zhang, Y., Wang, J., Wang, J., et al. (2020). M6A-mediated Upregulation of LINC00958 Increases Lipogenesis and Acts as a Nanotherapeutic Target in Hepatocellular Carcinoma. *J. Hematol. Oncol.* 13, 5. doi:10.1186/s13045-019-0839-x

Conflict of Interest: The authors declare that the research was conducted in the absence of any commercial or financial relationships that could be construed as a potential conflict of interest.

Publisher's Note: All claims expressed in this article are solely those of the authors and do not necessarily represent those of their affiliated organizations, or those of the publisher, the editors and the reviewers. Any product that may be evaluated in this article, or claim that may be made by its manufacturer, is not guaranteed or endorsed by the publisher.

frontiers in Cell and Developmental Biology

ORIGINAL RESEARCH
published: 16 February 2022
doi: 10.3389/fcell.2022.842220

Identification of the Expression Patterns and Potential Prognostic Role of 5-Methylcytosine Regulators in Hepatocellular Carcinoma

Yong Liu[1†], Shunzhen Zheng[2†], Tao Wang[1], Ziqi Fang[3], Junjie Kong[1,2] and Jun Liu[1,2]*

[1]Department of Liver Transplantation and Hepatobiliary Surgery, Shandong Provincial Hospital, Cheeloo College of Medicine, Shandong University, Jinan, China, [2]Department of Liver Transplantation and Hepatobiliary Surgery, Shandong Provincial Hospital Affiliated to Shandong First Medical University, Jinan, China, [3]Department of Clinical Laboratory, Shandong Provincial Hospital, Cheeloo College of Medicine, Shandong University, Jinan, China

OPEN ACCESS

Edited by:
Xiao Zhu,
Guangdong Medical University, China

Reviewed by:
Xinyi Zhang,
University of Texas Southwestern Medical Center, United States
Chongming Jiang,
Baylor College of Medicine, United States

***Correspondence:**
Jun Liu
dr_liujun1967@126.com

[†]These authors have contributed equally to this work and share first authorship

Specialty section:
This article was submitted to Epigenomics and Epigenetics, a section of the journal Frontiers in Cell and Developmental Biology

Received: 23 December 2021
Accepted: 28 January 2022
Published: 16 February 2022

Citation:
Liu Y, Zheng S, Wang T, Fang Z, Kong J and Liu J (2022) Identification of the Expression Patterns and Potential Prognostic Role of 5-Methylcytosine Regulators in Hepatocellular Carcinoma. Front. Cell Dev. Biol. 10:842220. doi: 10.3389/fcell.2022.842220

Background: Hepatocellular carcinoma (HCC) is the most common primary liver cancer with a poor prognosis. 5-methylcytosine (m5C) modification plays a nonnegligible role in tumor pathogenesis and progression. However, little is known about the role of m5C regulators in HCC.

Methods: Based on 9 m5C regulators, the m5C modification patterns of HCC samples extracted from public databases were systematically evaluated and correlated with tumor immune and prognosis characteristics. An integrated model called the "m5Cscore" was constructed using principal component analysis, and its prognostic value was evaluated.

Results: Almost all m5C regulators were differentially expressed between HCC and normal tissues. Through unsupervised clustering, three different m5Cclusters were ultimately uncovered; these clusters were characterized by differences in prognosis, immune cell infiltration, and pathway signatures. The m5Cscore was constructed to quantify the m5C modifications of individual patients. Subsequent analysis revealed that the m5Cscore was an independent prognostic factor of HCC and could be a novel indicator to predict the prognosis of HCC.

Conclusion: This study comprehensively explored and systematically profiled the features of m5C modification in HCC. m5C modification patterns play a crucial role in the tumor immune microenvironment (TIME) and prognosis of HCC. The m5Cscore provides a more holistic understanding of m5C modification in HCC and provides a practical tool for predicting the prognosis of HCC. This study will help clinicians identify effective indicators of HCC to improve the poor prognosis of this disease.

Keywords: 5-Methylcytosine, hepatocellular carcinoma, tumor immune microenvironment, m5Cscore, prognosis

INTRODUCTION

Hepatocellular carcinoma (HCC) is the most common primary liver cancer and is currently the third leading cause of cancer-related death worldwide (Bray et al., 2018; Islami et al., 2021). Although effective measures such as HBV vaccine immunization and health education have been implemented, the incidence of HCC has increased from 46.3 per 100,000 to 62.8 per 100,000 between 2005 and 2014 (Bosetti et al., 2014; Sayiner et al., 2017; Hester et al., 2020). Despite improvements in surveillance and treatment, the prognosis of HCC remains poor and the median overall survival (OS) time is only approximately 6–2 months once diagnosed (Bosetti et al., 2014). Prognostic assessment is a crucial step in the management of patients with HCC. An increased concentration of α-fetoprotein (AFP) is associated with poorer prognosis. Disappointingly, relevant studies reported that its sensitivity was approximately 60%, and more worryingly, its specificity was 80% (Marrero et al., 2009; Lok et al., 2010). Other tumor markers, such as angiopoietin 2 or vascular endothelial growth factor, might refine prognostic prediction in statistical modeling, but cannot yet be incorporated into the individual assessment of a specific patient (Forner et al., 2018). Therefore, searching for effective biomarkers for predicting the prognosis of HCC and developing novel targets for HCC treatment are urgent.

RNA modifications, which are more than 150 types of modifications reported thus far, are prevalent posttranscriptional modifications and play a critical role in regulating biological processes (Roundtree et al., 2017; Boccaletto et al., 2018). 5-methylcytosine (m5C), an important posttranscriptional modification, is present in diverse RNA species and participates in many aspects of gene expression, including RNA export, ribosome assembly, translation, and RNA stability (Trixl and Lusser, 2019). Increasing evidence has suggested that m5C modification plays a nonnegligible role in tumor pathogenesis and progression. It was reported that the m5C regulator YBX1 maintained the mRNA stability of the oncogenic gene heparin binding growth factor (HDGF) by binding to m5C methylated sites and recruiting ELAVL1, thus exerting an oncogenic role in bladder cancer development through the activation of HDGF (Chen et al., 2019). In addition, Gao et al. (Gao et al., 2019) found that high expression of NSUN2 could promote the proliferation and tumorigenesis of gallbladder carcinoma cells both *in vitro* and *in vivo* by closely cooperating with ribosomal protein L6. Recently, the role of m5C modification in cancers, including lung cancer, colon carcinoma, bladder cancer, and thyroid carcinoma, has been explored (Pan et al., 2021a; Pan et al., 2021b; Chen et al., 2021; Gao et al., 2021; Geng et al., 2021; Gu et al., 2021; Hu et al., 2021; Li et al., 2021; Liu et al., 2021; Xu et al., 2021). In addition, He et al. (He et al., 2020a) built a gene signature including 2 m5C regulators and found that it could effectively predict the prognosis of HCC. However, the signature is limited to the number of m5C regulators, while their role in the pathogenesis and progression of HCC depends on the interaction among the multiple m5C regulators.

In this study, we systematically evaluated the m5C modification pattern and tumor immune microenvironment (TIME) in HCC patients. We revealed three distinct m5C modification patterns in HCC; these clusters were characterized by differences in prognosis, immune cell infiltration, and pathway signatures. Based on the m5C regulators and related genes, a model (termed "m5Cscore") was constructed to quantify the m5C modification patterns of individual patients. The study also demonstrated that the m5Cscore could serve as a practical tool to predict the prognosis of HCC.

MATERIALS AND METHODS

Data Extraction and Preprocessing

The RNA sequencing data and relevant clinicopathological features of 374 HCC and 50 normal samples were obtained from The Cancer Genome Atlas database (TCGA; https://portal.gdc.cancer.gov/). Gene expression data (measured in fragments per kilobase of exon per million fragments mapped or FPKM) were transformed into transcripts per kilobase million (TPM). Somatic mutation data were extracted from the TCGA data portal. Furthermore, an eligible HCC set was downloaded from the International Cancer Genome Consortium database (ICGC; https://icgc.org/) and served as the validation cohort. All human HCC tissue samples used in this study were obtained from patients who underwent surgery in the Shandong Provincial Hospital Affiliated to Shandong First Medical University. This project was approved by the Ethics Committee of Shandong Provincial Hospital Affiliated to Shandong First Medical University and was performed in accordance with the Declaration of Helsinki. Each participant provided written informed consent.

The Landscape of m5C Regulators in Hepatocellular Carcinoma

A total of 10 m5C regulators were obtained and curated from previous studies (Guo et al., 2021; Bohnsack et al., 2019; Delaunay and Frye, 2019); these regulators included 7 "writers" (NOP2, NSUN2, NUSN3, NSUN4, NSUN5, NSUN6, and NSUN7), 1 "reader" (YBX1), and 2 "erasers" (TET2 and TET3). The expression profile of these regulators was systematically extracted and analyzed in normal and tumor samples. The somatic mutation of HCC was assessed with the "maftools" R package. The tumor mutation burden (TMB) was calculated, and the correlation between TMB and clinical characteristics was evaluated. The expression levels of m5C regulators in special immune cells were investigated using the Tumor Immune Single-Cell Hub (TISCH) (http://tisch.comp-genomics.org/) (Sun et al., 2021). A pie plot was used to show the cell number of each cell type. UMAP and violin plots were used to show the expression of m5C regulators in different immune cell types. The prognostic value of the m5C regulators was assessed using the Kaplan–Meier (KM) curve with log-rank test.

Model-Based Clustering Analysis for m5C Regulators

Based on the expression matrix of m5C regulators, unsupervised clustering was performed to identify distinct m5C modification patterns in HCC patients according to the best cutoff using the "ConsensusClusterPlus" R package, and the stability of clustering was guaranteed by 1,000 repetitions (Wilkerson and Hayes, 2010). The optimal number of clusters was determined by the consensus clustering algorithm. Survival analysis was performed between distinct clusters with the KM method. The differences in the biological processes between the distinct clusters were investigated through gene set variation analysis (GSVA) using the "GSVA" R package. The "c2.cp.kegg.v7.4.symbols" gene set was obtained from the Molecular Signatures Database (MSigDB). An adjusted p value <0.05 was considered statistically significant.

Comparison of the Tumor Immune Microenvironment Between Distinct m5Cclusters

Single-sample gene set enrichment analysis (ssGSEA) was used to quantify the relative infiltration levels of 23 immune cell types in HCC samples (Charoentong et al., 2017). The ratios of the immune stromal components in the tumor microenvironment (TME) were measured using Estimation of Stromal and Immune cells in Malignant Tumor tissues using Expression data (ESTIMATE) analysis with the "estimate" R package (Yoshihara et al., 2013). The differences in the TME between the different clusters were analyzed with the Wilcoxon rank sum test. Furthermore, the "limma" R package was used to investigate the differences in the expression of targeted immune checkpoint molecules between the different clusters.

Identification of Prognosis-Related Differentially Expressed Genes Between the Distinct m5Cclusters

Principal component analysis (PCA) was used to investigate whether there were different m5C modification patterns in HCC. The empirical Bayesian approach was applied to extract differentially expressed genes (DEGs) between the distinct m5Cclusters. The significance criterion of DEGs was set as an adjusted p value <0.001. Gene Ontology (GO) biological process analysis and Kyoto Encyclopedia of Genes and Genomes (KEGG) pathway analysis were performed to investigate the enriched functional annotations of DEGs. A critical value of adjusted p-value = 0.05 was selected as the filter criterion. After obtaining the DEGs, univariate Cox regression analysis was performed to identify prognosis-related genes. The significance criterion was set as an adjusted p value <0.001 and abs (logFC) > 0.

Construction of the m5C Gene Signature

To quantify the m5C modification patterns of individual HCC patients, a set of scoring systems (termed "m5Cscore") was constructed by PCA. Both principal components 1 and 2 were selected to act as signature scores. The m5Cscore was defined using a method similar to the Genomic Grade Index (GGI) (Sotiriou et al., 2006; Zeng et al., 2019):

$$\text{m5Cscore} = \sum (\text{PC1 i} + \text{PC2 i})$$

where i is the expression of overlapping genes with significant prognosis-related DEGs among the m5Cclusters. The m5Cscore was calculated in both the TCGA and ICGC cohorts.

According to the score, samples were divided into high- and low-m5Cscore groups. Correlation analyses were performed to investigate the relationships between the m5Cscore and some related biological pathways, including (Bray et al., 2018) survival analysis, (Islami et al., 2021), immunocorrelation analysis, (Bosetti et al., 2014), clinical correlation analysis, (Hester et al., 2020), TMB, and (Sayiner et al., 2017) targeted immune checkpoint molecules.

The Human Protein Atlas

The immunohistochemistry (IHC) results showing the protein expression of m5C regulators were downloaded from The Human Protein Atlas (HPA) website (https://www.proteinatlas.org/). The corresponding patient information, staining, intensity and quantity were obtained online (**Supplementary Table S1**).

RNA Isolation and Quantitative Real-Time PCR

Total RNA from 10 HCC samples and 10 adjacent tissues was extracted using the FastPure® Cell/Tissue Total RNA Isolation Kit V2 (Vazyme, RC112-01) according to the manufacturer's instructions. The total RNA concentration and purity were detected by a Nanodrop 2000 spectrophotometer (Thermo Fisher, United States). Samples were then reverse-transcribed into cDNA with HiScript® III RT SuperMix for qPCR (Vazyme, RC323-01) according to the manufacturer's protocol. qRT–PCR analysis was performed using ChamQ Universal SYBR qPCR Master Mix (Vazyme, Q711-02/03) on a QuantStudio 3 (Applied Biosystems, United States) to measure the expression levels of m5C regulators. The expression levels of the gene were normalized to β-actin and analyzed by the 2−ΔΔCt method. The primers used in this study are shown in **Supplementary Table S2**.

Statistical Analysis

All statistical analyses were performed with R software (version 4.0.5) and GraphPad Prism software (version 8.3.0). Paired t tests were performed to compare the expression levels of m5C regulators in HCC tissues. Continuous variables were dichotomized for patient survival using the optimal cutoff values determined by the "survminer" R package. The survival curves for the prognostic analysis were constructed by the KM method, and log-rank tests were used to identify the significance of differences. Receiver operating characteristic (ROC) curves (R package "timeROC") and the area under the curve (AUC) values

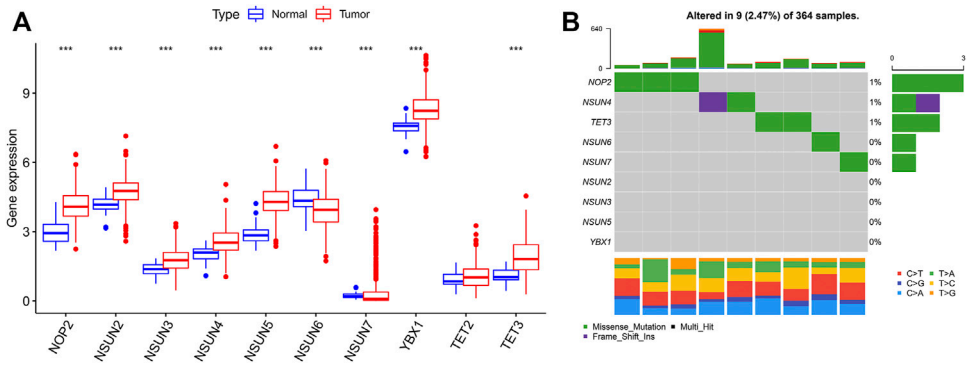

FIGURE 1 | 5C modification pattern in HCC. **(A)** The expression of m5C regulators in tumor and normal tissues; **(B)** The mutation frequency of m5C regulators in HCC (Each column represents a patient with a m5C regulator mutation, and the upper panel shows the tumor mutation burden. 0–3 means the number of patients with mutation, and 0–640 means the total mutation frequency of each patient).

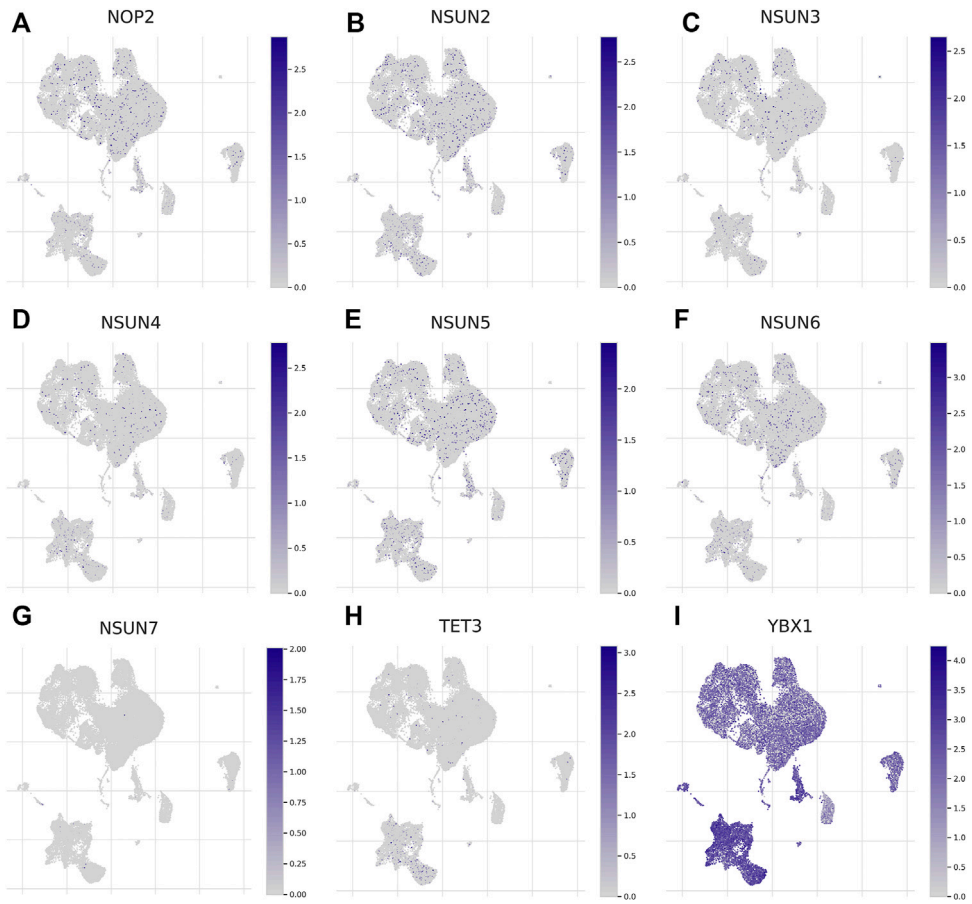

FIGURE 2 | Expression of m5C regulators in tumor microenvironment-related cells (TISCH). **(A-I)** The expression of m5C regulators in immune cells.

were used to evaluate the prognostic value of the m5Cscore (Blanche et al., 2013). Univariate and multivariate independent prognostic analyses were performed to assess whether the model was an independent prognostic factor for HCC. All statistical p values were two-sided, with $p < 0.05$ deemed statistically significant.

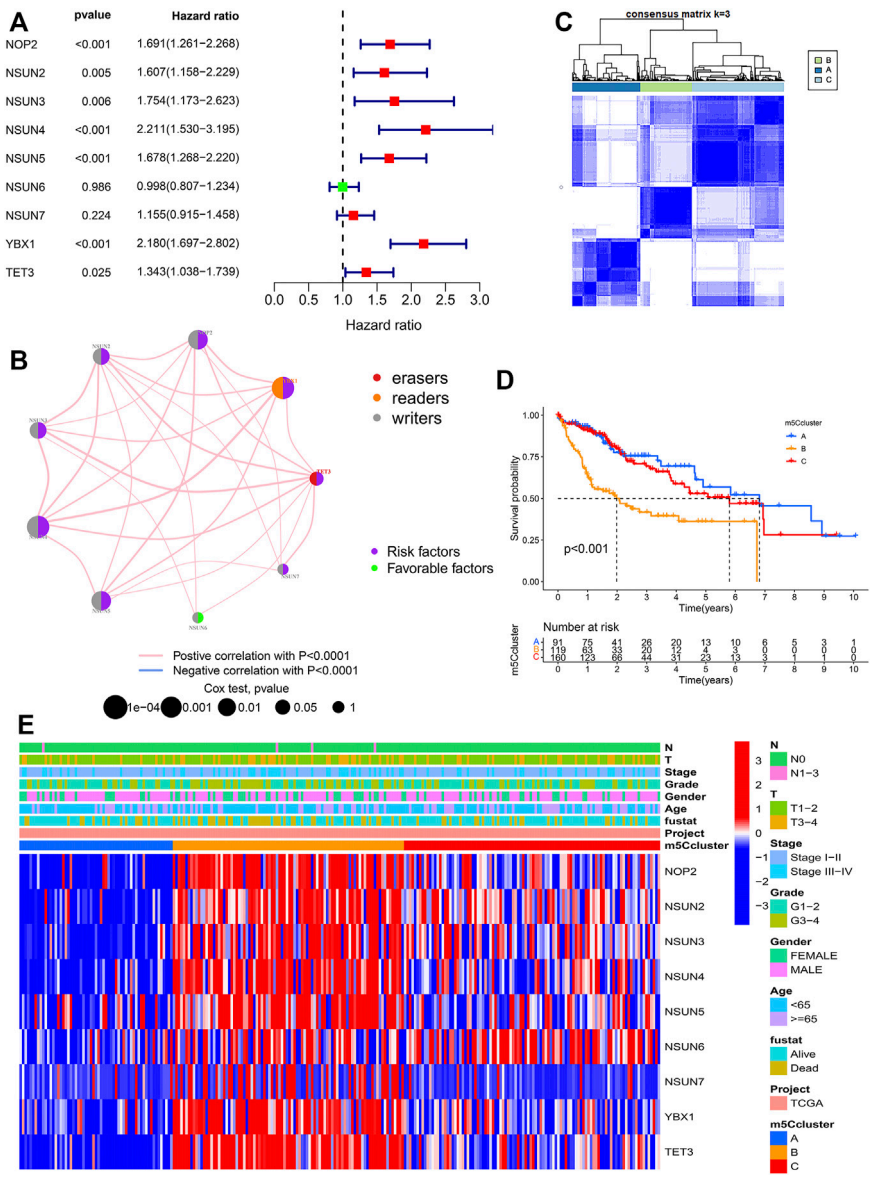

FIGURE 3 | Molecular characteristics of m5Cclusters. **(A)** Forest plot of univariate Cox regression analysis results; **(B)** Interaction of m5C regulators in HCC; **(C)** Consensus clustering matrix for k = 3; **(D)** Survival analysis of patients in distinct m5Cclusters; **(E)** Heatmap depicting the expression levels of m5C regulators in distinct m5Cclusters.

RESULTS

Expression Variation of the m5C Regulators in Hepatocellular Carcinoma

In this study, 374 HCC and 50 normal samples in the TCGA cohort were analyzed. The results revealed that almost all enrolled m5C regulators were differentially expressed between HCC and normal tissues, while there was no difference in the expression of TET2 (**Figure 1A**). Most m5C regulators were upregulated in HCC tissues ($p < 0.001$), while the expression levels of NSUN6 and NSUN7 were downregulated in HCC tissues. Somatic mutations were investigated to explore the prevalence of m5C regulator variations in HCC. The overall average mutation frequency of m5C regulators was low, with only 9 of 364 samples having m5C regulator mutations (**Figure 1B**). The mutation frequency was higher in NOP2 than in other regulators. Furthermore, the TMB was different in HCC patients with different clinicopathological characteristics. Variation analysis showed that patients in the male or N0 stage had a higher TMB, and a similar result could be found in patients older than 65 years (**Supplementary Figure S1**).

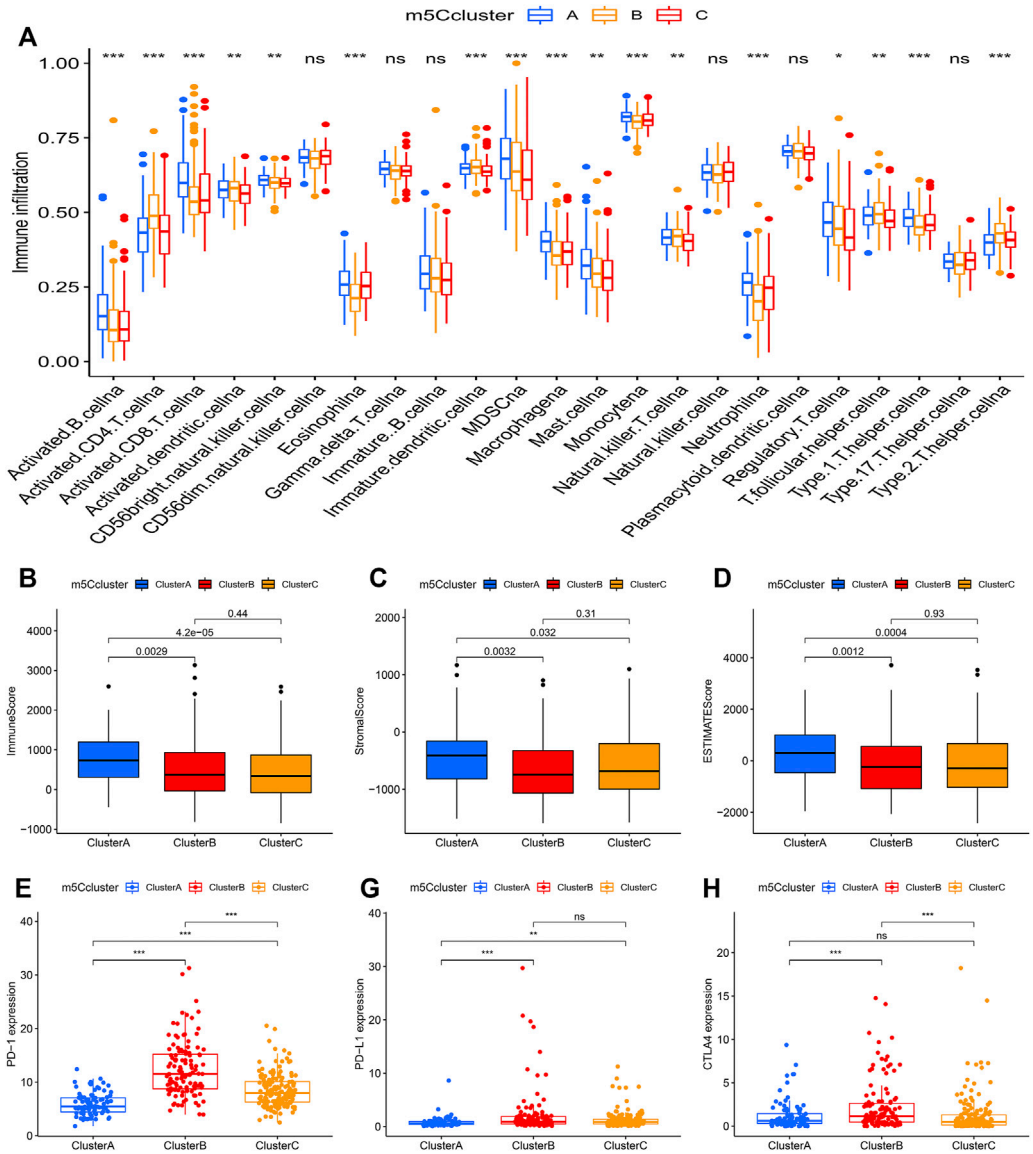

FIGURE 4 | Tumor immune landscape in distinct m5Cclusters. **(A)** ssGSEA of patients in distinct m5Cclusters, the asterisks represent the statistical *p* value between the three m5Cclusters (*$p < 0.05$; **$p < 0.01$; ***$p < 0.001$); **(B)** Immune score of patients in distinct m5Cclusters; **(C)** Stromal score of patients in distinct m5Cclusters; **(D)** ESTIMATE score of patients in distinct m5Cclusters; **(E)** PD-1 expression in distinct m5Cclusters (*$p < 0.05$; **$p < 0.01$; ***$p < 0.001$); **(F)** PD-L1 expression in distinct m5Cclusters (*$p < 0.05$; **$p < 0.01$; ***$p < 0.001$); **(G)** CTLA-4 expression in distinct m5Cclusters (*$p < 0.05$; **$p < 0.01$; ***$p < 0.001$).

Considering the role of the TME in tumor occurrence and progression, we used a data set (GSE140228) in the TISCH database to analyze the expression levels of m5C regulators in TME-related cells. As shown in **Supplementary Figure S2**, GSE140228 was divided into 20 cell clusters and 12 types of cells, and $CD8^+$ T cells were the most abundant immune cells (n = 19969). The expression level of YBX1 was highest in TME-related cells, while NSUN7 and TET3 were hardly expressed (**Figures 2A–I**). In addition, the expression levels of m5C regulators were different in distinct immune cells (**Supplementary Figure S3**).

Univariate Cox regression analysis and the KM method showed that most m5C regulators were potential prognostic risk factors for HCC patients (**Supplementary Table S3**, **Figure 3A**, **Supplementary Figure S4**). The network of m5C regulators comprehensively demonstrated the interactions, connections, and prognostic significance of m5C regulators in HCC patients (**Figure 3B**). The results showed that there were distinct positive correlations between each other. Most regulators, such as NSUN4 and YBX1, presented tumorigenic characteristics, with higher gene expression levels correlated with poor prognosis. Conversely, NSUN6 presented tumor-suppressing characteristics, with higher gene expression levels related to favorable prognosis. Overall, the above results presented high heterogeneity of the genome and expression variations of m5C

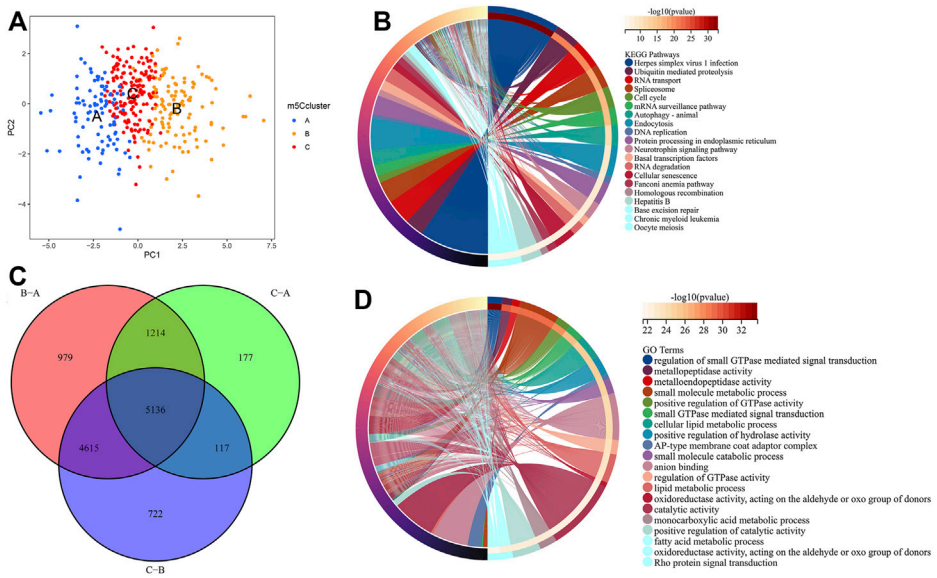

FIGURE 5 | Molecular characteristics of differentially expressed genes (DEGs) among m5Cclusters. **(A)** PCA among distinct m5Cclusters; **(B)** DEGs extracted among three m5Cclusters; **(C)** KEGG pathway analysis for the DEGs; **(D)** GO enrichment analysis for the DEGs.

regulators between normal and HCC tissues, indicating that m5C regulators may play a crucial role in HCC occurrence and progression.

m5C Modification Patterns Mediated by m5C Regulators

Based on the expression of the 9 m5C regulators, model-based clustering was performed to classify HCC patients using the "ConsensusClusterPlus" R package. Through unsupervised clustering, three distinct m5C modification patterns were ultimately uncovered (identified as m5Cclusters A-C), including 91 cases in cluster A, 119 cases in cluster B, and 160 cases in cluster C (**Figure 3C**). Prognostic analysis showed that there was a survival advantage in cluster A and a survival disadvantage in cluster B (**Figure 3D**). Further analysis revealed that there was a significant difference in three distinct m5C modification patterns. m5Ccluster A presented significantly low expression of all m5C regulators, while m5Ccluster B was characterized by high expression of all regulators (**Figure 3E**). Therefore, it was not surprising that m5Ccluster B had the poorest prognosis. In addition, GSVA was performed to investigate the differences in the biological process among the distinct m5Cclusters. The results indicated that distinct m5C modifications had a significant effect on the biological behaviors of HCC (**Supplementary Figure S5**).

Tumor Immune Characteristics in Distinct m5C Modification Patterns

Through ssGSEA, the difference in the infiltration of 23 different immune cell types was assessed in the distinct m5Cclusters (**Figure 4A**). m5Ccluster A showed high infiltration of activated B cells, activated $CD8^+$ T cells, eosinophils and monocytes, while m5Ccluster B was characterized by high infiltration of activated $CD4^+$ T cells and T helper type 2 (Th2) cells. In addition, the results of the ESTIMATE algorithm revealed that the immune, stromal, and ESTIMATE scores ($p < 0.05$) were higher in cluster A than in clusters B and C, while there was no difference between clusters B and C (**Figures 4B–D**). Meanwhile, the expression of targeted immune checkpoint molecules was different among the distinct clusters. The boxplots showed that the expression of the PD-1, PD-L1 and CTLA-4 genes was markedly higher in cluster B and significantly lower in cluster A (**Figures 4E–G**). It was surprising that the expression levels of targeted immune checkpoint molecules showed a similar trend with the expression levels of the m5C regulators. Characterized by high expression levels of the m5C regulators, m5Ccluster B also had high expression levels of the targeted immune checkpoint molecules.

Generation of the m5Cscore Model

PCA indicated that there were distinct m5C modification patterns in HCC (**Figure 5A**). To further investigate the potential biological behavior of each m5Ccluster, a total of 5,136 DEGs were extracted from the distinct m5Cclusters (**Figure 5B**). GO enrichment analysis and KEGG pathway analysis were performed with the "clusterProfiler" R package. The results showed that the DEGs were enriched in biological processes related to tumorigenesis and tumor progression, such as the cell cycle and autophagy (**Figures 5C,D**).

Univariate Cox regression analysis was performed to investigate the prognostic value of each DEG, and 1,183 genes with prognostic utility were eventually extracted to construct the patients' individual m5Cscore. The best cutoff value was calculated, and the patients were divided into low- and high-

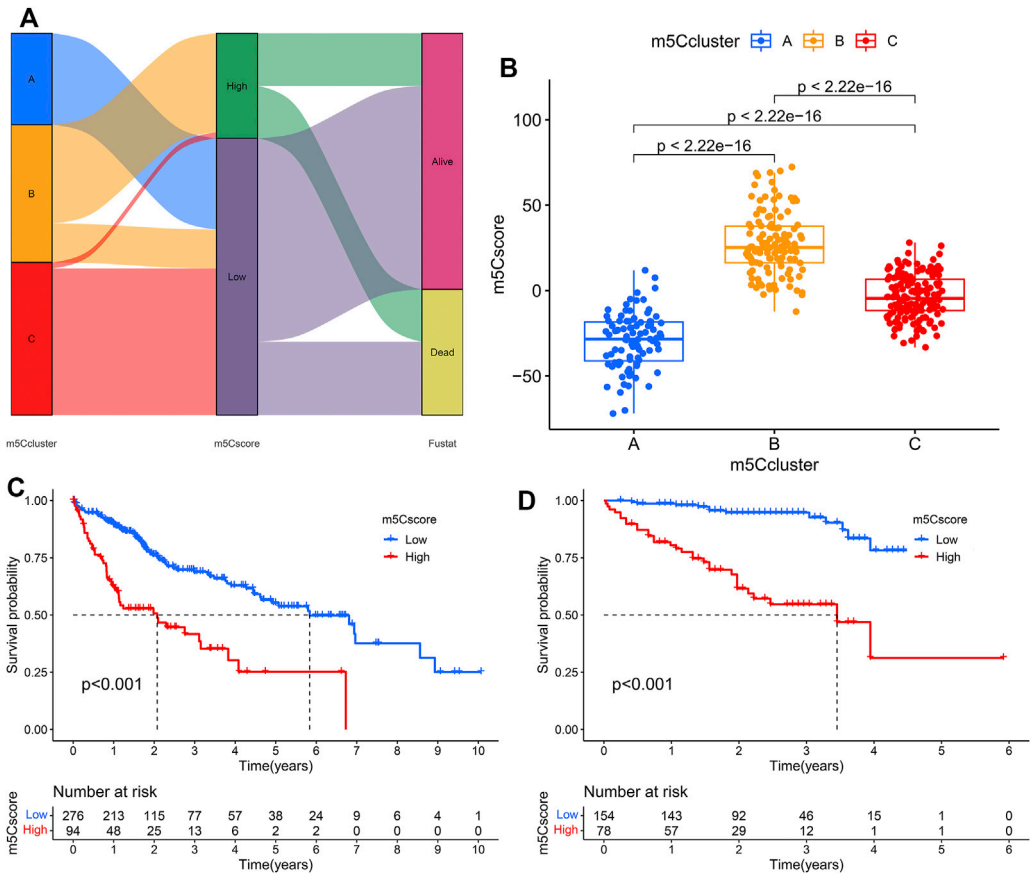

FIGURE 6 | Construction of the m5Cscore model. **(A)** Alluvial diagram showing the changes in m5Cclusters and m5Cscore; **(B)** Differences in m5Cscore among the three m5Cclusters; **(C)** KM analysis of patients in the high- and low-m5Cscore groups (TCGA cohort); **(D)** KM analysis of patients in the high- and low-m5Cscore groups (ICGC cohort).

m5Cscore groups. An alluvial diagram was used to visualize the changes in the attributes of individual HCC patients and showed that m5Ccluster B was linked to a high m5Cscore and had the highest proportion of deaths (**Figure 6A**). Furthermore, the relationship between m5C modification and the m5Cscore was explored. Differential analysis found that m5Ccluster B had the highest m5Cscore, while m5Ccluster A had the lowest m5Cscore (**Figure 6B**).

Patients with low m5Cscores demonstrated a prominent survival benefit in both the TCGA and ICGC cohorts (**Figures 6C,D**). In addition, univariate and multivariate Cox regression analyses including sex, age, tumor grade, m5Cscore, and tumor stage were performed in the TCGA and ICGC cohorts, which confirmed that m5Cscore was an independent prognostic factor of HCC (in TCGA cohort: HR: 1.045, 95% CI: 1.029–1.061, $p < 0.001$; in ICGC cohort: HR: 1.038, 95% CI: 1.022–1.054, $p < 0.001$, respectively) (**Figures 7A–D**). The AUC curves indicated that the m5Cscore had an acceptable prognostic value for HCC patients. The AUC values for predicting 1-, 2-, 3-, and 4-years OS in the TCGA cohort were 0.75, 0.64, 0.66, and 0.67, respectively, and those in the ICGC cohort were 0.79, 0.78, 0.80, and 0.83, respectively (**Figures 7E,F**).

To investigate the potential biological mechanism of the m5Cscore, we analyzed the correlations between the m5Cscore and some biological processes. As shown in **Figure 8A**, there were significantly positive correlations between the m5Cscore and some infiltrated immune cells, such as activated $CD4^+$ T cells and Th2 cells, while there was a negative correlation between the m5Cscore and the infiltration of eosinophils, monocytes and neutrophils. Unfortunately, there was no significant relationship between TMB and the m5Cscore ($p = 0.96$) (**Figure 8B**). In addition, patients with high m5Cscores had a high proportion of deaths (**Figures 8C,D**). Furthermore, the model validation results indicated that the m5Cscore model could be suitable for patients with different tumor grades (**Figures 8E,F**). Immunotherapies involving PD-1, PD-L1 and CTLA-4 blockade have undoubtedly emerged as a major breakthrough in cancer therapy. Patients with high m5Cscores showed obviously high expression levels of PD-1, PD-L1, and CTLA-4, which indicated a potential response to anti-PD-1/PD-L1/CTLA-4 therapy (**Figures 8G–I**).

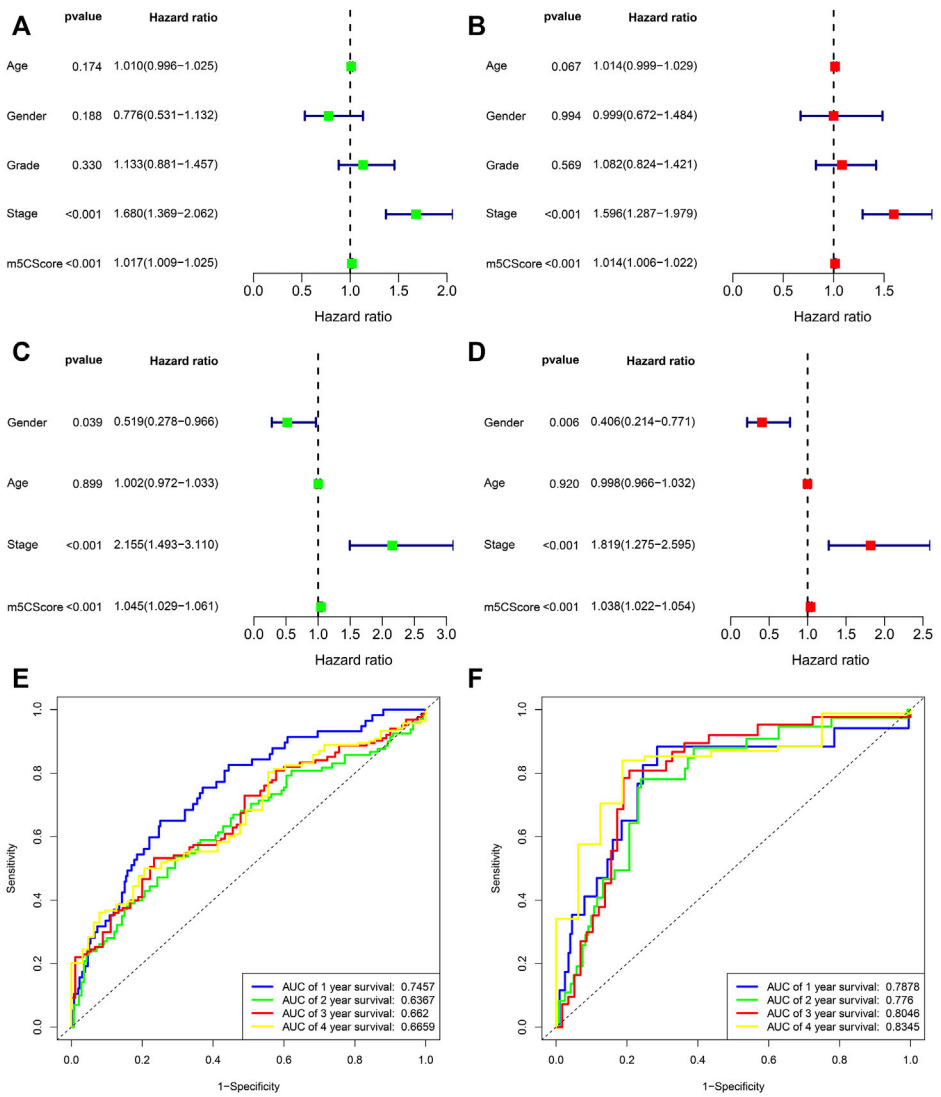

FIGURE 7 | Prognostic value of the m5Cscore model. **(A)** Univariate independent prognostic analysis in TCGA cohort; **(B)** Multivariate independent prognostic analysis in TCGA cohort; **(C)** Univariate independent prognostic analysis in ICGC cohort; **(D)** Multivariate independent prognostic analysis in ICGC cohort; **(E)** Receiver operating characteristic (ROC) curves of m5Cscore for predicting the 1/2/3/4/5-years survival in TCGA cohort; **(F)** Receiver operating characteristic (ROC) curves of m5Cscore for predicting the 1/2/3/4/5-years survival in ICGC cohort.

The mRNA and Protein Expression Levels of m5C Regulators in Hepatocellular Carcinoma

To further verify the trend of m5C regulator expression in HCC tissues, we performed a qPCR assay and acquired IHC pathological specimen data from the HPA. As shown in **Figures 9**, **10**, almost all m5C regulators were differentially expressed between HCC and normal tissues. Most m5C regulators were upregulated in HCC tissues, while the expression levels of NSUN6 and NSUN7 were significantly downregulated in HCC tissues.

DISCUSSION

Multiple m^5C regulators have been identified as participants in the development and progression of cancer. Specifically, m^5C plays an important role in cancer cell proliferation and metastasis, as well as cancer stem cell development, by regulating mRNA stability, expression, and translation (Lu et al., 2018; Shen et al., 2018; Chen et al., 2019; Mei et al., 2020). For instance, Ban et al. (Ban et al., 2021) found that YBX1 could promote nasopharyngeal carcinoma (NPC) cell proliferation and invasiveness by enhancing the protein synthesis of AURKA. As one of the most widespread malignances worldwide, HCC

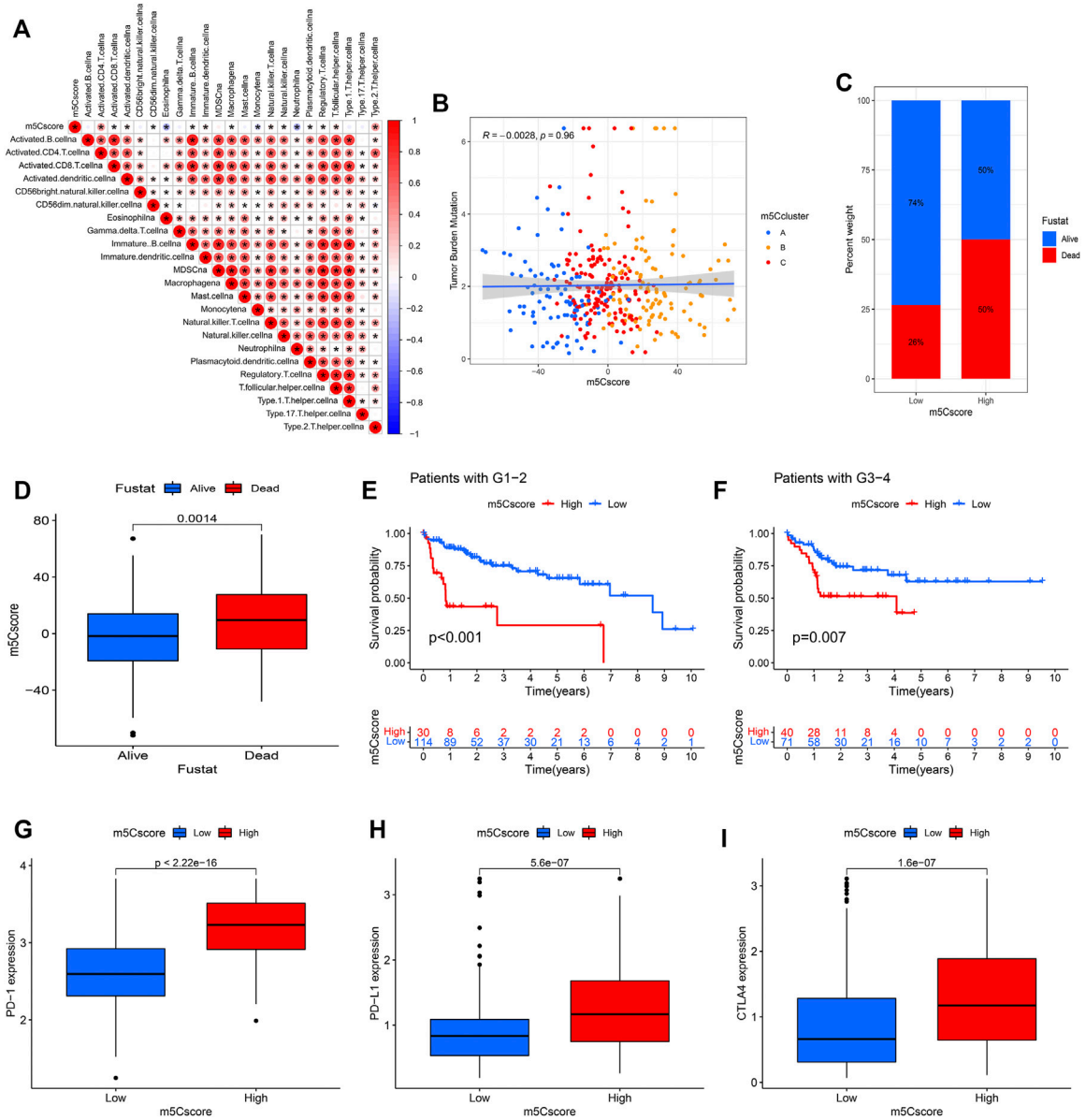

FIGURE 8 | Correlation analysis between the m5Cscore and some related biological pathways. **(A)** Immunocorrelation analysis; **(B)** Tumor mutation burden (TMB) correlation analysis; **(C,D)** Clinical correlation analysis; **(E,F)** Model validation in patients with different tumor grades; **(G)** PD-1 expression in distinct m5Cscore groups; **(H)** PD-L1 expression in distinct m5Cscore groups; **(I)** CTLA-4 expression in distinct m5Cscore groups.

remains poorly understood in terms of its pathogenesis and development (Xue et al., 2020). Recently, the role of m5C modification in tumors has attracted great attention, and increasing evidence has revealed that m5C modification is closely related to the tumorigenesis and tumor progression of HCC (He et al., 2020b; He et al., 2020c; Zhang et al., 2020). Sun et al. (Sun et al., 2020) found that the NSUN2-mediated m^5C modification of H19 lncRNA exerts an important function in the progression and malignancy of HCC. However, most of these studies focused on a single m5C regulator or only explored the distribution of m5C in HCC, and the overall influence of m5C regulator-related modification patterns on tumor prognosis has not been fully established.

In this study, we demonstrated that m5C modification played a crucial role in the tumorigenesis and tumor progression of HCC and had potential prognostic value for HCC. To clarify the role of m5C in HCC, we comprehensively profiled the m5C modification patterns in HCC samples obtained from public databases. Through unsupervised clustering analyses, we identified three distinct m5C modification patterns in HCC, characterized by differences in prognosis, immune cell infiltration, and pathway signatures. In addition, to quantify the m5C modifications of

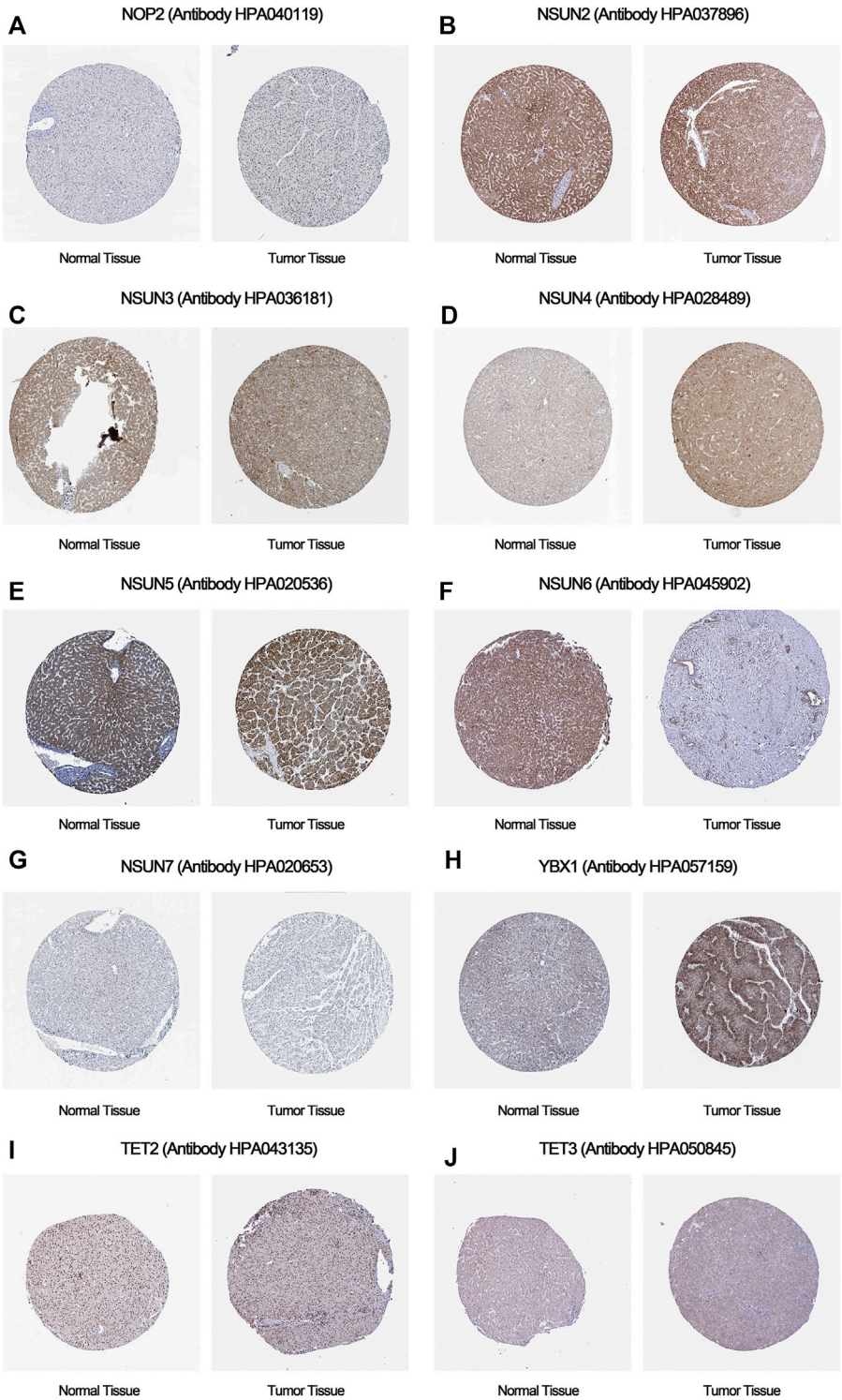

FIGURE 9 | The protein expression of m5C regulators in HCC and normal tissues. **(A)** The protein expression of NOP2 in HCC and normal tissues; **(B)** The protein expression of NSUN2 in HCC and normal tissues; **(C)** The protein expression of NSUN3 in HCC and normal tissues; **(D)** The protein expression of NSUN4 in HCC and normal tissues; **(E)** The protein expression of NSUN5 in HCC and normal tissues; **(F)** The protein expression of NSUN6 in HCC and normal tissues; **(G)** The protein expression of NSUN7 in HCC and normal tissues; **(H)** The protein expression of YBX1 in HCC and normal tissues; **(I)** The protein expression of TET2 in HCC and normal tissues; **(J)** The protein expression of TET3 in HCC and normal tissues.

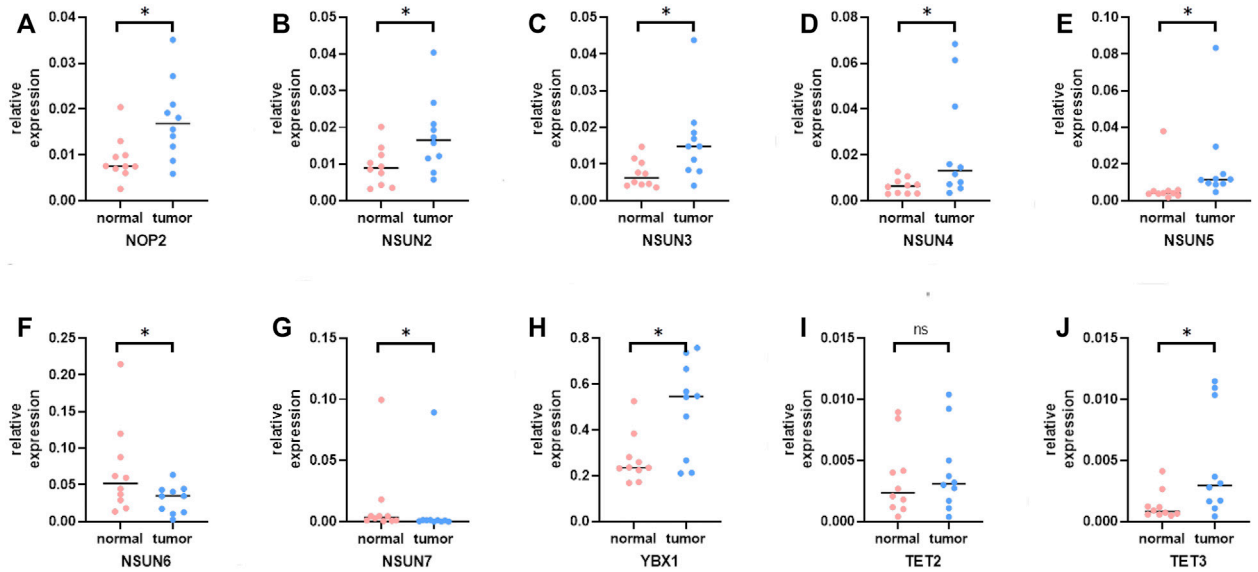

FIGURE 10 | The mRNA expression of m5C regulators in HCC and normal tissues. **(A)** The mRNA expression of NOP2 in HCC and normal tissues; **(B)** The mRNA expression of NSUN2 in HCC and normal tissues; **(C)** The mRNA expression of NSUN3 in HCC and normal tissues; **(D)** The mRNA expression of NSUN4 in HCC and normal tissues; **(E)** The mRNA expression of NSUN5 in HCC and normal tissues; **(F)** The mRNA expression of NSUN6 in HCC and normal tissues; **(G)** The mRNA expression of NSUN7 in HCC and normal tissues; **(H)** The mRNA expression of YBX1 in HCC and normal tissues; **(I)** The mRNA expression of TET2 in HCC and normal tissues; **(J)** The mRNA expression of TET3 in HCC and normal tissues.

individual patients, we constructed a model (termed "m5Cscore"), which was proven to be an independent prognostic factor of HCC. Our results indicated that m5C modification was different in HCC patients and could be a novel prognostic biomarker.

The expression levels of almost all m5C regulators were significantly higher in HCC tissues than in adjacent tissues, and a previous study showed that the degree of mRNA methylation in HCC was significantly higher than that in adjacent tissues (Zhang et al., 2020). These results suggested that the alteration of m5C modification was correlated with the pathogenesis of HCC. As shown in **Figure 3D**, three distinct m5C modification patterns identified by unsupervised clustering analyses had different survival outcomes. m5Ccluster A, which was characterized by low expression levels of m5C regulators, had a survival advantage, while m5Ccluster B, which presented significantly high expression of m5C regulators, had a survival disadvantage. The results indicated that the expression levels of m5C regulators were closely related to the tumor progression of HCC. Considering the heterogeneity of m5C modification, the m5Cscore model was constructed to quantify the m5C modification patterns of individual HCC patients. Through a comprehensive analysis and validation with the training cohort (TCGA) and validation cohort (ICGC), the m5Cscore was identified as a robust and independent prognostic factor of HCC. In addition, subsequent analysis found that the m5Cscore was closely related to immune cell infiltration. The m5Cscore had a significantly positive correlation with the infiltration of activated $CD4^+$ T cells and Th2 cells and a negative correlation with the infiltration of eosinophils, monocytes and neutrophils.

The immune environment that surrounds cancer tissues can affect tumor cell growth and metastasis (Ostrand-Rosenberg, 2008). The different types of immune cells have the potential to either promote or delay tumor development and progression. In this study, we investigated the expression levels of m5C regulators in TME-related cells and found that they were different in distinct immune cells. The results indicated that m5C regulators were closely related to the TME in HCC. In addition, we quantified the infiltration of 23 different immune cell types in HCC samples through ssGSEA. Subsequent analysis found that there was a significant difference in immune cell infiltration among the distinct m5Cclusters. Patients in m5Ccluster A showed high infiltrations of activated B cells, activated $CD8^+$ T cells, eosinophils and monocytes, while those in m5Ccluster B were characterized by high infiltrations of activated $CD4^+$ T cells and Th2 cells. Renata et al. (Rossetti et al., 2018) demonstrated that activated B cells could induce antigen specific T cell responses and play an antitumor role. Similarly, activated $CD8^+$ T cells and eosinophils can inhibit tumor growth in different ways (Wieckowski et al., 2009; Grisaru et al., 2021). In addition, previous research showed that a high number of Th2 cells was associated with poor prognosis in tumors (De Monte et al., 2011). Therefore, with a high infiltration of antitumor immune cells, patients in m5Ccluster A had a survival advantage, while those in m5Ccluster B characterized by high infiltration of tumor promoting immune cells had a worse outcome.

Immune checkpoint inhibitor (ICI) therapy targeting the PD-1/PD-L1/CTLA-4 pathway has been approved for the treatment of more than 10 cancer types (Callahan et al., 2016; Hoos, 2016). As a chance for cure, ICI therapy has revolutionized cancer

treatment (Xie et al., 2021). However, only a portion of patients had an expected response during immune checkpoint blockade therapy (Agdashian et al., 2019). For patients with advanced HCC, the anti-PD-1 agents nivolumab and pembrolizumab demonstrated an objective response rate (ORR) of only 15% in patients who had prior treatment with sorafenib (El-Khoueiry et al., 2017; Zhu et al., 2018). A similar situation has occurred in anti-CTLA-4 therapy (Duffy et al., 2017). Recently, the expression levels of PD-1, PD-L1 and CTLA-4 were identified as predictive biomarkers for immunotherapy response (Ferris et al., 2016; Herbst et al., 2016; Muro et al., 2016; Ott et al., 2017). In this study, we found that the expression levels of these targeted immune checkpoint molecules were different in HCC patients. Patients in m5Ccluster B had higher expression of PD-1, PD-L1 and CTLA-4 than those in m5Ccluster A, and a similar situation showed that the expression levels of PD-1, PD-L1 and CTLA-4 were higher in the high m5Cscore group. The results indicated that those patients would have a better response to ICI therapy. This needs to be further evaluated through experiments.

There were several limitations in this study. First, immune cell infiltration was assessed based on algorithms owing to technical limitations. Second, due to a lack of data, we could not directly explore the difference in the response to immunotherapy between the high- and low-m5Cscore groups. Last, there was no clinical cohort to verify the predictive value of the m5Cscore in HCC; thus, further research based on large cohort prospective clinical trials is needed.

In conclusion, this study comprehensively explored and systematically profiled the expression features of m5C-related regulators in HCC. The m5C modification patterns play a crucial role in the TIME and prognosis of HCC. Our work will enhance the understanding of the tumor immune landscape and provide a practical tool for predicting the prognosis of HCC. This study will help clinicians identify effective indicators for HCC to improve the poor prognosis of this disease.

DATA AVAILABILITY STATEMENT

The datasets presented in this study can be found in online repositories. The names of the repository/repositories and accession number(s) can be found in the article/ **Supplementary Material**.

ETHICS STATEMENT

This project was approved by the Ethics Committee of Shandong Provincial Hospital Affiliated to Shandong First Medical University and was performed in accordance with the Declaration of Helsinki. Each participant provided written informed consent.

AUTHOR CONTRIBUTIONS

YL, JL and SZ contributed to the conception and design of the study. YL and TW extracted data. YL and ZF analyzed the data. YL, JK and TW drafted the manuscript. WT, JK and ZF contributed to a critical revision of the manuscript. All authors have read and approved the final version of the manuscript.

FUNDING

This work was supported by the National Natural Science Foundation of China under Grant (No. 81373172, 81770646).

ACKNOWLEDGMENTS

The authors thank American Journal Experts for language editing.

SUPPLEMENTARY MATERIAL

The Supplementary Material for this article can be found online at: https://www.frontiersin.org/articles/10.3389/fcell.2022.842220/full#supplementary-material

Supplementary Figure 1 | Variation analysis between TMB and clinical status. **(A)** Variation analysis between TMB and age; **(B)** Variation analysis between TMB and sex; **(C)** Variation analysis between TMB and tumor grade; **(D)** Variation analysis between TMB and tumor stage; **(E)** Variation analysis between TMB and T stage; **(F)** Variation analysis between TMB and N stage.

Supplementary Figure 2 | Annotation of all cell types in GSE140228 and the percentage of each type of cell.

Supplementary Figure 3 | The expression levels of m5C regulators in HCC tumor microenvironment-related cells.

Supplementary Figure 4 | KM analysis of patients with distinct m5C regulator expression. **(A)** KM analysis of patients with distinct NOP2 expression; **(B)** KM analysis of patients with distinct NSUN2 expression; **(C)** KM analysis of patients with distinct NSUN3 expression; **(D)** KM analysis of patients with distinct NSUN4 expression; **(E)** KM analysis of patients with distinct NSUN5 expression; **(F)** KM analysis of patients with distinct TET3 expression; **(G)** KM analysis of patients with distinct YBX1 expression.

Supplementary Figure 5 | .GSVA enrichment analysis between different m5Cclustters. **(A)** GSVA enrichment analysis between m5Ccluster A and m5Ccluster B; **(B)** GSVA enrichment analysis between m5Ccluster A and m5Ccluster C; **(C)** GSVA enrichment analysis between m5Ccluster B and m5Ccluster C.

REFERENCES

Agdashian, D., ElGindi, M., Xie, C., Sandhu, M., Pratt, D., Kleiner, D. E., et al. (2019). The Effect of Anti-CTLA4 Treatment on Peripheral and Intra-tumoral T Cells in Patients with Hepatocellular Carcinoma. *Cancer Immunol. Immunother.* 68 (4), 599–608. doi:10.1007/s00262-019-02299-8

Ban, Y., Tan, Y., Li, X., Li, X., Zeng, Z., Xiong, W., et al. (2021). RNA-binding Protein YBX1 Promotes Cell Proliferation and Invasiveness of Nasopharyngeal Carcinoma Cells via Binding to AURKA mRNA. *J. Cancer* 12 (11), 3315–3324. doi:10.7150/jca.56262

Blanche, P., Dartigues, J.-F., and Jacqmin-Gadda, H. (2013). Estimating and Comparing Time-dependent Areas under Receiver Operating Characteristic Curves for Censored Event Times with Competing Risks. *Statist. Med.* 32 (30), 5381–5397. doi:10.1002/sim.5958

Boccaletto, P., Machnicka, M. A., Purta, E., Piątkowski, P., Bagiński, B., Wirecki, T. K., et al. (2018). MODOMICS: a Database of RNA Modification Pathways. 2017 Update. *Nucleic Acids Res.* 46, D303–D307. doi:10.1093/nar/gkx1030

Bohnsack, K. E., Höbartner, C., and Bohnsack, M. T. (2019). Eukaryotic 5-methylcytosine (m^5C) RNA Methyltransferases: Mechanisms, Cellular Functions, and Links to Disease. *Genes (Basel)* 10 (2). doi:10.3390/genes10020102

Bosetti, C., Turati, F., and La Vecchia, C. (2014). Hepatocellular Carcinoma Epidemiology. *Best Pract. Res. Clin. Gastroenterol.* 28 (5), 753–770. doi:10.1016/j.bpg.2014.08.007

Bray, F., Ferlay, J., Soerjomataram, I., Siegel, R. L., Torre, L. A., and Jemal, A. (2018). Global Cancer Statistics 2018: GLOBOCAN Estimates of Incidence and Mortality Worldwide for 36 Cancers in 185 Countries. *CA: a Cancer J. clinicians* 68 (6), 394–424. doi:10.3322/caac.21492

Callahan, M. K., Postow, M. A., and Wolchok, J. D. (2016). Targeting T Cell Co-receptors for Cancer Therapy. *Immunity* 44 (5), 1069–1078. doi:10.1016/j.immuni.2016.04.023

Charoentong, P., Finotello, F., Angelova, M., Mayer, C., Efremova, M., Rieder, D., et al. (2017). Pan-cancer Immunogenomic Analyses Reveal Genotype-Immunophenotype Relationships and Predictors of Response to Checkpoint Blockade. *Cell Rep.* 18 (1), 248–262. doi:10.1016/j.celrep.2016.12.019

Chen, H., Ge, X.-L., Zhang, Z.-Y., Liu, M., Wu, R.-Y., Zhang, X.-F., et al. (2021). M5C Regulator-Mediated Methylation Modification Patterns and Tumor Microenvironment Infiltration Characterization in Lung Adenocarcinoma. *Transl Lung Cancer Res.* 10 (5), 2172–2192. doi:10.21037/tlcr-21-351

Chen, X., Li, A., Sun, B.-F., Yang, Y., Han, Y.-N., Yuan, X., et al. (2019). 5-methylcytosine Promotes Pathogenesis of Bladder Cancer through Stabilizing mRNAs. *Nat. Cell Biol* 21 (8), 978–990. doi:10.1038/s41556-019-0361-y

De Monte, L., Reni, M., Tassi, E., Clavenna, D., Papa, I., Recalde, H., et al. (2011). Intratumor T Helper Type 2 Cell Infiltrate Correlates with Cancer-Associated Fibroblast Thymic Stromal Lymphopoietin Production and Reduced Survival in Pancreatic Cancer. *J. Exp. Med.* 208 (3), 469–478. doi:10.1084/jem.20101876

Delaunay, S., and Frye, M. (2019). RNA Modifications Regulating Cell Fate in Cancer. *Nat. Cell Biol* 21 (5), 552–559. doi:10.1038/s41556-019-0319-0

Duffy, A. G., Ulahannan, S. V., Makorova-Rusher, O., Rahma, O., Wedemeyer, H., Pratt, D., et al. (2017). Tremelimumab in Combination with Ablation in Patients with Advanced Hepatocellular Carcinoma. *J. Hepatol.* 66 (3), 545–551. doi:10.1016/j.jhep.2016.10.029

El-Khoueiry, A. B., Sangro, B., Yau, T., Crocenzi, T. S., Kudo, M., Hsu, C., et al. (2017). Nivolumab in Patients with Advanced Hepatocellular Carcinoma (CheckMate 040): an Open-Label, Non-comparative, Phase 1/2 Dose Escalation and Expansion Trial. *The Lancet* 389 (10088), 2492–2502. doi:10.1016/s0140-6736(17)31046-2

Ferris, R. L., Blumenschein, G., Fayette, J., Guigay, J., Colevas, A. D., Licitra, L., et al. (2016). Nivolumab for Recurrent Squamous-Cell Carcinoma of the Head and Neck. *N. Engl. J. Med.* 375 (19), 1856–1867. doi:10.1056/nejmoa1602252

Forner, A., Reig, M., and Bruix, J. (2018). Hepatocellular Carcinoma. *The Lancet* 391 (10127), 1301–1314. doi:10.1016/s0140-6736(18)30010-2

Gao, L., Chen, R., Sugimoto, M., Mizuta, M., Zhou, L., Kishimoto, Y., et al. (2021). The RNA Methylation Modification 5-Methylcytosine Impacts Immunity Characteristics, Prognosis and Progression of Oral Squamous Cell Carcinoma by Bioinformatics Analysis. *Front. Bioeng. Biotechnol.* 9, 760724. doi:10.3389/fbioe.2021.760724

Gao, Y., Wang, Z., Zhu, Y., Zhu, Q., Yang, Y., Jin, Y., et al. (2019). NOP 2/Sun RNA Methyltransferase 2 Promotes Tumor Progression via its Interacting Partner RPL 6 in Gallbladder Carcinoma. *Cancer Sci.* 110 (11), 3510–3519. doi:10.1111/cas.14190

Geng, Q., Wei, Q., Shen, Z., Zheng, Y., Wang, L., Xue, W., et al. (2021). Comprehensive Analysis of the Prognostic Value and Immune Infiltrates of the Three-m5C Signature in Colon Carcinoma. *Cmar* 13, 7989–8002. doi:10.2147/cmar.s331549

Grisaru, S., Itan, M., and Munitz, A. (2021). Analysis of Mouse Eosinophil Migration and Killing of Tumor Cells. *Methods Mol. Biol. (Clifton, NJ)* 2241, 89–97. doi:10.1007/978-1-0716-1095-4_8

Gu, X., Zhou, H., Chu, Q., Zheng, Q., Wang, J., and Zhu, H. (2021). Uncovering the Association between m5C Regulator-Mediated Methylation Modification Patterns and Tumour Microenvironment Infiltration Characteristics in Hepatocellular Carcinoma. *Front. Cell Dev. Biol.* 9, 727935. doi:10.3389/fcell.2021.727935

Guo, G., Pan, K., Fang, S., Ye, L., Tong, X., Wang, Z., et al. (2021). Advances in mRNA 5-methylcytosine Modifications: Detection, Effectors, Biological Functions, and Clinical Relevance. *Mol. Ther. - Nucleic Acids* 26, 575–593. doi:10.1016/j.omtn.2021.08.020

He, Y., Yu, X., Li, J., Zhang, Q., Zheng, Q., and Guo, W. (2020). Role of m5C-Related Regulatory Genes in the Diagnosis and Prognosis of Hepatocellular Carcinoma. *Am. J. Transl Res.* 12 (3), 912–922. doi:10.18632/aging.102669

He, Y., Zhang, Q., Zheng, Q., Yu, X., and Guo, W. (2020). Distinct 5-methylcytosine Profiles of Circular RNA in Human Hepatocellular Carcinoma. *Am. J. Transl Res.* 12 (9), 5719–5729.

He, Y., Shi, Q., Zhang, Y., Yuan, X., and Yu, Z. (2020). Transcriptome-Wide 5-Methylcytosine Functional Profiling of Long Non-coding RNA in Hepatocellular Carcinoma. *Cmar* 12, 6877–6885. doi:10.2147/cmar.s262450

Herbst, R. S., Baas, P., Kim, D.-W., Felip, E., Pérez-Gracia, J. L., Han, J.-Y., et al. (2016). Pembrolizumab versus Docetaxel for Previously Treated, PD-L1-Positive, Advanced Non-small-cell Lung Cancer (KEYNOTE-010): a Randomised Controlled Trial. *The Lancet* 387 (10027), 1540–1550. doi:10.1016/s0140-6736(15)01281-7

Hester, D., Golabi, P., Paik, J., Younossi, I., Mishra, A., and Younossi, Z. M. (2020). Among Medicare Patients with Hepatocellular Carcinoma, Non-alcoholic Fatty Liver Disease Is the Most Common Etiology and Cause of Mortality. *J. Clin. Gastroenterol.* 54 (5), 459–467. doi:10.1097/mcg.0000000000001172

Hoos, A. (2016). Development of Immuno-Oncology Drugs - from CTLA4 to PD1 to the Next Generations. *Nat. Rev. Drug Discov.* 15 (4), 235–247. doi:10.1038/nrd.2015.35

Hu, J., Othmane, B., Yu, A., Li, H., Cai, Z., Chen, X., et al. (2021). 5mC Regulator-Mediated Molecular Subtypes Depict the Hallmarks of the Tumor Microenvironment and Guide Precision Medicine in Bladder Cancer. *BMC Med.* 19 (1), 289. doi:10.1186/s12916-021-02163-6

Islami, F., Ward, E., Sung, H., Cronin, K., Tangka, F., Sherman, R., et al. (2021). Annual Report to the Nation on the Status of Cancer, Part 1: National Cancer Statistics. *J. Natl. Cancer Inst.* 113 (12), 1648–1669. doi:10.1093/jnci/djab131

Li, F., Deng, Q., Pang, X., Huang, S., Zhang, J., Zhu, X., et al. (2021). m5C Regulator-Mediated Methylation Modification Patterns and Tumor Microenvironment Infiltration Characterization in Papillary Thyroid Carcinoma. *Front. Oncol.* 11, 729887. doi:10.3389/fonc.2021.729887

Liu, T., Guo, L., Liu, G., Hu, X., Li, X., Zhang, J., et al. (2021). Molecular Characterization of the Clinical and Tumor Immune Microenvironment Signature of 5-Methylcytosine-Related Regulators in Non-small Cell Lung Cancer. *Front. Cell Dev. Biol.* 9, 779367. doi:10.3389/fcell.2021.779367

Lok, A. S., Sterling, R. K., Everhart, J. E., Wright, E. C., Hoefs, J. C., Di Bisceglie, A. M., et al. (2010). Des-γ-Carboxy Prothrombin and α-Fetoprotein as Biomarkers for the Early Detection of Hepatocellular Carcinoma. *Gastroenterology* 138 (2), 493–502. doi:10.1053/j.gastro.2009.10.031

Lu, L., Zhu, G., Zeng, H., Xu, Q., and Holzmann, K. (2018). High tRNA Transferase NSUN2 Gene Expression Is Associated with Poor Prognosis in Head and Neck Squamous Carcinoma. *Cancer Invest.* 36 (4), 246–253. doi:10.1080/07357907.2018.1466896

Marrero, J. A., Feng, Z., Wang, Y., Nguyen, M. H., Befeler, A. S., Roberts, L. R., et al. (2009). α-Fetoprotein, Des-γ Carboxyprothrombin, and Lectin-Bound α-Fetoprotein in Early Hepatocellular Carcinoma. *Gastroenterology* 137 (1), 110–118. doi:10.1053/j.gastro.2009.04.005

Mei, L., Shen, C., Miao, R., Wang, J.-Z., Cao, M.-D., Zhang, Y.-S., et al. (2020). RNA Methyltransferase NSUN2 Promotes Gastric Cancer Cell Proliferation by Repressing p57Kip2 by an m5C-dependent Manner. *Cell Death Dis* 11 (4), 270. doi:10.1038/s41419-020-2487-z

Muro, K., Chung, H. C., Shankaran, V., Geva, R., Catenacci, D., Gupta, S., et al. (2016). Pembrolizumab for Patients with PD-L1-Positive Advanced Gastric Cancer (KEYNOTE-012): a Multicentre, Open-Label, Phase 1b Trial. *Lancet Oncol.* 17 (6), 717–726. doi:10.1016/s1470-2045(16)00175-3

Ostrand-Rosenberg, S. (2008). Immune Surveillance: a Balance between Protumor and Antitumor Immunity. *Curr. Opin. Genet. Development* 18 (1), 11–18. doi:10.1016/j.gde.2007.12.007

Ott, P. A., Elez, E., Hiret, S., Kim, D.-W., Morosky, A., Saraf, S., et al. (2017). Pembrolizumab in Patients with Extensive-Stage Small-Cell Lung Cancer: Results from the Phase Ib KEYNOTE-028 Study. *Jco* 35 (34), 3823–3829. doi:10.1200/jco.2017.72.5069

Pan, J., Huang, Z., and Xu, Y. (2021). m5C RNA Methylation Regulators Predict Prognosis and Regulate the Immune Microenvironment in Lung Squamous Cell Carcinoma. *Front. Oncol.* 11, 657466. doi:10.3389/fonc.2021.657466

Pan, J., Huang, Z., and Xu, Y. (2021). m5C-Related lncRNAs Predict Overall Survival of Patients and Regulate the Tumor Immune Microenvironment in Lung Adenocarcinoma. *Front. Cell Dev. Biol.* 9, 671821. doi:10.3389/fcell.2021.671821

Rossetti, R. A. M., Lorenzi, N. P. C., Yokochi, K., Rosa, M. B. S. d. F., Benevides, L., Margarido, P. F. R., et al. (2018). B Lymphocytes Can Be Activated to Act as Antigen Presenting Cells to Promote Anti-tumor Responses. *PloS one* 13 (7), e0199034. doi:10.1371/journal.pone.0199034

Roundtree, I. A., Evans, M. E., Pan, T., and He, C. (2017). Dynamic RNA Modifications in Gene Expression Regulation. *Cell* 169 (7), 1187–1200. doi:10.1016/j.cell.2017.05.045

Sayiner, M., Otgonsuren, M., Cable, R., Younossi, I., Afendy, M., Golabi, P., et al. (2017). Variables Associated with Inpatient and Outpatient Resource Utilization Among Medicare Beneficiaries with Nonalcoholic Fatty Liver Disease with or without Cirrhosis. *J. Clin. Gastroenterol.* 51 (3), 254–260. doi:10.1097/mcg.0000000000000567

Shen, Q., Zhang, Q., Shi, Y., Shi, Q., Jiang, Y., Gu, Y., et al. (2018). Tet2 Promotes Pathogen Infection-Induced Myelopoiesis through mRNA Oxidation. *Nature* 554 (7690), 123–127. doi:10.1038/nature25434

Sotiriou, C., Wirapati, P., Loi, S., Harris, A., Fox, S., Smeds, J., et al. (2006). Gene Expression Profiling in Breast Cancer: Understanding the Molecular Basis of Histologic Grade to Improve Prognosis. *J. Natl. Cancer Inst.* 98 (4), 262–272. doi:10.1093/jnci/djj052

Sun, D., Wang, J., Han, Y., Dong, X., Ge, J., Zheng, R., et al. (2021). TISCH: a Comprehensive Web Resource Enabling Interactive Single-Cell Transcriptome Visualization of Tumor Microenvironment. *Nucleic Acids Res.* 49, D1420–D1430. doi:10.1093/nar/gkaa1020

Sun, Z., Xue, S., Zhang, M., Xu, H., Hu, X., Chen, S., et al. (2020). Aberrant NSUN2-Mediated m5C Modification of H19 lncRNA Is Associated with Poor Differentiation of Hepatocellular Carcinoma. *Oncogene* 39 (45), 6906–6919. doi:10.1038/s41388-020-01475-w

Trixl, L., and Lusser, A. (2019). The Dynamic RNA Modification 5-methylcytosine and its Emerging Role as an Epitranscriptomic Mark. *Wiley Interdiscip. Rev. RNA* 10 (1), e1510. doi:10.1002/wrna.1510

Wieckowski, E. U., Visus, C., Szajnik, M., Szczepanski, M. J., Storkus, W. J., and Whiteside, T. L. (2009). Tumor-derived Microvesicles Promote Regulatory T Cell Expansion and Induce Apoptosis in Tumor-Reactive Activated CD8+ T Lymphocytes. *J. Immunol.* 183 (6), 3720–3730. doi:10.4049/jimmunol.0900970

Wilkerson, M. D., and Hayes, D. N. (2010). ConsensusClusterPlus: a Class Discovery Tool with Confidence Assessments and Item Tracking. *Bioinformatics (Oxford, England)* 26 (12), 1572–1573. doi:10.1093/bioinformatics/btq170

Xie, D., Sun, Q., Wang, X., Zhou, J., Fan, J., Ren, Z., et al. (2021). Immune Checkpoint Inhibitor Plus Tyrosine Kinase Inhibitor for Unresectable Hepatocellular Carcinoma in the Real World. *Ann. Transl Med.* 9 (8), 652. doi:10.21037/atm-20-7037

Xu, W., Zhu, W., Tian, X., Liu, W., Wu, Y., Anwaier, A., et al. (2021). Integrative 5-Methylcytosine Modification Immunologically Reprograms Tumor Microenvironment Characterizations and Phenotypes of Clear Cell Renal Cell Carcinoma. *Front. Cell Dev. Biol.* 9, 772436. doi:10.3389/fcell.2021.772436

Xue, C., Zhao, Y., and Li, L. (2020). Advances in RNA Cytosine-5 Methylation: Detection, Regulatory Mechanisms, Biological Functions and Links to Cancer. *Biomark Res.* 8, 43. doi:10.1186/s40364-020-00225-0

Yoshihara, K., Shahmoradgoli, M., Martínez, E., Vegesna, R., Kim, H., Torres-Garcia, W., et al. (2013). Inferring Tumour Purity and Stromal and Immune Cell Admixture from Expression Data. *Nat. Commun.* 4, 2612. doi:10.1038/ncomms3612

Zeng, D., Li, M., Zhou, R., Zhang, J., Sun, H., Shi, M., et al. (2019). Tumor Microenvironment Characterization in Gastric Cancer Identifies Prognostic and Immunotherapeutically Relevant Gene Signatures. *Cancer Immunol. Res.* 7 (5), 737–750. doi:10.1158/2326-6066.cir-18-0436

Zhang, Q., Zheng, Q., Yu, X., He, Y., and Guo, W. (2020). Overview of Distinct 5-methylcytosine Profiles of Messenger RNA in Human Hepatocellular Carcinoma and Paired Adjacent Non-tumor Tissues. *J. Transl Med.* 18 (1), 245. doi:10.1186/s12967-020-02417-6

Zhu, A. X., Finn, R. S., Edeline, J., Cattan, S., Ogasawara, S., Palmer, D., et al. (2018). Pembrolizumab in Patients with Advanced Hepatocellular Carcinoma Previously Treated with Sorafenib (KEYNOTE-224): a Non-randomised, Open-Label Phase 2 Trial. *Lancet Oncol.* 19 (7), 940–952. doi:10.1016/s1470-2045(18)30351-6

Conflict of Interest: The authors declare that the research was conducted in the absence of any commercial or financial relationships that could be construed as a potential conflict of interest.

Publisher's Note: All claims expressed in this article are solely those of the authors and do not necessarily represent those of their affiliated organizations, or those of the publisher, the editors, and the reviewers. Any product that may be evaluated in this article, or claim that may be made by its manufacturer, is not guaranteed or endorsed by the publisher.

frontiers in Genetics

ORIGINAL RESEARCH
published: 24 February 2022
doi: 10.3389/fgene.2022.783016

Evaluation of the Prognostic Relevance of Differential Claudin Gene Expression Highlights Claudin-4 as Being Suppressed by TGFβ1 Inhibitor in Colorectal Cancer

Linqi Yang[1], Wenqi Zhang[2], Meng Li[1], Jinxi Dam[3], Kai Huang[1], Yihan Wang[1], Zhicong Qiu[1], Tao Sun[1], Pingping Chen[1], Zhenduo Zhang[4]* and Wei Zhang[1]**

[1]Department of Pharmacology, Hebei University of Chinese Medicine, Shijiazhuang, China, [2]Department of Hematology, The Fourth Hospital of Hebei Medical University, Shijiazhuang, China, [3]College of Natural Science, Michigan State University, East Lansing, MI, United States, [4]Shijiazhuang People's Hospital, Shijiazhuang, China

OPEN ACCESS

Edited by:
Xiao Zhu,
Guangdong Medical University, China

Reviewed by:
Jenny Paredes,
Memorial Sloan Kettering Cancer Center, United States
Mohamed Abd Elhamid Tantawy,
National Research Centre, Egypt

***Correspondence:**
Wei Zhang
zhangwei@hebcm.edu.cn
Pingping Chen
chenpp@hebcm.edu.cn
Zhenduo Zhang
289230116@qq.com

Specialty section:
This article was submitted to Epigenomics and Epigenetics, a section of the journal Frontiers in Genetics

Received: 25 September 2021
Accepted: 25 January 2022
Published: 24 February 2022

Citation:
Yang L, Zhang W, Li M, Dam J, Huang K, Wang Y, Qiu Z, Sun T, Chen P, Zhang Z and Zhang W (2022) Evaluation of the Prognostic Relevance of Differential Claudin Gene Expression Highlights Claudin-4 as Being Suppressed by TGFβ1 Inhibitor in Colorectal Cancer. Front. Genet. 13:783016. doi: 10.3389/fgene.2022.783016

Background: Claudins (CLDNs) are a family of closely related transmembrane proteins that have been linked to oncogenic transformation and metastasis across a range of cancers, suggesting that they may be valuable diagnostic and/or prognostic biomarkers that can be used to evaluate patient outcomes. However, CLDN expression patterns associated with colorectal cancer (CRC) remain to be defined.

Methods: The mRNA levels of 21 different CLDN family genes were assessed across 20 tumor types using the Oncomine database. Correlations between these genes and patient clinical outcomes, immune cell infiltration, clinicopathological staging, lymph node metastasis, and mutational status were analyzed using the GEPIA, UALCAN, Human Protein Atlas, Tumor Immune Estimation Resource, STRING, Genenetwork, cBioportal, and DAVID databases in an effort to clarify the potential functional roles of different CLDN protein in CRC. Molecular docking analyses were used to probe potential interactions between CLDN4 and TGFβ1. Levels of CLDN4 and CLDN11 mRNA expression in clinical CRC patient samples and in the HT29 and HCT116 cell lines were assessed via qPCR. CLDN4 expression levels in these 2 cell lines were additionally assessed following TGFβ1 inhibitor treatment.

Results: These analyses revealed that COAD and READ tissues exhibited the upregulation of CLDN1, CLDN2, CLDN3, CLDN4, CLDN7, and CLDN12 as well as the downregulation of CLDN5 and CLDN11 relative to control tissues. Higher CLDN11 and CLDN14 expression as well as lower CLDN23 mRNA levels were associated with poorer overall survival (OS) outcomes. Moreover, CLDN2 and CLDN3 or CLDN11 mRNA levels were significantly associated with lymph node metastatic progression in COAD or READ lower in COAD and READ tissues. A positive correlation between the expression of CLDN11 and predicted macrophage, dendritic cell, and $CD4^+$ T cell infiltration was identified in CRC, with CLDN12 expression further being positively correlated with $CD4^+$ T cell infiltration whereas a negative correlation was observed between such

infiltration and the expression of CLDN3 and CLDN15. A positive correlation between CLDN1, CLDN16, and neutrophil infiltration was additionally detected, whereas neutrophil levels were negatively correlated with the expression of CLDN3 and CLDN15. Molecular docking suggested that CLDN4 was able to directly bind via hydrogen bond with TGFβ1. Relative to paracancerous tissues, clinical CRC tumor tissue samples exhibited CLDN4 and CLDN11 upregulation and downregulation, respectively. LY364947 was able to suppress the expression of CLDN4 in both the HT29 and HCT116 cell lines.

Conclusion: Together, these results suggest that the expression of different CLDN family genes is closely associated with CRC tumor clinicopathological staging and immune cell infiltration. Moreover, CLDN4 expression is closely associated with TGFβ1 in CRC, suggesting that it and other CLDN family members may represent viable targets for antitumor therapeutic intervention.

Keywords: colorectal cancer, CLDNs, public databases, TGFβ1, molecular docking, prognostic value

INTRODUCTION

Colorectal cancer (CRC) is the third most common and fourth deadliest cancer (Mármol et al., 2017). As CRC is often diagnosed at an early stage, it generally has a good 5-year overall survival (OS) rate, but patients diagnosed at a later stage with metastatic disease often fair poorly (Yamagishi et al., 2016). Diagnostic and prognostic biomarkers of CRC thus offer clear clinical value for identifying and monitoring affected patients.

Claudins (CLDNs) are members of a 27 + gene family of transmembrane proteins with four transmembrane helical domains, two extracellular loops, and short N- and C-terminal domains (Suzuki et al., 2014). These CLDNs play important roles in tumorigenesis and can influence aggressive growth and motility owing to their role as regulators of intercellular adhesion. Indeed, there is growing evidence that CLDN dysregulation is common across many cancer types such as gastric, lung, breast, ovarian, and colorectal cancer (Yu et al., 2009; Tabariès and Siegel, 2017).

Herein, we surveyed patterns of CLDN mRNA and protein expression in different CRC patient subsets in order to elucidate the links between these different genes and outcomes associated with different CRC stages. In addition, relationships between CLDN expression, mutational status, and immune cell infiltration in CRC tumors were assessed to better clarify the mechanistic role of these CLDNs and to guide the selection of future targets for therapeutic intervention when treating patients with this cancer type.

MATERIALS AND METHODS

Clinical Samples

CRC patient tumor and paracancerous tissues were collected from the First Department of General Surgery, Shijiazhuang People's Hospital (Hebei Province, China), and Hebei Medical University Fourth Hospital (China). Pathologists confirmed the diagnosis and staging of all patients, and the Ethical Committee of Shijiazhuang People's Hospital approved this study. All patients provided written informed consent to participate.

Cell Culture

Human HT29 and HCT116 cell lines were grown in McCoy's 5A media (Gibco, CA, USA) containing 10% FBS and penicillin/streptomycin at 37°C in a 5% CO_2 incubator (Yang et al., 2021).

Oncomine Database Analysis of CLDN mRNA Profiles

The Oncomine database (http://www.oncomine.com) (Rhodes et al., 2004) was utilized to evaluate the expression of 21 different CLDN family members in 20 cancer types, using the following criteria for differential expression: $p = 0.01$, Fold-change > 1.5, gene rank ≤10%.

GEPIA Analyses

The GEPIA database (http://gepia.cancer-pku.cn/) (Tang et al., 2017) was used to analyze colon adenocarcinoma (COAD) and rectal adenocarcinoma (READ) tissue samples in order to explore the relationships between different CLDN family members and key clinical outcomes including staging, overall survival (OS), and disease-free survival (DFS). Default GEPIA parameters were utilized for these analyses.

Human Protein Atlas Analyses

IHC staining data pertaining to the protein level expression of different CLDN family members were assessed with the Human Protein Atlas database (https://www.proteinatlas.org/) in CRC patient tumors and normal tissue samples (Pontén et al., 2008).

Immune Cell Infiltration Analysis

The association between different CLDN family members and the infiltration of immune cells into CRC tumors was assessed with the TIMER database (https://cistrome.shinyapps.io/timer/), with scatter plots for different CLDN genes being generated to demonstrate purity-corrected partial Spearman's r values and corresponding significance metrics (Li et al., 2021).

UALCAN Database Analyses

Staging and nodal metastasis status for COAD (n = 324) and READ (n = 172) patient clinicopathologic parameters were evaluated using the UALCAN database (Lyu et al., 2020). According to multivariate Kaplan-Meier survival analysis, with *p*-values calculated using the log-rank test (log-rank test). The Ualcan database uses TCGA RNA-seq and clinical data for 31 cancer types.

Analysis of CLDN Mutational Status in CRC

The mutational status of different CLDN family genes in CRC was assessed using the cBioPortal database (http://cbioportal.org) (Cerami et al., 2012). Assessed mutations included deep deletions, missense mutations, copy number amplifications, and mRNA upregulation.

CLDN Matrix Interaction Analyses

An interaction matrix for CLDN family genes was generated using the "matrix" command in the GeneNetwork database (Mulligan et al., 2017), enabling a correlation analysis between different CLDN family members.

Protein-Protein Interaction Network

The STRING database (http://string-db.org; version 11.0) was used to construct a CLDN family gene PPI network incorporating 24 co-expressed genes with a score of >0.4 (Franceschini et al., 2013). The network was visualized using Cytoscape (v 3.8.2).

GO and KEGG Enrichment Analysis

GO analyses were used to assess the enrichment of particular genes in specific functional categories including biological processes (BPs), cellular components (CCs), and molecular functions (MFs), enabling efficient analyses of transcriptomic datasets (Thomas et al., 2019). The Kyoto Encyclopedia of Genes and Genomes (KEGG) database compiles functional data pertaining to a diverse array of regulatory pathways (Kanehisa et al., 2016). The online DAVID database (https://david.ncifcrf.gov/; version 6.8) was used for GO annotation and KEGG pathway analyses in this study (Huang et al., 2007). R was used to visualize the enrichment data.

Molecular Docking Analysis

Full-length wild-type protein sequences were obtained from UniProt (https://www.uniprot.org/) (UniProt Consortium, 2021), with Uniprot ID. O14493 and Uniprot ID. P01137 being used for CLDN4 and TGFβ1, respectively. Three-dimensional structures for these proteins were obtained from the RCSB PDB database (https://www.rcsb.org/) (Berman et al., 2000), using PDB IDs of 7KP4 and 5VQP, respectively, for docking analyses. The CLDN4 and TGFβ1 proteins were docked with the Zdock server 3.0.2 (https://zdock.umassmed.edu/) (Pierce et al., 2014). Prior to docking, PyMOL was utilized to remove water molecules, heteroatoms, and repeated subunits, with the best docked complex being assessed for hydrogen bonding.

qRT-PCR

The ISOGEN reagent (Nippon Gene Co. Ltd., Kokyo, Japan) was utilized to isolate RNA from tissue and cell line samples, after which qPCR was conducted by initially reverse transcribing 1 μg of total RNA per sample using a Revert Aid first strand cDNA synthesis kit (ThermoFisher Scientific). Primers used for qPCR are compiled in **Supplementary Table S1**. A Real-Time PCR system (BIOER Co. Ltd., Kokyo, Japan) was used for all qPCR analyses, and the relative expression of CLDN11, CLDN4, and TGFβ1 was assessed via the ΔCT method as in prior reports (Yang et al., 2021). For appropriate experiments, the HT29 and HCT116 cells were treated for 48 h with the TGFβ1 inhibitor LY364947 (5.00 or 10.0uM).

Western Blot

HT29 and HCT116 cells were treated for 48 h with LY364947 at concentrations of 5, and 10 μM. After being washed three times with PBS, the cells were lysed for 30 min on ice before being centrifuged at 10000 g for 5 min at 4°C for 5 min. The protein concentrations in cell lysates were determined using an ND-1000 Spectrophotometer (National Instruments) (NanoDrop, ThermoFisher Scientific). SDS-PAGE was used to separate out equal amounts of total protein, which was then transferred to PVDF membranes (Millipore, Billerica, MA, USA). After blocking with 5% milk for 2 h, we did overnight immunoblotting with primary antibodies at 4°C. The primary antibodies were raised against TGFβ1 (1:1,000; Abcam, Cambridge, MA, USA), CLDN4 (1:500; abways technology) and β-actin (AC026, at 1 : 10000 dilution). A secondary antibody of goat anti-rabbit IG (KPL074-1,506, at 1: 5,000 dilution) was then used to incubate the membranes for 1 h at 37°C. Fusion FX5 Spectra was used to determine the intensity of protein bands (Fusion, France). The membranes were then incubated for 1 h at 37°C with secondary antibodies of goat anti-rabbit IG (KPL074-1,506, at 1:5,000 dilution). The intensity of protein bands was estimated via executing Fusion FX5 Spectra (Fusion, France).

RESULTS

The Association Between CLDN Family Gene Expression and CRC Pathological Type

We began by using the Oncomine database to evaluate CLDN family member expression in CRC. In total, 19 CLDNs were found to be differentially expressed between normal tissues and COAD and READ patient samples. At the mRNA level, CLDN1, CLDN2, CLDN12, and CLDN14 were upregulated whereas CLDN3, CLDN5, CLDN7, CLDN8, CLDN11, CLDN15, and CLDN23 were downregulated (FC > 1.5) in patients with CRC (**Figure 1**). Specifically, fold-change values for CLDN1, CLDN2, and CLDN12 in COAD tissues were 6.755, 3.006, and 2.096, respectively (**Supplementary Table S1**), while in READ tissues these respective fold-change values were 4.301, 1.849, and 1.583 in the dataset analysis of Kaiser et al. (2007). CLDN19 expression was altered by 1.117 and 1.158-fold in COAD and READ tissues from this same dataset,

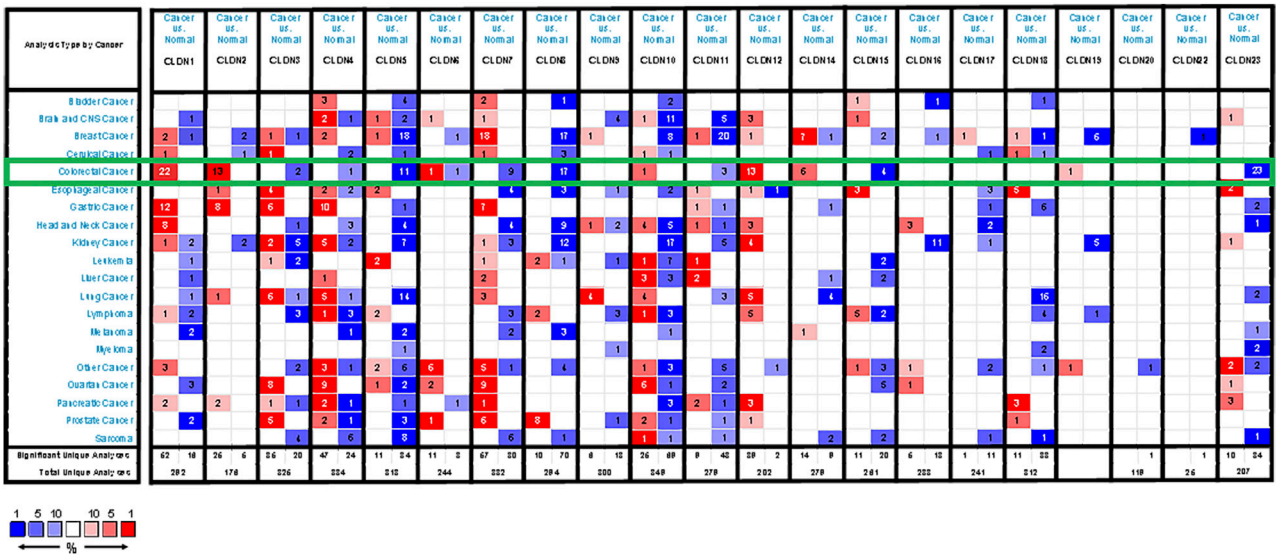

FIGURE 1 | CLDN family member expression levels across human cancers. Cut-off values for these mRNA analyses were as follows: *p*-value = 0.01, Fold-change = 1.5, gene rank = 10%. Red and blue correspond to overexpression and underexpression, respectively, with the strength of the color be proportional to the expression level for that gene.

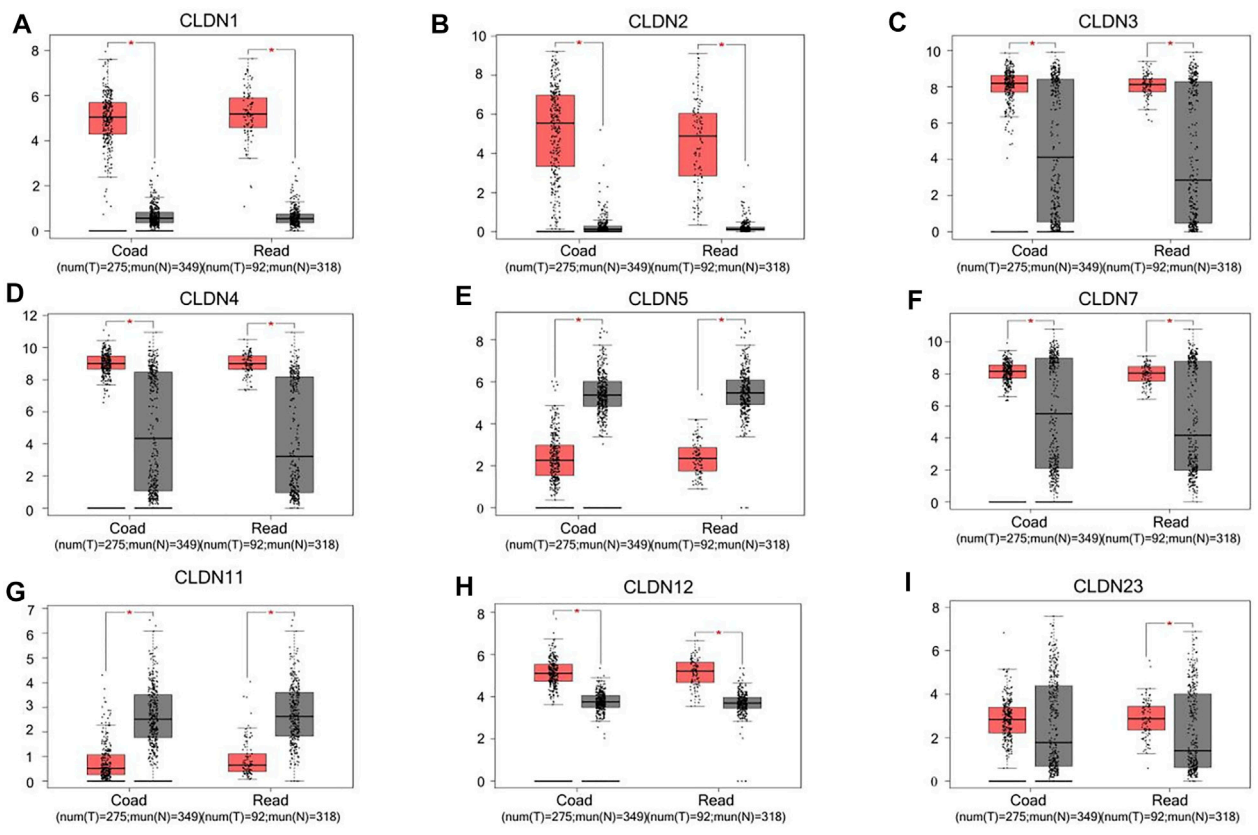

FIGURE 2 | CLDN family gene expression in COAD and READ tissues. Tumors and normal tissue controls are respectively shown in red and grey **(A-I)**. *$p < 0.05$.

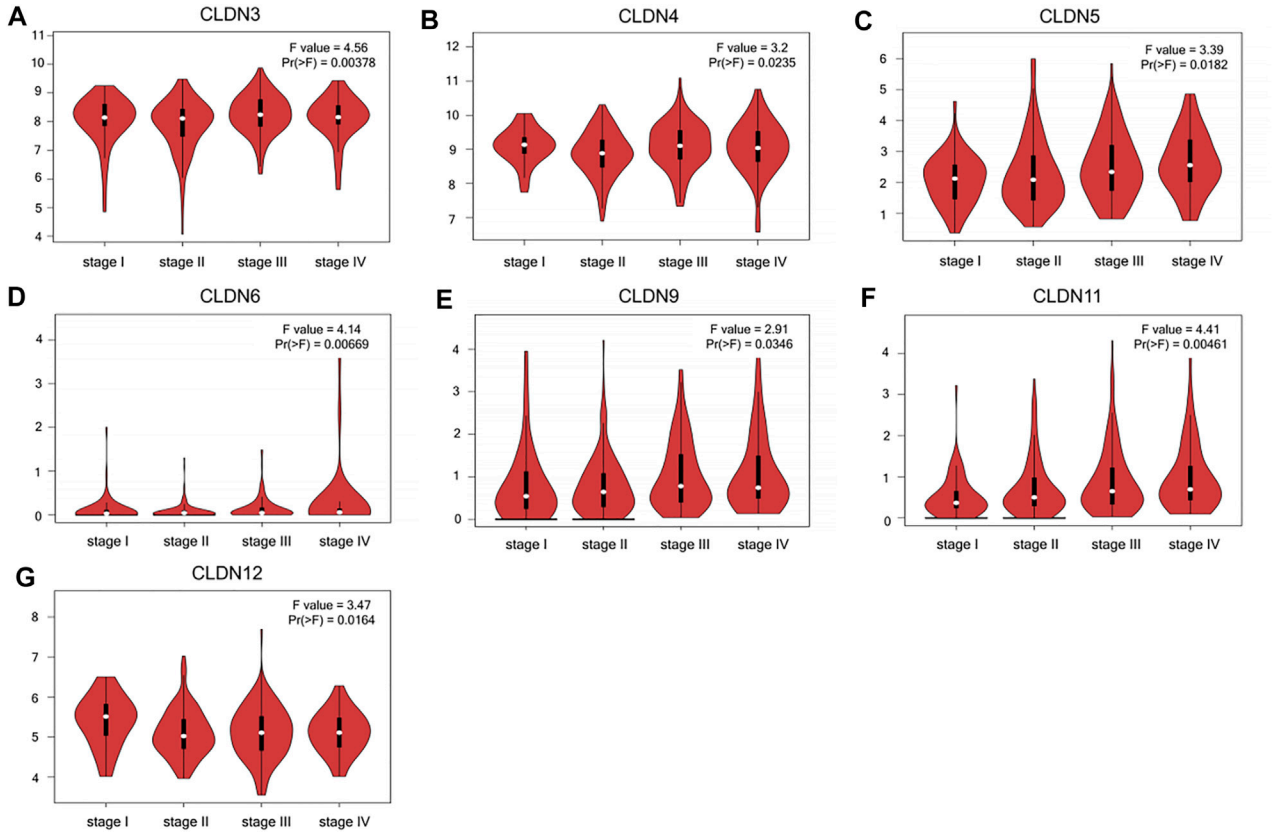

FIGURE 3 | CLDN family gene expression as a function of CRC patient disease staging **(A-G)**.

while CLDN20 expression was changed by 1.075- and 1.091-fold, respectively. Gaedcke et al. (2010) found fold-change values for the expression of CLDN1, CLDN10, CLDN11, CLDN15, and CLDN22 of 19.563, 1.583, 1.718, 1.417, and 1.05, respectively, in READ tissues. Skrzypczak et al. (2010) further reported CLDN1 and CLDN2 expression levels in CRC tissues that were altered by 6.351- and 7.754-fold, respectively. In the TCGA dataset, CLDN14 expression in READ and COAD was altered by 4.876-fold and 4.368-fold, respectively, while it was altered by 3.471-fold in the dataset generated by Gaedke et al. CLDN18 expression was altered by 1.298-fold and 1.184-fold in COAD data from TCGA and Kaiser et al., and by 1.216-fold and 1.25-fold in READ samples from these two respective data sources.

The GEPIA database was next utilized to compare the expression of different CLDN family members in CRC and in normal colon tissue samples, revealing CLDN1, CLDN2, CLDN3, CLDN4, CLDN7, and CLDN12 to have been upregulated and CLDN5 and CLDN11 to have been downregulated in COAD and READ tissues relative to control samples (**Figure 2**). Significant differences in CLDN3, CLDN4, CLDN5, CLDN6, CLDN9, CLDN11, and CLDN12 expression were evident as a function of tumor stage (**Figure 3**). CLDN3, CLDN4 and CLDN6 were related with clinicopathological stage in CRC. The more CLDN5, CLDN9, and CLDN11 are expressed in CRC, the worse the stage. CLDN12 expression in CRC associated with pathological stage. We additionally examined the link between CLDN family gene mRNA levels and CRC patient lymph node metastasis, revealing a significant relationship between the expression of CLDN1, CLDN2, CLDN3, CLDN7, CLDN8, CLDN9, CLDN11, CLDN14, CLDN16 and CLDN23 nodal metastasis in COAD and READ (**Figures 4A, B, C, G, H, I, K, M, N, R**) (**Figures 5A, B, C, E, F, G, I, K, M, O**).

The Association Between CLDN Expression and CRC Patient Survival Outcomes

Kaplan-Meier curves and log-rank tests were next performed, revealing a relationship between the upregulation of CLDN11, CLDN14, and CLDN23 at the mRNA level and COAD and READ patient OS (**Figure 6**). Specifically, high levels of CLDN11 and CLDN14 expression were correlated with worse patient OS, whereas CLDN23 overexpression was linked to better OS outcomes.

Analysis of CLDN Protein Levels in CRC

The Human Protein Atlas yielded findings that were somewhat consistent with the mRNA level data above, with higher CLDN1 and CLDN12 protein levels and lower

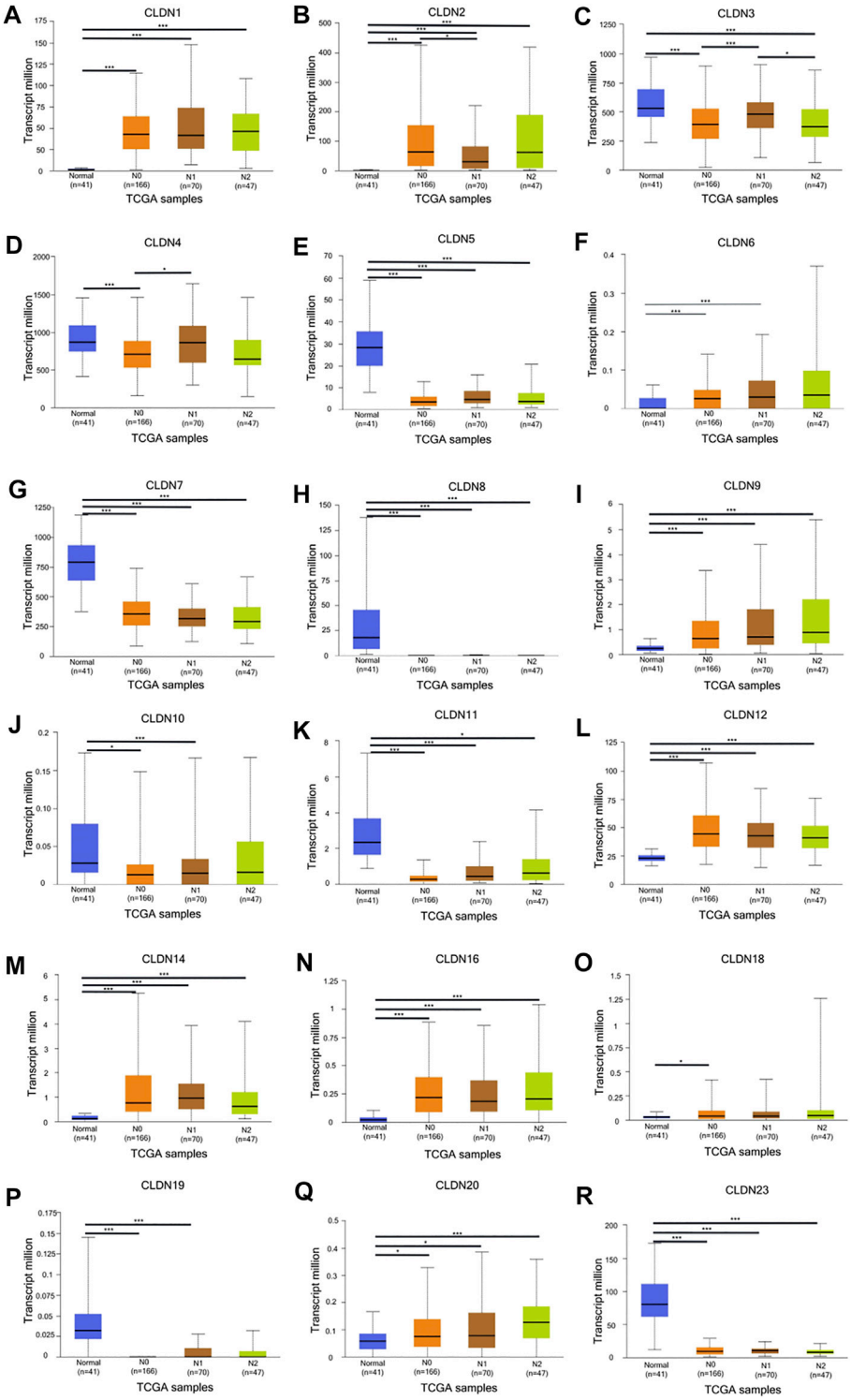

FIGURE 4 | The UALCAN database shows a link between CLDN gene expression and nodal metastases in COAD patients. Box plots represent the CLDN mRNA expression levels in normal tissues or in COAD patients with N0–N2 disease **(A–R)**. *$p < 0.05$; **$p < 0.01$; ***$p < 0.001$.

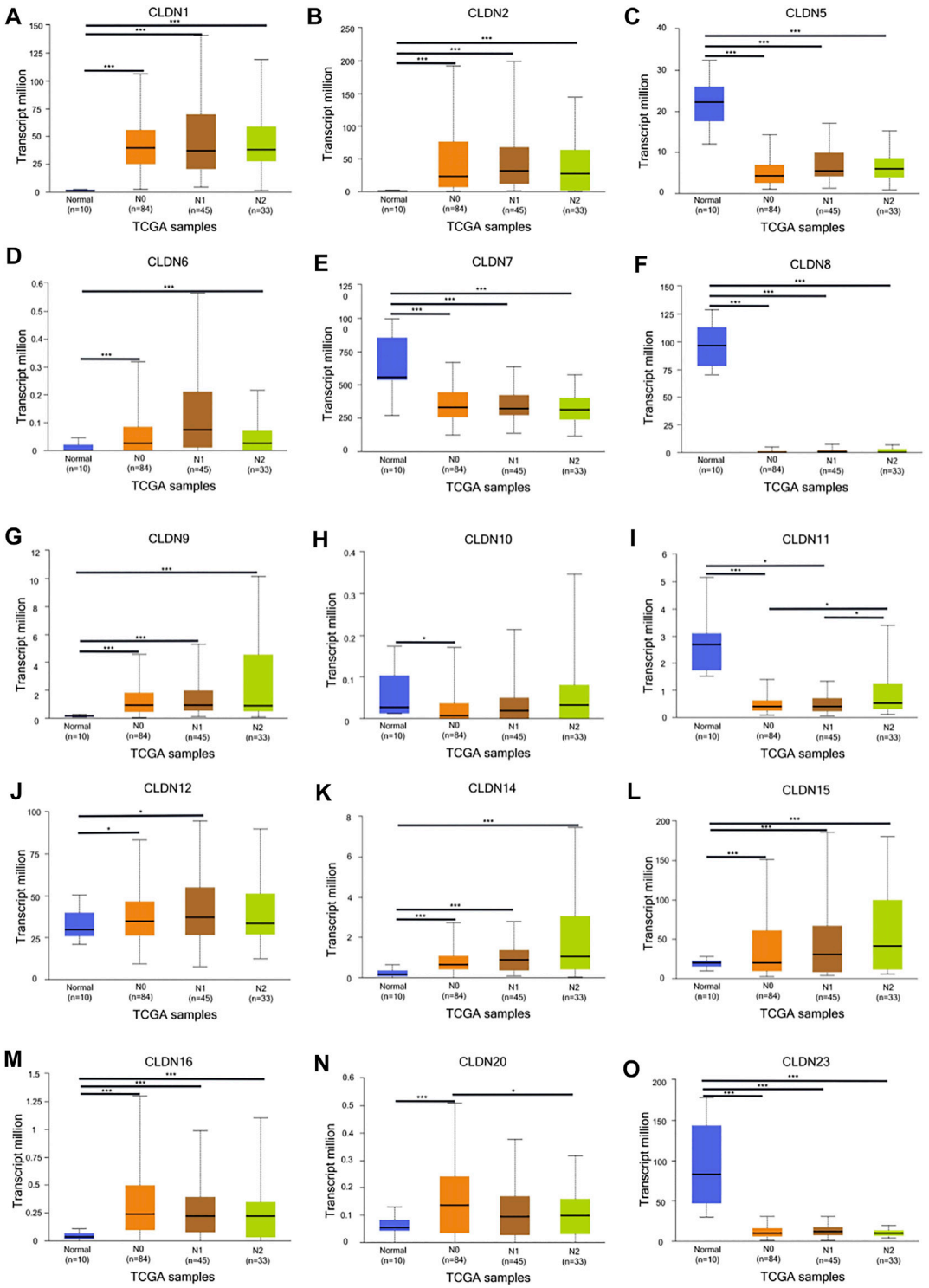

FIGURE 5 | The UALCAN database shows a link between CLDN gene expression and nodal metastases in READ patients. Box plots represent the CLDN mRNA expression levels in normal tissues or in READ patients with N0–N2 disease **(A–O)**. *$p < 0.05$; **$p < 0.01$; ***$p < 0.001$.

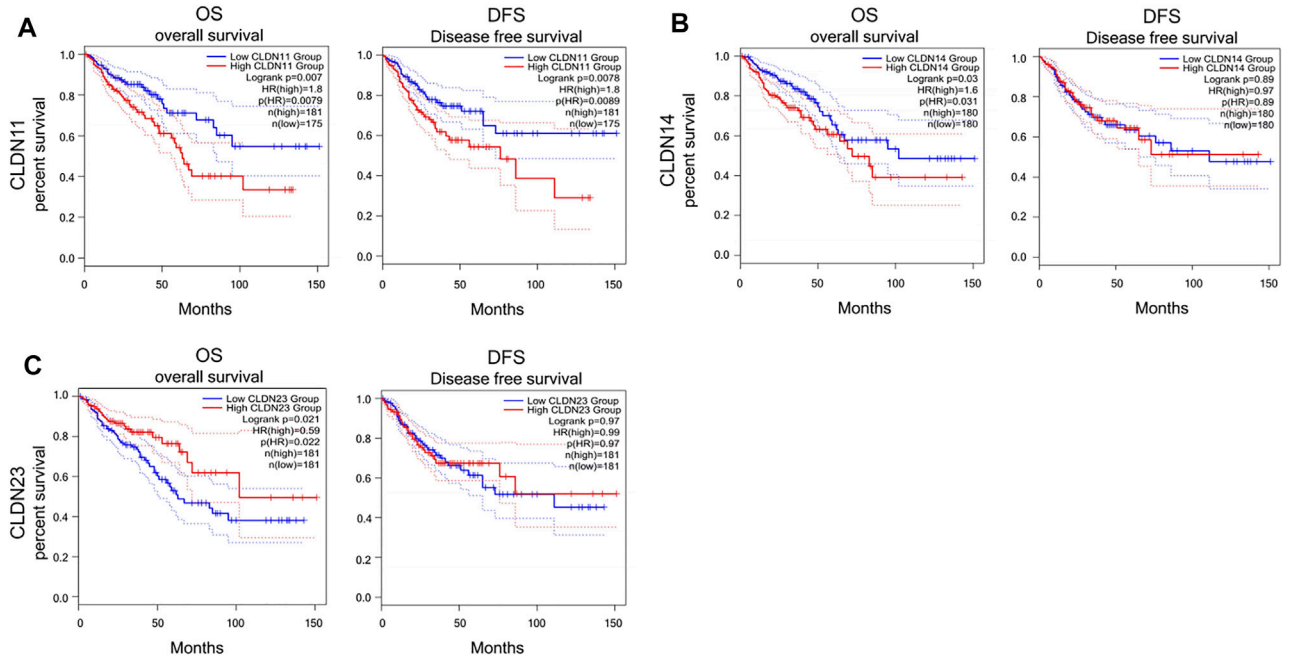

FIGURE 6 | Kaplan–Meier survival analyses assing the link between CLDN expression and CRC patient survival in GEPIA database **(A-C)** ($p < 0.05$).

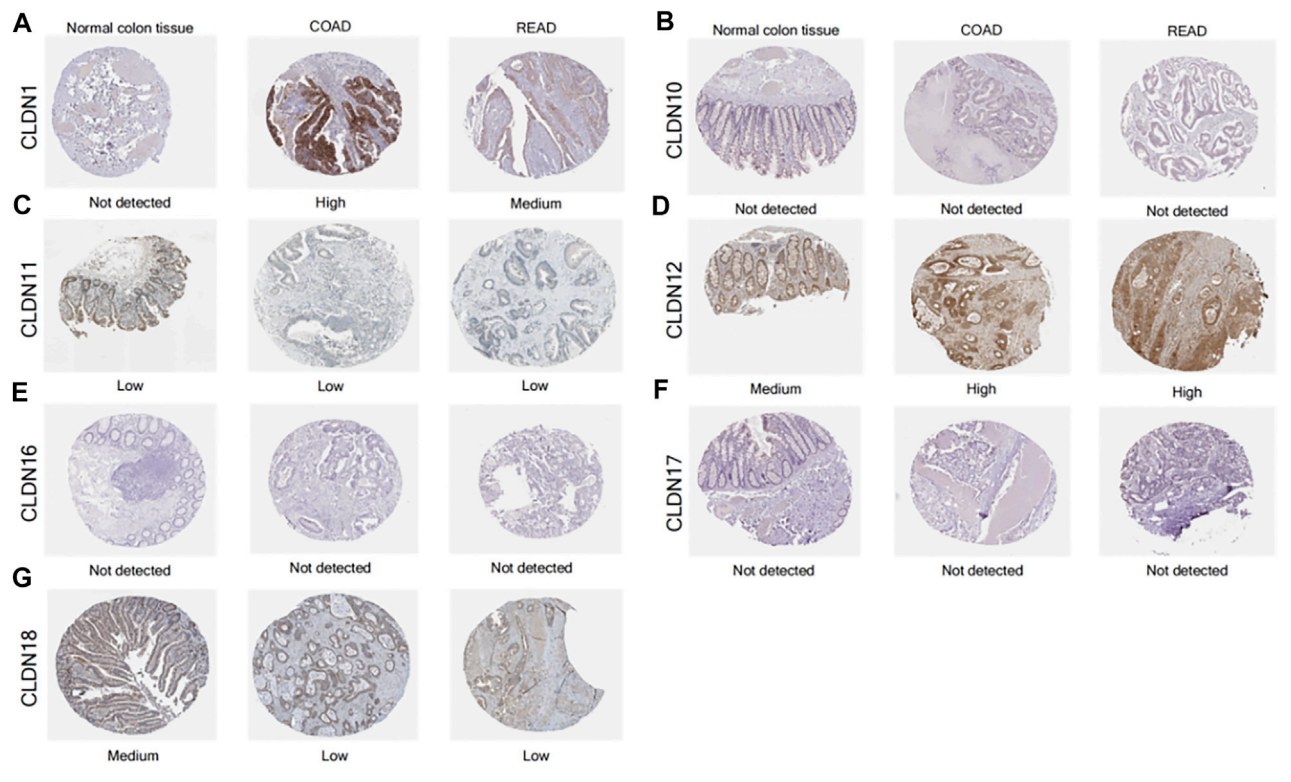

FIGURE 7 | IHC staining for CLDN protein expression levels in tumor samples from CRC patients and normal colon tissue samples **(A-G)**.

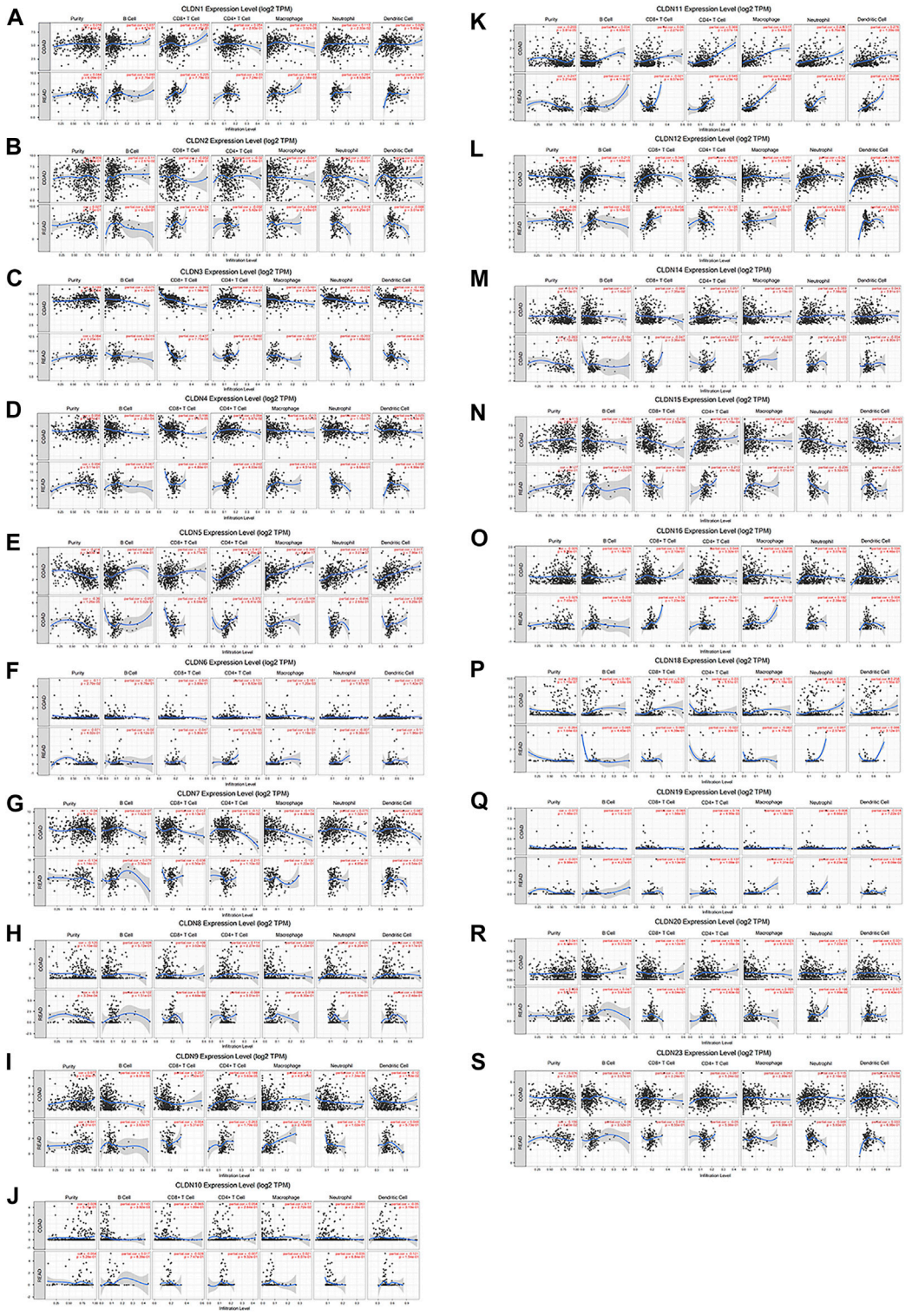

FIGURE 8 | The relationship between CLDN mRNA level expression and CRC tumor immune cell infiltration **(A-S)**.

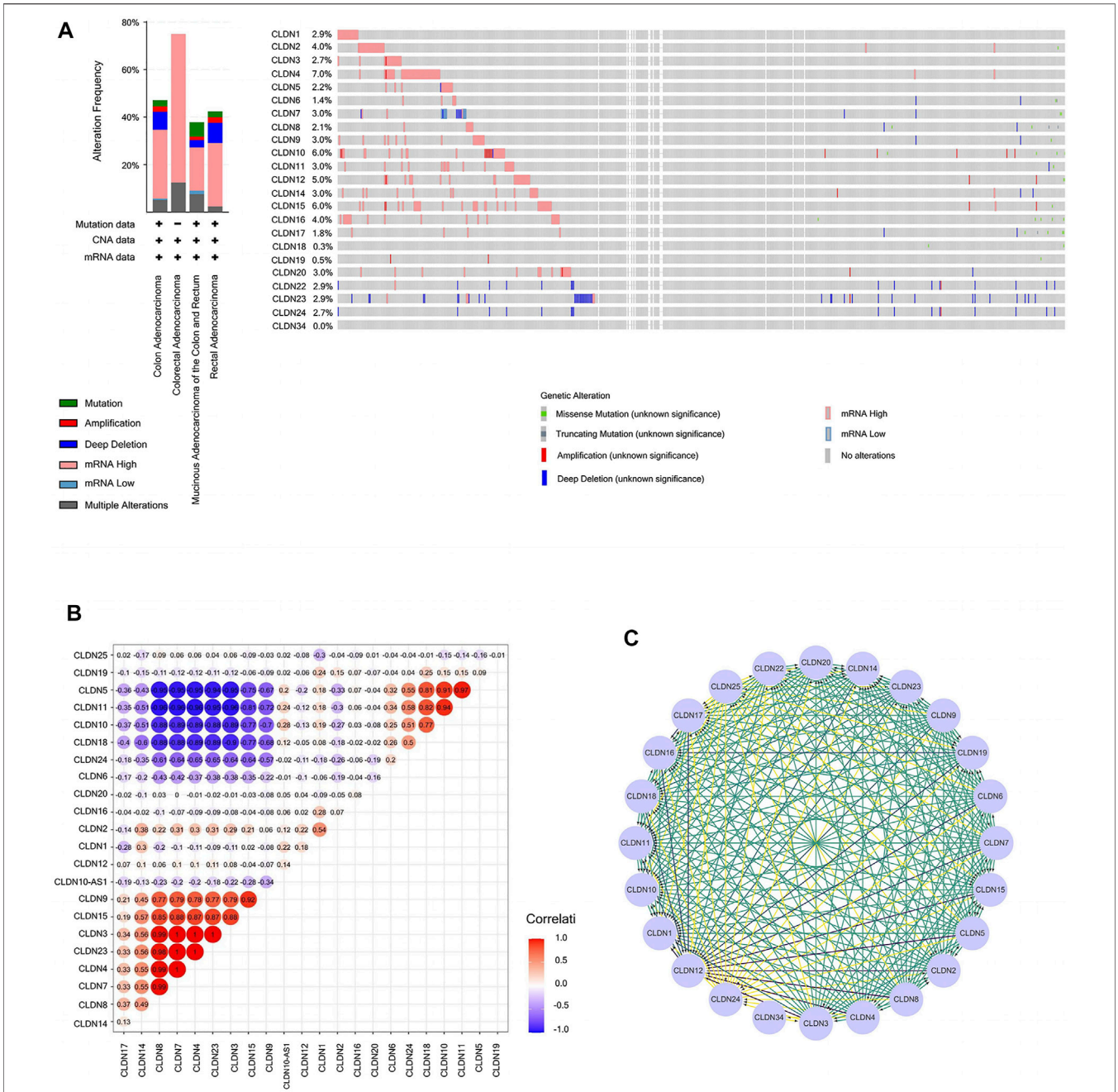

FIGURE 9 | (A) Cancer type summary and Oncoprint for CLDN family genes in BioPortal. **(B)** Heatmap demonstrating correlations among CLDN family genes with respect to mRNA expression. Colors correspond to Pearson correlation coefficients, which span from blue to red (negative and positively correlated, respectively). **(C)** A PPI network of CLDNs was generated using the STRING database to clarify interactions among these proteins.

CLDN11 levels in CRC tumors relative to samples of normal colon tissue (**Figure 7**).

The Relationship Between CLDN Expression and CRC Tumor Immune Cell Infiltration

Using the TIMER database, we detected a negative correlation between the mRNA level expression of CLDN5, CLDN8, CLDN11, and CLDN18 and CRC tumor purity (**Figures 8E, H, J, O**). Moreover, CLDN12 expression was correlated with B cell infiltration and positively correlated with $CD8^+$ T cells (**Figures 8K**). Additionally, CLDN5, CLDN9, CLDN11, CLDN15, and CLDN20 were significantly positively correlated with $CD4^+$ T cell infiltration into CRC tumors, while CLDN7 expression was negatively correlated with such infiltration (**Figures 8E, H, J, M, Q**). Additionally, a clear positive correlation was observed between macrophage infiltration

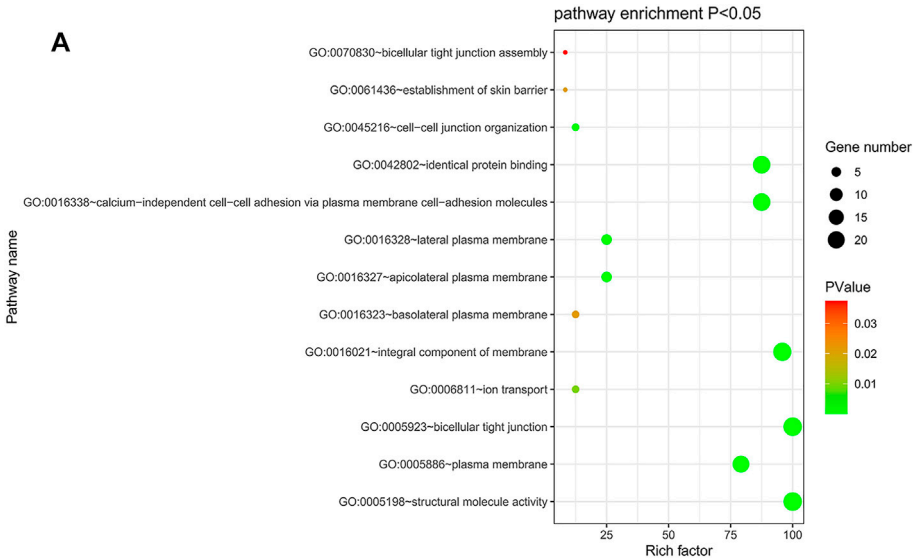

FIGURE 10 | (A) DAVID was used for the functional enrichment analysis of CLDN family genes, with results shown using a bubble chart.

and the expression of CLDN1, CLDN9, CLDN11, and CLDN16 (**Figures 8A,H,J,N**). Neutrophil infiltration was negatively correlated with CLDN15 expression and positively correlated with CLDN1 and CLDN16 expression (**Figures 8A, M, N**), while CLDN11 expression was positively correlated with dendritic cell infiltration (**Figures 8J**).

CLDN Mutation and the Relationships in CLDN Family in COAD Patients

Next, we assessed CLDN family gene mutations in 640 COAD samples using the online cBioPortal tool, revealing mutations in 283 samples (44%) (**Figures 9A**). Mutations in CLDN10 (6%) were attributable to missense mutations and gene amplification.

The Genenetwork database was also used to explore relationships among CLDN gene expression levels in COAD samples, revealing the following correlative relationships: CLDN1 with CLDN2; CLDN3 with CLDN4, CLDN7, CLDN8, CLDN14, and CLDN23; CLDN4 with CLDN7, CLDN8, and CLDN14; CLDN5 with CLDN10, CLDN11, CLDN18, and CLDN24; CLDN7 with CLDN8 and CLDN14; CLDN8 with CLDN14; CLDN9 with CLDN3, CLDN4, CLDN7, CLDN8, CLDN14, CLDN15, and CLDN23; CLDN10 with CLDN18 and CLDN24; CLDN11 with CLDN10, CLDN18, and CLDN24; CLDN15 with CLDN3, CLDN4, CLDN7, CLDN8, CLDN14, and CLDN23; CLDN18 with CLDN24; and CLDN23 with CLDN4, CLDN7, CLDN8, CLDN14, and CLDN23. A co-expression network for these CLDNs is shown in **Figures 9B**.

A PPI network for these CLDN family genes was generated composed of 24 nodes and 254 edges (**Figures 9C**).

GO Function and KEGG Pathway Enrichment Analyses of CLDN Genes in CRC

The DAVID database was utilized to predict the functional roles of different CLDNs in key CRC-related biological processes, molecular functions, and cellular components (**Figures 10A**). KEGG pathway analyses further revealed a close relationship between these CLDN family members and tight junctions, cell adhesion molecules, leukocyte transendothelial migration, and Hepatitis C (**Supplementary Table S2**).

Molecular Docking Analyses

A prior study of inflammatory bowel disease demonstrated the ability of TGFβ1 signaling inhibition to suppress CLDN4 expression (Marincola Smith et al., 2021). A molecular docking analysis was therefore conducted to explore putative interactions between CLDN4 and TGFβ1. For this approach, ZDOCK scores were used to estimate protein-protein binding affinity, with higher scores being indicating of greater binding affinity (Pierce et al., 2011). This approach revealed that nine hydrogen bonds were predicted to form between CLDN4 and TGFβ1, with interactions between Glu109 of CLDN4 and Gln177 of TGFβ1, Cys107 of CLDN4 and Gly173 and Arg181 of TGFβ1, Val95 of CLDN4 rand Ser244 of TGFβ1, Ser98 of CLDN4 and His247 and Arg249 of TGFβ1, Trp18 of CLDN4 and Leu242 of TGFβ1, Ala20 of CLDN4 and Glu261 of TGFβ1, and Leu173 of CLDN4 and Thr260 of TGFβ1 (**Figures 11A**).

Assessment of CLDN4 and CLDN11 Expression and the Responsiveness of CLDN4 to TGFβ1 Inhibitor Treatment

At the mRNA level, we found that CLDN11 and CLDN4 expression were respectively reduced and increased in CRC tumor samples relative to paracancerous controls as measured via qPCR ($n = 10$, $p < 0.05$). At the protein level, CLDN4 expression was increased by WB ($n = 5$, $p < 0.05$) (**Figures 11B,C,D**) (**Supplementary Table S3**). Treatment with LY364947 (TGFβ1 inhibitor) at a dose of five or 10 uM was sufficient to

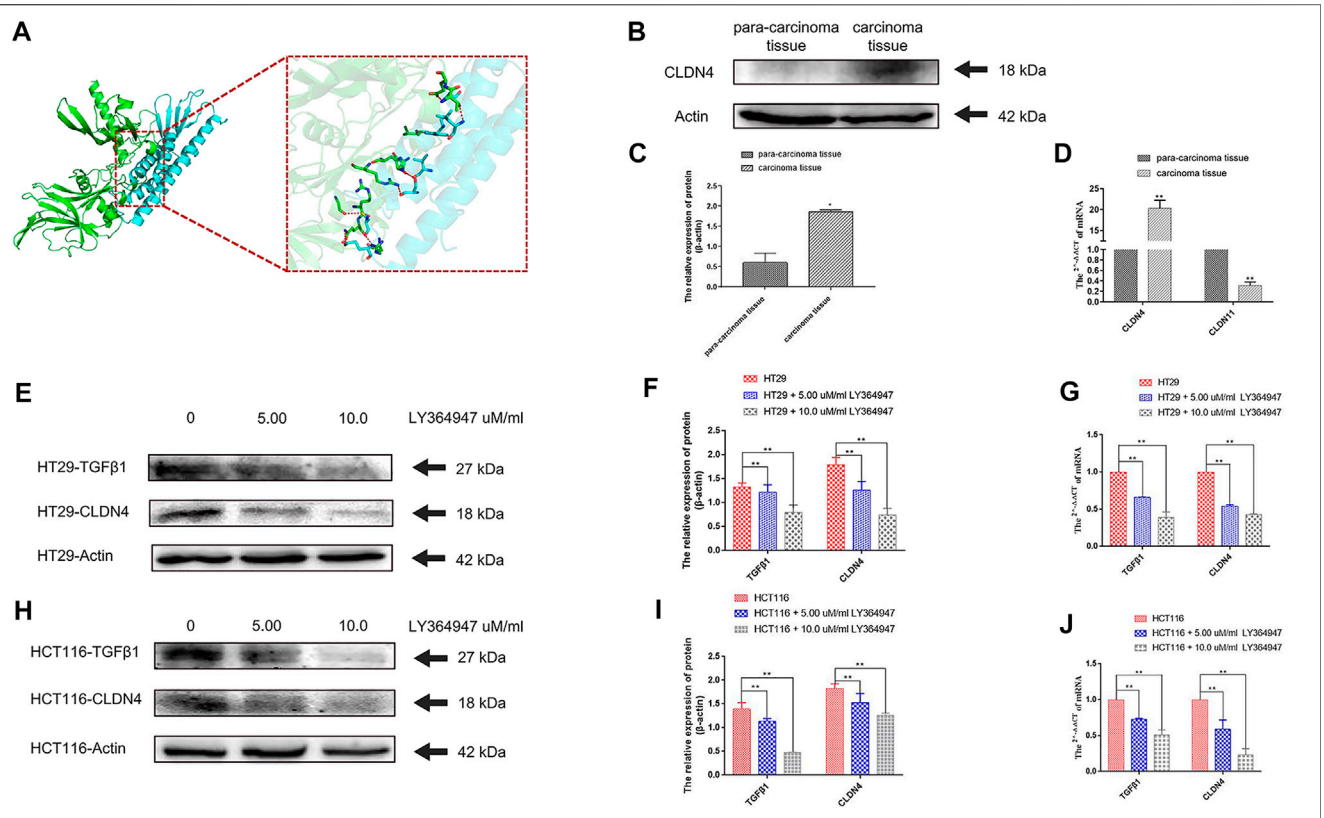

FIGURE 11 | (A) A docking analysis of CLDN4 and TGFβ1. **(B) (C)** The protein of CLDN4 levels was increased in human CRC tissues (n = 5, $*p < 0.05$; $**p < 0.01$). **(D)** CLDN4 and CLDN11 mRNA levels were respectively increased and decreased in human CRC tissues (n = 10, $*p < 0.05$; $**p < 0.01$). **(E) (F) (G)** Western blot and qRT-PCR showed TGFβ1 and CLDN4 were remarkably downregulated at both protein and mRNA levels after treatment with LY364947 at 5.0 and 10.0 uM/ml, respectively, on HT29 cells. **(H) (I) (J)** Western blot and qRT-PCR showed TGFβ1 and CLDN4 were remarkably downregulated at both protein and mRNA levels after treatment with LY364947 at 5.0 and 10.0 uM/ml, respectively, on HCT116 cells. TGFβ1 reduced CLDN4 expression in colorectal cancer cell lines.

suppress CLDN4 mRNA and protein expression at 48 h post-treatment in both HT29 and HCT116 cells (**Figure 11E, F, G, H, I, J**).

DISCUSSION

Claudin (CLDN) genes encode a family of proteins that play a critical role in the generation and functioning of tight junctions between epithelial and endothelial cells (Hewitt et al., 2006). Many malignancies rely on this protein family for their development, progression, and metastasis. Although some studies have demonstrated the importance of claudins in tumorigenesis and the prognosis of human cancers (Arabzadeh et al., 2007; Morel et al., 2012), no extensive bioinformatic analyses of this gene family have been performed in colorectal cancer to date. In this study, each gene in the claudin family was evaluated to examine its expression and prognostic relevance in colorectal cancer using bioinformatics tools, offering an opportunity to better understand how claudin gene dysregulation affects colorectal cancer, as well as how treatment can be optimized to improve patient prognosis.

Our findings revealed that the mRNA expression levels of CLDN1, CLDN2, CLDN12, and CLDN14 were upregulated in colorectal cancer tissues relative to normal tissues in the Oncomine database, whereas CLDN3, CLDN5, CLDN7, CLDN8, CLDN11, CLDN15, and CLDN23 were downregulated, as previously reported. However, when comparing colorectal cancer tissues from the GEPIA database to normal colonic mucosa, the mRNA level expression of CLDN3, CLDN7, and CLDN23 was shown to be significantly higher in these tumor tissues. Given the inconsistencies in claudin gene expression in these two databases, we focused on those claudins exhibiting comparable gene expression patterns in both databases. In addition, three genes were shown to be related with advanced colorectal cancer: CLDN11 ($p = 0.007$), and CLDN14 ($p = 0.03$) and CLDN23 ($p = 0.021$). Moreover, we found that CLDN11 and CLDN18 protein levels were decreased in CRC tumors relative to normal tissues. At the same time, high levels of CLDN11 expression were associated with an increase in the proportion of $CD4^+$ T cells, macrophages, neutrophils, and dendritic cells within tumors. We further determined that CLDN4 and TGFβ1 were capable of forming hydrogen bonds, and that CLDN4 was overexpressed in CRC cell lines and inhibited by TGFβ inhibitor treatment.

Claudin expression is related to tumor proliferation, migration, and invasion (Mori et al., 2011; Pope et al., 2014; Wang and Zöller,

2019; Li et al., 2020a). Many claudins are dysregulated in a range of cancers, as in the case of the CLDN1 and CLDN2 genes, which are overexpressed in colorectal cancer (Dhawan et al., 2011; Mori et al., 2011; Pope et al., 2014; Wang et al., 2019). CLDN3 is similarly overexpressed at the mRNA level in CRC tumors that belong to the consensus molecular subgroup (CMS)-CMS2 and CMS3, which correspond to a poor prognosis (Tang et al., 2011; Perez et al., 2020). Colorectal cancers have significant levels of CLDN4 expression (Georges et al., 2012). It has been shown that combination treatment with 5-fluorouracil (FU) and an anti-CLDN4 extracellular domain antibody (4D3) enhances antitumor efficacy against CRC (Fujiwara-Tani et al., 2018). CLDN5 expression has been shown to be reduced in squamous cell carcinomas of the lung (Akizuki et al., 2017), cervical cancer (Zhu et al., 2015), hepatocellular carcinoma (Sakaguchi et al., 2008), oral squamous cell carcinoma (Phattarataratip and Sappayatosok, 2016), breast cancer (Escudero-Esparza et al., 2012), and pancreatic cancer (Jakab et al., 2011). Similarly, compared to normal mucosal tissues, CLDN5 expression was downregulated in CRC tumors (Cherradi et al., 2019), although the mechanistic basis for this change remains poorly understood. CLDN6 is a cellular adhesion protein that is abundantly expressed in gastric tumors tissues and cell lines, and is associated with a poor prognosis. CLDN6 enhances gastric cancer cell proliferation and invasiveness via the YAP1 and YAP1-Snail1 axis (Li et al., 2020a). High expression of CLDN7 has been shown to accelerate pancreatic and colon cancer progression (Mu et al., 2019; Wang and Zöller, 2019). Cancer initiation cells (CICs) and nasopharyngeal carcinoma metastases in gastrointestinal tumors can be detected using CLDN7 as a marker protein (Liu et al., 2017; Kyuno et al., 2019). The MAPK/ERK signaling pathway is activated in colorectal cancers when CLDN8 is overexpressed (Cheng et al., 2019). In contrast, low levels of CLDN8 expression slow the progression of renal clear cell carcinoma via the EMT/AKT signaling pathway (Zhu et al., 2020). Colonic epithelial barrier function in mice is influenced by TGF family signaling, which regulates CLDN2, CLDN4, CLDN7, and CLDN8 in colonic epithelial cells. We additionally confirmed that TGFβ1 and CLDN4 engage in molecular structural interactions and that TGFβ1 inhibits CLDN4 transcription and protein expression in human colorectal cancer cell lines. Increased levels of TGFβ1 may affect the expression of CLDN4, potentially influencing CRC development. CLDN9 can be employed as a prognostic biomarker for gastric and esophageal cancer (Kang et al., 2020; Yu et al., 2020). CLDN10 overexpression promotes carcinogenesis in papillary thyroid cancer, which has a poor prognosis (Zhou et al., 2018). However, infiltration of B cells, CD8 + T cells, and macrophages as a consequence of increased CLDN10 expression improves the prognosis of patients with papillary thyroid carcinoma (Xiang et al., 2020). TGFβ or WNT/β-catenin-induced epithelial-mesenchymal transition (EMT) and tumor resistance may be linked to CLDN10, which offers promise as a prognostic biomarker in ovarian cancer (Gao et al., 2017; Li et al., 2020b). Hypermethylated CLDN11 can be utilized as a biomarker for the early detection of CRC melanoma, and gastric cancer (Agarwal et al., 2009; Karagiannis et al., 2014; Guo et al., 2019). While CLDN11 is perhaps the best-studied claudin in oncogenic contexts to date, it has yet to be identified as either a promoter or repressor of tumor growth (Bhat et al., 2020). CLDN12 is involved in the formation of Ca2+ channels in intestinal epithelial cells and is involved in Ca2+ uptake in intestinal epithelial cells (Fujita et al., 2008). According to prior studies, CLDN12 is the most uniformly expressed of these genes across murine organs (Hwang et al., 2014). By activating PI3K/AKT/mTOR, CLDN14 promotes CRC development (Qiao et al., 2021). CLDN15 has been shown to be a positive indicator associated with malignant pleural mesothelioma in clinical contexts (Watanabe et al., 2021), while CLDN16 is a predictor of oral squamous cell carcinoma, breast cancer, and thyroid cancer (Chen et al., 2010; Gomez-Rueda et al., 2016; Ribeiro et al., 2021). In gastric cancer, CLDN18 can be employed as a tumor marker (Matsusaka et al., 2016). Moreover, CRC patients with low levels of CLDN23 expression may benefit from its use as a prognostic, diagnostic, or therapeutic target (Oh et al., 2017; Liu et al., 2020).

Previous studies exploring the effects of CLDN1, CLDN2, CLDN4, CLDN11, CLDN12, CLDN14, and CLDN23 expression on CRC tumor growth have yielded findings consistent with our results in the present study. However, the influence of additional genes expressed in CRC on tumor growth remains unknown. In addition, as many of these studies are subject to various limitations, the same genes may not be consistently expressed in both databases analyzed in the present study, and the results may thus be skewed. Secondly, as we used an online database to analyze gene expression patterns, our findings remain to be verified in a large-scale colorectal cancer clinical study.

In conclusion, we herein found that many claudin family genes and proteins were dysregulated in CRC by querying multiple publicly available databases. Claudin family proteins have also been implicated in various phases of cancer development, lymph node metastasis, and immune cell infiltration. In addition, TGFβ1 was found to suppress the expression of CLDN4 in CRC cell lines. In general, claudin family genes contribute to the progression and prognosis of colorectal cancer, and they may thus be prospective targets for the development of novel pharmaceutical preparations capable of treating CRC.

DATA AVAILABILITY STATEMENT

The datasets presented in this study can be found in online repositories. The names of the repository/repositories and accession number(s) can be found in the article/**Supplementary Material**.

ETHICS STATEMENT

The studies involving human participants were reviewed and approved by The Ethic Committee of Hebei University of Chinese Medicine. The patients/participants provided their written informed consent to participate in this study.

AUTHOR CONTRIBUTIONS

WZ, PC and ZZ designed the study. WZ, PC and ZZ supervised the study and wrote the manuscript. LY and WZ performed the

experiments. ML, KH, YW, ZQ and TS collected and analyzed the data. All authors contributed to the article and approved the submitted version.

FUNDING

The work was supported by the Key Basic Applied Project of Hebei Provincial Department of Science & Technology (grant NO. 15967730D) and Hebei Provincial Administration of Traditional Chinese Medicine (2022077).

SUPPLEMENTARY MATERIAL

The Supplementary Material for this article can be found online at: https://www.frontiersin.org/articles/10.3389/fgene.2022.783016/full#supplementary-material

REFERENCES

Agarwal, R., Mori, Y., Cheng, Y., Jin, Z., Olaru, A. V., Hamilton, J. P., et al. (2009). Silencing of Claudin-11 Is Associated with Increased Invasiveness of Gastric Cancer Cells. *PLoS One* 4 (11), e8002. doi:10.1371/journal.pone.0008002

Akizuki, R., Shimobaba, S., Matsunaga, T., Endo, S., and Ikari, A. (2017). Claudin-5, -7, and -18 Suppress Proliferation Mediated by Inhibition of Phosphorylation of Akt in Human Lung Squamous Cell Carcinoma. *Biochim. Biophys. Acta (Bba) - Mol. Cel Res.* 1864, 293–302. doi:10.1016/j.bbamcr.2016.11.018

Arabzadeh, A., Troy, T.-C., and Turksen, K. (2007). Changes in the Distribution Pattern of Claudin Tight junction Proteins during the Progression of Mouse Skin Tumorigenesis. *BMC Cancer* 7, 196. doi:10.1186/1471-2407-7-196

Berman, H. M., Westbrook, J., Feng, Z., and Bourne, P. E. (2000). The Protein Data Bank. *Nucleic Acids Res.* 28 (1), 235–242. doi:10.1093/nar/28.1.235

Bhat, A. A., Syed, N., Therachiyil, L., Nisar, S., Hashem, S., Macha, M. A., et al. (2020). Claudin-1, A Double-Edged Sword in Cancer. *Ijms* 21 (2), 569. doi:10.3390/ijms21020569

Cerami, E., Gao, J., Dogrusoz, U., Gross, B. E., Sumer, S. O., Aksoy, B. A., et al. (2012). The cBio Cancer Genomics Portal: An Open Platform for Exploring Multidimensional Cancer Genomics Data: Figure 1. *Cancer Discov.* 2 (5), 401–404. doi:10.1158/2159-8290.CD-12-0095

Chen, S. J., Chien, S. Y., Lin, C., and Chen, D. R. (2010). Significant Elevation of CLDN16 and HAPLN3 Gene Expression in Human Breast Cancer. *Oncol. Rep.* 24 (3), 759–766. doi:10.3892/or_00000918

Cheng, B., Rong, A., Zhou, Q., and Li, W. (2019). CLDN8 Promotes Colorectal Cancer Cell Proliferation, Migration, and Invasion by Activating MAPK/ERK Signaling. *Cmar* 11, 3741–3751. doi:10.2147/CMAR.S189558

Cherradi, S., Martineau, P., Gongora, C., and Del Rio, M. (2019). Claudin Gene Expression Profiles and Clinical Value in Colorectal Tumors Classified According to Their Molecular Subtype. *Cmar* 11, 1337–1348. doi:10.2147/CMAR.S188192

Dhawan, P., Ahmad, R., Chaturvedi, R., Smith, J. J., Midha, R., Mittal, M. K., et al. (2011). Claudin-2 Expression Increases Tumorigenicity of colon Cancer Cells: Role of Epidermal Growth Factor Receptor Activation. *Oncogene* 30 (29), 3234–3247. doi:10.1038/onc.2011.43

Escudero-Esparza, A., Jiang, W. G., and Martin, T. A. (2012). Claudin-5 Is Involved in Breast Cancer Cell Motility through the N-WASP and ROCK Signalling Pathways. *J. Exp. Clin. Cancer Res.* 31, 43. doi:10.1186/1756-9966-31-43

Franceschini, A., Szklarczyk, D., Frankild, S., Kuhn, M., Simonovic, M., Roth, A., et al. (2013). STRING v9.1: Protein-Protein Interaction Networks, with Increased Coverage and Integration. *Nucleic Acids Res.* 41, D808–D815. doi:10.1093/nar/gks1094

Fujita, H., Sugimoto, K., Inatomi, S., Maeda, T., Osanai, M., Uchiyama, Y., et al. (2008). Tight junction Proteins Claudin-2 and -12 Are Critical for Vitamin D-dependent Ca2+ Absorption between Enterocytes. *MBoC* 19 (5), 1912–1921. doi:10.1091/mbc.e07-09-0973

Fujiwara-Tani, R., Sasaki, T., Luo, Y., Goto, K., Kawahara, I., Nishiguchi, Y., et al. (2018). Anti-claudin-4 Extracellular Domain Antibody Enhances the Antitumoral Effects of Chemotherapeutic and Antibody Drugs in Colorectal Cancer. *Oncotarget* 9 (100), 37367–37378. doi:10.18632/oncotarget.26427

Gaedcke, J., Grade, M., Jung, K., Camps, J., Jo, P., Emons, G., et al. (2010). Mutated KRAS Results in Overexpression of DUSP4, a MAP-Kinase Phosphatase, and SMYD3, a Histone Methyltransferase, in Rectal Carcinomas. *Genes Chromosom. Cancer* 49 (11), 1024–1034. doi:10.1002/gcc.20811

Gao, Y., Liu, X., Li, T., Wei, L., Yang, A., Lu, Y., et al. (2017). Cross-validation of Genes Potentially Associated with Overall Survival and Drug Resistance in Ovarian Cancer. *Oncol. Rep.* 37 (5), 3084–3092. doi:10.3892/or.2017.5534

Georges, R., Bergmann, F., Hamdi, H., Zepp, M., Eyol, E., Hielscher, T., et al. (2012). Sequential Biphasic Changes in Claudin1 and Claudin4 Expression Are Correlated to Colorectal Cancer Progression and Liver Metastasis. *J. Cel Mol Med* 16 (2), 260–272. doi:10.1111/j.1582-4934.2011.01289.x

Gomez-Rueda, H., Palacios-Corona, R., Gutiérrez-hermosillo, H., and Trevino, V. (2016). A Robust Biomarker of Differential Correlations Improves the Diagnosis of Cytologically Indeterminate Thyroid Cancers. *Int. J. Mol. Med.* 37 (5), 1355–1362. doi:10.3892/ijmm.2016.2534

Guo, Y., Long, J., and Lei, S. (2019). Promoter Methylation as Biomarkers for Diagnosis of Melanoma: A Systematic Review and Meta-analysis. *J. Cel Physiol* 234 (5), 7356–7367. doi:10.1002/jcp.27495

Hewitt, K. J., Agarwal, R., and Morin, P. J. (2006). The Claudin Gene Family: Expression in normal and Neoplastic Tissues. *BMC Cancer* 6, 186. doi:10.1186/1471-2407-6-186

Huang, D., Sherman, B. T., Tan, Q., Collins, J. R., Alvord, W. G., Roayaei, J., et al. (2007). The DAVID Gene Functional Classification Tool: a Novel Biological Module-Centric Algorithm to Functionally Analyze Large Gene Lists. *Genome Biol.* 8 (9), R183. doi:10.1186/gb-2007-8-9-r183

Hwang, I., Yang, H., Kang, H.-S., Ahn, C.-H., Lee, G.-S., Hong, E.-J., et al. (2014). Spatial Expression of Claudin Family Members in Various Organs of Mice. *Mol. Med. Rep.* 9 (5), 1806–1812. doi:10.3892/mmr.2014.2031

Jakab, C., Rusvai, M., Gálfi, P., Halász, J., and Kulka, J. (2011). Expression of Claudin-5 in Canine Pancreatic Acinar Cell Carcinoma - an Immunohistochemical Study. *Acta Vet. Hung* 59 (1), 87–98. doi:10.1556/AVet.59.2011.1.8

Kaiser, S., Park, Y.-K., Franklin, J. L., Halberg, R. B., Yu, M., Jessen, W. J., et al. (2007). Transcriptional Recapitulation and Subversion of Embryonic colon Development by Mouse colon Tumor Models and Human colon Cancer. *Genome Biol.* 8 (7), R131. doi:10.1186/gb-2007-8-7-r131

Kanehisa, M., Sato, Y., Kawashima, M., Furumichi, M., and Tanabe, M. (2016). KEGG as a Reference Resource for Gene and Protein Annotation. *Nucleic Acids Res.* 44 (D1), D457–D462. doi:10.1093/nar/gkv1070

Kang, H., Wang, N., Wang, X., Zhang, Y., Lin, S., Mao, G., et al. (2020). A Glycolysis-Related Gene Signature Predicts Prognosis of Patients with Esophageal Adenocarcinoma. *Aging* 12 (24), 25828–25844. doi:10.18632/aging.104206

Karagiannis, G. S., Schaeffer, D. F., Cho, C.-K. J., Musrap, N., Saraon, P., Batruch, I., et al. (2014). Collective Migration of Cancer-Associated Fibroblasts Is Enhanced by Overexpression of Tight junction-associated Proteins Claudin-11 and Occludin. *Mol. Oncol.* 8 (2), 178–195. doi:10.1016/j.molonc.2013.10.008

Kyuno, D., Zhao, K., Schnölzer, M., Provaznik, J., Hackert, T., and Zöller, M. (2019). Claudin7-dependent Exosome-promoted Reprogramming of Nonmetastasizing Tumor Cells. *Int. J. Cancer* 145 (8), 2182–2200. doi:10.1002/ijc.32312

Li, D., Zhao, W., Zhang, X., Lv, H., Li, C., and Sun, L. (2021). NEFM DNA Methylation Correlates with Immune Infiltration and Survival in Breast Cancer. *Clin. Epigenet* 13 (1), 112. doi:10.1186/s13148-021-01096-4

Li, X., Li, H., Liu, C., Leng, X., Liu, T., Zhang, X., et al. (2020). CLDN6-mediates SB431542 Action through MMPs to Regulate the Invasion, Migration, and EMT of Breast Cancer Cells. *Int. J. Clin. Exp. Pathol.* 13 (7), 1590–1600.

Li, Z., Xuan, W., Huang, L., Chen, N., Hou, Z., Lu, B., et al. (2020). Claudin 10 Acts as a Novel Biomarker for the Prognosis of Patients with Ovarian Cancer. *Oncol. Lett.* 20 (1), 373–381. doi:10.3892/ol.2020.11557

Liu, H., Jiang, F., Jia, X., Lan, J., Guo, H., Li, E., et al. (2017). Cycling Hypoxia Affects Cell Invasion and Proliferation through Direct Regulation of Claudin1/Claudin7 Expression, and Indirect Regulation of P18 through Claudin7. *Oncotarget* 8 (6), 10298–10311. doi:10.18632/oncotarget.14397

Liu, X., Bing, Z., Wu, J., Zhang, J., Zhou, W., Ni, M., et al. (2020). Integrative Gene Expression Profiling Analysis to Investigate Potential Prognostic Biomarkers for Colorectal Cancer. *Med. Sci. Monit.* 26, e918906. doi:10.12659/MSM.918906

Lyu, L., Xiang, W., Zheng, F., Huang, T., Feng, Y., Yuan, J., et al. (2020). Significant Prognostic Value of the Autophagy-Related Gene P4HB in Bladder Urothelial Carcinoma. *Front. Oncol.* 10, 1613. doi:10.3389/fonc.2020.01613

Marincola Smith, P., Choksi, Y. A., Markham, N. O., Hanna, D. N., Zi, J., Weaver, C. J., et al. (2021). Colon Epithelial Cell TGFβ Signaling Modulates the Expression of Tight junction Proteins and Barrier Function in Mice. *Am. J. Physiology-Gastrointestinal Liver Physiol.* 320 (6), G936–G957. doi:10.1152/ajpgi.00053.2021

Mármol, I., Sánchez-de-Diego, C., Pradilla Dieste, A., Cerrada, E., and Rodriguez Yoldi, M. (2017). Colorectal Carcinoma: A General Overview and Future Perspectives in Colorectal Cancer. *Ijms* 18 (1), 197. doi:10.3390/ijms18010197

Matsusaka, K., Ushiku, T., Urabe, M., Fukuyo, M., Abe, H., Ishikawa, S., et al. (2016). Coupling CDH17 and CLDN18 Markers for Comprehensive Membrane-Targeted Detection of Human Gastric Cancer. *Oncotarget* 7 (39), 64168–64181. doi:10.18632/oncotarget.11638

Morel, A.-P., Hinkal, G. W., Thomas, C., Fauvet, F., Courtois-Cox, S., Wierinckx, A., et al. (2012). EMT Inducers Catalyze Malignant Transformation of Mammary Epithelial Cells and Drive Tumorigenesis towards Claudin-Low Tumors in Transgenic Mice. *Plos Genet.* 8 (5), e1002723. doi:10.1371/journal.pgen.1002723

Mori, M., Miyoshi, N., Ishii, H., and Mori, M. (2011). Expression of CLDN1 in Colorectal Cancer: a Novel Marker for Prognosis. *Int. J. Oncol.* 39 (4), 791–796. doi:10.3892/ijo.2011.1102

Mu, W., Wang, Z., and Zöller, M. (2019). Ping-Pong-Tumor and Host in Pancreatic Cancer Progression. *Front. Oncol.* 9, 1359. doi:10.3389/fonc.2019.01359

Mulligan, M. K., Mozhui, K., Prins, P., and Williams, R. W. (2017). GeneNetwork: A Toolbox for Systems Genetics. *Methods Mol. Biol.* 1488, 75–120. doi:10.1007/978-1-4939-6427-7_4

Oh, B. Y., Cho, J., Hong, H. K., Bae, J. S., Park, W.-Y., Joung, J.-G., et al. (2017). Exome and Transcriptome Sequencing Identifies Loss of PDLIM2 in Metastatic Colorectal Cancers. *Cmar* 9, 581–589. doi:10.2147/cmar.s149002

Perez, A., Andrade-Da-Costa, J. s., De Souza, W., De Souza Ferreira, M., Boroni, M., De Oliveira, I., et al. (2020). N-glycosylation and R-eceptor T-yrosine K-inase S-ignaling A-ffect C-laudin-3 L-evels in C-olorectal C-ancer C-ells. *Oncol. Rep.* 44 (4), 1649–1661. doi:10.3892/or.2020.7727

Phattarataratip, E., and Sappayatosok, K. (2016). Expression of Claudin-5, Claudin-7 and Occludin in Oral Squamous Cell Carcinoma and Their Clinico-Pathological Significance. *J. Clin. Exp. Dent* 8 (3), e299–306. doi:10.4317/jced.52801

Pierce, B. G., Hourai, Y., and Weng, Z. (2011). Accelerating Protein Docking in ZDOCK Using an Advanced 3D Convolution Library. *PLoS One* 6 (9), e24657. doi:10.1371/journal.pone.0024657

Pierce, B. G., Wiehe, K., Hwang, H., Kim, B.-H., Vreven, T., and Weng, Z. (2014). ZDOCK Server: Interactive Docking Prediction of Protein-Protein Complexes and Symmetric Multimers. *Bioinformatics* 30 (12), 1771–1773. doi:10.1093/bioinformatics/btu097

Pontén, F., Jirström, K., and Uhlen, M. (2008). The Human Protein Atlas-A Tool for Pathology. *J. Pathol.* 216 (4), 387–393. doi:10.1002/path.2440

Pope, J. L., Ahmad, R., Bhat, A. A., Washington, M. K., Singh, A. B., and Dhawan, P. (2014). Claudin-1 Overexpression in Intestinal Epithelial Cells Enhances Susceptibility to Adenamatous Polyposis Coli-Mediated colon Tumorigenesis. *Mol. Cancer* 13, 167. doi:10.1186/1476-4598-13-167

Qiao, T.-Y., Yuan, Z.-M., Ma, T.-Y., Hu, H.-Q., Zhu, Y.-H., Zhang, W.-Y., et al. (2021). Claudin14 Promotes Colorectal Cancer Progression via the PI3K/AKT/mTOR Pathway. *neo* 68, 947–954. doi:10.4149/neo_2021_210210N203

Rhodes, D. R., Yu, J., Shanker, K., Deshpande, N., Varambally, R., Ghosh, D., et al. (2004). ONCOMINE: a Cancer Microarray Database and Integrated Data-Mining Platform. *Neoplasia* 6 (1), 1–6. doi:10.1016/s1476-5586(04)80047-2

Ribeiro, I. P., Esteves, L., Santos, A., Barroso, L., Marques, F., Caramelo, F., et al. (2021). A Seven-Gene Signature to Predict the Prognosis of Oral Squamous Cell Carcinoma. *Oncogene* 40 (22), 3859–3869. doi:10.1038/s41388-021-01806-5

Sakaguchi, T., Suzuki, S., Higashi, H., Inaba, K., Nakamura, S., Baba, S., et al. (2008). Expression of Tight junction Protein Claudin-5 in Tumor Vessels and Sinusoidal Endothelium in Patients with Hepatocellular Carcinoma. *J. Surg. Res.* 147 (1), 123–131. doi:10.1016/j.jss.2007.07.013

Skrzypczak, M., Goryca, K., Rubel, T., Paziewska, A., Mikula, M., Jarosz, D., et al. (2010). Modeling Oncogenic Signaling in colon Tumors by Multidirectional Analyses of Microarray Data Directed for Maximization of Analytical Reliability. *PLoS One* 5 (10), e13091. doi:10.1371/journal.pone.0013091

Suzuki, H., Nishizawa, T., Tani, K., Yamazaki, Y., Tamura, A., Ishitani, R., et al. (2014). Crystal Structure of a Claudin Provides Insight into the Architecture of Tight Junctions. *Science* 344 (6181), 304–307. doi:10.1126/science.1248571

Tabariès, S., and Siegel, P. M. (2017). The Role of Claudins in Cancer Metastasis. *Oncogene* 36 (9), 1176–1190. doi:10.1038/onc.2016.289

Tang, W., Dou, T., Zhong, M., and Wu, Z. (2011). Dysregulation of Claudin Family Genes in Colorectal Cancer in a Chinese Population. *Biofactors* 37 (1), 65–73. doi:10.1002/biof.138

Tang, Z., Li, C., Kang, B., Gao, G., Li, C., and Zhang, Z. (2017). GEPIA: a Web Server for Cancer and normal Gene Expression Profiling and Interactive Analyses. *Nucleic Acids Res.* 45 (W1), W98–W102. doi:10.1093/nar/gkx247

Thomas, P. D., Hill, D. P., Mi, H., Osumi-Sutherland, D., Van Auken, K., Carbon, S., et al. (2019). Gene Ontology Causal Activity Modeling (GO-CAM) Moves beyond GO Annotations to Structured Descriptions of Biological Functions and Systems. *Nat. Genet.* 51 (10), 1429–1433. doi:10.1038/s41588-019-0500-1

UniProt Consortium Nucleic Acids Res. UniProt: the Universal Protein Knowledgebase in 2021. *UniProt Consortium*.2021 ;49(D1):D480–D489. doi:10.1093/nar/gkaa1100

Wang, Y.-B., Shi, Q., Li, G., Zheng, J.-H., Lin, J., and Qiu, W. (2019). MicroRNA-488 Inhibits Progression of Colorectal Cancer via Inhibition of the Mitogen-Activated Protein Kinase Pathway by Targeting Claudin-2. *Am. J. Physiology-Cell Physiol.* 316 (1), C33–C47. doi:10.1152/ajpcell.00047.2018

Wang, Z., and Zöller, M. (2019). Exosomes, Metastases, and the Miracle of Cancer Stem Cell Markers. *Cancer Metastasis Rev.* 38 (1-2), 259–295. doi:10.1007/s10555-019-09793-6

Watanabe, M., Higashi, T., Ozeki, K., Higashi, A. Y., Sugimoto, K., Mine, H., et al. (2021). CLDN15 Is a Novel Diagnostic Marker for Malignant Pleural Mesothelioma. *Sci. Rep.* 11 (1), 12554. doi:10.1038/s41598-021-91464-0

Xiang, Z., Zhong, C., Chang, A., Ling, J., Zhao, H., Zhou, W., et al. (2020). Immune-related Key Gene CLDN10 Correlates with Lymph Node Metastasis but Predicts Favorable Prognosis in Papillary Thyroid Carcinoma. *Aging* 12 (3), 2825–2839. doi:10.18632/aging.102780

Yamagishi, H., Kuroda, H., Imai, Y., Hiraishi, H., Yamagishi, H., Kuroda, H., et al. (2016). Molecular Pathogenesis of Sporadic Colorectal Cancers. *Chin. J. Cancer* 35, 4. doi:10.1186/s40880-015-0066-y

Yang, T., Wang, H., Li, M., Yang, L., Han, Y., Liu, C., et al. (2021). CD151 Promotes Colorectal Cancer Progression by a Crosstalk Involving CEACAM6, LGR5 and Wnt Signaling via TGFβ1. *Int. J. Biol. Sci.* 17 (3), 848–860. doi:10.7150/ijbs.53657

Yu, A. S. L., Cheng, M. H., Angelow, S., Günzel, D., Kanzawa, S. A., Schneeberger, E. E., et al. (2009). Molecular Basis for Cation Selectivity in Claudin-2-Based Paracellular Pores: Identification of an Electrostatic Interaction Site. *J. Gen. Physiol.* 133 (1), 111–127. doi:10.1085/jgp.200810154

Yu, S., Hu, C., Cai, L., Du, X., Lin, F., Yu, Q., et al. (2020). Seven-Gene Signature Based on Glycolysis Is Closely Related to the Prognosis and Tumor Immune Infiltration of Patients with Gastric Cancer. *Front. Oncol.* 10, 1778. doi:10.3389/fonc.2020.01778

Zhou, Y., Xiang, J., Bhandari, A., Guan, Y., Xia, E., Zhou, X., et al. (2018). CLDN10 Is Associated with Papillary Thyroid Cancer Progression. *J. Cancer* 9 (24), 4712–4717. doi:10.7150/jca.28636

Zhu, J., Wang, R., Cao, H., Zhang, H., Xu, S., Wang, A., et al. (2015). Expression of Claudin-5, -7, -8 and -9 in Cervical Carcinoma Tissues and Adjacent Non-neoplastic Tissues. *Int. J. Clin. Exp. Pathol.* 8 (8), 9479–9486.

Zhu, Z., Xu, C., Lin, L., Lv, T., Cai, T., and Lin, J. (2020). Prognostic Value and Potential Biological Functions of CLDN8 in Patients with Clear Cell Renal Cell Carcinoma. *Ott* 13, 9135–9145. doi:10.2147/ott.s266846

Conflict of Interest: The authors declare that the research was conducted in the absence of any commercial or financial relationships that could be construed as a potential conflict of interest.

Publisher's Note: All claims expressed in this article are solely those of the authors and do not necessarily represent those of their affiliated organizations, or those of the publisher, the editors, and the reviewers. Any product that may be evaluated in this article, or claim that may be made by its manufacturer, is not guaranteed or endorsed by the publisher.

frontiers in Cell and Developmental Biology

ORIGINAL RESEARCH
published: 01 March 2022
doi: 10.3389/fcell.2022.827657

Integrating the Epigenome and Transcriptome of Hepatocellular Carcinoma to Identify Systematic Enhancer Aberrations and Establish an Aberrant Enhancer-Related Prognostic Signature

Peng Huang[1], *Bin Zhang*[1], *Junsheng Zhao*[1] *and Ming D. Li*[1,2]*

[1]State Key Laboratory for Diagnosis and Treatment of Infectious Diseases, National Clinical Research Center for Infectious Diseases, Collaborative Innovation Center for Diagnosis and Treatment of Infectious Diseases, The First Affiliated Hospital, Zhejiang University School of Medicine, Hangzhou, China, [2]Research Center for Air Pollution and Health, Zhejiang University, Hangzhou, China

OPEN ACCESS

Edited by:
Zhenhua Xu,
Children's National Hospital,
United States

Reviewed by:
Qi Liao,
Ningbo University, China
Oliver Bischof,
Délégation Ile-de-France Ouest et Nord (CNRS), France

***Correspondence:**
Ming D. Li
ml2km@zju.edu.cn

Specialty section:
This article was submitted to Epigenomics and Epigenetics, a section of the journal Frontiers in Cell and Developmental Biology

Received: 02 December 2021
Accepted: 31 January 2022
Published: 01 March 2022

Citation:
Huang P, Zhang B, Zhao J and Li MD (2022) Integrating the Epigenome and Transcriptome of Hepatocellular Carcinoma to Identify Systematic Enhancer Aberrations and Establish an Aberrant Enhancer-Related Prognostic Signature. Front. Cell Dev. Biol. 10:827657. doi: 10.3389/fcell.2022.827657

Recently, emerging evidence has indicated that aberrant enhancers, especially super-enhancers, play pivotal roles in the transcriptional reprogramming of multiple cancers, including hepatocellular carcinoma (HCC). In this study, we performed integrative analyses of ChIP-seq, RNA-seq, and whole-genome bisulfite sequencing (WGBS) data to identify intergenic differentially expressed enhancers (DEEs) and genic differentially methylated enhancers (DMEs), along with their associated differentially expressed genes (DEE/DME-DEGs), both of which were also identified in independent cohorts and further confirmed by HiC data. Functional enrichment and prognostic model construction were conducted to explore the functions and clinical significance of the identified enhancer aberrations. We identified a total of 2,051 aberrant enhancer-associated DEGs (AE-DEGs), which were highly concurrent in multiple HCC datasets. The enrichment results indicated the significant overrepresentations of crucial biological processes and pathways implicated in cancer among these AE-DEGs. A six AE-DEG-based prognostic signature, whose ability to predict the overall survival of HCC was superior to that of both clinical phenotypes and previously published similar prognostic signatures, was established and validated in TCGA-LIHC and ICGC-LIRI cohorts, respectively. In summary, our integrative analysis depicted a landscape of aberrant enhancers and associated transcriptional dysregulation in HCC and established an aberrant enhancer-derived prognostic signature with excellent predictive accuracy, which might be beneficial for the future development of epigenetic therapy for HCC.

Keywords: enhancer, super-enhancer, DNA methylation, histone modification, prognostic model, eRNA, RNA-seq, hepatocellular carcinoma

INTRODUCTION

Liver cancer is the sixth most common malignant tumor and the third leading cause of cancer-related deaths, accounting for approximately 700,000 deaths annually worldwide and poses a severe health threat and economic burden to the world (Likhitsup and Parikh, 2020; Sung et al., 2021). This is especially true in China, which has the largest HCC risk population (HBV carriers) throughout the world. The latest epidemiological report showed that primary liver cancer is the fourth most common tumor in China (Feng et al., 2019) and the vast majority of liver cancers are HCCs. Since there are usually no evident symptoms in the early developmental state of liver cancer, patients are often diagnosed in the late stage of liver cancer, resulting in an extremely high probability of death (Grandhi et al., 2016). Although the survival duration of early- and intermediate-stage HCCs has improved over the past decades, the prognosis for advanced-stage HCC patients has remained poor, with no significant improvement. Even with the survival benefits of several first- and second-line therapeutic options available for patients with advanced HCC, such as sorafenib and lenvatinib, the median survival time of intermediate to advanced HCC is only 1–2 years (Marrero et al., 2018). Clinical studies of immune checkpoint inhibitors have yielded promising survival benefits, although the suppressive milieu and tumor immunosurveillance escape mechanisms in the liver still dampen the effectiveness of immunotherapy (Nakano et al., 2020). Hence, there is an urgent need to explore the underlying genetic and epigenetic mechanisms implicated in hepatocarcinogenesis to identify potential targets/biomarkers for the diagnosis, treatment and prognosis of HCC.

Cancer is a complex disease involving both genetic mutations and epigenetic aberrations. By definition, epigenetics refers to heritable states of gene activities that do not involve alteration of DNA sequence itself. Epigenetic changes such as DNA hypermethylation or hypomethylation, dysregulation of histone modification patterns, chromatin remodeling, and aberrant expression of noncoding RNAs are demonstrated to be involved in the initiation and progression of HCC (Wahid et al., 2017). Unlike genetic mutations, epigenetic alterations are reversible and various drugs targeting epigenetic regulators have exhibited viable therapeutic potential for solid tumors in both preclinical and clinical studies (Cheng et al., 2019). A better understanding of the epigenetic mechanisms underlying hepatocarcinogenesis will facilitate the discovery of new targets and biomarkers for HCC therapy.

Like most malignancies, HCC is also characterized by widespread abnormal gene expression. Enhancers are distal, noncoding genomic regulatory elements with multiple transcription factor binding sites that interact with promoters to enhance the transcription of target genes. Nucleosomes in the neighborhood of active enhancers usually contain histones with iconic posttranslational modifications, such as H3 lysine monomethylation (H3K4me1) and H3 lysine acetylation (H3K27ac) at their amino termini (Shlyueva et al., 2014). Super-enhancers are large clusters of enhancers that synergistically promote gene transcription (Herranz et al., 2014). Emerging evidence shows that cancer cells can acquire super-enhancers in the vicinity of key oncogenes, such as *MYC* and *TAL1*, during the development of cancer (Hnisz et al., 2013; Herranz et al., 2014; Mansour et al., 2014). Moreover, pancancer studies of TCGA data also showed wide-spread aberrant super-enhancer activities in cancers (Chen et al., 2018a; Chen and Liang, 2020).

In HCC, Wong et al. demonstrated that the super-enhancer landscape and components of the *trans*-acting super-enhancer complex, composed of *CDK7*, *BRD4*, *EP300*, and *MED1*, were significantly altered (Tsang et al., 2019). Additionally, Deng et al. reported an aberrant landscape of active enhancers developed in cirrhosis and conserved in hepatocarcinogenesis (Yang et al., 2020). However, those two studies lacked a comprehensive collection of enhancers in the liver, reliable identification of enhancer target genes, and replication of enhancer aberrations in independent cohorts.

In the present study, through the integration of transcriptome and epigenome data, we aimed to: 1) manually curate a comprehensive catalog of enhancers in the liver; 2) systematically identify and replicate enhancer aberrations and associated target genes in HCC; and 3) explore the function and prognostic significance of identified aberrant enhancers.

MATERIALS AND METHODS

Patient Data and Tissues Collection

Paired tumor tissues and adjacent non-tumor tissues used in this study were collected from 33 HCC patients who underwent hepatectomy at the First Affiliated Hospital, Zhejiang University School of Medicine. Board-certified pathologists reviewed each specimen to confirm that all frozen sections were histologically consistent with tumor or non-tumor tissues. This study was approved by the Institutional Review Board of The First Affiliated Hospital. Written informed consent was obtained from each participant.

High-Throughput Sequencing and Computational Preprocessing

DNA methylation and gene expression of 33 pairs of tumour and adjacent tissues were assessed by whole-genome bisulfite sequencing (WGBS) and mRNA-seq on the Illumina X Ten platform with standard procedures. After quality control, clean WGBS reads were aligned with the reference genome (hg38) using Bismark (v. 0.16.1) (Krueger and Andrews, 2011) with default parameters. The harvested count data for each strand were combined for methylation level estimation. Differentially methylated loci (DML) and differentially methylated regions (DMRs) were detected with customized R scripts like our previous WGBS study (Huang et al., 2021). For RNAseq data, clean reads that passed quality control were aligned with the hg38 genome, and the reference transcriptome was downloaded from GENCODE (v. 29) (Harrow et al., 2012) with STAR (v. 2.5.2a) (Dobin et al., 2013). Estimated raw count gene expression from STAR was imported into DESeq2 (Love et al., 2014) for

differential expression analysis. STAR generated alignment BAM files were utilized as input for enhancer RNA (eRNA) expression quantification via bedtools (v. 2.27.1) (Quinlan and Hall, 2010). More details about high-throughput sequencing and bioinformatic preprocessing can be found in the Supplementary Methods.

Curation of a Comprehensive Catalog of Enhancers in Liver

Eleven histone ChIP-seq liver relevant samples were collected from the public domain. Specifically, bed files containing the pseudo-replicated peaks identified from six H3K4me1- and H3K27ac-based ChIPseq profiled samples (i.e., one HepG2, one Hepatocyte, and four normal adult liver tissue samples) were downloaded from ENCODE (Consortium, 2004). For each ENCODE sample, regions with overlapped H3K27ac and H3K4me1 peaks were annotated as active enhancers, and regions with only H3K4me1 peaks were considered as primed enhancers. In one case of an adult liver ENCODE sample without H3K27ac profiling data, H3K4me1 peaks were included as enhancers (primed or active). Four types of histone (including H3K4me1 and H3K27ac) ChIP-seq profiling-based ChromHMM state annotation files of five adult liver tissue samples (i.e., one normal liver sample and two tumor and matched adjacent cirrhosis samples from two HCC patients) were retrieved from the recent integrative epigenomic study on HCC (Hlady et al., 2019). Specifically, regions whose ChromHMM states were annotated as "poised enhancer" (refers to regions with only H3K4me1 peaks) were included as primed enhancers, and regions annotated as "active enhancer" (refer to regions with both H3K4me1 and H3K27ac) were collected as active enhancers. All (active or primed) enhancers from each sample were merged together via bedtools (Quinlan and Hall, 2010). Afterwards, enhancers with a lenth of <50 bp or overlapped with any promoter (upstream 1,500 bp to downstream 500 bp from TSS) were excluded from further analysis. The concurrence of each merged enhancer was estimated as the number of ChIP-seq samples in which the merged enhancer was annotated as a primed or active enhancer. In other words, a merged enhancer with higher concurrence represents a more highly conserved and reliable enhancer among those 11 liver-related ChIP-seq samples.

Identification of Intergenic Differentially Expressed Enhancers and Associated Differentially Expressed Genes

The collected enhancers in the liver were divided into two groups, namely, intergenic enhancers and genic enhancers, according to their genomic locations. For intergenic enhancers, the read count-based expression levels of eRNAs were estimated via the "coverage" module of bedtools (Quinlan and Hall, 2010). A paired *t*-test was applied to the normalized expression ($\log_2$ transformed fragment per million, $\log_2$ FPM) of each eRNA to identify significant differentially expressed eRNA ($|\log_2$ fold change of FPM$| > 0.5$ and BH-FDR < 0.05). Intergenic enhancers with significant differential expression of eRNA were defined as intergenic differentially expressed enhancers (intergenic DEEs). Nearby (TSS located ± 1 Mb from the center of corresponding intergenic DEEs) differentially expressed genes (DEG) ($|\log_2$ fold change (LFC)$| > 0.5$ and BH-FDR < 0.05) displayed a significant correlation (Spearman Rho ≥ 0.7 and Bonferroni-corrected *p*-value < 0.01) with eRNA expression were identified as intergenic DEE-associated DEGs (intergenic DEE-DEGs).

Replication of Intergenic DEE-DEGs

For independent replication of intergenic DEE-DEGs, four HCC RNA-seq datasets were downloaded from the GEO: GSE77314 (paired tumor and adjacent nontumor tissue samples from 50 HCC patients) (Liu et al., 2016), GSE124535 (paired tumor and adjacent nontumor tissue samples from 35 HCC patients) (Jiang et al., 2019), GSE148355 (62 tumor and 47 adjacent nontumor samples) (Yoon et al., 2021), and GSE77509 (paired tumor and adjacent nontumor samples from 20 HCC patients) (Yang et al., 2017). The same protocols in the discovery cohort were applied to detect intergenic DEEs and associated DEE-DEGs in these four datasets. Afterward, identified intergenic DEEs and DEE-DEGs from each dataset were compared with those from the discovery cohort to calculate the concurrence of each intergenic DEE and DEE-DEG. Specifically, the concurrence of each DEE was calculated as one plus the number of GEO datasets in which the DEE was successfully replicated, while the concurrence of each DEE-DEG was calculated as one plus the number of GEO datasets in which the corresponding DEE and DEG were significant and the correlation between them was also significant.

Assessment of the Roles of Epigenetic Modification Aberrations in Intergenic DEEs

Intergenic DEEs that overlapped with at least one DMR and displayed significant methylation-eRNA Spearman correlation (BH-FDR < 0.05) were defined as methylation-associated DEEs, and corresponding DEE-DEGs were classified as methylation-associated DEE-DEGs. Meanwhile, we further investigated the dysregulation of histone posttranslational modification (PTM) modifiers and their potential implications in those identified intergenic enhancer aberrations. Top differentially expressed histone PTM modifiers ($|\text{LFC}| > 1$ and BH-FDR $< 5\%$) in the discovery cohort were screened out for subsequent coexpression analyses to determine the ratios of DEEs and DEE-DEGs that significantly correlated ($|$Spearman correlation coefficient$| > 0.5$ and BH-FDR $< 5\%$) with the mRNA expression of those histone PTM modifiers.

Identification of Genic Differentially Methylated Enhancers and Associated Differentially Expressed Genes

Reliable genic enhancers (concurrence among the 11 ChIP-seq samples ≥2) that overlapped ($\text{length}_{\text{overlap}} \geq 200$ bp, $\text{length}_{\text{overlap}}/\text{length}_{\text{enhancer}} \geq 0.3$, and with at least 5 CpGs) with at least one

DMR were identified as potential genic differentially methylated enhancers (genic DMEs). For each potential genic DME, their associated DEGs were screened *via* the Spearman correlation test. Nearby (distance of enhancer to TSS ≤ ± 1 Mb) DEGs (|LFC|> 0.5 and BH-FDR < 0.05) that show significant correlation (|Rho| ≥ 0.5 and FDR ≤ 0.01) between gene expression and DNA methylation level were identified as genic DEE-associated DEGs (genic DME-DEGs). Genic DME candidates with at least one associated DEG were identified as genic DMEs.

Replication of Genic DMEs and DME-DEGs

The normalized gene expression and DNA methylation level matrix of TCGA-LIHC were retrieved *via* the RTCGA R package (Kosinski and Biecek, 2015). For each genic DEE-DEG pair identified in the discovery cohort, we examined the significance of differential methylation, differential expression, and Spearman correlation between DNA methylation and gene expression in TCGA-LIHC. A genic DEE-DEG pair was considered as "successful replication" only when there was simultaneous significant differential methylation, differential expression, and a significant correlation between methylation and expression in TCGA-LIHC. Considering the platform limitation of the 450 k methylation array in covering enhancer CpG, we classified all replication failures of DEE-DEGs into two groups: 1) "type I failure" refers to replication failure due to the lack of CpG for corresponding genic DMEs in TCGA-LIHC, and 2) "type II failure" refers to replication failure except type I failure. The raw replication rate of genic DEE-DEGs was calculated as the ratio of genic DEE-DEGs that achieved successful replication, while the platform-adjusted replication rate was defined as: $Count_{Successful\ replication}/(Count_{Successful\ replication} + Count_{Type\ II\ failure})*100$.

Functional Enrichment of Aberrant Enhancer-Associated Differentially Expressed Genes

AE-DEGs were defined as the union of those identified intergenic DEE-DEGs and genic DME-DEGs. Pathway/gene ontology (GO) enrichment analyses of upregulated and downregulated AE-DEGs were performed *via* the online web tool Metascape (Zhou et al., 2019). In addition, 10 cancer hallmark gene sets were downloaded from the Cancer Hallmark Gene (CHG) database (Zhang et al., 2020a). The enrichment degrees of AE-DEGs for cancer hallmarks were evaluated through a hypergeometric test followed by BH-FDR multitest correction in R.

Bioinformatic Confirmation of AE-DEGs Using Public Hi-C Data

The bed files containing topologically associated domains (TADs) and chromatin loops of Hi-C-profiled HepG2 and one normal adult liver tissue sample were downloaded from the 3D Genome Browser (http://3dgenome.fsm.northwestern.edu/) (Wang et al., 2018). Each pair of AE and AE-DEG was examined to determine whether both the enhancer and its associated DEG were located in the same TAD or located in the two elements of a chromatin loop, respectively.

Establishment of an AE-Derived Prognostic Model

Clinical phenotype data, including overall survival (OS) time and status, were retrieved from the integrated TCGA pancancer clinical data resource (Liu et al., 2018a). Univariate Cox proportional hazards regression analysis was conducted to screen for AE-DEGs associated with the OS of HCC patients in TCGA-LIHC via the function "coxph" in the R package "survival" (Therneau, 2020). AE-DEGs with univariate Cox *p*-value < 0.05 were incorprated into the least absolute shrinkage and selection operator (LASSO) regression model by using the glmnet package (Friedman et al., 2010) for identification of the most prominent survival-associated AE-DEGs in TCGA-LIHC. Afterward, the multivariate proportional hazards Cox regression model was employed to establish a gene signature for predicting the OS of HCC patients. Multivariate Cox regression-derived coefficients (β) were used to calculate the risk score as follows: risk score = (β_{gene1} * normalized expression level of gene1 + β_{gene2} * normalized expression level of gene2 + . . . + β_{geneN} * normalized expression of geneN) (Lossos et al., 2004). Based on the optimal cutoff of risk score determined by minimizing log-rank test *p*-value, HCC patients were divided into high- and low-risk groups, whose differences in OS probability across time were visualized through a Kaplan-Meier survival curve by using the function "ggsurvplot" in the survminer package (Alboukadel Kassambara, 2021). The prognostic performance of the risk score was evaluated by time-dependent receiver operating characteristic (ROC) curve analysis via the function "survivalROC" in the survivalROC package (Patrick, 2013). The independent prognostic role of the identified gene signature in TCGA-LIHC was assessed by building a multivariate Cox regression model including the risk group, age, gender, and pathologic tumor-node-metastasis (TNM) stage of each patient. All factors that passed through the multivariate Cox regression model were utilized for the construction of a predictive nomogram *via* the rms package (RMS, 2021). Calibration plots and time-dependent ROC curves were applied to assess the predictive performance of the established nomogram.

Validtion of the AE-Derived Prognostic Model

Regarding the independent validation of the prognostic signature, clinical phenotypes and gene expression data of the International Cancer Genome Consortium Liver Cancer-RIKEN (LIRI-JP) were downloaded from the ICGC website. Multivariate Cox regression-derived coefficients from TCGA-LIHC were used to calculate the corresponding risk score for each patient in ICGC-LIRI. Similarly, ICGC-LIRI patients

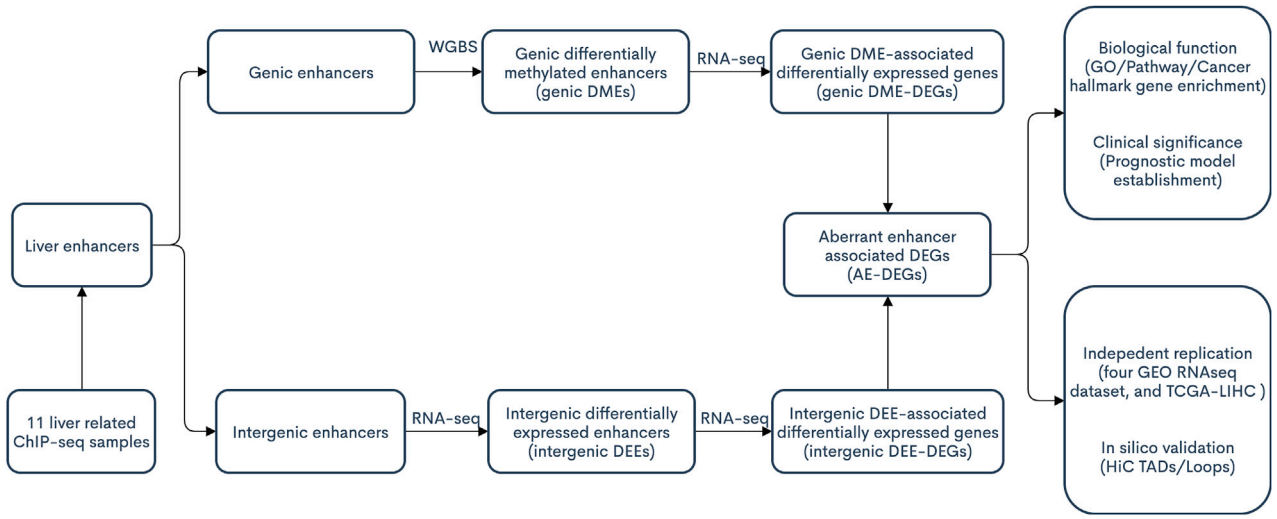

FIGURE 1 | The schematic flowchart of the present study.

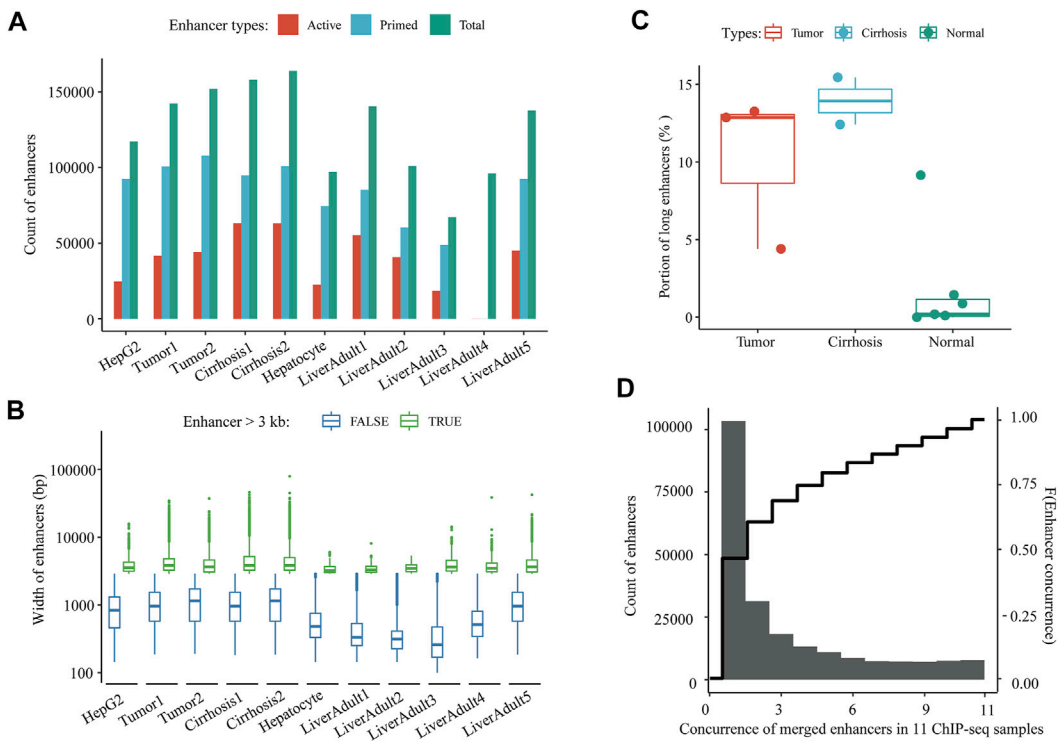

FIGURE 2 | A comprehensive catalog of enhancers in the liver. **(A)** Count of active and primed enhancers in each liver-relevant ChIP-seq sample. **(B)** Length distribution of enhancers in each liver-relevant ChIP-seq sample. **(C)** Proportions of long enhancers in three types of liver-relevant ChIP-seq samples. And **(D)** Distribution of the concurrence of all merged enhancers among 11 liver-relevant ChIP-seq samples.

were divided into high- and low-risk groups according to the cutoff determined by minimizing the log-rank test *p*-value. Comparison of the difference in OS probability, evaluation of predictive performance, and assessment of predictive independence were performed with identical procedures employed for TCGA-LIHC.

TABLE 1 | Characteristics and enhancer identification strategies applied for 11 liver-relevant ChIP-seq samples.

Sample name	Source	H3K4me1	H3K27ac	Enhancer identification strategy
HepG2	ENCODE (Consortium, 2004)	√	√	H3K4me1 only (primed enhancer) + H3K4me1 and H3K27ac (active enhancer)
Hepatocyte		√	√	
LiverAdult 1		√	√	
LiverAdult 2		√	√	
LiverAdult 3		√	√	
LiverAdult 4		√	X	H3K4me1 (primed or active enhancer)
LiverAdult 5	The integrative epigenomic HCC study (Hlady et al., 2019)	√	√	H3K4me1 only (primed enhancer) + H3K4me1 and H3K27ac (active enhancer)
Cirrhosis 1		√	√	
Cirrhosis 2		√	√	
Tumor 1		√	√	
Tumor 2		√	√	

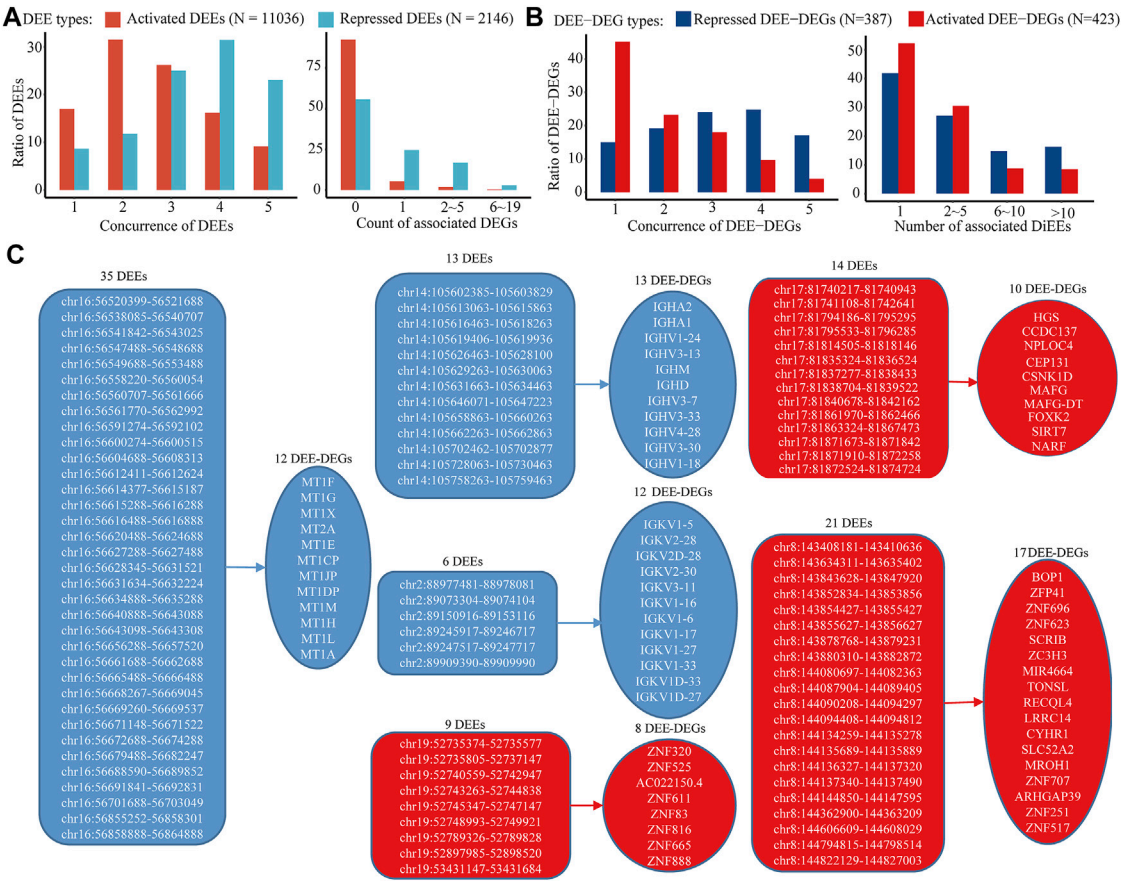

FIGURE 3 | Distinct patterns of activated and repressed intergenic enhancers in HCC. **(A)** (left) Distribution of the concurrence of identified intergenic DEEs among five RNA-seq datasets and (right) distribution of the number of associated intergenic DEE-DEG of each DEE. **(B)** (left) Distribution of the concurrence of identified intergenic DEE-DEGs among five RNA-seq datasets and (right) distribution of the number of associated DEE of each DEE-DEG. **(C)** Gene clusters associated with aberrant super-enhancers. Only gene clusters with at least five DEE-DEGs and super-enhancers with at least five DEEs were displayed. Activated DEEs and DEE-DEGs are shown in red color, and repressed DEEs and DEE-DEGs are shown in blue.

RESULTS

Comprehensive Collection of Enhancers in the Liver

The procedures of this study are shown in the schematic flowchart (**Figure 1**). Among 11 liver-relevant ChIP-seq profiled samples, we identified numerous enhancers whose counts ranged from 96,124 to 163,953 (**Figure 2A**; Table S1.1). On average, there were 124,838 enhancers in each sample, among which approximately one third (32.08%) were active enhancers with both H3K4me1 and H3K27ac peak signals (**Table 1**; **Supplementary Table S1.1**). Interestingly, there was a higher proportion of long enhancers (length > 3 kb) in nonnormal samples (i.e., tumoral and cirrhosis samples), and the median widths of classical enhancers (length ≤ 3 kb) were also higher than those of normal samples (**Figures 2B,C**; **Supplementary Table S1.2**). Specifically, the mean percentages of long enhancers (>3 kb) in tumor samples, adjacent cirrhosis samples, and normal liver samples were 10.17, 12.93, and 1.97%, respectively (**Figure 2C**). After combining these enormous enhancers, we obtained a comprehensive catalog of 223,007 unique enhancers in the liver. Over one half (53.64%) of them were concurrent enhancers that consistently existed in at least two samples (**Figure 2D**; **Supplementary Table S1.3**). In addition, genomic location-based annotation showed that approximately 29.84% (66,551/223,007) of those 223,007 enhancers were located in intergenic regions (**Supplementary Table S1.3**).

Activated and Repressed Intergenic Enhancers Show Different Patterns in Concurrence and Transcriptional Regulation in HCC

In the discovery cohort, 23,601 of the 66,551 collected intergenic enhancers displayed active transcription of eRNA, and 13,182 of them were identified as intergenic DEEs, including 11,036 activated DEEs and 2,146 repressed DEEs (**Figure 3A**). Through bioinformatic inferrence for target genes, 842 activated DEEs and 951 repressed DEEs were found to be correlated with 423 upregulated DEE-DEGs, and 387 downregulated DEE-DEGs, respectively (**Figure 3B**; **Supplementary Table S2**). Although the number of activated DEEs was over fivefold that of repressed DEEs (11036 *vs.* 2,146), each repressed DEE was found to be simultaneously associated with more DEE-DEGs (**Figure 3A**). Specifically, 19.67% of repressed DEEs displayed high correlations with multiple DEE-DEGs, while only 2.28% of activated DEEs showed this pattern (**Figure 3A**). Moreover, 387 downregulated and 423 upregulated DEE-DEGs also showed differences in terms of the number of associated DEEs. Compared with upregulated DEE-DEG, each downregulated DEE-DEG tended to be simultaneously regulated by more DEEs (**Figure 3B**). Taken together, we found a higher portion of potential transcriptional master regulators among the repressed DEEs, and more downregulated DEE-DEGs were simultaneously associated with aberrant super-enhancers that were consisted of multiple adjacent synergistic enhancers (**Figure 3C**). For example, in 16q13, a cluster of 35 repressed intergenic DEEs was identified as potential regulators of the metallothionein (MT) family (i.e., each of the 35 DEEs was significantly correlated with the expressions of all 12 metallothionein genes) (**Figure 3C**; **Table 2**). A literature searching revealed that nine of those 12 MT genes were previously implicated in HCC (**Table 2**). Besides, in chromosome 17, we also identified a super-enhancer whose activation was correlated with upregulation of 10 DEGs including nine previously-reported oncogenes in HCC or other cancers (**Table 2**). Beyond these, we also identified another four gene clusters likely regulated by super-enhancers on chromosomes 14, 2, 19, and 8 (**Figure 3C**).

Moreover, the identified intergenic DEEs and DEE-DEGs were overall highly replicated in four independent GEO datasets (**Table 3**). A total of 83.03% of activated DEEs, and 91.33% of repressed DEEs were observed in at least one GEO dataset (i.e., concurrence ≥ 2) (**Figure 3A**). Furthermore, 54.85% of upregulated DEE-DEGs and 85.01% of downregulated DEE-DEGs were identified in at least one GEO dataset (**Figure 3B**). Compared with activated DEEs and upregulated DEE-DEGs, those repressed DEEs and downregulated DEE-DEGs were more likely to be conserved in multiple GEO datasets (i.e., concurrence higher than three) (**Figures 3A,B**). For instance, 54.52% of repressed DEEs and 41.86% of downregulated DEE-DEGs were consistently replicated in more than three GEO datasets, while only 25.34% activated DEEs and 13.71% upregulated DEE-DEGs were also observed in three or more GEO datasets (**Figures 3A,B**).

Potential Roles of Epigenetic Modification Aberrations in Identified Aberrant Intergenic Enhancers

Through integration with matched WGBS data in the discovery cohort, the differential expression of 10.61% of the activated DEEs and 11.14% of the repressed DEEs was significantly correlated with regional differential DNA methylation, especially hypomethylation, in corresponding enhancers (**Figure 4A**). Nevertheless, these differential methylation-associated DEEs correlated with 34.04% of the upregulated DEE-DEGs and 37.21% of the downregulated DEE-DEGs (**Figure 4B**), suggesting that those methylation-associated DEEs were more likely to be transcriptional master regulators that targeted multiple genes. In addition to DNA methylation, there was also substantial dysregulation of histone modification in HCC. Three histone methyltransferases (EZH2, EHMT2, and SMYD3), two demethylases (KDM5B and KDM6B), and two deacetylases (HDAC11 and HDAC9) were differentially expressed in both the discovery and four GEO datasets (**Figure 4C**; **Supplementary Table S2.2**). Coexpression tests showed that many DEEs and DEE-DEGs were significantly correlated with the differential expression of those seven histone modification regulators, especially EZH2, EHMT2, and SMYD3 (**Figures 4D,E**). Notably, 75.89% of the upregulated DEE-DEGs and 63.57% of the downregulated DEE-DEGs displayed significant coexpression with EZH2 and SMYD3,

TABLE 2 | Summary information about two representative sets of DEE-DEGs regulated by intergenic DEE clusters.

Enhancer cluster	Average LFC.DEE	Avergae LogFDR.DEE	Gene name	LFC DEG	FDR DEG	Average rho	Average concurrence	Implicated cancers
chr16:56520399–56864888 (~344 kb, 35 DEEs)	–3.3	6.62	*MT1A*	**–2.08**	**1.45E-06**	**0.76**	**2.56**	HCC (Ning et al., 2021)
			MT1CP	–2.01	1.20E-03	0.82	3.51	Unknown
			MT1DP	**–1.37**	**1.64E-03**	**0.81**	**3.71**	HCC (Yu et al., 2014a) and others (Gai et al., 2020)
			MT1E	**–3.58**	**2.35E-16**	**0.88**	**3.72**	HCC (Liu et al., 2020) and others (Hur et al., 2016)
			MT1F	**–3.70**	**3.24E-17**	**0.91**	**3.75**	HCC (Lu et al., 2003) and others (Lin et al., 2017a)
			MT1G	**–3.43**	**6.06E-10**	**0.90**	**3.67**	HCC (Wang et al., 2019) and others (Fu et al., 2013)
			MT1H	**–2.13**	**1.48E-03**	**0.86**	**2.43**	HCC (Zheng et al., 2017)
			MT1JP	**–5.27**	**1.36E-20**	**0.82**	**3.64**	HCC (Wu et al., 2020a) and others (Zhang et al., 2018; Yu et al., 2019)
			MT1L	–2.58	5.28E-10	0.86	2.86	Unknown
			MT1M	**–3.65**	**2.33E-12**	**0.90**	**2.78**	HCC (Fu et al., 2017) and others (Li et al., 2021)
			MT1X	**–3.55**	**1.47E-17**	**0.88**	**3.86**	HCC (Liu et al., 2018b)
			MT2A	–3.35	4.85E-24	0.91	3.83	Breast cancer (Kim et al., 2011) and others (Pan et al., 2013)
chr17: 81740217–81874724 (~134 kb, 14 DEEs)	1.05	4.53	*HGS*	**1.04**	**1.95E-20**	**0.87**	**1.22**	HCC (Canal et al., 2015)
			CCDC137	0.95	3.37E-16	0.80	1.78	Unknown
			NPLOC4	0.82	3.53E-11	0.79	1.22	Bladder cancer (Lu et al., 2019) and others (Skrott et al., 2017; Pan et al., 2021)
			CEP131	**1.42**	**2.39E-19**	**0.79**	**1.78**	HCC (Liu et al., 2017) and others (Kim et al., 2019; Wang et al., 2020)
			CSNK1D	0.55	8.36E-08	0.76	1.22	Breast cancer (Bar et al., 2018) and others (Peer et al., 2021)
			MAFG	**0.98**	**3.10E-07**	**0.71**	**1.00**	HCC (Liu et al., 2018c)
			MAFG-DT	**3.03**	**3.42E-28**	**0.73**	**1.33**	HCC (Ouyang et al., 2019) and others (Cui et al., 2018; Li et al., 2019; Sui et al., 2019; Qu and Liu, 2020; Xiao et al., 2020)
			FOXK2	**0.68**	**3.22E-07**	**0.73**	**1.67**	HCC (Lin et al., 2017b) and others (Shan et al., 2016; Nestal de Moraes et al., 2019)
			SIRT7	**0.61**	**8.43E-06**	**0.72**	**1.00**	HCC (Zhao et al., 2019) and others (Yu et al., 2014b; Zhang et al., 2015)
			NARF	1.07	9.12E-15	0.74	2.00	Glioblastoma (Anderson et al., 2010)

Notes: Enhancer cluster: the cluster of intergenic DEEs that were simultaneously associated with the corresponding cluster of genes; average LFC.DEE: the arithmetic mean of log_2 fold change of the FPM of all DEEs in the enhancer cluster; average LogFDR.DEE: the arithmetic mean of the–log_{10}FDR of the differential expression test of all DEEs in the enhancer cluster; average rho: the arithmetic mean of Spearman correlation coefficients of all DEE-DEG pairs between corresponding DEGs and DEEs in the enhancer cluster; average concurrence: the arithmetic mean of the concurrence of all DEE-DEG pairs between corresponding DEGs and DEEs in the enhancer cluster; implicated cancers: results of literature searching (only molecular mechanism studies) to determine the relevance between DEE-DEG and cancers (genes implicated in HCC were highlighted with a bold font).

TABLE 3 | Characteristics of five RNA-seq datasets used in the present study.

Dataset	No. of tumor tissues	No. of adjacent tissues	Additional data type	Reference (PMID)
Discovery cohort	33	33	WGBS	—
GSE77314	50	50	—	27119355 (Liu et al., 2016)
GSE124535	35	35	—	30814741 (Jiang et al., 2019)
GSE148355	62	47	—	33772139 (Yoon et al., 2021)
GSE77509	20	20	—	28194035 (Yang et al., 2017)

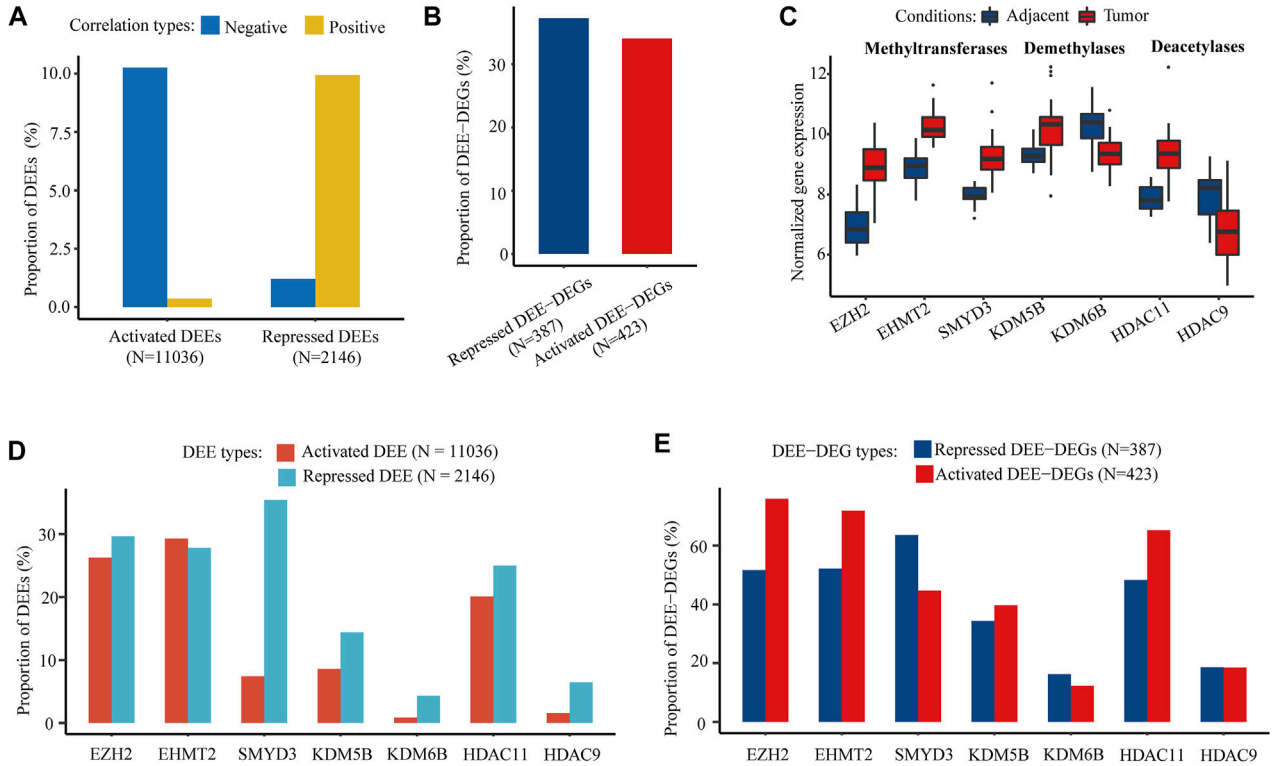

FIGURE 4 | DNA methylation and histone PTM modifer-associated intergenic DEEs and DEE-DEGs. **(A)** Percentage of DNA methylation-associated intergenic DEEs. **(B)** Percentage of DNA methylation-associated intergenic DEE-DEGs. **(C)** Significant differential expression of seven histone modification regulators (three histone methyltransferases, two histone demethylases, and three histone deacetylases) in the discovery cohort. **(D)** Proportion of histone modification regulator-associated intergenic DEEs. **(E)** Percentage of histone modification regulator-associated intergenic DEE-DEGs.

respectively, which were much higher than the corresponding percentages for significantly correlated DEEs (26.26 and 35.41%, respectively) (**Figures 4D,E**), suggesting that histone modification-associated DEEs are also more likely to be transcriptional master regulators.

Aberrant Genic Enhancers-Associated With DNA Methylation Alterations

Among those collected genic enhancers, 1,119 DMEs and their associated DME-DEGs were identified through the integration of WGBS, ChIP-seq, and RNA-seq data. Overall, hypomethylated and hypermethylated DMEs displayed similar transcriptional regulation patterns (i.e., they tended to be correlated with equal number of DME-DEGs) (**Figure 5A**). In total, there were 1,442 genic DEE-DEGs, including 120 hypermethylated upregulated DEE-DEGs (HyperUp), 168 hypermethylated downregulated DEE-DEGs (HyperDown), 517 hypomethylated upregulated DEE-DEGs (HypoUp), and 637 hypomethylated downregulated DEE-DEGs (HypoDown) (**Figure 5B**; **Supplementary Table S3.1**). Approximately half (52.50%) of the identified DEE-DEGs exhibited a nonclassical positive correlation between DNA methylation and gene expression. The results of independent replication of those 1,442 DME-DEGs in TCGA-LIHC showed that the raw replication rates of the four types of DEE-DEGs (i.e., HyperUp, HyperDown, HypoUp, and HypoDown) were 47.50, 42.86, 28.63, and 14.44%, respectively (**Figure 5C**). Since the 450 k methylation array barely covered CpGs located in the gene body and intergenic regions, which were primarily hypomethylated, it was not surprising to observe much lower raw replication rates and higher type I failure ratios for the HypoUp and HypoDown groups. In contrast, their platform-adjusted replication rates reached 67.86, 59.02, 65.78, and 50.00% (**Figure 5D**), which were comparable to each other.

Intergration of Aberrant Enhancer-Associated Transcriptional Dysregulation and Sucessfully in Silico Verification Based on HiC Data

After combining 1,442 genic DME-DEGs with the 810 intergenic DEE-DEGs, we obtained a set of 2,051 aberrant enhancer-associated DEGs (AE-DEGs), which was composed of 1,092 upregulated AE-DEGs and 959 downregulated AE-DEGs (**Figure 6A**; **Supplementary Table S3.2**). Pathway/biological process enrichment analyses demonstrated that 1,092 activated AE-DEGs were overrepresented for genes implicated in the cell cycle, nuclear division, DNA repair, and DNA replication

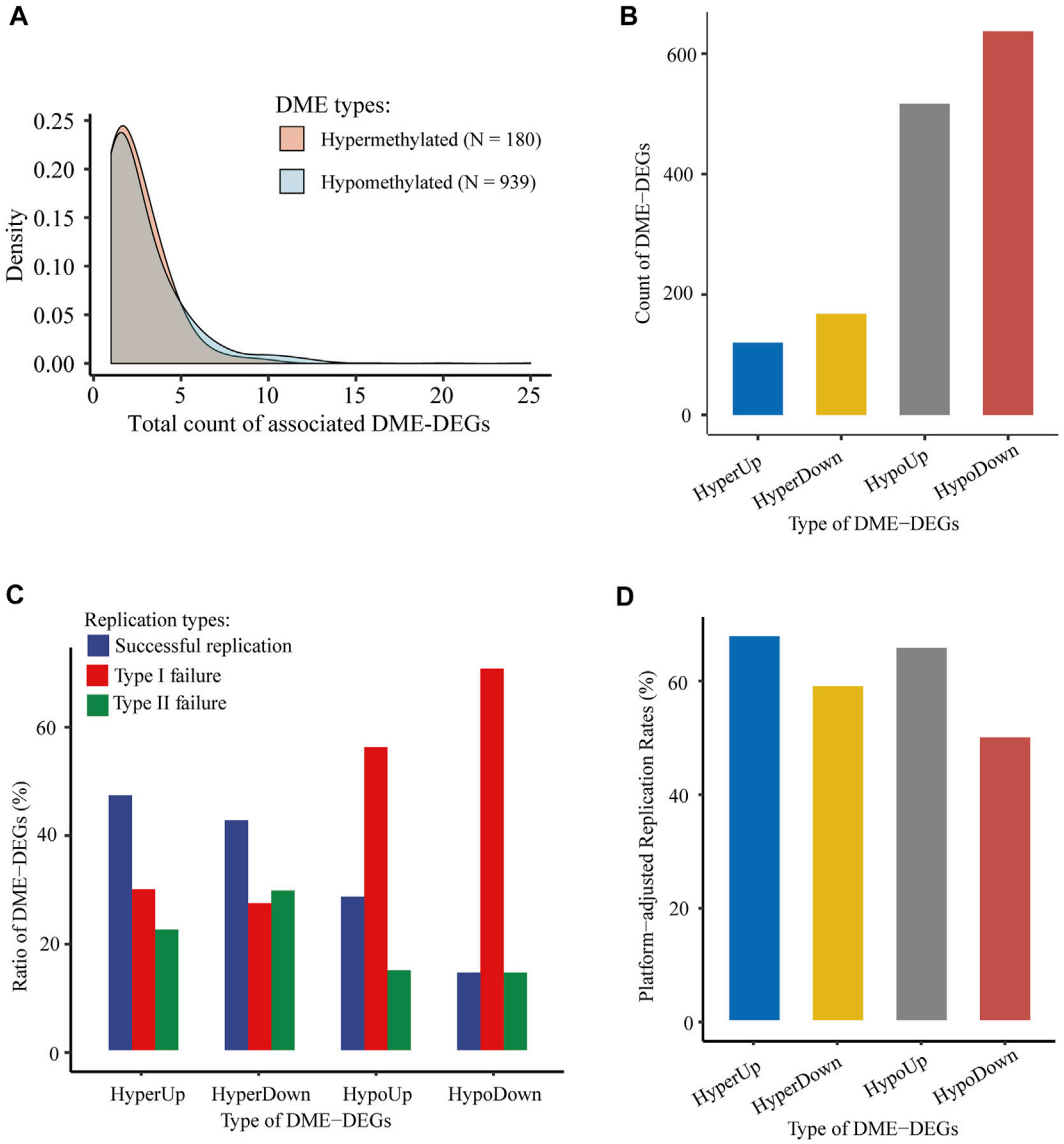

FIGURE 5 | Identification and validation of genic DMEs and associated DME-DEGs in HCC. **(A)** Distribution density of the number of associated DME-DEGs of hypermethylated and hypomethylated genic DME. **(B)** Count of four types of genic DME-DEGs. "HyperUp" refers to hypermethylated enhancer-associated upregulated DME-DEGs; "HyperDown" refers to hypomethylated enhancer-associated downregulated DME-DEGs; "HypoUp" refers to hypermethylated enhancer-associated upregulated DME-DEGs, and "HypoDown" refers to hypomethylated enhancer-associated downregulated DME-DEGs. **(C)** Distribution of the three types of replication results of genic DME-DEGs. "Successful replication" refers to the successful replication of genic DME-DEGs for correlated differential methylation and differential expression in TCGA-LIHC; "type I failure" refers to replication failure due to lack of CpG for the corresponding genic DMEs in TCGA-LIHC; and "type II failure" refers to replication failures except type I failure. **(D)** Platform-adjusted replication rates of four types of genic DME-DEGs in TCGA-LIHC. Platform-adjusted replication rates were calculated as $(Count_{Successful\ Replication} + Count_{Successful\ Replication} + Count_{Type\ I\ Failure}) * 100\%$.

(**Figure 6B**), while 959 repressed AE-DEGs were enriched for genes involved in monocarboxylic acid metabolism, adaptive immune response, biological oxidation, and cytochrome P450 epoxygenase pathway (**Figure 6C**). Moreover, hypergeometric test revealed that AE-DEGs showed significant enrichment for genes related to four cancer hallmarks including genome instability and mutation (FDR = 6.3e−9), reprogramming energy metabolism (FDR = 1.2e−3), resisting cell death (FDR = 7.3e−3), and evading immune destruction (FDR = 4.2e−2) (**Figure 6D**).

In addition, AE-DEGs were further verificated according to HiC-produced TADs and chromatin loops. The results showed that 63.24 and 71.62% of AE-DEGs were in the same TAD, in which their corresponding enhancers were located, in the HiC profiled HepG2 and normal adult liver tissue sample (**Figure 6E**; **Supplementary Table S3.3**). Moreover, the TAD validation results in two HiC samples were highly consistent. Specifically, 56.95 and 80.35% of AE-DEGs were successfully supported by TADs in both samples and either sample, respectively (**Figure 6E**;

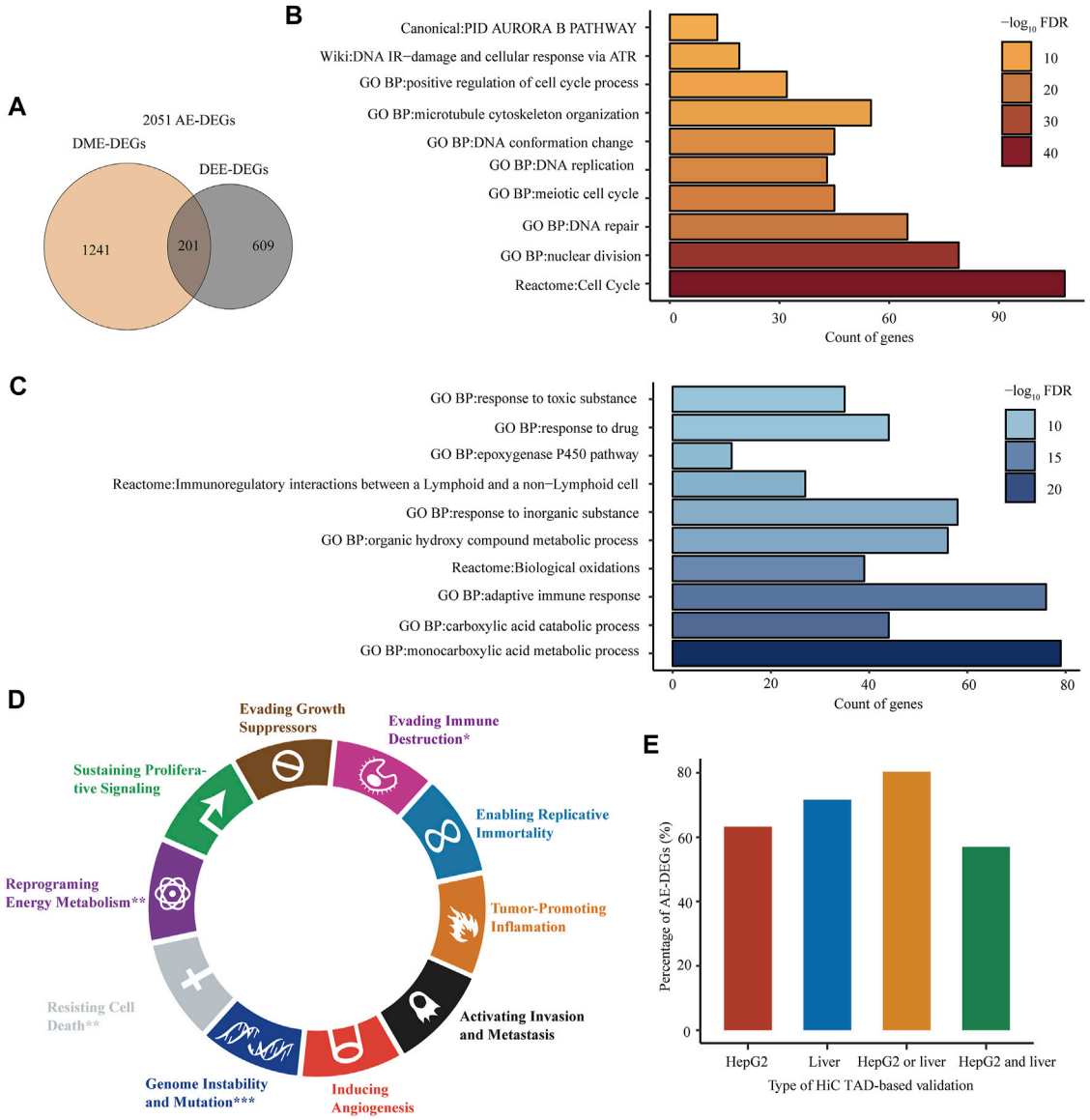

FIGURE 6 | Biological functions and in silico verification of AE-DEGs. **(A)** Venn diagram displaying the overlap between genic DME-DEGs and intergenic DEE-DEGs. The union of them were defined as aberrant enhancer-associated DEGs (AE-DEGs). **(B)** and **(C)** Top ten overrepresented pathways/GO terms of activated AE-DEGs and repressed AE-DEGs, respectively. **(D)** Enrichment of AE-DEGs for ten cancer hallmarks. "*"refers to hypergeometric test FDR < 0.05; "**"refers to FDR < 1e-2; and "***"refers to FDR < 1e-3. **(E)** Percentage of AE-DEGs that were successfully validated by TADs in HiC-profiled HepG2 and normal liver samples. "HepG2 or liver" refers to successful validation in HepG2 or the liver sample; "HepG2 and liver" refers to successful validation in both HepG2 and the liver sample.

Supplementary Table S3.3). Furthermore, 12 and one AE-DEG were confirmed by chromatin interaction loops in HepG2 and normal liver sample (**Supplementary Table S3.4**), respectively.

Construction of a Six AE-DEGs -Based Prognostic Model

Through univariate Cox regression, LASSO, and multivariate Cox regression model filtering, 2051 AE-DEGs were eventually filtered to six genes to build a prognostic model for OS in TCGA-LIHC. These six AE-DEGs included procollagen-lysine,2-oxoglutarate 5-dioxygenase 2 (PLOD2), homeobox D9 (HOXD9), BOP1 ribosomal biogenesis factor, which is also known as Block of Proliferation (BOP1), Ras-related protein Rab-26 (RAB26), killer cell lectin-like receptor K1 (KLRK1), and Ral guanine nucleotide dissociation stimulator like 4 (RGL4) (**Figure 7A**). A prognostic risk score was calculated for each patient as follows: the risk score = (0.424 * expression of PLOD2) + (0.109 * expression of HOXD9) + (0.184 * expression of BOP1) + (−0.134 * expression of RAB26) + (−0.185 * expression of KLRK1) + (−0.0547 * expression of RGL4). An optimal cutoff at 7.37 was applied to divide all

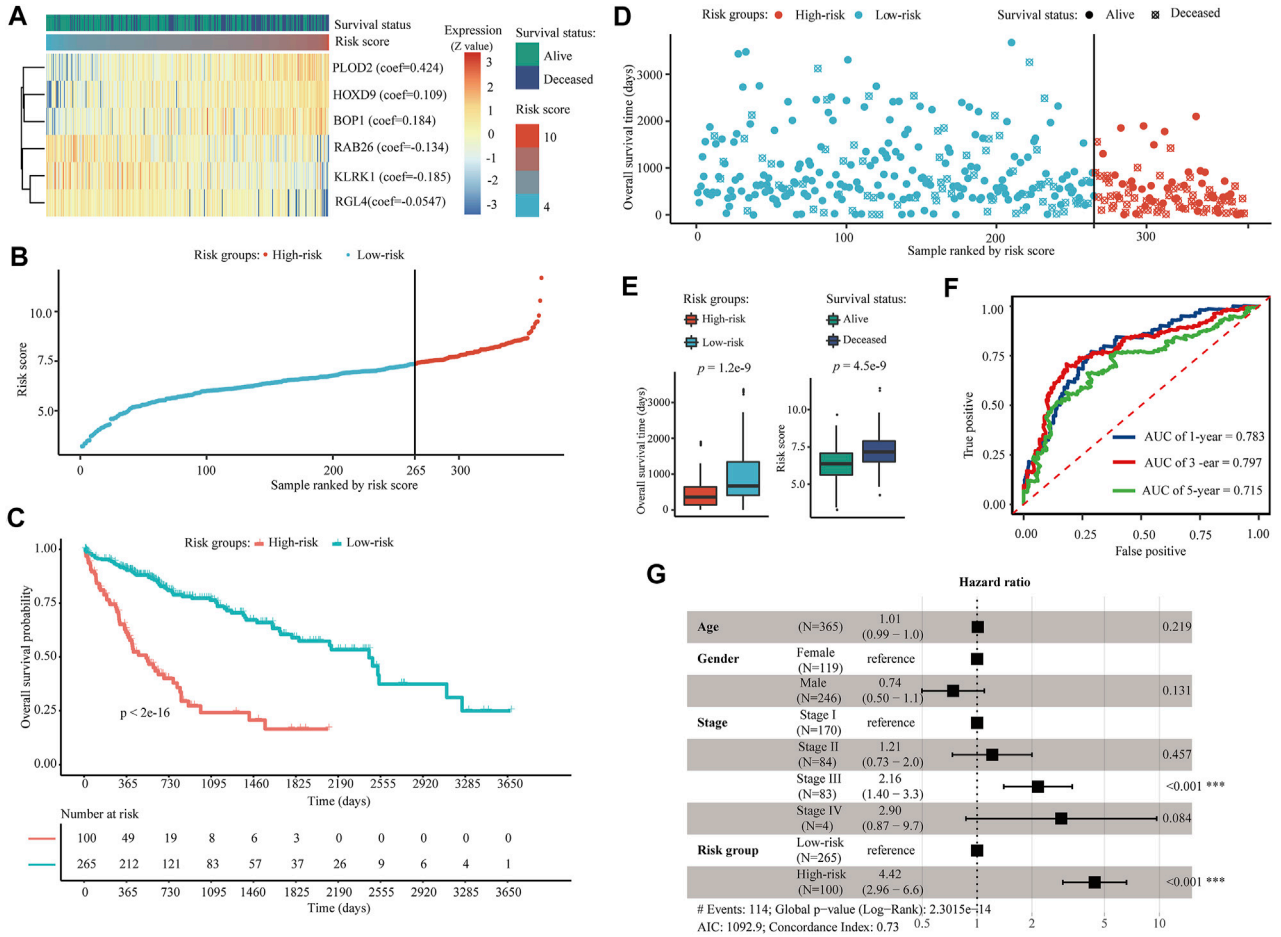

FIGURE 7 | Construction of a six AE-DEG-based prognostic model for HCC in TCGA-LIHC. **(A)** The expression heatmap of six AE-DEGs constituted the identified prognostic model for OS of HCC in TCGA-LIHC. Multivariate Cox regression derived coefficients used for the calculation of risk score are given in parentheses. Patients were ranked according to corresponding calculated risk scores. **(B)** Distribution of the calculated risk scores of HCC patients in TCGA-LIHC. **(C)** Kaplan-Meier analysis of the six AE-DEG-based prognostic signature in TCGA-LIHC. **(D)** Distribution of duration and survival status of HCC patients in TCGA-LIHC. **(E)** Box plots display the comparison of survival times between high- and low-risk HCC patients and the comparison of risk scores between alive and deceased HCC patients in TCGA-LIHC. Wilcox *p*-values were calculated and displayed with each boxplot. **(F)** Time-dependent ROC analyses of the six AE-DEG-based prognostic signature in TCGA-LIHC. **(G)** Forest plot of the multivariate Cox regression analysis in TCGA-LIHC.

patients into high-risk (N = 100) and low-risk (N = 265) groups (**Figure 7B**). Kaplan-Meier analysis revealed significant differences in OS probability across time between high-risk and low-risk groups ($p < 2.0e{-}16$) (**Figure 7C**). Wilcox rank-sum exact tests illuminated significantly less OS duration in high-risk patients ($p = 1.2e{-}9$), and lower risk scores among alive patients ($p = 4.5e{-}9$) (**Figures 7D,E**). The areas under the time-dependent ROC curves (AUCs) for 1-, 3-, and 5-years OS were estimated to be 0.783, 0.797, and 0.715, respectively (**Figure 7F**). A multivariate Cox regression model constructed using both age, gender, and pathologic TNM stage demonstrated that TNM stage ($p < 0.001$, HR = 2.16) and risk group ($p < 0.001$, HR = 4.42) were both independent prognostic biomarkers for OS of HCC patients in TCGA-LIHC (**Figure 7G**).

Subsequently, a predictive nomogram was built by combining the risk score and TNM stage for accurate prediction of overall survival probability in 1, 3, and 5 years (**Figure 8A**). The calibration plots for internal validation of the nomogram showed high consistency between the predicted OS outcomes and actual observations (**Figure 8B**). Time-dependent ROC curves revealed the best predictive performance of the nomogram, with AUCs of 0.796, 0.830, and 0.773 for 1-year, 3-years, and 5-years OS, respectively (**Figure 8C**).

Consistent Validation of the Six AE-DEGs-Based Prognostic Model in ICGC-LIRI

Univariate Cox regression revealed that all six AE-DEGs that constituted the identified prognostic signature were significant OS-related biomarkers in ICGC-LIRI cohort (**Figure 9A**). Risk scores were calculated for each ICGC-LIRI patient by using the coefficients estimated from TCGA-LIHC. Similarly, 198 ICGC-LIRI patients were divided into high-risk (N = 65) and low-risk (N = 135) groups according to the corresponding optimal cutoff (**Figure 9B**).

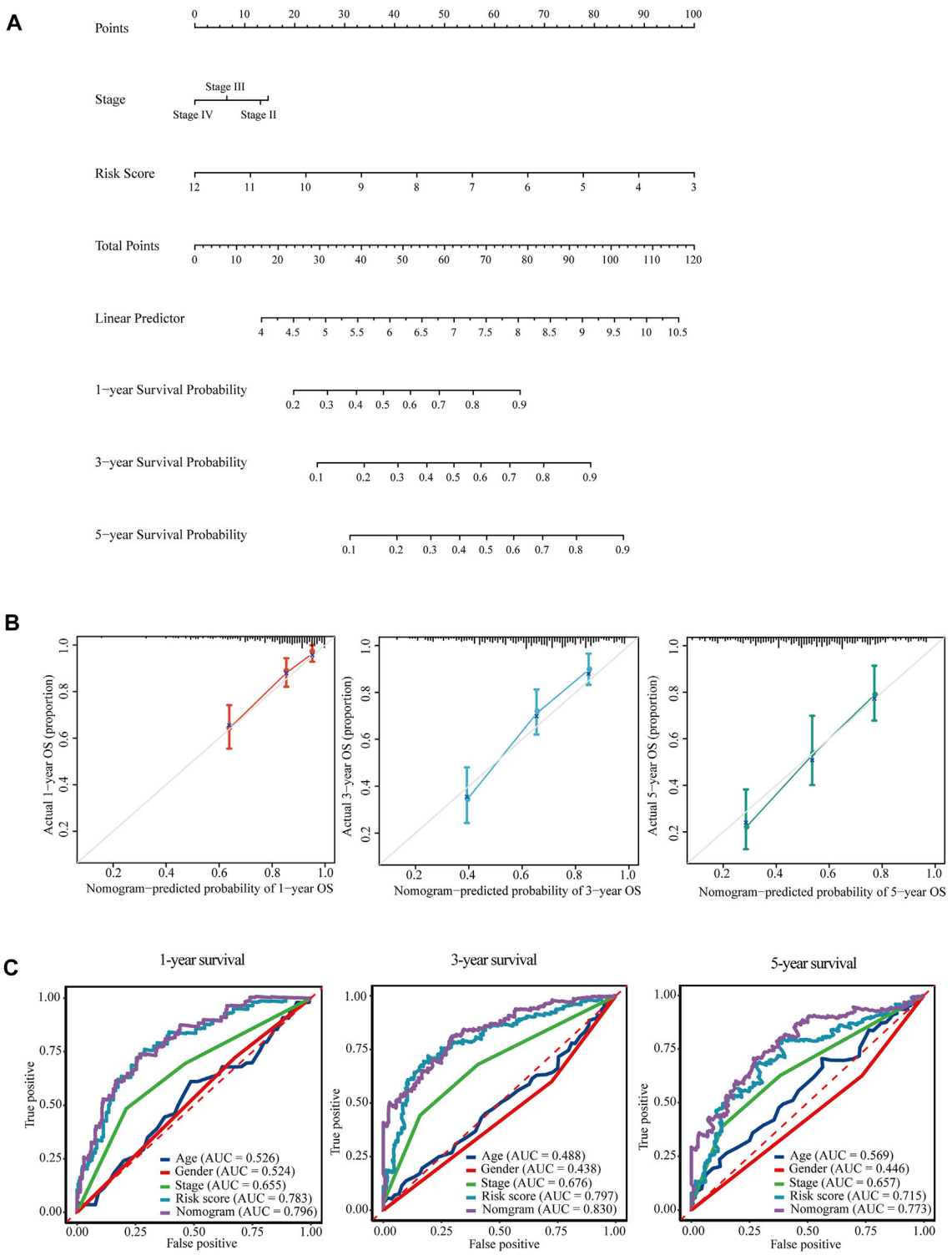

FIGURE 8 | Nomogram for the prediction of overall survival of HCC in TCGA-LIHC. **(A)** A prognostic nomogram for predicting the probabilities of 1-year, 3-years, and 5-years overall survival of HCC patients in TCGA-LIHC. **(B)** Calibration plots for evaluation of the predictive performance of the constructed nomogram. **(C)** Time-dependent ROC curves displayed the comparisons of AUCs among diverse prognostic models.

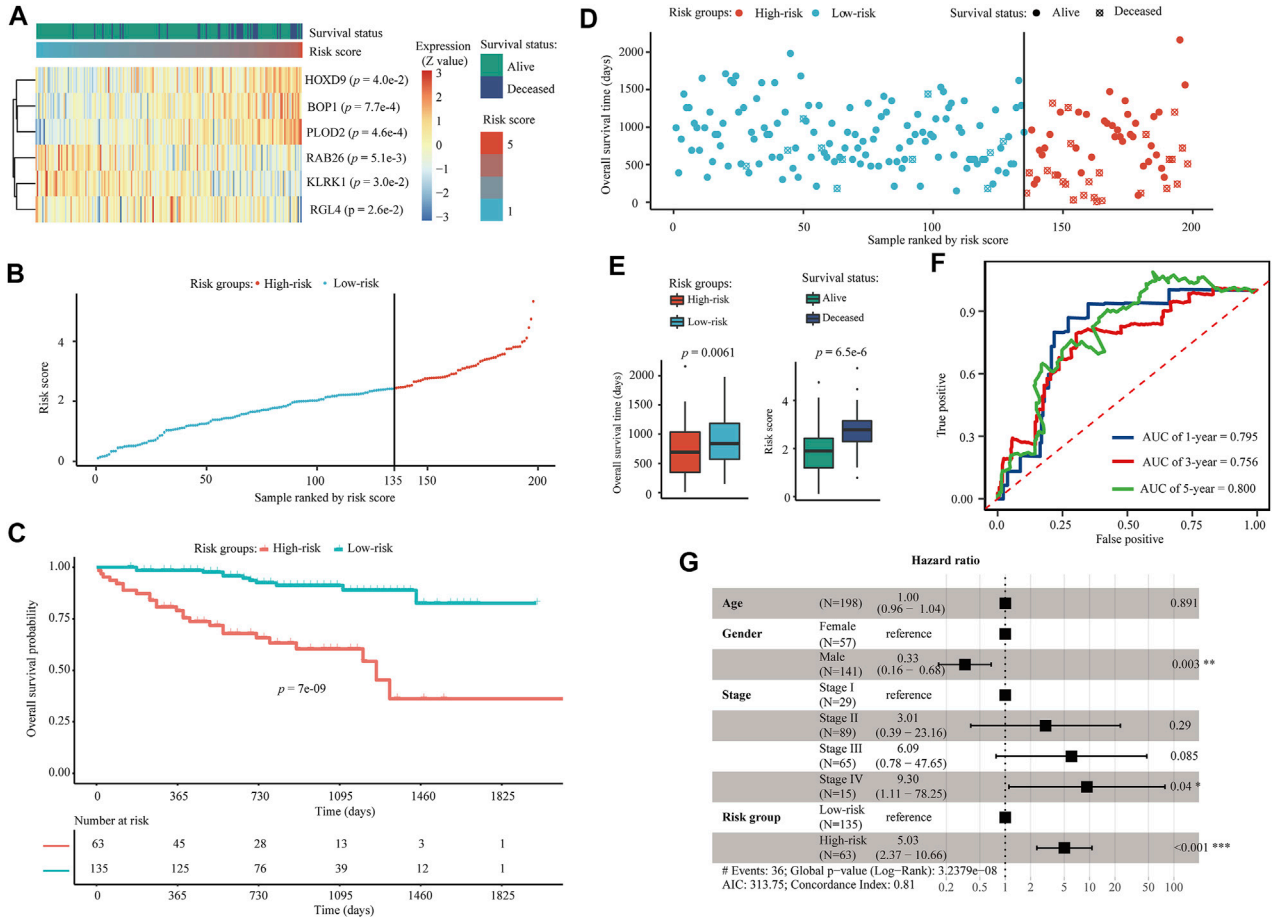

FIGURE 9 | Validation of the six AE-DEG-based prognostic model for OS of HCC in ICGC-LIRI cohort. **(A)** The expression heatmap of six AE-DEGs constituted the identified prognostic model for overall survival of HCC in ICGC-LIRI cohort. Patients were ranked according to their risk scores. **(B)** Distribution of the calculated risk scores of HCC patients in ICGC-LIRI. **(C)** Kaplan-Meier analysis of the 6-gene prognostic signature in ICGC-LIRI. **(D)** Distribution of duration and survival status of HCC patients in ICGC-LIRI. **(E)** Boxplots display the comparison of survival time between high- and low-risk HCC patients and the comparison of risk score between alive and deceased HCC patients in ICGC-LIRI. **(F)** Time-dependent ROC analysis of the six AE-DEG-based prognostic signature in ICGC-LIRI. **(G)** Forest plot of the multivariate Cox regression analysis in ICGC-LIRI.

Kaplan-Meier analysis revealed significant differences in OS probability across time between high-risk and low-risk group ICGC-LIRI patients (p = 7.0e−9) (**Figure 9C**). Wilcox rank-sum exact tests illuminated significantly less OS duration in high-risk patients (p = 0.0061), and lower risk scores among alive patients (p = 6.5e−6) (**Figures 9D,E**). The AUCs for 1-, 3-, and 5-years OS were estimated as 0.795, 0.756, and 0.800 (**Figure 9F**), respectively. A multivariate Cox regression model constructed using both age, gender, and pathologic TNM stage also confirmed that the risk group (p < 0.001, HR = 5.03) was an independent prognostic biomarker for OS of HCC patients in ICGC-LIRI (**Figure 9G**).

The Six AE-DEG-Based Prognostic Model Display Superb Predictive Performance for OS of HCC Patients

Furthermore, the good predictive performance of our identified AE-DEG-based signature was assessed through comparisons with seven established similar prognostic models (Long et al., 2019; Zhang et al., 2020b; Ouyang et al., 2020; Tang et al., 2020; Zhu et al., 2020; He et al., 2021; Wang et al., 2021). Among all signatures, the hypoxia-related gene-based signature and our AE-DEG-based signature were the only two models in which all AUCs were higher than 0.7, which is a well-accepted criterion for high predictive accuracy. Moreover, our model's average AUCs in the discovery and validation cohorts were both higher than those of the hypoxia-related model (0.765 and 0.784 *vs.* 0.723 and 0.763) (**Table 4**). Overall, our prognostic signature had more predictive power than others.

DISCUSSION

In the present study, integration of ChIP-seq and RNA-seq data revealed substantial intergenic DEEs and associated DEE-DEGs in HCC. Compared with activated DEEs and DEE-DEGs, the repressed DEEs and DEE-DEGs displayed higher consistency in multiple HCC

TABLE 4 | Comparison of the predictive performance of our AE-DEG-based signature with seven previously established prognostic signatures in HCC.

Signature name	AUCs for OS in discovery			AUCs for OS in validation		
	1-year	3-years	5-years	1-year	3-years	5-years
Methylation-driven gene based signature 1 (Long et al., 2019)	0.6885	0.6563	0.6548	0.6397	0.6644	0.5942
Methylation-driven gene based signature 2 (He et al., 2021)	0.742	0.661	—	0.695	0.655	—
Angiogenic gene based signature (Zhu et al., 2020)	0.74	0.66	0.66	0.78	0.74	—
EMT related gene based signature (Wang et al., 2021)	0.824	0.798	0.800	0.688	0.674	0.876
Ferroptosis and iron-metabolism related gene based signature (Tang et al., 2020)	0.77	0.71	0.64	0.67	0.73	—
Differentially expressed gene signature (Ouyang et al., 2020)	0.77	0.73	0.72	0.63	0.68	0.65
Hypoxia related gene based signature (Zhang et al., 2020b)	0.78	0.70	0.70	0.75	0.77	0.77
Our AE-DEG based signature	0.783	0.797	0.715	0.795	0.756	0.800

cohorts. Remarkably, 162 of those 387 intergenic DEE-DEGs were concurrent in at least four of the five HCC cohorts that were analyzed in this study. Functional enrichment analysis by Metascape (Zhou et al., 2019) revealed that half of those highly concurrent genes were liver-specific. Enrichment of repressed DEGs for liver-specific genes was previously reported in HCC (Lian et al., 2018). A highly plausible mechanism underlying this phenomenon might be cell dedifferentiation. Cell dedifferentiation is a process that implicates the epigenetic reprogramming of gene activity to transform cells into a less differentiated state like their parent cell type. In the development of HCC, stepwise dedifferentiation is a certain event that exhibits loss of hepatic functions and morphology and gain of hepatic progenitor markers (Chao et al., 2020). Moreover, the well-known demethylation agent 5-azacytidine (5-AZA) displayed potential for usage in dedifferentiation therapy in HCC cell lines and cell-derived xenograft (Gailhouste et al., 2018). In addition, it has been shown that upon loss of the mouse Igκ gene's downstream enhancers, E3′ and Ed, the mature B cells unexpectedly undergo reversible retrograde differentiation (Zhou et al., 2013). Hence, our finds about conservative enhancer repression associated suppression of liver-specific genes might shed new light on epigenetic mechanisms underlying the dedifferentiation that occurs in hepatocarcinogenesis and provide potential targets for dedifferentiation-targeted therapy of HCC.

Notably, highly conserved intergenic DEE-DEGs with counts less than 200 unexpectedly included the majority of all MT genes in the genome. MTs are small cysteine-rich proteins that play pivotal roles in metal homeostasis and protection against heavy metal-related cytotoxicity, DNA damage, and oxidative stress (Coyle et al., 2002). Dysregulation of MTs is ubiquitous in most malignancies, and emerging evidence shows that MTs are implicated in tumor formation, progression, and drug resistance (Si and Lang, 2018; Merlos Rodrigo et al., 2020). As mentioned earlier, nine identified DEE-associated differentially expressed MT isoforms were reported to be involved in liver cancer. Specifically, the upregulation of *MT1A* mediated the attenuation of malignant behaviors of *CT23* knockdown in HCC cells (Ning et al., 2021). *MT1DP* is a pivotal anticancer long noncoding RNA (lncRNA), whose suppression mediates the vital carcinogenetic roles of *RUNX2* and *YAP* in HCC (Yu et al., 2014a). *MT1E* was newly identified as a novel tumor suppressor for HCC that could induce apoptosis and suppress cell growth and metastasis (Liu et al., 2020). Exogenous expression of *MT1F* displayed a strong inhibitive effect on the growth of HepG2 cells (Lu et al., 2003). *MT1G* was uncovered as a tumor suppressor in HCC by inducing the transcriptional activity of p53 through direct interaction and supply of appropriate zinc ions to p53 (Wang et al., 2019). *MT1H* functions as a tumor suppressor that suppresses the proliferation and invasion of HCC cells by inhibiting the Wnt/β-catenin pathway (Zheng et al., 2017). Overexpression of the lncRNA *MT1JP* remarkably inhibited the proliferation and enhanced apoptosis, which might be mediated by regulating the expression of *AKT* (Wu et al., 2020a). Similarly, *MT1M* also showed a tumor-suppressive ability to suppress cell viability, migration, and invasion and activate apoptosis *in vitro* (Fu et al., 2017). *MT1X* was demonstrated to be a tumor suppressor that suppresses tumor growth and metastasis *in vivo* and induces cell cycle arrest and apoptosis by repressing the NF-κB signaling pathway in HCC (Liu et al., 2018b). The roles of *MT1CP*, *MT1L*, and *MT2A* in HCC are still unknown, while *MT2A* could promote breast cancer invasiveness and might play a suppressive role in gastric cancer through inhibition of the NK-κB signaling pathway (Kim et al., 2011; Pan et al., 2013).

Besides, there were also several sets of upregulated genes associated with activated super-enhancers in HCC. On chromosome 17, a group of 10 activated DEE-DEGs was found to be associated with increased enhancer activity for 14 intergenic DEEs. It is intriguing that six (*HGS*, *CEP131*, *MAFG*, *MAFG-DT*, *FOXK2*, and *SIRT7*) of them have already been discovered as proto-oncogenes in HCC (Canal et al., 2015; Lin et al., 2017b; Liu et al., 2017; Liu et al., 2018c; Ouyang et al., 2019; Zhao et al., 2019). In particular, the lncRNA *MAFG-DT*, which is likewise known as *MAFG-AS1*, was also recently shown to play oncogenic roles in multiple tumors in addition to HCC, including colorectal cancer (Cui et al., 2018), breast carcinoma (Li et al., 2019), bladder urothelial carcinoma (Xiao et al., 2020), esophageal squamous cell carcinoma (Qu and Liu, 2020), and lung adenocarcinoma (Sui et al., 2019). *NPLOC4*, also known as *NPL4*, is uncharacterized in HCC but has been revealed as an important oncogene in bladder cancer (Lu et al., 2019) and a critical target of the anticancer drug disulfiram (Skrott et al., 2017; Pan et al., 2021). Similarly, *CSNK1D* has recently been identified as a novel drug target in Hedgehog/GLI-driven cancers (Peer et al., 2021), and silencing of *CSNK1D* attenuates the migration and metastasis of triple-negative breast cancer cells (Bar et al., 2018). As an E3 ubiquitin

ligase, *NARF* was identified as a positive regulator of cell growth in glioblastoma (Anderson et al., 2010). *CCDC137* has not been characterized in any cancer, but its depletion via HIV could cause cell cycle arrest (Zhang and Bieniasz, 2020). Taken together, the elevated activity of the super-enhancer, which is composed of a cluster of 14 synergistic enhancers located on chromosome 17, was demonstrated to be associated with the activation of several critical oncogenes implicated in HCC and/or other cancers. Therefore, inhibition of this activated super-enhancer might be a promising therapy for HCC.

Our integrative transcriptomic analyses discovered massive concurrent DEEs in HCC, which might be caused by either genetic mutations or epigenetic aberrations. However, those DEEs, especially repressed DEEs, were ubiquitous and conserved in multiple HCC cohorts, which suggests a higher possibility of epigenetic aberration-relevant underlying mechanisms. Indeed, our investigation revealed that considerable DEEs and DEE-DEGs were linked to DNA methylation and histone modification. Notably, there were strong associations between the activation of three histone methyltransferases (*EZH2*, *EHMT2*, and *SMYD3*) and enhancer aberrations. This was consistent with the previous findings that mutations and expression changes of epigenetic modifiers are common events leading to an aggressive gene expression and poor clinical outcomes in HCC (Bayo et al., 2019). *EZH2*, *EHMT2*, and *SMYD3* are vital epigenetic regulators that could be targeted for cancer therapy (Cheng et al., 2019). Unlike those of *EZH2* (Gao et al., 2014; Liu et al., 2015; Zhuang et al., 2016; Chen et al., 2018b), the roles of *EHMT2* and *SMYD3* in mediating transcriptional regulation in carcinogenesis are still not fully characterized in HCC (Zhang et al., 2021a; Guo et al., 2021). Our findings serve as a proof-of-concept that activation of histone methyltransferases, such as *EZH2*, *EHMT2*, and *SMYD3* might promote hepatocarcinogenesis by inducing enhancer aberration of crucial cancer-related genes.

To better assess the clinical outcomes of HCC patients, in this study, we applied machine learning approaches to explore the prognostic significance of AE-DEGs in HCC and established a prognostic model based on a panel of six AE-DEGs, including *PLOD2*, *HOXD9*, *BOP1*, *RAB26*, *KLRK1*, and *RGL4*. Our identified AE-DEG-based signature outperformed clinical characteristics such as the TNM stage and seven previously established similar prognostic models in terms of predictive accuracy, suggesting that those six AE-DEGs might play important roles in HCC. *PLOD2* encodes a key enzyme mediating the formation of the stabilized collagen cross-links, which are considered as the "highway" for cancer cell migration and invasion (Provenzano et al., 2006). The roles of *PLOD2* in breast cancer, sarcoma, bladder cancer, and renal cell carcinoma were thoroughly discussed in a previous review (Du et al., 2017). *PLOD2* was first demonstrated as a prognostic marker for HCC in 2011 (Noda et al., 2012), while the function and mechanism of *PLOD2* activation in HCC have not been thoroughly explored. *HOXD9* and *BOP1* were both uncovered as the oncogenic promoters of epithelial-mesenchymal transition (EMT) in HCC (Chung et al., 2011; Lv et al., 2015), which was in line with their unfavorable prognostic contribution in our identified prognostic signature. On the other hand, *RAB26* was novel in HCC but was newly identified as a suppressor of the migration and invasion of breast cancer cells (Liu et al., 2021). The roles of *KLRK1* and *RGL4* have not been investigated in any malignancies but have been identified as prognostic factors in lung adenocarcinoma (Sun et al., 2020; Zhang et al., 2021b). In summary, previous studies revealed pivotal cancer-related functions of *PLOD2*, *HOXD9*, *BOP1*, and *RAB26,* manifesting our findings of their AE-associated dysregulation and prognostic significance in OS of HCC, and suggesting the possibility that *PLOD2*, *RAB26*, *KLRK1*, and *RGL4* play essential roles in the progression and survival of HCC, although further experimental investigations are warranted.

Our study uncovered systematic enhancer aberrations with important functions and excellent prognostic significance in HCC. There are still several potential limitations. First of all, RNA-seq is still commonly used in the literature (Chen et al., 2018a; Wu et al., 2020b; Chen and Liang, 2020) but is not one of the best choices for the comprehensive detection of eRNA; for example, GRO-seq would be a better approach (Danko et al., 2015; Zhang et al., 2020c). Second, aberrant genic enhancers might be only partially captured by identifying genic DMEs, especially considering the relatively low ratio of DNA methylation-associated DEEs in total intergenic DEEs. Moreover, although our identified AE-DEGs were successfully replicated in independent cohorts and confirmed by TADs from HiC, further validation of enhancer-mediated transcriptional regulation of particular genes *via* experimental technologies such as CRISPR, like in previous enhancer related studies (Chen et al., 2018a; Xiong et al., 2019), was lacking in our present study and will be part of our ongoing works.

CONCLUSION

In conclusion, our integrative analysis of the epigenome and transcriptome depicted and verified a systematic landscape of aberrant enhancers and 2051 associated DEGs, including many well-known cancer-related genes, in HCC. These findings provide new insight into the roles of epigenetic aberration induced aberrant enhancers in the progression of HCC. Furthermore, our established prognostic signature based on six AE-DEGs displayed superior predictive performance over previous models for predicting the long-term and short-term OS of HCC patients.

DATA AVAILABILITY STATEMENT

The datasets presented in this study can be found in online repositories. The names of the repository/repositories and accession number(s) can be found below: NCBI SRA database [accession: PRJNA762641].

ETHICS STATEMENT

The studies involving human participants were reviewed and approved by The institutional review board of the First Affiliated Hospital, Zhejiang University School of Medicine. The patients/participants provided their written informed consent to participate in this study.

AUTHOR CONTRIBUTIONS

PH, BZ, JZ, and ML contributed to the conception and design of the study. PH organized the database and performed the statistical analysis. PH wrote the first draft of the manuscript. All authors contributed to manuscript revision, read, and approved the submitted version.

FUNDING

This study was supported in part by the China Precision Medicine Initiative (2016YFC0906300), Research Center for Air Pollution and Health of Zhejiang University, and the Independent Task of State Key Laboratory for Diagnosis and Treatment of Infectious Diseases.

SUPPLEMENTARY MATERIAL

The Supplementary Material for this article can be found online at: https://www.frontiersin.org/articles/10.3389/fcell.2022.827657/full#supplementary-material

REFERENCES

Alboukadel Kassambara, M. K. (2021). *Przemyslaw Biecek, and Scheipl Fabian Survminer: Survival Analysis and Visualization*.

Anderson, T. W., Wright, C., and Brooks, W. S. (2010). The E3 Ubiquitin Ligase NARF Promotes colony Formation *In Vitro* and Exhibits Enhanced Expression Levels in Glioblastoma Multiforme *In Vivo*. *Am. J. Undergraduate Res.* 9, 23–30. doi:10.33697/ajur.2010.017

Bar, I., Merhi, A., Larbanoix, L., Constant, M., Haussy, S., Laurent, S., et al. (2018). Silencing of Casein Kinase 1 delta Reduces Migration and Metastasis of Triple Negative Breast Cancer Cells. *Oncotarget* 9 (56), 30821–30836. doi:10.18632/oncotarget.25738

Bayo, J., Fiore, E. J., Dominguez, L. M., Real, A., Malvicini, M., Rizzo, M., et al. (2019). A Comprehensive Study of Epigenetic Alterations in Hepatocellular Carcinoma Identifies Potential Therapeutic Targets. *J. Hepatol.* 71 (1), 78–90. doi:10.1016/j.jhep.2019.03.007

Canal, F., Anthony, E., Lescure, A., Del Nery, E., Camonis, J., Perez, F., et al. (2015). A Kinome siRNA Screen Identifies HGS as a Potential Target for Liver Cancers with Oncogenic Mutations in CTNNB1. *BMC Cancer* 15, 1020. doi:10.1186/s12885-015-2037-8

Chao, J., Zhao, S., and Sun, H. (2020). Dedifferentiation of Hepatocellular Carcinoma: Molecular Mechanisms and Therapeutic Implications. *Am. J. Transl Res.* 12 (5), 2099–2109.

Chen, H., Li, C., Peng, X., Zhou, Z., Weinstein, J. N., Caesar-Johnson, S. J., et al. (2018). A Pan-Cancer Analysis of Enhancer Expression in Nearly 9000 Patient Samples. *Cell* 173 (2), 386–e12. e312. doi:10.1016/j.cell.2018.03.027

Chen, H., and Liang, H. (2020). A High-Resolution Map of Human Enhancer RNA Loci Characterizes Super-enhancer Activities in Cancer. *Cancer Cell* 38 (5), 701–715. e705. doi:10.1016/j.ccell.2020.08.020

Chen, S., Pu, J., Bai, J., Yin, Y., Wu, K., Wang, J., et al. (2018). EZH2 Promotes Hepatocellular Carcinoma Progression through Modulating miR-22/galectin-9 axis. *J. Exp. Clin. Cancer Res.* 37 (1), 3. doi:10.1186/s13046-017-0670-6

Cheng, Y., He, C., Wang, M., Ma, X., Mo, F., Yang, S., et al. (2019). Targeting Epigenetic Regulators for Cancer Therapy: Mechanisms and Advances in Clinical Trials. *Sig Transduct Target. Ther.* 4, 62. doi:10.1038/s41392-019-0095-0

Chung, K.-Y., Cheng, I. K.-C., Ching, A. K.-K., Chu, J.-H., Lai, P. B.-S., and Wong, N. (2011). Block of Proliferation 1 (BOP1) Plays an Oncogenic Role in Hepatocellular Carcinoma by Promoting Epithelial-To-Mesenchymal Transition. *Hepatology* 54 (1), 307–318. doi:10.1002/hep.24372

Consortium, E. P. (2004). The ENCODE (ENCyclopedia of DNA Elements) Project. *Science* 306 (5696), 636–640. doi:10.1126/science.1105136

Coyle, P., Philcox, J. C., Carey, L. C., and Rofe, A. M. (2002). Metallothionein: the Multipurpose Protein. *Cell Mol. Life Sci. (Cmls)* 59 (4), 627–647. doi:10.1007/s00018-002-8454-2

Cui, S., Yang, X., Zhang, L., Zhao, Y., and Yan, W. (2018). LncRNA MAFG-AS1 Promotes the Progression of Colorectal Cancer by Sponging miR-147b and Activation of NDUFA4. *Biochem. Biophysical Res. Commun.* 506 (1), 251–258. doi:10.1016/j.bbrc.2018.10.112

Danko, C. G., Hyland, S. L., Core, L. J., Martins, A. L., Waters, C. T., Lee, H. W., et al. (2015). Identification of Active Transcriptional Regulatory Elements from GRO-Seq Data. *Nat. Methods* 12 (5), 433–438. doi:10.1038/nmeth.3329

Dobin, A., Davis, C. A., Schlesinger, F., Drenkow, J., Zaleski, C., Jha, S., et al. (2013). STAR: Ultrafast Universal RNA-Seq Aligner. *Bioinformatics* 29 (1), 15–21. doi:10.1093/bioinformatics/bts635

Du, H., Pang, M., Hou, X., Yuan, S., and Sun, L. (2017). PLOD2 in Cancer Research. *Biomed. Pharmacother.* 90, 670–676. doi:10.1016/j.biopha.2017.04.023

Feng, R.-M., Zong, Y.-N., Cao, S.-M., and Xu, R.-H. (2019). Current Cancer Situation in China: Good or Bad News from the 2018 Global Cancer Statistics? *Cancer Commun.* 39 (1), 22. doi:10.1186/s40880-019-0368-6

Friedman, J., Hastie, T., and Tibshirani, R. (2010). Regularization Paths for Generalized Linear Models via Coordinate Descent. *J. Stat. Softw.* 33 (1), 1–22. doi:10.18637/jss.v033.i01

Fu, C.-L., Pan, B., Pan, J.-H., and Gan, M.-F. (2017). Metallothionein 1M Suppresses Tumorigenesis in Hepatocellular Carcinoma. *Oncotarget* 8 (20), 33037–33046. doi:10.18632/oncotarget.16521

Fu, J., Lv, H., Guan, H., Ma, X., Ji, M., He, N., et al. (2013). Metallothionein 1G Functions as a Tumor Suppressor in Thyroid Cancer through Modulating the PI3K/Akt Signaling Pathway. *BMC Cancer* 13, 462. doi:10.1186/1471-2407-13-462

Gai, C., Liu, C., Wu, X., Yu, M., Zheng, J., Zhang, W., et al. (2020). MT1DP Loaded by Folate-Modified Liposomes Sensitizes Erastin-Induced Ferroptosis via Regulating miR-365a-3p/NRF2 axis in Non-small Cell Lung Cancer Cells. *Cell Death Dis* 11 (9), 751. doi:10.1038/s41419-020-02939-3

Gailhouste, L., Liew, L. C., Yasukawa, K., Hatada, I., Tanaka, Y., Nakagama, H., et al. (2018). Differentiation Therapy by Epigenetic Reconditioning Exerts Antitumor Effects on Liver Cancer Cells. *Mol. Ther.* 26 (7), 1840–1854. doi:10.1016/j.ymthe.2018.04.018

Gao, S.-B., Zheng, Q.-F., Xu, B., Pan, C.-B., Li, K.-L., Zhao, Y., et al. (2014). EZH2 Represses Target Genes through H3K27-dependent and H3K27-independent Mechanisms in Hepatocellular Carcinoma. *Mol. Cancer Res.* 12 (10), 1388–1397. doi:10.1158/1541-7786.mcr-14-0034

Grandhi, M. S., Kim, A. K., Ronnekleiv-Kelly, S. M., Kamel, I. R., Ghasebeh, M. A., and Pawlik, T. M. (2016). Hepatocellular Carcinoma: From Diagnosis to Treatment. *Surg. Oncol.* 25 (2), 74–85. doi:10.1016/j.suronc.2016.03.002

Guo, Y., Zhao, Y.-R., Liu, H., Xin, Y., Yu, J.-Z., Zang, Y.-J., et al. (2021). EHMT2 Promotes the Pathogenesis of Hepatocellular Carcinoma by Epigenetically Silencing APC Expression. *Cell Biosci* 11 (1), 152. doi:10.1186/s13578-021-00663-9

Harrow, J., Frankish, A., Gonzalez, J. M., Tapanari, E., Diekhans, M., Kokocinski, F., et al. (2012). GENCODE: the Reference Human Genome Annotation for the ENCODE Project. *Genome Res.* 22 (9), 1760–1774. doi:10.1101/gr.135350.111

He, D., Liao, S., Cai, L., Huang, W., Xie, X., and You, M. (2021). Integrated Analysis of Methylation-Driven Genes and Pretreatment Prognostic Factors in Patients with Hepatocellular Carcinoma. *BMC Cancer* 21 (1), 599. doi:10.1186/s12885-021-08314-5

Herranz, D., Ambesi-Impiombato, A., Palomero, T., Schnell, S. A., Belver, L., Wendorff, A. A., et al. (2014). A NOTCH1-Driven MYC Enhancer Promotes

T Cell Development, Transformation and Acute Lymphoblastic Leukemia. *Nat. Med.* 20 (10), 1130–1137. doi:10.1038/nm.3665

Hlady, R. A., Sathyanarayan, A., Thompson, J. J., Zhou, D., Wu, Q., Pham, K., et al. (2019). Integrating the Epigenome to Identify Drivers of Hepatocellular Carcinoma. *Hepatology* 69 (2), 639–652. doi:10.1002/hep.30211

Hnisz, D., Abraham, B. J., Lee, T. I., Lau, A., Saint-André, V., Sigova, A. A., et al. (2013). Super-enhancers in the Control of Cell Identity and Disease. *Cell* 155 (4), 934–947. doi:10.1016/j.cell.2013.09.053

Huang, P., Xu, M., Han, H., Zhao, X., Li, M. D., and Yang, Z. (2021). Integrative Analysis of Epigenome and Transcriptome Data Reveals Aberrantly Methylated Promoters and Enhancers in Hepatocellular Carcinoma. *Front. Oncol.* 11, 769390. doi:10.3389/fonc.2021.769390

Hur, H., Ryu, H.-H., Li, C.-H., Kim, I. Y., Jang, W.-Y., and Jung, S. (2016). Metallothinein 1E Enhances Glioma Invasion through Modulation Matrix Metalloproteinases-2 and 9 in U87MG Mouse Brain Tumor Model. *J. Korean Neurosurg. Soc.* 59 (6), 551–558. doi:10.3340/jkns.2016.59.6.551

Jiang, Y., Sun, A., Sun, A., Zhao, Y., Ying, W., Sun, H., et al. (2019). Proteomics Identifies New Therapeutic Targets of Early-Stage Hepatocellular Carcinoma. *Nature* 567 (7747), 257–261. doi:10.1038/s41586-019-0987-8

Kim, D. H., Ahn, J. S., Han, H. J., Kim, H.-M., Hwang, J., Lee, K. H., et al. (2019). Cep131 Overexpression Promotes Centrosome Amplification and colon Cancer Progression by Regulating Plk4 Stability. *Cel Death Dis* 10 (8), 570. doi:10.1038/s41419-019-1778-8

Kim, H. G., Kim, J. Y., Han, E. H., Hwang, Y. P., Choi, J. H., Park, B. H., et al. (2011). Metallothionein-2A Overexpression Increases the Expression of Matrix Metalloproteinase-9 and Invasion of Breast Cancer Cells. *FEBS Lett.* 585 (2), 421–428. doi:10.1016/j.febslet.2010.12.030

Kosinski, M., and Biecek, P. (2015). *RTCGA:The Cancer Genome Atlas Data Integration*. R bioconductor package. Available at: https://rtcga.github.io

Krueger, F., and Andrews, S. R. (2011). Bismark: a Flexible Aligner and Methylation Caller for Bisulfite-Seq Applications. *Bioinformatics* 27 (11), 1571–1572. doi:10.1093/bioinformatics/btr167

Li, D., Peng, W., Wu, B., Liu, H., Zhang, R., Zhou, R., et al. (2021). Metallothionein MT1M Suppresses Carcinogenesis of Esophageal Carcinoma Cells through Inhibition of the Epithelial-Mesenchymal Transition and the SOD1/PI3K Axis. *Mol. Cell* 44 (4), 267–278. doi:10.14348/molcells.2021.2179

Li, H., Zhang, G. Y., Pan, C. H., Zhang, X. Y., and Su, X. Y. (2019). LncRNA MAFG-AS1 Promotes the Aggressiveness of Breast Carcinoma through Regulating miR-339-5p/MMP15. *Eur. Rev. Med. Pharmacol. Sci.* 23 (7), 2838–2846. doi:10.26355/eurrev_201904_17561

Lian, Q., Wang, S., Zhang, G., Wang, D., Luo, G., Tang, J., et al. (2018). HCCDB: A Database of Hepatocellular Carcinoma Expression Atlas. *Genomics, Proteomics & Bioinformatics* 16 (4), 269–275. doi:10.1016/j.gpb.2018.07.003

Likhitsup, A., and Parikh, N. D. (2020). Economic Implications of Hepatocellular Carcinoma Surveillance and Treatment: A Guide for Clinicians. *Pharmacoeconomics* 38 (1), 5–24. doi:10.1007/s40273-019-00839-9

Lin, M.-F., Yang, Y.-F., Peng, Z.-P., Zhang, M.-F., Liang, J.-Y., Chen, W., et al. (2017). FOXK2, Regulted by miR-1271-5p, Promotes Cell Growth and Indicates Unfavorable Prognosis in Hepatocellular Carcinoma. *Int. J. Biochem. Cel Biol.* 88, 155–161. doi:10.1016/j.biocel.2017.05.019

Lin, Z., Lai, S., He, X., Zhuo, W., Wang, L., Si, J., et al. (2017). Decreased Long Non-coding RNA MTM Contributes to Gastric Cancer Cell Migration and Invasion via Modulating MT1F. *Oncotarget* 8 (57), 97371–97383. doi:10.18632/oncotarget.22126

Liu, G., Hou, G., Li, L., Li, Y., Zhou, W., and Liu, L. (2016). Potential Diagnostic and Prognostic Marker Dimethylglycine Dehydrogenase (DMGDH) Suppresses Hepatocellular Carcinoma Metastasis *In Vitro* and *In Vivo*. *Oncotarget* 7 (22), 32607–32616. doi:10.18632/oncotarget.8927

Liu, H., Liu, Y., Liu, W., Zhang, W., and Xu, J. (2015). EZH2-mediated Loss of miR-622 Determines CXCR4 Activation in Hepatocellular Carcinoma. *Nat. Commun.* 6, 8494. doi:10.1038/ncomms9494

Liu, H., Zhou, Y., Qiu, H., Zhuang, R., Han, Y., Liu, X., et al. (2021). Rab26 Suppresses Migration and Invasion of Breast Cancer Cells through Mediating Autophagic Degradation of Phosphorylated Src. *Cel Death Dis* 12 (4), 284. doi:10.1038/s41419-021-03561-7

Liu, J., Lichtenberg, T., Hoadley, K. A., Poisson, L. M., Lazar, A. J., Cherniack, A. D., et al. (2018). An Integrated TCGA Pan-Cancer Clinical Data Resource to Drive High-Quality Survival Outcome Analytics. *Cell* 173 (2), 400–e11. e411. doi:10.1016/j.cell.2018.02.052

Liu, Q., Lu, F., and Chen, Z. (2020). Identification of MT1E as a Novel Tumor Suppressor in Hepatocellular Carcinoma. *Pathol. - Res. Pract.* 216 (11), 153213. doi:10.1016/j.prp.2020.153213

Liu, T., Yang, H., Fan, W., Tu, J., Li, T. W. H., Wang, J., et al. (2018). Mechanisms of MAFG Dysregulation in Cholestatic Liver Injury and Development of Liver Cancer. *Gastroenterology* 155 (2), 557–571. e514. doi:10.1053/j.gastro.2018.04.032

Liu, X.-H., Yang, Y.-F., Fang, H.-Y., Wang, X.-H., Zhang, M.-F., and Wu, D.-C. (2017). CEP131 Indicates Poor Prognosis and Promotes Cell Proliferation and Migration in Hepatocellular Carcinoma. *Int. J. Biochem. Cel Biol.* 90, 1–8. doi:10.1016/j.biocel.2017.07.001

Liu, Z., Ye, Q., Wu, L., Gao, F., Xie, H., Zhou, L., et al. (2018). Metallothionein 1 Family Profiling Identifies MT1X as a Tumor Suppressor Involved in the Progression and Metastastatic Capacity of Hepatocellular Carcinoma. *Mol. Carcinogenesis* 57 (11), 1435–1444. doi:10.1002/mc.22846

Long, J., Chen, P., Lin, J., Bai, Y., Yang, X., Bian, J., et al. (2019). DNA Methylation-Driven Genes for Constructing Diagnostic, Prognostic, and Recurrence Models for Hepatocellular Carcinoma. *Theranostics* 9 (24), 7251–7267. doi:10.7150/thno.31155

Lossos, I. S., Czerwinski, D. K., Alizadeh, A. A., Wechser, M. A., Tibshirani, R., Botstein, D., et al. (2004). Prediction of Survival in Diffuse Large-B-Cell Lymphoma Based on the Expression of Six Genes. *N. Engl. J. Med.* 350 (18), 1828–1837. doi:10.1056/nejmoa032520

Love, M. I., Huber, W., and Anders, S. (2014). Moderated Estimation of Fold Change and Dispersion for RNA-Seq Data with DESeq2. *Genome Biol.* 15 (12), 550. doi:10.1186/s13059-014-0550-8

Lu, B.-S., Yin, Y.-W., Zhang, Y.-P., Guo, P.-Y., Li, W., and Liu, K.-L. (2019). Upregulation of NPL4 Promotes Bladder Cancer Cell Proliferation by Inhibiting DXO Destabilization of Cyclin D1 mRNA. *Cancer Cel Int* 19, 149. doi:10.1186/s12935-019-0874-2

Lu, D. D., Chen, Y. C., Zhang, X. R., Cao, X. R., Jiang, H. Y., and Yao, L. (2003). The Relationship between metallothionein-1F (MT1F) Gene and Hepatocellular Carcinoma. *Yale J. Biol. Med.* 76 (2), 55–62.

Lv, X., Li, L., Lv, L., Qu, X., Jin, S., Li, K., et al. (2015). HOXD9 Promotes Epithelial-Mesenchymal Transition and Cancer Metastasis by ZEB1 Regulation in Hepatocellular Carcinoma. *J. Exp. Clin. Cancer Res.* 34, 133. doi:10.1186/s13046-015-0245-3

Mansour, M. R., Abraham, B. J., Anders, L., Berezovskaya, A., Gutierrez, A., Durbin, A. D., et al. (2014). An Oncogenic Super-enhancer Formed through Somatic Mutation of a Noncoding Intergenic Element. *Science* 346 (6215), 1373–1377. doi:10.1126/science.1259037

Marrero, J. A., Kulik, L. M., Sirlin, C. B., Zhu, A. X., Finn, R. S., Abecassis, M. M., et al. (2018). Diagnosis, Staging, and Management of Hepatocellular Carcinoma: 2018 Practice Guidance by the American Association for the Study of Liver Diseases. *Hepatology* 68 (2), 723–750. doi:10.1002/hep.29913

Merlos Rodrigo, M. A., Jimenez Jimemez, A. M., Haddad, Y., Bodoor, K., Adam, P., Krizkova, S., et al. (2020). Metallothionein Isoforms as Double Agents - Their Roles in Carcinogenesis, Cancer Progression and Chemoresistance. *Drug Resist. Updates* 52, 100691. doi:10.1016/j.drup.2020.100691

Nakano, S., Eso, Y., Okada, H., Takai, A., Takahashi, K., and Seno, H. (2020). Recent Advances in Immunotherapy for Hepatocellular Carcinoma. *Cancers (Basel)* 12 (4), 775. doi:10.3390/cancers12040775

Nestal de Moraes, G., Carneiro, L. D. T., Maia, R. C., Lam, E. W., and Sharrocks, A. D. (2019). FOXK2 Transcription Factor and its Emerging Roles in Cancer. *Cancers (Basel)* 11 (3). doi:10.3390/cancers11030393

Ning, W., Huang, M., Wu, S., Wang, H., Yao, J., Ge, Y., et al. (2021). CT23 Knockdown Attenuating Malignant Behaviors of Hepatocellular Carcinoma Cell Is Associated with Upregulation of Metallothionein 1. *Cell Biol Int* 45 (6), 1231–1245. doi:10.1002/cbin.11567

Noda, T., Yamamoto, H., Takemasa, I., Yamada, D., Uemura, M., Wada, H., et al. (2012). PLOD2 Induced under Hypoxia Is a Novel Prognostic Factor for Hepatocellular Carcinoma after Curative Resection. *Liver Int.* 32 (1), 110–118. doi:10.1111/j.1478-3231.2011.02619.x

Ouyang, G., Yi, B., Pan, G., and Chen, X. (2020). A Robust Twelve-Gene Signature for Prognosis Prediction of Hepatocellular Carcinoma. *Cancer Cel Int* 20, 207. doi:10.1186/s12935-020-01294-9

Ouyang, H., Zhang, L., Xie, Z., and Ma, S. (2019). Long Noncoding RNA MAFG-AS1 Promotes Proliferation, Migration and Invasion of Hepatocellular

Carcinoma Cells through Downregulation of miR-6852. *Exp. Ther. Med.* 18 (4), 2547–2553. doi:10.3892/etm.2019.7850

Pan, M., Zheng, Q., Yu, Y., Ai, H., Xie, Y., Zeng, X., et al. (2021). Seesaw Conformations of Npl4 in the Human P97 Complex and the Inhibitory Mechanism of a Disulfiram Derivative. *Nat. Commun.* 12 (1), 121. doi:10.1038/s41467-020-20359-x

Pan, Y., Huang, J., Xing, R., Yin, X., Cui, J., Li, W., et al. (2013). Metallothionein 2A Inhibits NF-Kb Pathway Activation and Predicts Clinical Outcome Segregated with TNM Stage in Gastric Cancer Patients Following Radical Resection. *J. Transl Med.* 11, 173. doi:10.1186/1479-5876-11-173

Patrick, J. (2013). *Heagerty aPS-C: survivalROC: Time-dependent ROC Curve Estimation from Censored Survival Data*.

Peer, E., Aichberger, S. K., Vilotic, F., Gruber, W., Parigger, T., Grund-Gröschke, S., et al. (2021). Casein Kinase 1D Encodes a Novel Drug Target in Hedgehog-GLI Driven Cancers and Tumor-Initiating Cells Resistant to SMO Inhibition. *bioRxiv* 13 (16), 4227. doi:10.3390/cancers13164227

Provenzano, P. P., Eliceiri, K. W., Campbell, J. M., Inman, D. R., White, J. G., and Keely, P. J. (2006). Collagen Reorganization at the Tumor-Stromal Interface Facilitates Local Invasion. *BMC Med.* 4 (1), 38. doi:10.1186/1741-7015-4-38

Qu, Y., and Liu, J. (2020). lncRNA MAFG-AS1 Contributes to Esophageal Squamous-Cell Carcinoma Progression via Regulating miR143/LASP1. *Ott* 13, 8359–8370. doi:10.2147/ott.s258157

Quinlan, A. R., and Hall, I. M. (2010). BEDTools: a Flexible Suite of Utilities for Comparing Genomic Features. *Bioinformatics* 26 (6), 841–842. doi:10.1093/bioinformatics/btq033

Rms (2021). *Rms: Regression Modeling Strategies*. R package.

Shan, L., Zhou, X., Liu, X., Wang, Y., Su, D., Hou, Y., et al. (2016). FOXK2 Elicits Massive Transcription Repression and Suppresses the Hypoxic Response and Breast Cancer Carcinogenesis. *Cancer Cell* 30 (5), 708–722. doi:10.1016/j.ccell.2016.09.010

Shlyueva, D., Stampfel, G., and Stark, A. (2014). Transcriptional Enhancers: from Properties to Genome-wide Predictions. *Nat. Rev. Genet.* 15 (4), 272–286. doi:10.1038/nrg3682

Si, M., and Lang, J. (2018). The Roles of Metallothioneins in Carcinogenesis. *J. Hematol. Oncol.* 11 (1), 107. doi:10.1186/s13045-018-0645-x

Skrott, Z., Mistrik, M., Andersen, K. K., Friis, S., Majera, D., Gursky, J., et al. (2017). Alcohol-abuse Drug Disulfiram Targets Cancer via P97 Segregase Adaptor NPL4. *Nature* 552 (7684), 194–199. doi:10.1038/nature25016

Sui, Y., Lin, G., Zheng, Y., and Huang, W. (2019). LncRNA MAFG-AS1 Boosts the Proliferation of Lung Adenocarcinoma Cells via Regulating miR-744-5p/MAFG axis. *Eur. J. Pharmacol.* 859, 172465. doi:10.1016/j.ejphar.2019.172465

Sun, Y., Zhang, Y., Ren, S., Li, X., Yang, P., Zhu, J., et al. (2020). Low Expression of RGL4 Is Associated with a Poor Prognosis and Immune Infiltration in Lung Adenocarcinoma Patients. *Int. Immunopharmacology* 83, 106454. doi:10.1016/j.intimp.2020.106454

Sung, H., Ferlay, J., Siegel, R. L., Laversanne, M., Soerjomataram, I., Jemal, A., et al. (2021). Global Cancer Statistics 2020: GLOBOCAN Estimates of Incidence and Mortality Worldwide for 36 Cancers in 185 Countries. *CA A. Cancer J. Clin.* 71 (3), 209–249. doi:10.3322/caac.21660

Tang, B., Zhu, J., Li, J., Fan, K., Gao, Y., Cheng, S., et al. (2020). The Ferroptosis and Iron-Metabolism Signature Robustly Predicts Clinical Diagnosis, Prognosis and Immune Microenvironment for Hepatocellular Carcinoma. *Cell Commun Signal* 18 (1), 174. doi:10.1186/s12964-020-00663-1

Therneau, T. M. (2020). *A Package for Survival Analysis in R*.

Tsang, F. H., Law, C. T., Tang, T. C., Cheng, C. L., Chin, D. W., Tam, W. V., et al. (2019). Aberrant Super-enhancer Landscape in Human Hepatocellular Carcinoma. *Hepatology* 69 (6), 2502–2517. doi:10.1002/hep.30544

Wahid, B., Ali, A., Rafique, S., and Idrees, M. (2017). New Insights into the Epigenetics of Hepatocellular Carcinoma. *Biomed. Res. Int.* 2017, 1609575. doi:10.1155/2017/1609575

Wang, J., Yang, X., Han, S., and Zhang, L. (2020). CEP131 Knockdown Inhibits Cell Proliferation by Inhibiting the ERK and AKT Signaling Pathways in Non-small Cell Lung Cancer. *Oncol. Lett.* 19 (4), 3145–3152. doi:10.3892/ol.2020.11411

Wang, X., Xing, Z., Xu, H., Yang, H., and Xing, T. (2021). Development and Validation of Epithelial Mesenchymal Transition-Related Prognostic Model for Hepatocellular Carcinoma. *Aging* 13 (10), 13822–13845. doi:10.18632/aging.202976

Wang, Y., Song, F., Zhang, B., Zhang, L., Xu, J., Kuang, D., et al. (2018). The 3D Genome Browser: a Web-Based Browser for Visualizing 3D Genome Organization and Long-Range Chromatin Interactions. *Genome Biol.* 19 (1), 151. doi:10.1186/s13059-018-1519-9

Wang, Y., Wang, G., Tan, X., Ke, K., Zhao, B., Cheng, N., et al. (2019). MT1G Serves as a Tumor Suppressor in Hepatocellular Carcinoma by Interacting with P53. *Oncogenesis* 8 (12), 67. doi:10.1038/s41389-019-0176-5

Wu, J. H., Xu, K., Liu, J. H., Du, L. L., Li, X. S., Su, Y. M., et al. (2020). LncRNA MT1JP Inhibits the Malignant Progression of Hepatocellular Carcinoma through Regulating AKT. *Eur. Rev. Med. Pharmacol. Sci.* 24 (12), 6647–6656. doi:10.26355/eurrev_202006_21651

Wu, Y., Yang, Y., Gu, H., Tao, B., Zhang, E., Wei, J., et al. (2020). Multi-omics Analysis Reveals the Functional Transcription and Potential Translation of Enhancers. *Int. J. Cancer* 147 (8), 2210–2224. doi:10.1002/ijc.33132

Xiao, M., Liu, J., Xiang, L., Zhao, K., He, D., Zeng, Q., et al. (2020). MAFG-AS1 Promotes Tumor Progression via Regulation of the HuR/PTBP1 axis in Bladder Urothelial Carcinoma. *Clin. Transl Med.* 10 (8), e241. doi:10.1002/ctm2.241

Xiong, L., Wu, F., Wu, Q., Xu, L., Cheung, O. K., Kang, W., et al. (2019). Aberrant Enhancer Hypomethylation Contributes to Hepatic Carcinogenesis through Global Transcriptional Reprogramming. *Nat. Commun.* 10 (1), 335. doi:10.1038/s41467-018-08245-z

Yang, Y., Deng, X., Chen, X., Chen, S., Song, L., Meng, M., et al. (2020). Landscape of Active Enhancers Developed De Novo in Cirrhosis and Conserved in Hepatocellular Carcinoma. *Am. J. Cancer Res.* 10 (10), 3157–3178.

Yang, Y., Chen, L., Gu, J., Zhang, H., Yuan, J., Lian, Q., et al. (2017). Recurrently Deregulated lncRNAs in Hepatocellular Carcinoma. *Nat. Commun.* 8, 14421. doi:10.1038/ncomms14421

Yoon, S.-H., Choi, S.-W., Nam, S. W., Lee, K. B., and Nam, J.-W. (2021). Preoperative Immune Landscape Predisposes Adverse Outcomes in Hepatocellular Carcinoma Patients with Liver Transplantation. *Npj Precis. Onc.* 5 (1), 27. doi:10.1038/s41698-021-00167-2

Yu, H., Wang, S., Zhu, H., and Rao, D. (2019). LncRNA MT1JP Functions as a Tumor Suppressor via Regulating miR-214-3p Expression in Bladder Cancer. *J. Cel Physiol* 1, 1. doi:10.1002/jcp.28274

Yu, H., Ye, W., Wu, J., Meng, X., Liu, R.-y., Ying, X., et al. (2014). Overexpression of Sirt7 Exhibits Oncogenic Property and Serves as a Prognostic Factor in Colorectal Cancer. *Clin. Cancer Res.* 20 (13), 3434–3445. doi:10.1158/1078-0432.ccr-13-2952

Yu, W., Qiao, Y., Tang, X., Ma, L., Wang, Y., Zhang, X., et al. (2014). Tumor Suppressor Long Non-coding RNA, MT1DP Is Negatively Regulated by YAP and Runx2 to Inhibit FoxA1 in Liver Cancer Cells. *Cell Signal.* 26 (12), 2961–2968. doi:10.1016/j.cellsig.2014.09.011

Zhang, B., Tang, B., Gao, J., Li, J., Kong, L., and Qin, L. (2020). A Hypoxia-Related Signature for Clinically Predicting Diagnosis, Prognosis and Immune Microenvironment of Hepatocellular Carcinoma Patients. *J. Transl Med.* 18 (1), 342. doi:10.1186/s12967-020-02492-9

Zhang, D., Huo, D., Xie, H., Wu, L., Zhang, J., Liu, L., et al. (2020). CHG: A Systematically Integrated Database of Cancer Hallmark Genes. *Front. Genet.* 11, 29. doi:10.3389/fgene.2020.00029

Zhang, F., and Bieniasz, P. D. (2020). HIV-1 Vpr Induces Cell Cycle Arrest and Enhances Viral Gene Expression by Depleting CCDC137. *Elife* 9, e55806. doi:10.7554/eLife.55806

Zhang, G., Li, S., Lu, J., Ge, Y., Wang, Q., Ma, G., et al. (2018). LncRNA MT1JP Functions as a ceRNA in Regulating FBXW7 through Competitively Binding to miR-92a-3p in Gastric Cancer. *Mol. Cancer* 17 (1), 87. doi:10.1186/s12943-018-0829-6

Zhang, H., Zheng, Z., Zhang, R., Yan, Y., Peng, Y., Ye, H., et al. (2021). SMYD3 Promotes Hepatocellular Carcinoma Progression by Methylating S1PR1 Promoters. *Cel Death Dis* 12 (8), 731. doi:10.1038/s41419-021-04009-8

Zhang, S., Chen, P., Huang, Z., Hu, X., Chen, M., Hu, S., et al. (2015). Sirt7 Promotes Gastric Cancer Growth and Inhibits Apoptosis by Epigenetically Inhibiting miR-34a. *Sci. Rep.* 5, 9787. doi:10.1038/srep09787

Zhang, Y., Chen, Z., and Gao, G. (2021). *KLRK1 as a Prognostic Biomarker for Lung Adenocarcinoma Cancer*.

Zhang, Y., Qian, M., Tang, F., Huang, Q., Wang, W., Li, Y., et al. (2020). Identification and Analysis of P53-Regulated Enhancers in Hepatic Carcinoma. *Front. Bioeng. Biotechnol.* 8, 668. doi:10.3389/fbioe.2020.00668

Zhao, J., Wozniak, A., Adams, A., Cox, J., Vittal, A., Voss, J., et al. (2019). SIRT7 Regulates Hepatocellular Carcinoma Response to Therapy by Altering the P53-dependent Cell Death Pathway. *J. Exp. Clin. Cancer Res.* 38 (1), 252. doi:10.1186/s13046-019-1246-4

Zheng, Y., Jiang, L., Hu, Y., Xiao, C., Xu, N., Zhou, J., et al. (2017). Metallothionein 1H (MT1H) Functions as a Tumor Suppressor in Hepatocellular Carcinoma through Regulating Wnt/β-Catenin Signaling Pathway. *BMC Cancer* 17 (1), 161. doi:10.1186/s12885-017-3139-2

Zhou, X., Xiang, Y., Ding, X., and Garrard, W. T. (2013). Loss of an Igκ Gene Enhancer in Mature B Cells Results in Rapid Gene Silencing and Partial Reversible Dedifferentiation. *Mol. Cel Biol* 33 (10), 2091–2101. doi:10.1128/mcb.01569-12

Zhou, Y., Zhou, B., Pache, L., Chang, M., Khodabakhshi, A. H., Tanaseichuk, O., et al. (2019). Metascape Provides a Biologist-Oriented Resource for the Analysis of Systems-Level Datasets. *Nat. Commun.* 10 (1), 1523. doi:10.1038/s41467-019-09234-6

Zhu, J., Tang, B., Li, J., Shi, Y., Chen, M., Lv, X., et al. (2020). Identification and Validation of the Angiogenic Genes for Constructing Diagnostic, Prognostic, and Recurrence Models for Hepatocellular Carcinoma. *Aging* 12 (9), 7848–7873. doi:10.18632/aging.103107

Zhuang, C., Wang, P., Huang, D., Xu, L., Wang, X., Wang, L., et al. (2016). A Double-Negative Feedback Loop between EZH2 and miR-26a Regulates Tumor Cell Growth in Hepatocellular Carcinoma. *Int. J. Oncol.* 48 (3), 1195–1204. doi:10.3892/ijo.2016.3336

Conflict of Interest: The authors declare that the research was conducted in the absence of any commercial or financial relationships that could be construed as a potential conflict of interest.

Publisher's Note: All claims expressed in this article are solely those of the authors and do not necessarily represent those of their affiliated organizations, or those of the publisher, the editors and the reviewers. Any product that may be evaluated in this article, or claim that may be made by its manufacturer, is not guaranteed or endorsed by the publisher.

frontiers in Cell and Developmental Biology

ORIGINAL RESEARCH
published: 02 March 2022
doi: 10.3389/fcell.2022.832803

Identification of a Methylation-Regulating Genes Prognostic Signature to Predict the Prognosis and Aid Immunotherapy of Clear Cell Renal Cell Carcinoma

Li Zhang[1], *Zhixiong Su*[2], *Fuyuan Hong*[1]* *and Lei Wang*[2]*

[1]Department of Nephrology, Fujian Provincial Hospital, Shengli Clinical Medical College of Fujian Medical University, Fuzhou, China, [2]Department of Radiation Oncology, Fujian Cancer Hospital, Fujian Medical University Cancer Hospital, Fuzhou, China

OPEN ACCESS

Edited by:
Biaoru Li,
Augusta University, United States

Reviewed by:
Shukui Wang,
Nanjing Medical University, China
Borbala Mifsud,
Hamad bin Khalifa University, Qatar

***Correspondence:**
Fuyuan Hong
hongdoc@163.com
Lei Wang
wangleiy001@126.com

Specialty section:
This article was submitted to Epigenomics and Epigenetics, a section of the journal Frontiers in Cell and Developmental Biology

Received: 10 December 2021
Accepted: 04 February 2022
Published: 02 March 2022

Citation:
Zhang L, Su Z, Hong F and Wang L (2022) Identification of a Methylation-Regulating Genes Prognostic Signature to Predict the Prognosis and Aid Immunotherapy of Clear Cell Renal Cell Carcinoma. Front. Cell Dev. Biol. 10:832803. doi: 10.3389/fcell.2022.832803

Methylation is one of the most extensive modifications of biological macromolecules and affects cell-fate determination, development, aging, and cancer. Several methylation modifications, including 5-methylcytosine and N6-methyladenosine, play an essential role in many cancers. However, little is known about the relationship between methylation and the prognosis of clear cell renal cell carcinoma (ccRCC). Here, we established a methylation-regulating genes prognostic signature (MRGPS) to predict the prognoses of ccRCC patients. We obtained ccRCC samples from The Cancer Genome Atlas and identified methylation-regulatingd genes (MRGs) from the Gene Set Enrichment Analysis database. We also determined differentially expressed genes (DEGs) and performed cluster analysis to identify candidate genes. Subsequently, we established and validated an MRGPS to predict the overall survival of ccRCC patients. This was also verified in 15 ccRCC samples collected from the Fujian Provincial Hospital via quantitative real-time transcription (qRT-PCR). While 95 MRGs were differentially expressed (DEGs1) between tumor and normal tissues, 17 MRGs were differentially expressed (DEGs2) between cluster 1 and 2. Notably, 13 genes common among DEGs1 and DEGs2 were identified as hub genes. In fact, we established three genes (*NOP2, NSUN6*, and *TET2*) to be an MRGPS based on their multivariate Cox regression analysis coefficients ($p < 0.05$). A receiver operating characteristic curve analysis confirmed this MRGPS to have a good prognostic performance. Moreover, the MRGPS was associated with characteristics of the tumor immune microenvironment and responses to inhibitor checkpoint inhibitors. Data from "IMvigor 210" demonstrated that patients with a low MRGPS would benefit more from atelozumab ($p < 0.05$). Furthermore, a multivariate analysis revealed that MRGPS was an independent risk factor associated with ccRCC prognosis ($p < 0.05$). Notably, a nomogram constructed by combining with clinical characteristics (age, grade, stage, and MRGPS risk score) to predict the overall survival of a ccRCC patient had a favorable predictive value. Eventually, our qRT-PCR results showed that tumor tissues had higher *NOP2* and *NSUN6* expression levels and lower *TET2* expression than normal tissues of ccRCC samples. While the proposed MRGPS comprising *NOP2*, *NSUN6*, and *TET2* can be an

alternative prognostic biomarker for ccRCC patients, it is a promising index for personalized ICI treatments against ccRCC.

Keywords: methylation, clear cell renal cell carcinoma, quantitative real-time transcription, immune checkpoint inhibitor, prognosis, risk signature

INTRODUCTION

Clear cell renal cell carcinoma (ccRCC) is one of the most lethal malignancies of the genitourinary tract, accounting for 70–80% of renal cell carcinoma patients (Zhao et al., 2018). Despite substantial advances in the diagnosis and treatment of ccRCC, long-term prognosis remains far from satisfactory (Siegel et al., 2017). Approximately 20–30% of patients initially present with metastasis (Reiter et al., 2015), indicating that the current screening index for ccRCC is inadequate; thus, it is necessary to immediately identify an aggressive diagnostic marker for ccRCC. In addition, approximately 30–40% of patients with localized ccRCC relapse or exhibit metastasis within 2 years of undergoing radical surgeries (Miao et al., 2018). This implies that the ccRCC patient population is greatly heterogeneous and highlights the inaccuracies in the existing staging system integrated with clinicopathological characteristics.

Interestingly, ccRCC is a highly immunogenic tumor characterized by an abundance of suppressed immune cells (Díaz-Montero et al., 2020). A randomized phase II study has demonstrated that immune checkpoint inhibitor (ICI) monotherapy exhibits non-inferiority efficacy to sunitinib (Mcdermott et al., 2018). However, a CheckMate-214 trial (Cella et al., 2019; Albiges et al., 2020) has revealed that nivolumab combined with iplimumab has positive outcomes compared with sunitinib. Thus, this combination has been approved by the United States Food and Drug Administration as a frontline therapeutic approach for ccRCC patients with intermediate severity. Nonetheless, the objective response rates (ORRs) of avelumab, pembrolizumab, and nivolumab are 16, 36, and 17%, respectively (Tzeng et al., 2021), whereas that of avelumab combined with nivolumab is 42% (Cella et al., 2019). Additionally, continuing treatment with nivolumab has been found to be associated with reduced tumor burden in approximately 50% of patients (Hellmann et al., 2018). Hence, an aggressive biomarker, except PD-1/PD-L1, tumor mutation burden (TMB), and microsatellite status, is urgently warranted in ICI management for ccRCC.

Methylation is one of the most abundant modifications that is widespread across all biological processes. It involves an alkylation reaction, wherein a methyl group replaces a hydrogen atom (Michalak et al., 2019). Methyltransferases, also called "writers," use the methyl donor S-adenosylmethionine to catalyze methylation; "writers" cooperate with dedicated "erasers" (demethylases) and methyl "readers" (Dawson and Kouzarides, 2012). Genomic studies have demonstrated that hypo- and/or hyper-methylation occur in various enzymes and can result in loss of histone modification (Michalak et al., 2019). Few examples include mutations in metabolic enzymes that regulate histone and DNA demethylation and somatic mutations in core histone genes (You and Jones, 2012). In fact, previous studies have demonstrated that aberrant changes in DNA or RNA methylation can be prospectively utilized in the diagnosis, prognosis, and individualized treatment of various cancers, including ccRCC (Fang et al., 2020; Zhang et al., 2020; Li et al., 2021). Therefore, we systematically analyzed the transcriptomic data of ccRCC patient tissues to identify methylation-regulating genes (MRGs) and accurately predict the prognoses and guide the ICI management of ccRCC patients.

MATERIALS AND METHODS

Patients and Datasets

We retrieved 359 human MRGs from the Gene Set Enrichment Analysis (GSEA) database (https://www.gsea-msigdb.org/gsea/index.Jsp; **Supplementary Table S1**) (Subramanian et al., 2005). Moreover, we obtained RNA sequencing (RNA-Seq) expression profile dataset of 537 ccRCC patients and 72 corresponsonding normal samples from The Cancer Genome Atlas (TCGA; https://portal.gdc.cancer.gov/) (Tomczak et al., 2015). The clinicopathological characteristics and survival data of these patients was also retrieved from TCGA. The RNA-seq profiles and clinical data of"IMvigor 210" cohort were obtained from http://research-pub.gene.com/IMvigor210CoreBiologies/.

Furthermore, 15 frozen, surgically resected tumor specimens were acquired from patients pathologically diagnosed with ccRCC at the Fujian Provincial Hospital (FPH) between December 2018 and December 2020. Additionally, we validated the immunohistochemical staining of prognostic genes using The Human Protein Atlas (HPA) database (http://www.proteinatlas.org/) (Uhlén et al., 2015). This study was approved by the ethics committee of the FPH.

Identification of Methylation-Regulating Hub Genes

Based on the RNA-seq data of the ccRCC samples (537 tumors vs 72 normal samples) obtained from TCGA, we analyzed the differentially expressed genes (DEGs1) between tumor and normal tissues. We also functionally explored the biological properties of MRGs in the TCGA ccRCC patients by clustering ccRCC patients into different clusters using the "ConsensusClusterPluspackage" (Wilkerson and Hayes, 2010) (http://www.bioconductor.org/; 1,000 iterations and resampling rate of 80%). The cumulative distribution function (CDF) and delta area were considered to determine the optimal number of groups (k). Subsequently, we identified DEGs between the different clusters (DEGs2) and defined the hub genes as genes common to both DEGs1 and DEGs2.

Construction and Validation of Methylation-Regulating Genes Prognostic Signature

We divided TCGA patients into training and validation cohorts at a ratio of 3:7 (11 samples were deleted because their OS was 0 or unknown), and prognostically significant hub genes ($p < 0.05$) were screened by univariate Cox regression analysis. In fact, these candidate genes were used to establish a methylation-regulating genes prognostic signature (MRGPS) via multivariate Cox regression analysis. The risk score for each patient was determined using the following formula:

$$\text{Risk score} = \sum_{i=1}^{n} \text{Coef}(i) \times x(i)$$

Thereafter, the patients were classified into low-risk and high-risk groups based on the median risk score. We determined the prognostic ability of the MRGPS in the training cohort by generating Kaplan–Meier survival curves and receiving operating characteristic (ROC) curves using the R packages "survminer" and "survivalROC". The prognostic performance of this MRGPS was further tested in the testing cohort in the same manner as mentioned above.

Functional Analysis

We conducted Gene Ontology (GO) and Kyoto Encyclopedia of Genes and Genomes (KEGG) analysis to analyze the main function using the "clusterProfiler" (Yu et al., 2012) R package and visualized it using the "Treemap" (Liu et al., 2021) and "ggplot2" packages. Additionally, GSEA was performed to understand the biological processes prevalent in the different subgroups using the "clusterProfiler" R package. Predefined gene sets were identified in the GSEA using the GO Biological Process; 5,000 permutations were performed to determine the p values of these gene sets. Significant pathways were defined as having a p value of <0.05 and a false discovery rate (FDR) of <0.05 (Powers et al., 2018).

Immune Score and Immunotherapy Benefits Analyses

We conducted a single sample GSEA (ssGSEA) analysis, where (Bustin and Mueller, 2005)in we analyzed 20 immune cells of 537 ccRCC samples based on the expression profile of a single sample; we used the "gsva" R package to perform this analysis (Hänzelmann et al., 2013). The ESTIMATE algorithm (i.e., the "estimate" R package) was used to calculate the immune score of each patient. Subsequently, we assessed the immune score difference between the two cluster subgroups. A semi-quantitative analysis of 22 immune cell types in the two MRGPS groups was performed using CIBERSORT via the "cibersort" R package (Chen et al., 2018). Moreover, we calculated tumor immune dysfunction and exclusion (TIDE) and microsatellite instability (MSI) scores from the website of http://tide.dfci.harvar.edu to assess the potential efficacy of ICIs in the two MRGPS subgroups (Fu et al., 2020). We also compared the somatic mutations between the two MRGPS subgroups by obtaining the TMB, i.e., the total number of somatic mutations.

Predicting the Benefits of MRGPS for Tyrosine Kinase Inhibitors

Since VEGFR-targeted therapy remains the first line of treatment for ccRCC, we explored the sensitivity of TKIs, such as sunitinib, sorafenib, pazopanib, and axitinib, stratified by MRGPS. The sensitivity of each TKI was evaluated by IC_{50} calculation using the "pRRophetic" package (Geeleher et al., 2014), and the corresponding data were obtained from the Genomics of Drug Sensitivity in Cancer database (Yang et al., 2013).

Development of Risk Prediction Model

Furthermore, we conducted a multivariate Cox analysis to evaluate whether the signature-based risk score was independent of other clinical characteristics. The testing cohort was used to further test the performance of the signature in the same manner mentioned above. Thereafter, we generated a nomogram consisting of the current MRGPS and clinical characteristics with $p < 0.1$. This helped predict the 1-, 3- and 5-years overall survival (OS) of the TCGA ccRCC patients using the "rms" package. Additionally, we evaluated this nomogram using the calibration curve, ROC curve, and decision-making curve (DCA).

Quantitative Reverse Transcription PCR

Relative quantitation of the 15 paired mRNAs was determined by quantitative reverse transcription polymerase chain reaction (qRT-PCR; SuperScript IV Reverse Transcriptase 18090010; Thermo Fisher, United States). The amplification reactions were performed as described previously (Bustin and Mueller, 2005). NSUN6-specific primers were: forward primer, 5′-ATC TGCGTCCGTTTCACC-3′ and reverse primer, 5′-GCTTCC ACCACACCTCATC-3'. NOP2-specific primers were: forward primer, 5′-GGGCACAGACACACAAACA-3′ and reverse primer, 5′-GAACGGATGGGAGACACAG-3'. TET2-specific primers were: forward primer, 5′-CACAACCATCCCAGAGTT CA-3′ and reverse primer, 5′-ACTTCCTCCAGTCCCATTTG-3'. Human β-actin-specific primers were: forward primer, 5′-GAAGAGCTACGAGCTGCCTGA-3′ and reverse primer 5′-CAGACAGCACTGTGTTGGCG-3'. Data analysis was performed using the ΔΔCT method.

Statistical Analyses

Distributed data were compared by performing the Student's t-test and Wilcoxon test, whereas proportion differences were calculated by the chi-square test. Additionally, component analysis in subgroups were compared by the Fisher's test. While survival differences between different groups were assessed via the log-rank test, prognostic factors were identified by the Cox regression analyses. All statistical analyses were performed using RStudio version 4.0.3, and two-sided $p < 0.05$ was considered as statistically significant.

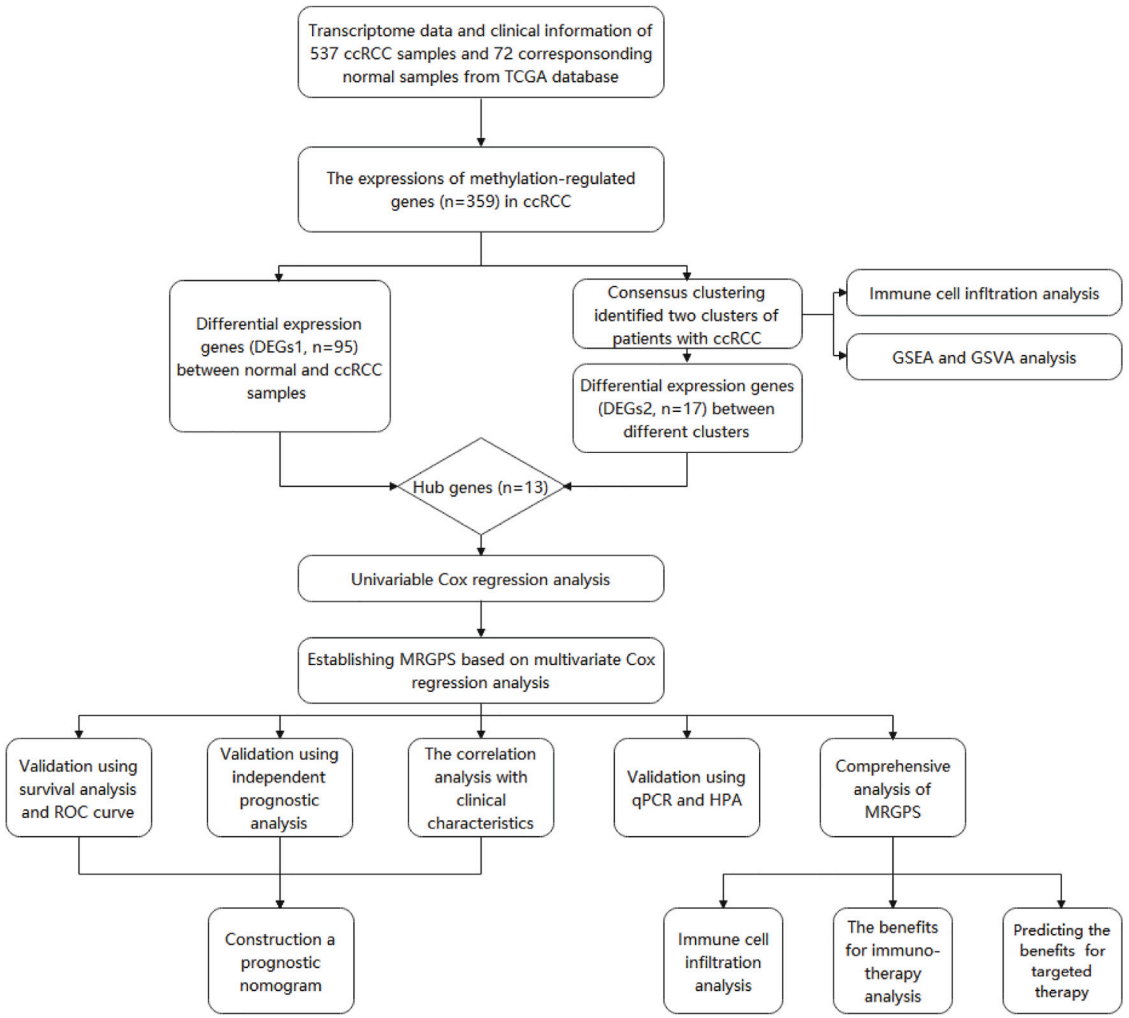

FIGURE 1 | The entire analytical process of the study.

RESULTS

Identification of Methylation-Regulating Hub Genes

The entire analytical process of this study is presented in **Figure 1**, and the clinical characteristics of the ccRCC patients in the TCGA and FPH cohorts are listed in **Table 1**. Additionally, **Figure 2A** presents all 95 DEGs among tumor and normal tissues (DEGs1: FDR<0.05 and |log2FC|>0.5), including 51 upregulated and 44 downregulated genes; the top 50 DEGs are presented in a heatmap (**Figure 2B**). The GO analysis of DEGs1 revealed that methylation-relate biological process (BP), cellular component (CC), and molecular function (MF) were enriched in tumor tissues (**Figure 2C**).

Subsequently, we performed consensus clustering to explore the molecular characteristics between different MRG expression samples. We observed a relative change in the CDF of the consensus cluster from k = 2 to k = 9 (**Figure 2D**); the delta area under the CDF curve from k = 2 to 9 is depicted in **Supplementary Figure S1H**. The corresponding heatmap presents the results of this consensus from k = 2 to 9 (k = 2, **Figure 2E**; k = 3–9, **Supplementary Figure S1A–G**). The criteria for deciding the cluster number was determined by a relatively high consistency and a low variation coefficient and an appreciable increase in the area under the CDF curve. Thus, after comprehensive consideration, we chose k = 2 as the optimal cut-off for the clusters number.

A significant difference in the OS was observed between patients of clusters 1 and 2 ($p < 0.001$, **Figure 2F**). To determine which genes contributed to this difference in prognosis, we first identified 17 genes as DEGs between cluster 1 and cluster 2 (DEGs2: FDR<0.05, |log2FC| >0.5; **Figure 2G**); these genes are also represented in a heatmap (**Figure 2H**). Eventually, 13 overlapping genes between DEGs1 and DEGs2 were identified as the hub genes (**Figure 2I**, **Supplementary Table S2**).

We further evaluated the molecular characteristics of the different clusters by conducting immune-related analyses between clusters 1 and 2. The ssGSEA demonstrated that

TABLE 1 | Clinical characteristics of the ccRCC patients in TCGA cohort and FPH cohort.

Characteristic	TCGA cohort	FPH cohort
n (%)	537 (100%)	15 (100%)
Age, n (%)	—	—
≤65	352 (65.55%)	11 (73.33%)
>65	185 (34.45%)	4 (26.67%)
Gender, n (%)	—	—
Female	191 (35.57%)	6 (40.00%)
Male	346 (64.43%)	9 (60.00%)
Histologic grade, n (%)	—	—
G1	14 (2.61%)	NA
G2	230 (42.83%)	NA
G3	207 (38.55%)	NA
G4	78 (14.53%)	NA
NA	8 (1.48%)	NA
Pathologic stage, n (%)	—	—
Stage I	269 (50.09%)	12 (80.00%)
Stage II	57 (10.61%)	2 (13.33%)
Stage III	125 (23.28%)	1 (4.67%)
Stage IV	83 (15.46%)	0 (0%)
NA	3 (0.56%)	0 (0%)
T stage, n (%)	—	—
T1	275 (51.21%)	12 (80.00%)
T2	69 (12.85%)	2 (13.33%)
T3	182 (33.89%)	1 (4.67%)
T4	11 (2.05%)	0 (0%)
N stage, n (%)	—	—
N0	240 (44.69%)	15 (100%)
N1	17 (3.17%)	0 (0%)
NA	280 (52.14%)	0 (0%)
M stage, n (%)	—	—
M0	426 (79.33%)	15 (100%)
M1	79 (14.71%)	0 (0%)
NA	32 (5.96%)	0 (0%)

cluster 2 had a high abundance of approximately all immune cell types compared to cluster 1 ($p < 0.05$, **Figure 3A**). Moreover, the tumor microenvironment estimate scores, including the stromal, immune, and total scores, were higher in cluster 2 than those in cluster 1 ($p < 0.05$, **Figure 3B**). Notably, immune-related signaling pathways were enriched in cluster 2, as determined by the GSEA (**Figure 3C** and **Supplementary Table S3**). Furthermore, we obtained the enrichment score of each negative immune-related signaling pathway in each ccRCC sample by performing a gene set variation analysis (GSVA). Consequently, we observed significant survival differences between high- and low-GSVA scores regarding the negative regulation of adaptive immune response, negative regulation of immune response, and negative regulation of leukocyte-mediated immunity ($p < 0.05$, **Figures 3D–F**); however, this did not hold true for the negative regulation of natural killer cell-mediated immunity ($p > 0.05$, **Figure 3G**).

Construction and Validation of the Methylation-Regulating Genes Prognostic Signature

In the training cohort, we screened prognosis-associated seven hub genes by univariate Cox regression analysis (**Figure 4A**). Then, a multivariate Cox regression analysis was conducted to screen the optimal model and was depicted in **Figure 4B**; based on their regression coefficients, three MRGS (*NOP2, NSUN6,* and *TET2*) were identified to form an MRGPS. The MRGPS score of each patient was calculated according to the following formula: *Risk score* = [*NOP2 expression**(*0.656940513*)] + [*NSUN6 expression**(0.911107243)] + [TET2 expression*(-1.180533124)]. Considering the median score as the cut-off value, patients in the training cohort were divided into low- and high-risk groups; these patients had apparent survival differences ($p < 0.001$, **Figure 4C**). The corresponding risk scores and survival statuses are presented in **Figure 4D**. The ROC curves demonstrated the excellent predictive capability of the current MRGPS with 1-, 3-, and 5-years AUCs being 0.798, 0.750, and 0.768, respectively (**Figure 4E**). Likewise, the advantages of the current MRGPS were observed in the validation (**Figures 4F–H**) and the whole cohorts (**Figures 4I,J**).

In addition, relationships between clinicopathological characteristics and risk scores were further explored. As shown in **Supplementary Figure S2A**, differences were observed regarding the age (age ≤65 years, age >65 years), differentiation (G1, G2, G3, G4), T stage (T1, T2, T3, T4), M stage (M0, M1), and cancer stage (I, II, III, IV). Furthermore, Kaplan–Meier survival curves showed that the high-risk patients had worse prognoses than the low-risk patients in the following attributes: age ≤65 years, age >65 years, male sex, female sex, G1-2, G3-4, T1-2, T3-4, M0, M1, stage I–II, and stage III–IV ($p < 0.05$, **Supplementary Figure S2B–M**).

Immune Analyses and Immunotherapy

We further explored the immune microenvironment characteristics of patients belonging to the different risk subgroups by conducting immune cell infiltration and immune function analysis on the TCGA cohort patients. We observed significantly decreased number of naive B cells, memory B cells, plasma cells, CD4+T cells, CD4+T memory cells, gamma T cells, resting NK cells, M0/M1/M2 and resting dendritic cells, activated dendritic cells, and resting mast cells and also observed increased number of CD8+T cells and regulatory T cells in the high-risk group ($p < 0.05$, **Figure 5A**). Relative expression levels of MHC molecules and co-stimulatory molecules and adhesion factors, such as CD40, CD58, HLA-A, HLA-B, HLA-C, HLA-DMA, HLA-DOB, HLA-DPB1, and HLA-F, were all higher in the high-risk group than those in the low-risk group ($p < 0.05$, **Figure 5B**). Importantly, the expression levels of immune checkpoint proteins, such as PDCD1, CTLA4, TBX2, TNF, LAG3, CD8A, IFNG, and GZMB were all significantly higher in the high-risk group than those in the low-risk group ($p < 0.05$, **Figure 5C**).

Furthermore, patients in the high-risk group were found to have a higher TIDE score, lower MSI score, and higher TMB than those in the low-risk group ($p < 0.05$, **Figures 5D–F**). This suggested that low-risk patients may benefit more from immunotherapy compared to high-risk ones according to the current MRGPS. We further validated this observation using the "IMvigor 210" dataset containing clinical information and RNA-seq data of metastatic urothelial cancer patients who were treated with the ICI atezolizumab (PD-L1 inhibitor). Remarkably, data

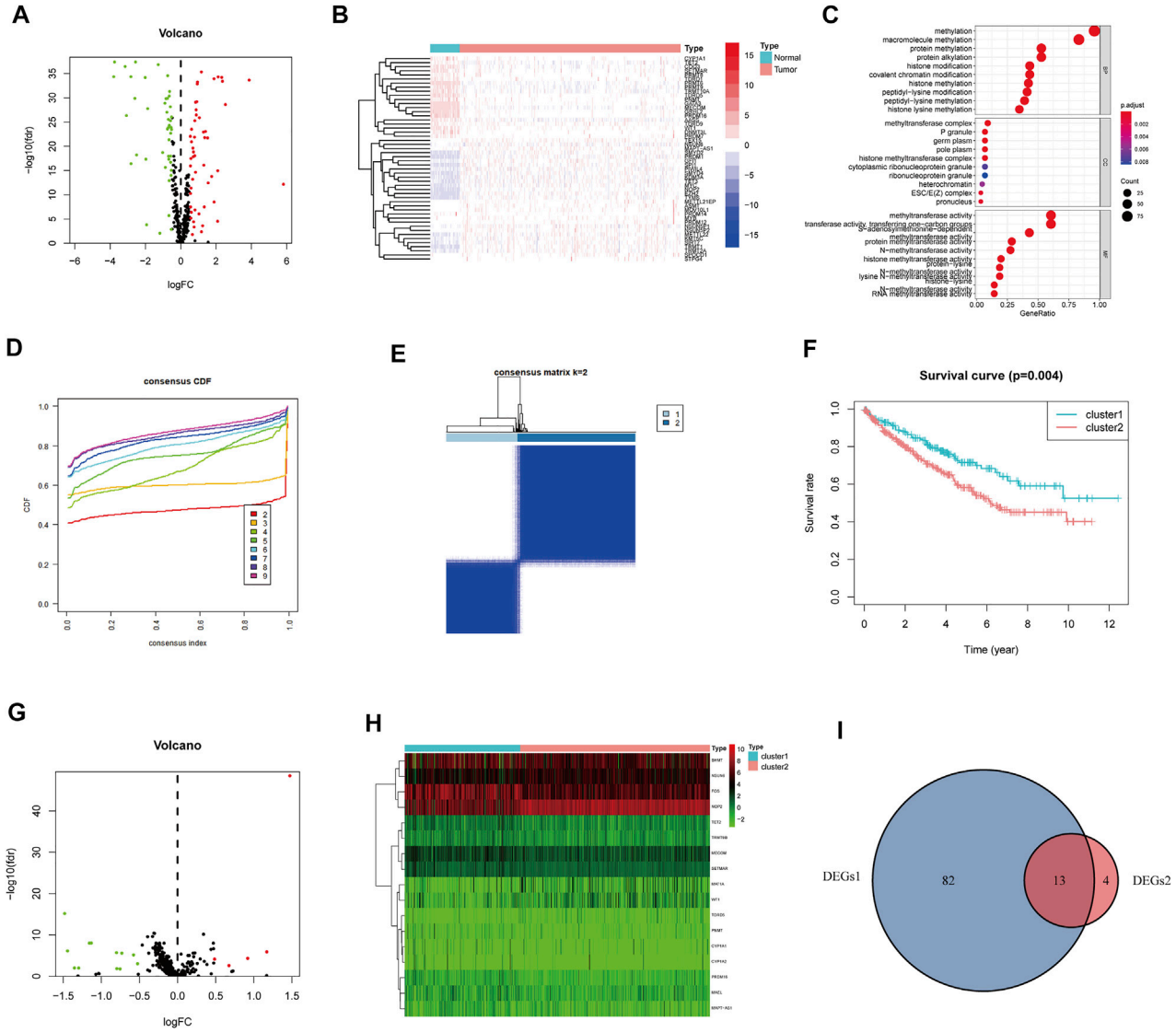

FIGURE 2 | Identification of methylation-regulating Hub Genes. **(A)** Volcano plot demonstrates DEGs1. **(B)** Heatmap demonstrates the top 50 DEGs1. **(C)** The Gene Ontology (GO) analysis of DEGs1 in ccRCC. **(D)** Consensus clustering cumulative distribution function (CDF) for k = 2 to 9. **(E)** The consensus heatmap showed the ccRCC patients was divided into two distinct clusters when k = 2. **(F)** Overall Survival (OS) analysis of different clusters in the TCGA dataset. **(G)** Volcano plot demonstrates the DEGs2. **(H)** Heatmap demonstrates the DEGs2. **(I)** Venn diagram demonstrates the intersect between DEGs1 and DEGs2.

from the 298 IMvigor patients also validated the clinical utility of the current MRGPS in response to atezolizumab ($p < 0.05$, **Figure 5G**).

Potential Biological Pathway Analysis of Methylation-Regulating Genes Prognostic Signature

We further determined the potential biological pathways prevalent in different risk group by performing a KEGG analysis on the DEGs among high- and low-risk groups (FDR<0.05 and |log2FC|>0.5). We observed that the "PI3K–Akt signaling pathway", "mTOR signaling pathway", "Ras signaling pathway" and other carcinogenesis-related pathways were enriched in the high-risk group (**Figure 6A**). Furthermore, the GSEA revealed that the high-risk group had higher enrichment score for the PI3K-AKT and mTOR pathways compared to the low-risk group (**Figures 6B,C**). These results revealed that the MRGPS possibly promotes cancer development by activating these pathways.

VEGF Family Expressions and TKI Sensitivity

As the VEGF family was an important molecular target, we compared their expression levels in high- and low-risk groups.

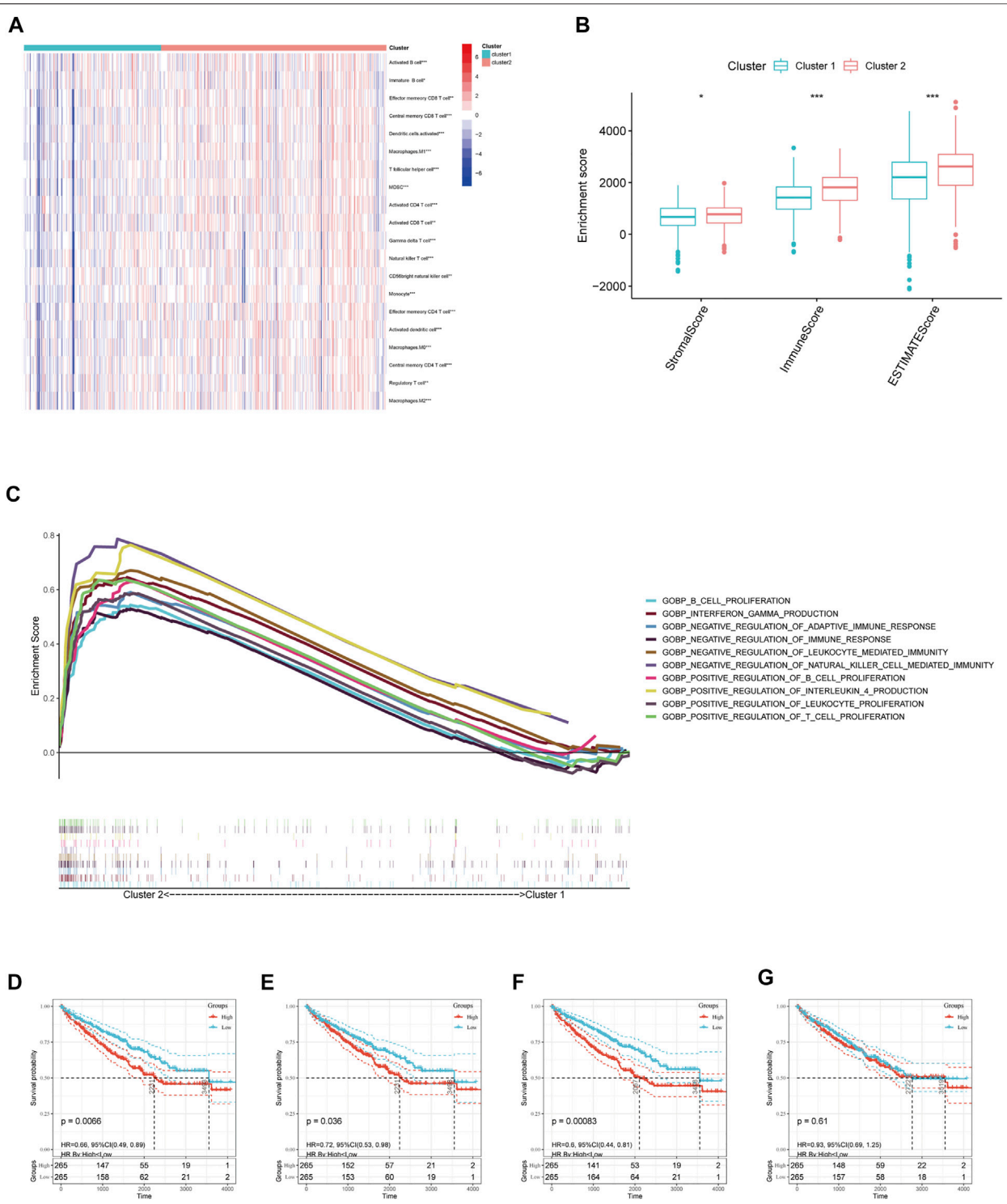

FIGURE 3 | Immune cell infiltration analysis and GSEA analysis between different clusters. **(A)** Estimated abundance of 20 immune cells using ssGSEA. **(B)** Tumor microenvironment (TME) estimate score in different clusters. **(C)** GSEA delineation of the biological pathways which enrich in cluster 2 using the gene set "c5. go.bp.v7.4. symbols". Overall Survival (OS) analysis in different GSVA score of **(D)** negative regulation of adaptive immune response, **(E)** negative regulation of immune response, and **(F)** negative regulation of leukocyte-mediated immunity, **(G)** negative regulation of natural killer cell-mediated immunity in TCGA-ccRCC patients. Significant statistical differences between the two clusters were assessed using the Wilcoxon test (ns, $p > 0.05$; *, $p < 0.05$; **, $p < 0.01$; ***, $p < 0.001$).

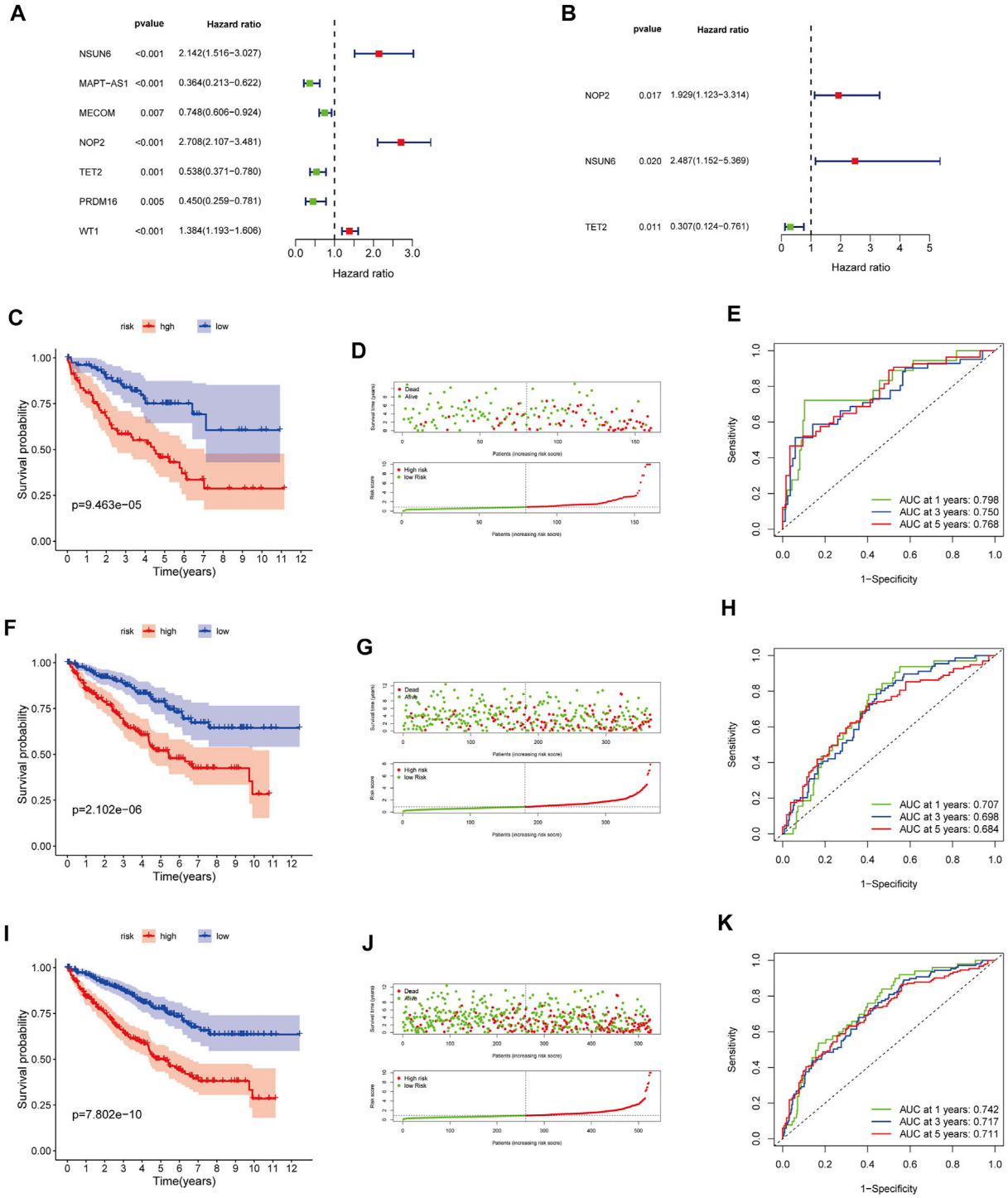

FIGURE 4 | Construction and validation of the MRGPS. **(A)** Forrest plot of the univariate Cox regression analysis in the training cohort. **(B)** Forrest plot of the multivariate Cox regression analysis in the training cohort. Kaplan-Meier analysis, risk score analysis and ROC curve of the MRGPS inthe training cohort **(C–E)**, validation cohort **(F–H)**, and whole TCGA cohort **(I–K)**.

Consequently, no significant differences in VEGFA expression were observed between the two groups ($p > 0.05$, **Figure 7A**). However, VEGFB and VEGFD expression levels were significantly upregulated in the high-risk group ($p < 0.05$, **Figures 7B,D**), whereas that of VEGFC was significantly downregulated in the high-risk group ($p < 0.05$, **Figure 7C**). Further analysis revealed that sunitinib had lower IC_{50} the higher-risk group than that in the low-risk groups ($p < 0.05$, **Figure 7E**).

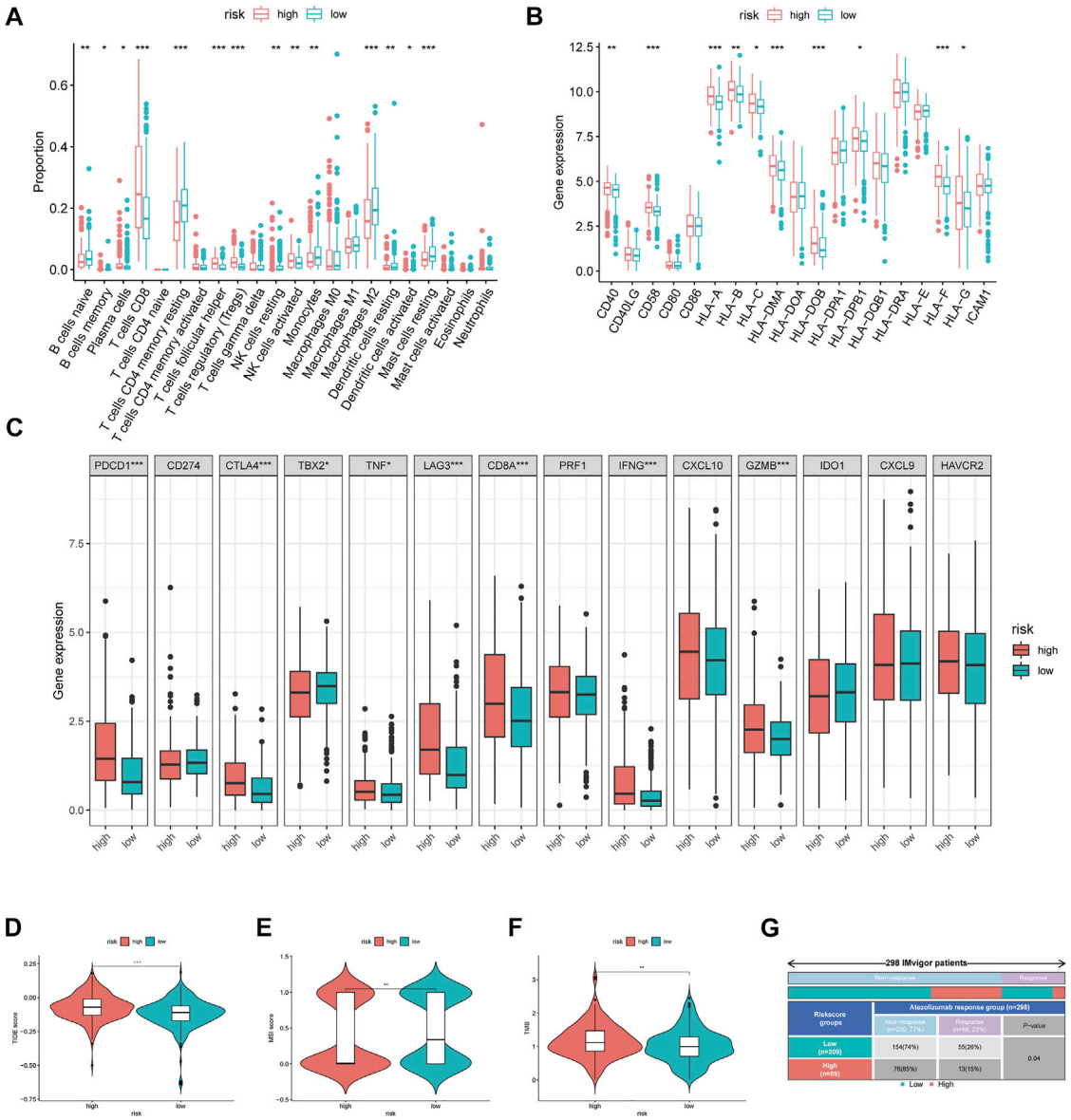

FIGURE 5 | Immune-related analysis between different MRGPS subgroup. **(A)** The proportions of TME cells in different MRGPS subgroups. **(B)** Relative expression of MHC molecules, co-stimulatory molecules, and adhesion factors. **(C)** Association of MRGPS with immune checkpoint molecules. **(D)** TIDE, **(E)** MSI, **(F)** TMB score in different MRGPS subgroups. **(G)** Distribution of immune response to ICIs therapy in different MRGPS subgroups in IMvigor patients. Significant statistical differences between the two subgroups were assessed using the Wilcoxon test (ns, $p > 0.05$; *, $p < 0.05$; **, $p < 0.01$; ***, $p < 0.001$).

In contrast, pazopanib ($p < 0.05$, **Figure 7G**), but not sorafenib and axitinib (both $p > 0.05$, **Figures 7F,H**), had lower IC_{50} in the low-risk group than that in the high-risk group. These results indicated that different risk groups had varying susceptibilities for different targeted drugs.

Methylation-Regulating Genes Prognostic Signature-Based Nomogram Construction

Furthermore, we discovered that the current risk score was an independent risk factor for OS in the training, validation, and whole cohorts ($p < 0.05$, **Table 2**). Subsequently, we developed a nomogram based on age, differentiation grade, stage, and MRGPS risk score to further predict the OS of ccRCC patients belonging to the TCGA cohort ($p < 0.1$, **Figure 8A**). We observed good calibrations regarding the predicted vs observed 1-, 3-, and 5-years OS of the patients (**Figure 8B**). Moreover, the ROC curves exhibited better predictive capability in the current nomogram to predict the 1-, 3-, and 5-years OS than the MRGPS and risk scores published by Wang et al. (2021), Chen et al. (2021), and Zheng et al. (2021) (**Figures 8C–E**). Additionally, DCA analysis revealed the superiority of the current nomogram over MRGPS and the

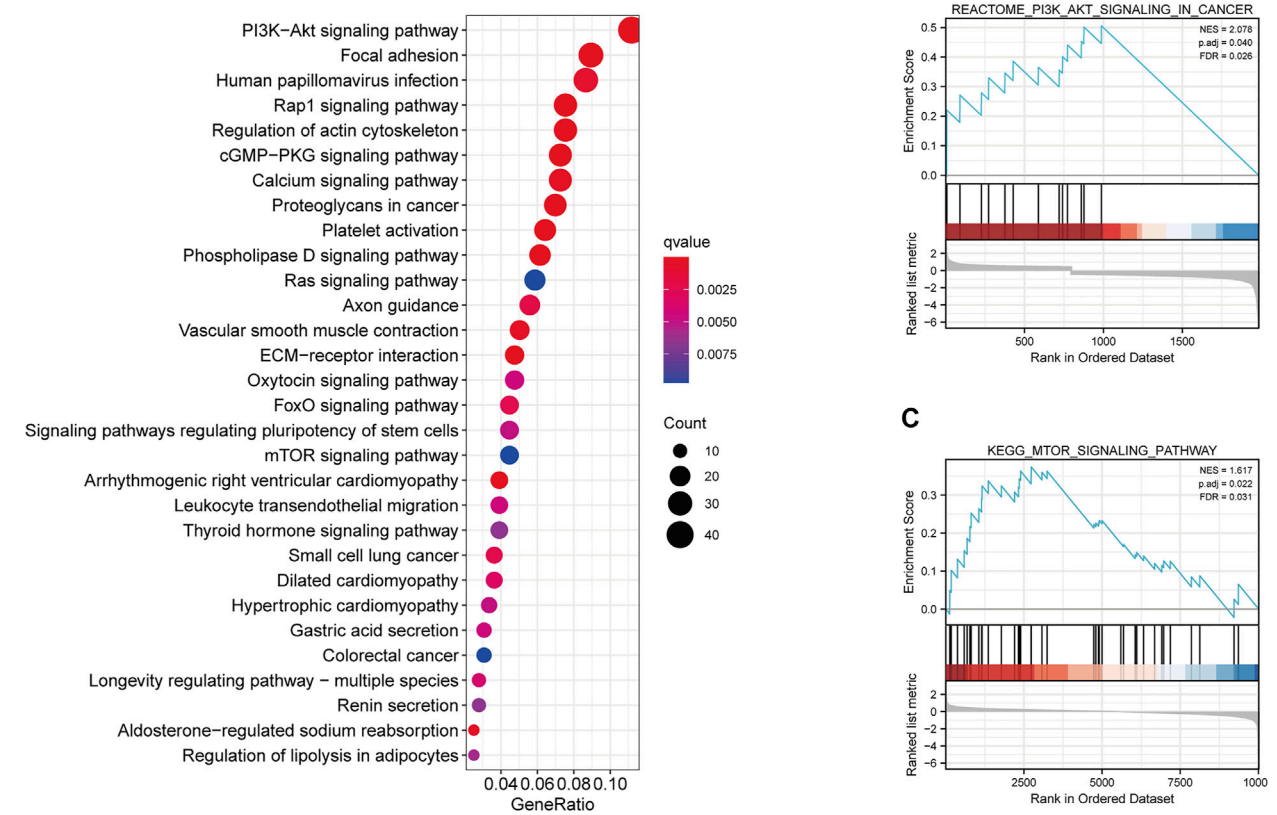

FIGURE 6 | KEGG and GSEA analysis of MRGPS. **(A)** KEGG analysis of the DEGs between high- and low-risk groups. **(B)** PI3K–Akt signaling pathway and **(C)** mTOR signaling pathway were identified in the high-risk group.

published risk scores in predicting the 1-, 3-, and 5-years OS (**Figures 8F–H**).

Validation Using Quantitative Real-Time Transcription-PCR and Human Protein Atlas Datasets

Our qRT-PCR analysis revealed elevated expression levels of NOP2 and NSUN6, but decreased expression of TET2 were in the tumor tissues compared to those in the paired normal tissues of 15 ccRCC samples obtained from FPH ($p < 0.05$, **Figures 9A–C**). The results of HPA database demonstrated that the expression levels of both NOP2 and NSUN6 were higher in the ccRCC tissues than those in the normal tissues; however, the expression of TET2 was significantly lower in the ccRCC tissues than that in the normal tissue (**Figures 9D–F**).

DISCUSSION

Global and local changes in DNA/RNA/histone methylation are seminal features of malignant tumor cells (Michalak et al., 2019). In the current study, we identified three MRGs (*NOP2*, *NSUN6*, and *TET2*) from TCGA data and established an MRGPS for the prognoses of ccRCC patients. This MRGPS exhibited excellent calibration and discrimination. In addition, we validated the three candidate genes in 15 paired ccRCC samples obtained from FPH by qRT-PCR. Furthermore, the current risk score was correlated with tumor immune microenvironment characteristics and could be used as a potential biomarker of ccRCC response to ICIs.

Of note, ccRCC is a highly heterogeneous malignancy (Jonasch et al., 2021). The existing prognosis models that incorporate clinicopathological characteristics, such as the AJCC staging system and the Mayo Clinic stage and necrosis score, have improved prognosis capacity (Parker et al., 2017). However, owing to the complex molecular mechanism of ccRCC, clinical parameters alone are inadequate for predicting the prognoses of ccRCC patients. Interestingly, chromatin methylations, such as m5C and m6A, play a fundamental role in the ccRCC carcinogenesis (Angulo et al., 2021). Nonetheless, comprehensive exploration of chromatin methylation in ccRCC is still lacking. In this study, we established a novel MRGPS using data from TCGA ccRCC patients; this MRGPs improved the prognoses of ccRCC patients with a C-index as high as 0.798 at 1-year OS. In addition, close links were identified between the clinical and pathological characteristics of ccRCC and MRGPS: age, sex, differentiation, and tumor node metastasis (TNM) stage. Furthermore, a MRGPS-incorporating nomogram demonstrated

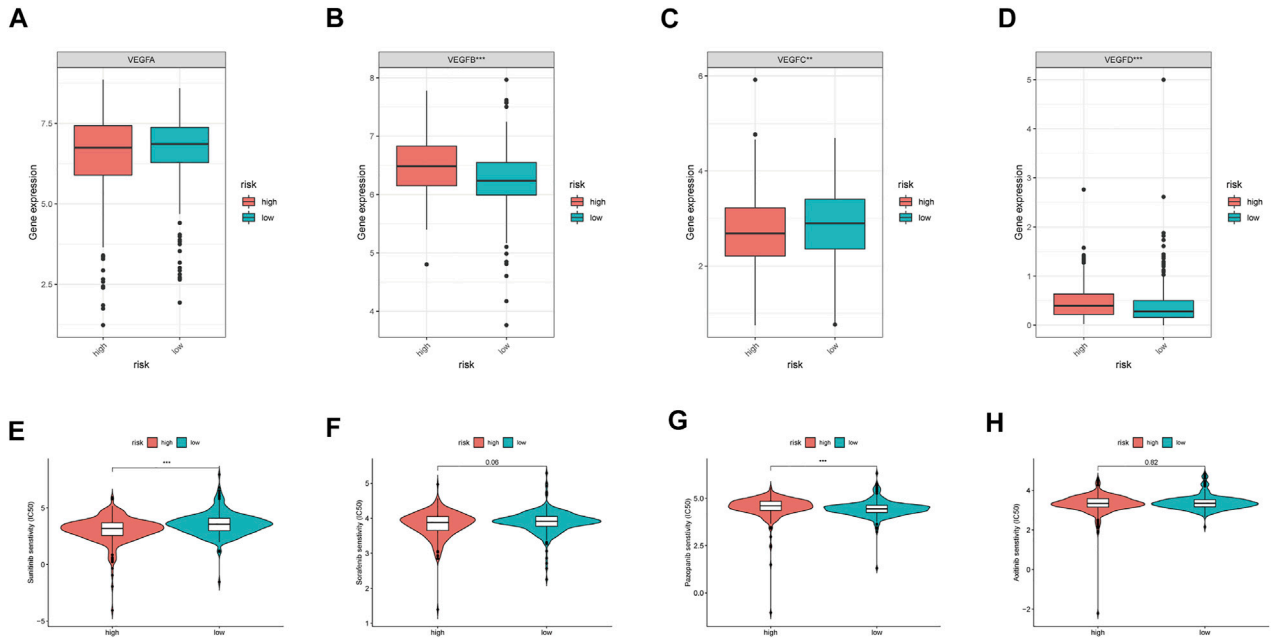

FIGURE 7 | VEGF family expressions and the sensibility of TKI inhibitors in different MRGPS subgroups. **(A–D)** VEGF family expressions in different MRGPS subgroups. Drug susceptibility analysis between different MRGPS subgroups about **(E)** Sunitinib, **(F)** Sorafenib, **(G)** Pazopanib, **(H)** Axitinib. Wilcoxon test (ns, $p > 0.05$; *, $p < 0.05$; **, $p < 0.01$; ***, $p < 0.001$).

TABLE 2 | Multivariate Cox regression analysis in training, validation, and the whole cohorts.

Characteristics	Multivariate analysis		
Hazard ratio (95% CI)	Training cohort	Validation cohort	The whole cohorts
Age	1.045 (1.019–1.072)[a]	1.027 (1.009–1.046)[a]	1.032 (1.017–1.047)[a]
Gender	0.955 (0.554–1.649)	0.879 (0.577–1.340)	0.958 (0.691–1.329)
Grade	1.168 (0.761–1.791)	1.474 (1.098–1.978)[a]	1.398 (1.108–1.765)[a]
Stage	2.123 (0.955–4.722)	1.504 (0.834–2.710)	1.559 (0.985–2.466)
T	0.687 (0.339–1.390)	0.914 (0.530–1.577)	0.894 (0.589–1.357)
M	1.561 (0.499–4.886)	1.426 (0.593–3.428)	1.523 (0.774–2.996)
Risk score	1.218 (1.115–1.332)[a]	1.230 (1.076–1.406)[a]	1.222 (1.141–1.308)[a]

[a]*Statistically significant* (p < *0.05).*

a higher prognostic capacity and clinical utility than published risk scores.

Among the three MRGs identified, *NOP2* and *NSUN6* were prognostic risk factors, whereas *TET2* was a prognostic protective factor. Notably, *NOP2* and *NSUN6* are key members of the NOP2/Sun domain family and possess S-adenosyl-L-methionine-dependent methyltransferase activity (Frye and Blanco, 2016). *NOP2* is upregulated in various cancers, including lung adenocarcinoma, breast cancer, and prostate cancer, and it is associated with tumor aggressiveness (Ma et al., 2017). Deficiency of *NSUN6*-mediated methylation can downregulate transcription and translation. While *NSUN6* expression is highest in the testis and lowest in the blood, it is heterogeneous in different tumors. However, it is downregulated in tumors originating from tissues that have high *NSUN6* expression, such as the testis, thyroid, and ovaries (Selmi et al., 2021). In contrast, it is upregulated in tumors originating from tissues that have low *NSUN6* expression, such as that in hematologic tumor and kidney cancer. Moreover, *NSUN6* is associated with prognosis of various cancers, including pancreatic cancer (Yang et al., 2021) and hepatocellular carcinoma (Wang et al., 2018). It also plays an important role in bone metastasis (Li et al., 2017). On the other hand, *TET2* mutations have been widely identified various myeloid malignancies. In fact, *TET2* inactivation leads to polyhematopoietic abnormalities in mice, which is a recurrent event in human lymphoma formation (Ferrone et al., 2020). Notably, *TET2* dysfunction mutations are generally associated with DNA hypermethylation, tumor progression, and poor patient outcomes (Cimmino et al., 2017). However, *NOP2,*

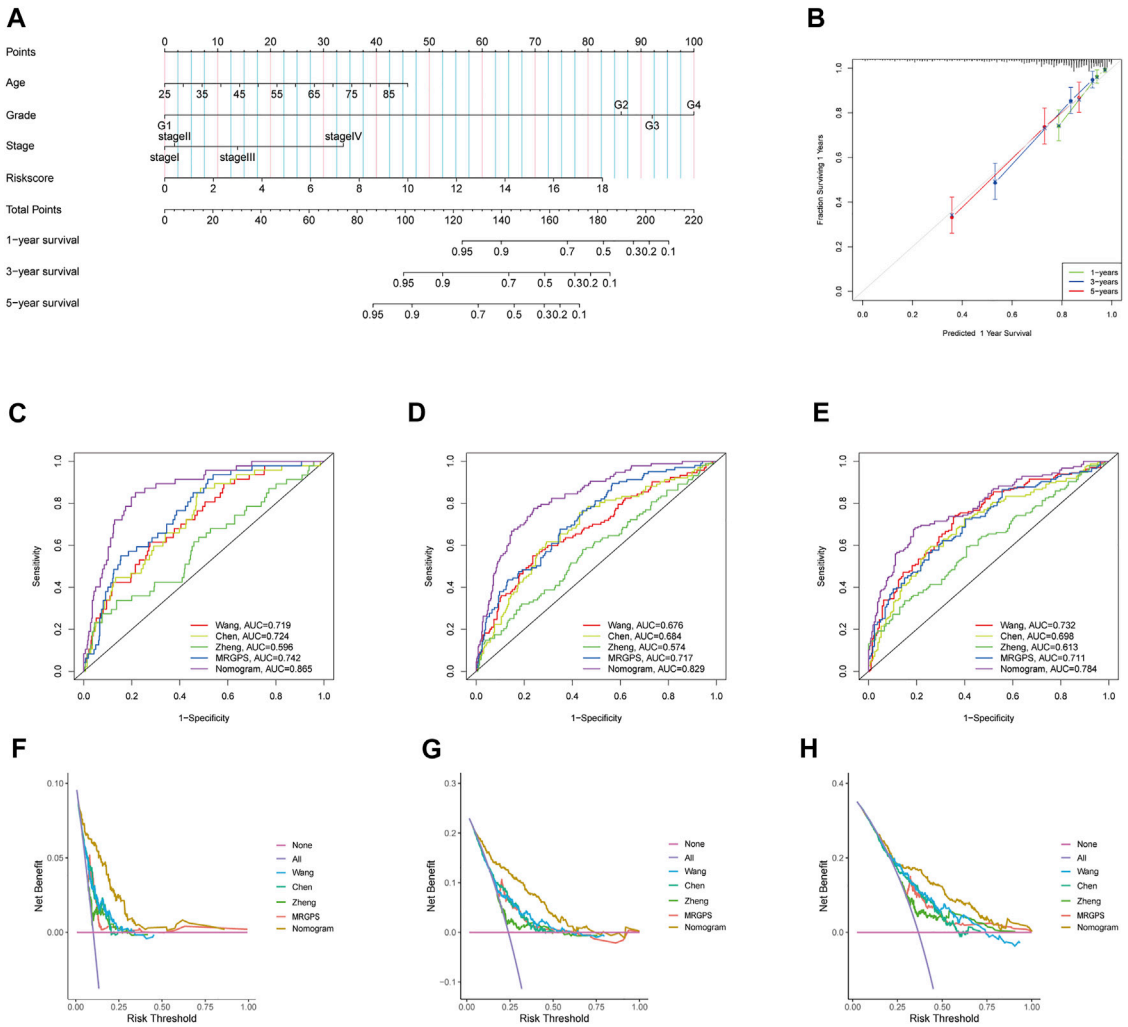

FIGURE 8 | Construction and verification of nomogram. **(A)** The prognostic nomogram constructed based on the risk score of MRGPS and clinicopathological parameters predicted the survival rate of TCGA-ccRCC patients at 1-, 3-, and 5-years. **(B)** Calibration curves showed the concordance between predicted and observed 1-, 3-, and 5-years survival rates. AUCs of the nomogram, MRGPS and other signatures in ROC analysis were calculated at **(C)** 1-, **(D)** 3-, and **(E)** 5-years OS time in TCGA-ccRCC cohort. Decision curve analyses (DCA) for nomogram, MRGPS and other signatures at **(F)** 1-, **(G)** 3-, and **(H)** 5-years to assess clinical utility in TCGA-ccRCC cohort.

NSUN6, and *TET2* have been rarely studied in ccRCC. In the present study, qRT-PCR data from 15 paired FPH ccRCC samples revealed that while *NOP2* and *NSUN6* were upregulated, *TET2* was downregulated in tumor tissues compared with those in normal tissues. In summary, *NOP2*, *NSUN6*, and *TET2* were identified as prognostic biomarkers for ccRCC; however, additional *in vitro* and *in vivo* research is needed to validate these findings.

The potential mechanisms of MRGPS regulating ccRCC prognosis deserved further study. In the present study, we found via KEGG analysis and GSEA that the PI3K-AKT and mTOR signaling pathways were highly enriched in the high-risk subgroup. The PI3K signaling pathway facilitates several essential cellular functions, such as cell proliferation, growth, migration, metabolism, and survival (Fruman and Rommel, 2014). In a large cohort of 419 primary ccRCC patients, aberrantly expressed components of the PI3K signaling cascade (e.g., PTEN, PI3K, p-AKT, mTOR, p-mTOR, p-S6, and p-4EBP1 proteins) exhibited aggressive pathological features and caused adverse survival (Darwish et al., 2013). Therefore, we hypothesized that poor prognoses of patients with a high MRGPS might be because of activation of the PI3K-AKT and mTOR pathways; nonetheless, this hypothesis requires further exploration.

Since ccRCC is a highly vascular tumor, the levels of angiogenic factors, including VEGF, are correlated with its prognosis (Choueiri and Kaelin, 2020). Inhibition of VEGFR generally causes vascular normalization, thereby activating anti-tumor immunity (Hsieh et al., 2017). Until 2017, the multikinase inhibitors sunitinib and pazopanib that primarily target VEGFR formed the frontline treatment for ccRCC (Powles et al., 2021). The median progress free survival (PFS), OS and ORR for sunitinib and pazopanib are 8.4 and 9.5 months, 28.4 months

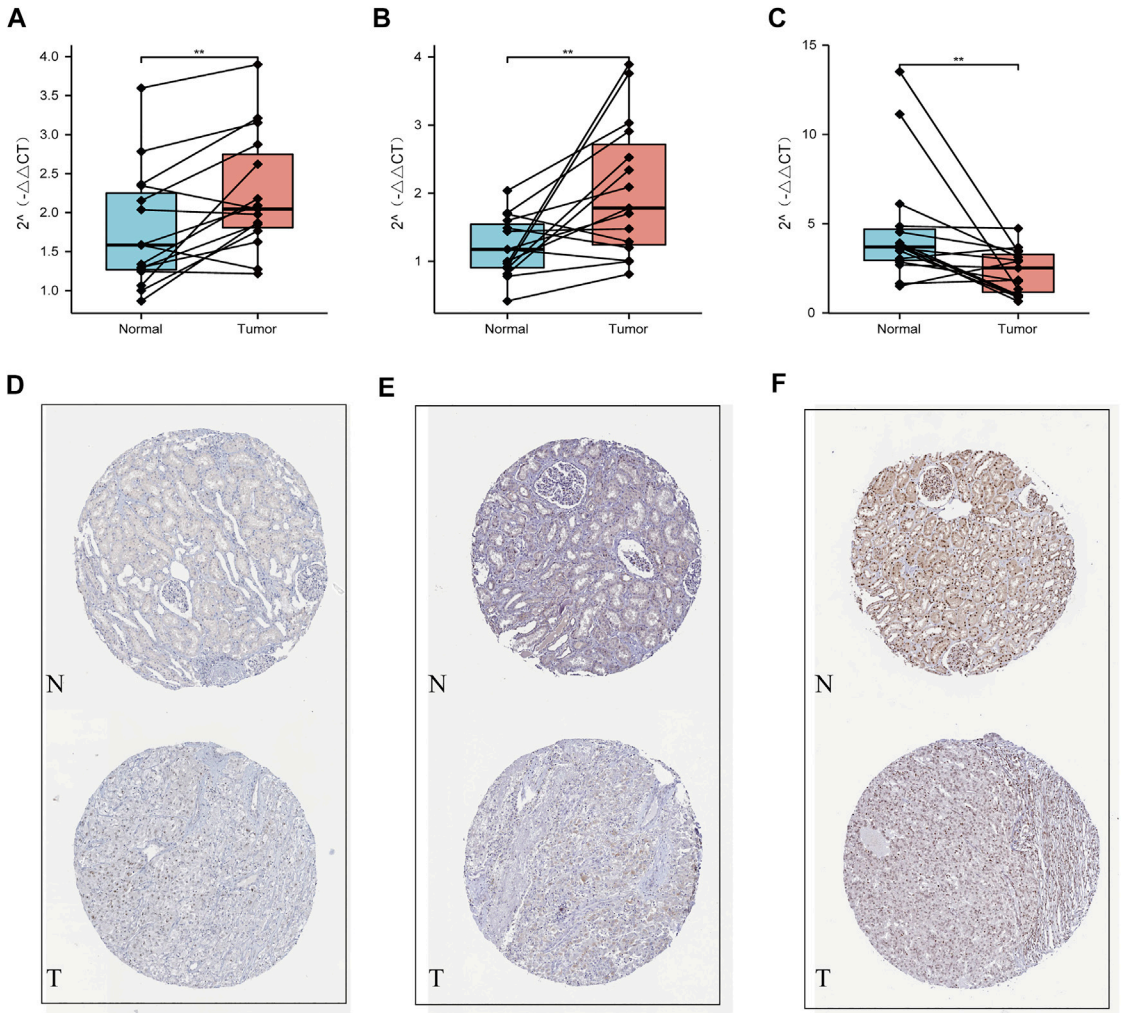

FIGURE 9 | Validation using qPCR and HPA datasets. **(A)** NOP2, **(B)** NSUN6, and **(C)** TET2 mRNA expression measured by qRT-PCR. Validation of the differences in expression of **(D)** NOP2, **(E)** NSUN6, and **(F)** TET2 between renal cancer and normal renal tissue at the translational level with data from the HPA database.

and 29.3 months, and 25 and 31%, respectively (George et al., 2021). The complexity of the VEGFR family may possibly be responsible for the inconsistent results. In this study, we found that the current MRGPS could be used as an alternative to VEGFRs. Remarkably, it had a positively correlation with VEGFB/D and negative correlation with VEGFC; however, it did not have a correlation with VEGFA. Furthermore, we also found that while sunitinib had a lower IC_{50}, pazopanib had a higher IC_{50} in high-risk patients than those in low-risk patients, according to the current MRGPS. This highlighted the response divergence between sunitinib and pazopanib and clarified personalized TKI treatment for ccRCC patients.

Although ccRCC patients have a typically suppressed immune status, they are highly abundant in immune cells (Şenbabaoğlu et al., 2016). In this study, we revealed that the current MRGPS was correlated with tumor-infiltrating lymphocytes: high MRGPS was associated with increased number of CD8+T cell number, activated NK cell, follicular helper cells T cells, and regulatory T cells. In contrast, low MRGPS was associated with decreased number of naïve B cells, resting memory $CD4^+$ T cells, monocytes, macrophages M2, and resting mast cells, as previously reported (Díaz-Montero et al., 2020). In addition, the current MRGPS was also associated with co-stimulatory molecules, such as CD40 and CD58. Immune checkpoints are cell surface receptors expressed on immune cells, and their inhibition causes immune activation. In the present study, we found that high MRGPS was associated with PDCD1 and CTLA4 expression levels (both $p < 0.001$). Further analysis revealed that low MRGPS was correlated with lower TIDE score and higher MSI score than high MRGPS (both $p < 0.05$), indicating that patients with low MRGPS would benefit more from ICIs. Importantly, this finding was validated in 298 IMvigor patients receiving atezolizumab. Therefore, MRGPS is a promising biomarker for predicting the response of ccRCC patients towards ICIs.

Nonetheless, our study has several limitations. First, both the data from TCGA and FPH are retrospective; therefore, the risk score needs to be verified in prospective cohorts. Second, merely incorporating MRGPS to build a prognostic model is inadequate, regardless of its importance. Third, samples from FPH were too few, and the results need to be validated in more samples. Finally, the associations of the current MRGPS with tumor mutations, tumor immune microenvironment, and TKI and ICI responses require further validation *in vitro* and *in vivo*.

In conclusion, the current MRGPS consisting of *NOP2, NSUN6,* and *TET2* is a potential alternative prognostic biomarker for ccRCC patients and is also be a promising index for personalized ICI treatments in ccRCC.

DATA AVAILABILITY STATEMENT

Publicly available datasets were analyzed in this study. This data can be found here: Expression profile data are available in The Cancer Genome Atlas (TCGA) (https://portal.gdc.cancer.gov/). Immunohistochemical staining of genes are available in The Human Protein Atlas (HPA) (http://www.proteinatlas.org/). And the experimental data of qRT-RCR can be downloaded from the supplementary file.

AUTHOR CONTRIBUTIONS

LZ, ZS, LW and FH were involved in the study concept and design and data analysis and interpretation and in drafting the manuscript. All authors contributed to the article and approved the submitted version.

FUNDING

Supported by Natural Science Foundation of Fujian Province of China (No. 2019J01185) and key Clinical Specialty Discipline Construction Program of Fujian, P.R.C (No. 2017739).

ACKNOWLEDGMENTS

We sincerely thank the researchers and study participants for their contributions towards this study.

SUPPLEMENTARY MATERIAL

The Supplementary Material for this article can be found online at: https://www.frontiersin.org/articles/10.3389/fcell.2022.832803/full#supplementary-material

Supplementary Figure S1 | The ccRCC patients from TCGA was divided into different clusters when k=3-9 **(A–G)**. Relative change in area under CDF curve for k=2 to 9 **(H)**.

Supplementary Figure S2 | The correlation analysis with clinical characteristic. **(A)** Bargraph demonstrates the proportion of patients in the high- and low- risk groups with different clinicopathological characteristics. **(B-M)** Kaplan-Meier analysis of subgroup patients based on risk scores.

REFERENCES

Albiges, L., Tannir, N. M., Burotto, M., Mcdermott, D., Plimack, E. R., Barthélémy, P., et al. (2020). Nivolumab Plus Ipilimumab versus Sunitinib for First-Line Treatment of Advanced Renal Cell Carcinoma: Extended 4-year Follow-Up of the Phase III CheckMate 214 Trial. *ESMO Open* 5, e001079. doi:10.1136/esmoopen-2020-001079

Angulo, J. C., Manini, C., López, J. I., Pueyo, A., Colás, B., and Ropero, S. (2021). The Role of Epigenetics in the Progression of Clear Cell Renal Cell Carcinoma and the Basis for Future Epigenetic Treatments. *Cancers (Basel)* 13, 2071. doi:10.3390/cancers13092071

Bustin, S. A., and Mueller, R. (2005). Real-time Reverse Transcription PCR (qRT-PCR) and its Potential Use in Clinical Diagnosis. *Clin. Sci. (Lond)* 109, 365–379. doi:10.1042/cs20050086

Cella, D., Grünwald, V., Escudier, B., Hammers, H. J., George, S., Nathan, P., et al. (2019). Patient-reported Outcomes of Patients with Advanced Renal Cell Carcinoma Treated with Nivolumab Plus Ipilimumab versus Sunitinib (CheckMate 214): a Randomised, Phase 3 Trial. *Lancet Oncol.* 20, 297–310. doi:10.1016/s1470-2045(18)30778-2

Chen, B., Khodadoust, M. S., Liu, C. L., Newman, A. M., and Alizadeh, A. A. (2018). Profiling Tumor Infiltrating Immune Cells with CIBERSORT. *Methods Mol. Biol.* 1711, 243–259. doi:10.1007/978-1-4939-7493-1_12

Chen, H., Pan, Y., Jin, X., and Chen, G. (2021). Identification of a Four Hypoxia-Associated Long Non-coding RNA Signature and Establishment of a Nomogram Predicting Prognosis of Clear Cell Renal Cell Carcinoma. *Front. Oncol.* 11, 346. doi:10.3389/fonc.2021.713346

Choueiri, T. K., and Kaelin, W. G., Jr (2020). Targeting the HIF2-VEGF axis in Renal Cell Carcinoma. *Nat. Med.* 26, 1519–1530. doi:10.1038/s41591-020-1093-z

Cimmino, L., Dolgalev, I., Wang, Y., Yoshimi, A., Martin, G. H., Wang, J., et al. (2017). Restoration of TET2 Function Blocks Aberrant Self-Renewal and Leukemia Progression. *Cell* 170, 1079–1095. e1020. doi:10.1016/j.cell.2017.07.032

Darwish, O. M., Kapur, P., Youssef, R. F., Bagrodia, A., Belsante, M., Alhalabi, F., et al. (2013). Cumulative Number of Altered Biomarkers in Mammalian Target of Rapamycin Pathway Is an Independent Predictor of Outcome in Patients with clear Cell Renal Cell Carcinoma. *Urology* 81, 581–586. doi:10.1016/j.urology.2012.11.030

Dawson, M. A., and Kouzarides, T. (2012). Cancer Epigenetics: from Mechanism to Therapy. *Cell* 150, 12–27. doi:10.1016/j.cell.2012.06.013

Díaz-Montero, C. M., Rini, B. I., and Finke, J. H. (2020). The Immunology of Renal Cell Carcinoma. *Nat. Rev. Nephrol.* 16, 721–735. doi:10.1038/s41581-020-0316-3

Fang, J., Hu, M., Sun, Y., Zhou, S., and Li, H. (2020). Expression Profile Analysis of m6A RNA Methylation Regulators Indicates They Are Immune Signature Associated and Can Predict Survival in Kidney Renal Cell Carcinoma. *DNA Cel Biol* 39, 2194–2211. doi:10.1089/dna.2020.5767

Ferrone, C. K., Blydt-Hansen, M., and Rauh, M. J. (2020). Age-Associated TET2 Mutations: Common Drivers of Myeloid Dysfunction, Cancer and Cardiovascular Disease. *Int. J. Mol. Sci.* 21, 626. doi:10.3390/ijms21020626

Fruman, D. A., and Rommel, C. (2014). PI3K and Cancer: Lessons, Challenges and Opportunities. *Nat. Rev. Drug Discov.* 13, 140–156. doi:10.1038/nrd4204

Frye, M., and Blanco, S. (2016). Post-transcriptional Modifications in Development and Stem Cells. *Development* 143, 3871–3881. doi:10.1242/dev.136556

Fu, J., Li, K., Zhang, W., Wan, C., Zhang, J., Jiang, P., et al. (2020). Large-scale Public Data Reuse to Model Immunotherapy Response and Resistance. *Genome Med.* 12, 21. doi:10.1186/s13073-020-0721-z

Geeleher, P., Cox, N., and Huang, R. S. (2014). pRRophetic: an R Package for Prediction of Clinical Chemotherapeutic Response from Tumor Gene Expression Levels. *PLoS One* 9, e107468. doi:10.1371/journal.pone.0107468

George, D. J., Lee, C. H., and Heng, D. (2021). New Approaches to First-Line Treatment of Advanced Renal Cell Carcinoma. *Ther. Adv. Med. Oncol.* 13, 17588359211034708. doi:10.1177/17588359211034708

Hänzelmann, S., Castelo, R., and Guinney, J. (2013). GSVA: Gene Set Variation Analysis for Microarray and RNA-Seq Data. *BMC Bioinformatics* 14, 7. doi:10.1186/1471-2105-14-7

Hellmann, M. D., Callahan, M. K., Awad, M. M., Calvo, E., Ascierto, P. A., Atmaca, A., et al. (2018). Tumor Mutational Burden and Efficacy of Nivolumab Monotherapy and in Combination with Ipilimumab in Small-Cell Lung Cancer. *Cancer Cell* 33, 853–861. e854. doi:10.1016/j.ccell.2018.04.001

Hsieh, J. J., Purdue, M. P., Signoretti, S., Swanton, C., Albiges, L., Schmidinger, M., et al. (2017). Renal Cell Carcinoma. *Nat. Rev. Dis. Primers* 3, 17009. doi:10.1038/nrdp.2017.9

Jonasch, E., Walker, C. L., and Rathmell, W. K. (2021). Clear Cell Renal Cell Carcinoma Ontogeny and Mechanisms of Lethality. *Nat. Rev. Nephrol.* 17, 245–261. doi:10.1038/s41581-020-00359-2

Li, C., Wang, S., Xing, Z., Lin, A., Liang, K., Song, J., et al. (2017). A ROR1-HER3-lncRNA Signalling axis Modulates the Hippo-YAP Pathway to Regulate Bone Metastasis. *Nat. Cel Biol* 19, 106–119. doi:10.1038/ncb3464

Li, H., Jiang, H., Huang, Z., Chen, Z., and Chen, N. (2021). Prognostic Value of an m5C RNA Methylation Regulator-Related Signature for Clear Cell Renal Cell Carcinoma. *Cancer Manag. Res.* 13, 6673–6687. doi:10.2147/cmar.s323072

Liu, L., Chandrashekar, P., Zeng, B., Sanderford, M. D., Kumar, S., and Gibson, G. (2021). TreeMap: a Structured Approach to fine Mapping of eQTL Variants. *Bioinformatics* 37, 1125–1134. doi:10.1093/bioinformatics/btaa927

Ma, P., Pan, Y., Li, W., Sun, C., Liu, J., Xu, T., et al. (2017). Extracellular Vesicles-Mediated Noncoding RNAs Transfer in Cancer. *J. Hematol. Oncol.* 10, 57. doi:10.1186/s13045-017-0426-y

Mcdermott, D. F., Huseni, M. A., Atkins, M. B., Motzer, R. J., Rini, B. I., Escudier, B., et al. (2018). Clinical Activity and Molecular Correlates of Response to Atezolizumab Alone or in Combination with Bevacizumab versus Sunitinib in Renal Cell Carcinoma. *Nat. Med.* 24, 749–757. doi:10.1038/s41591-018-0053-3

Miao, D., Margolis, C. A., Gao, W., Voss, M. H., Li, W., Martini, D. J., et al. (2018). Genomic Correlates of Response to Immune Checkpoint Therapies in clear Cell Renal Cell Carcinoma. *Science* 359, 801–806. doi:10.1126/science.aan5951

Michalak, E. M., Burr, M. L., Bannister, A. J., and Dawson, M. A. (2019). The Roles of DNA, RNA and Histone Methylation in Ageing and Cancer. *Nat. Rev. Mol. Cel Biol* 20, 573–589. doi:10.1038/s41580-019-0143-1

Parker, W. P., Cheville, J. C., Frank, I., Zaid, H. B., Lohse, C. M., Boorjian, S. A., et al. (2017). Application of the Stage, Size, Grade, and Necrosis (SSIGN) Score for Clear Cell Renal Cell Carcinoma in Contemporary Patients. *Eur. Urol.* 71, 665–673. doi:10.1016/j.eururo.2016.05.034

Powers, R. K., Goodspeed, A., Pielke-Lombardo, H., Tan, A.-C., and Costello, J. C. (2018). GSEA-InContext: Identifying Novel and Common Patterns in Expression Experiments. *Bioinformatics* 34, i555–i564. doi:10.1093/bioinformatics/bty271

Powles, T., Albiges, L., Bex, A., Grünwald, V., Porta, C., Procopio, G., et al. (2021). ESMO Clinical Practice Guideline Update on the Use of Immunotherapy in Early Stage and Advanced Renal Cell Carcinoma. *Ann. Oncol.*. 32:1511–1519. doi:10.1016/j.annonc.2021.09.014

Reiter, M. A., Kurosch, M., and Haferkamp, A. (2015). Renal Cell Carcinoma: Drug Therapy and Prognostic Models. *Urologe A* 54, 735–738. 735-746; quiz. doi:10.1007/s00120-015-3845-9

Selmi, T., Hussain, S., Dietmann, S., Heiß, M., Borland, K., Flad, S., et al. (2021). Sequence- and Structure-specific Cytosine-5 mRNA Methylation by NSUN6. *Nucleic Acids Res.* 49, 1006–1022. doi:10.1093/nar/gkaa1193

Şenbabaoğlu, Y., Gejman, R. S., Winer, A. G., Liu, M., Van Allen, E. M., De Velasco, G., et al. (2016). Tumor Immune Microenvironment Characterization in clear Cell Renal Cell Carcinoma Identifies Prognostic and Immunotherapeutically Relevant Messenger RNA Signatures. *Genome Biol.* 17, 231. doi:10.1186/s13059-016-1092-z

Siegel, R. L., Miller, K. D., and Jemal, A. (2017). Cancer Statistics, 2017. *CA: A Cancer J. Clinicians* 67, 7–30. doi:10.3322/caac.21387

Subramanian, A., Tamayo, P., Mootha, V. K., Mukherjee, S., Ebert, B. L., Gillette, M. A., et al. (2005). Gene Set Enrichment Analysis: a Knowledge-Based Approach for Interpreting Genome-wide Expression Profiles. *Proc. Natl. Acad. Sci.* 102, 15545–15550. doi:10.1073/pnas.0506580102

Tomczak, K., Czerwińska, P., and Wiznerowicz, M. (2015). The Cancer Genome Atlas (TCGA): an Immeasurable Source of Knowledge. *Contemp. Oncol. (Pozn)* 19, A68–A77. doi:10.5114/wo.2014.47136

Tzeng, A., Tzeng, T. H., and Ornstein, M. C. (2021). Treatment-free Survival after Discontinuation of Immune Checkpoint Inhibitors in Metastatic Renal Cell Carcinoma: a Systematic Review and Meta-Analysis. *J. Immunother. Cancer* 9, e003473. doi:10.1136/jitc-2021-003473

Uhlén, M., Fagerberg, L., Hallström, B. M., Lindskog, C., Oksvold, P., Mardinoglu, A., et al. (2015). Tissue-based Map of the Human Proteome. *Science* 347, 1260419. doi:10.1126/science.1260419

Wang, Z.-L., Li, B., Luo, Y.-X., Lin, Q., Liu, S.-R., Zhang, X.-Q., et al. (2018). Comprehensive Genomic Characterization of RNA-Binding Proteins across Human Cancers. *Cel Rep.* 22, 286–298. doi:10.1016/j.celrep.2017.12.035

Wang, B., Zhao, H., Ni, S., and Ding, B. (2021). Integrated Analysis of the Roles of RNA Binding Proteins and Their Prognostic Value in Clear Cell Renal Cell Carcinoma. *J. Healthc. Eng.* 2021, 5568411. doi:10.1155/2021/5568411

Wilkerson, M. D., and Hayes, D. N. (2010). ConsensusClusterPlus: a Class Discovery Tool with Confidence Assessments and Item Tracking. *Bioinformatics* 26, 1572–1573. doi:10.1093/bioinformatics/btq170

Yang, W., Soares, J., Greninger, P., Edelman, E. J., Lightfoot, H., Forbes, S., et al. (2013). Genomics of Drug Sensitivity in Cancer (GDSC): a Resource for Therapeutic Biomarker Discovery in Cancer Cells. *Nucleic Acids Res.* 41, D955–D961. doi:10.1093/nar/gks1111

Yang, R., Liang, X., Wang, H., Guo, M., Shen, H., Shi, Y., et al. (2021). The RNA Methyltransferase NSUN6 Suppresses Pancreatic Cancer Development by Regulating Cell Proliferation. *EBioMedicine* 63, 103195. doi:10.1016/j.ebiom.2020.103195

You, J. S., and Jones, P. A. (2012). Cancer Genetics and Epigenetics: Two Sides of the Same coin? *Cancer Cell* 22, 9–20. doi:10.1016/j.ccr.2012.06.008

Yu, G., Wang, L.-G., Han, Y., and He, Q.-Y. (2012). clusterProfiler: an R Package for Comparing Biological Themes Among Gene Clusters. *OMICS: A J. Integr. Biol.* 16, 284–287. doi:10.1089/omi.2011.0118

Zhang, D., Wang, Y., and Hu, X. (2020). Identification and Comprehensive Validation of a DNA Methylation-Driven Gene-Based Prognostic Model for Clear Cell Renal Cell Carcinoma. *DNA Cel Biol.* 39, 1799–1812. doi:10.1089/dna.2020.5601

Zhao, H., Cao, Y., Wang, Y., Zhang, L., Chen, C., Wang, Y., et al. (2018). Dynamic Prognostic Model for Kidney Renal clear Cell Carcinoma (KIRC) Patients by Combining Clinical and Genetic Information. *Sci. Rep.* 8, 17613. doi:10.1038/s41598-018-35981-5

Zheng, B., Niu, Z., Si, S., Zhao, G., Wang, J., Yao, Z., et al. (2021). Comprehensive Analysis of New Prognostic Signature Based on Ferroptosis-Related Genes in clear Cell Renal Cell Carcinoma. *Aging* 13, 19789–19804. doi:10.18632/aging.203390

Conflict of Interest: The authors declare that the research was conducted in the absence of any commercial or financial relationships that could be construed as a potential conflict of interest.

Publisher's Note: All claims expressed in this article are solely those of the authors and do not necessarily represent those of their affiliated organizations, or those of the publisher, the editors, and the reviewers. Any product that may be evaluated in this article, or claim that may be made by its manufacturer, is not guaranteed or endorsed by the publisher.

frontiers in Genetics

ORIGINAL RESEARCH
published: 23 March 2022
doi: 10.3389/fgene.2022.851384

A Novel Pyroptosis-Related Gene Signature for Predicting Prognosis in Kidney Renal Papillary Cell Carcinoma

*Jian Hu[1†], Yajun Chen[2†], Liang Gao[1], Chengguo Ge[1], Xiaodu Xie[1], Pan Lei[1], Yuanfeng Zhang[1] and Peihe Liang[1]**

[1]Department of Urology, The Second Affiliated Hospital of Chongqing Medical University, Chongqing, China, [2]Department of Hepatobiliary Surgery, The Second Affiliated Hospital of Chongqing Medical University, Chongqing, China

Pyroptosis is defined as an inflammatory form of programmed cell death. Increasing studies have demonstrated that pyroptosis is closely related to tumor development and antitumor process. However, the role of pyroptosis in kidney renal papillary cell carcinoma (KIRP) remains obscure. In this study, we analyzed the expression of 52 pyroptosis-related genes (PRGs) in KIRP, of which 20 differentially expressed PRGs were identified between tumor and normal tissues. Consensus clustering analysis based on these PRGs was used to divided patients into two clusters, from which a significant difference in survival was found (p = 0.0041). The prognostic risk model based on six PRGs (*CASP8*, *CASP9*, *CHMP2A*, *GPX4*, *IL6*, and *IRF1*) was built using univariate Cox regression and LASSO–Cox regression analysis, with good performance in predicting one-, three-, and five-year overall survival. Kaplan–Meier survival analysis showed that the high-risk group had a poor survival outcome (p < 0.001) and risk score was an independent prognostic factor (HR: 2.655, 95% CI 1.192–5.911, p = 0.016). Immune profiling revealed differences in immune cell infiltration between the two groups, and the infiltration of M2 macrophages was significantly upregulated in the tumor immune microenvironment, implying that tumor immunity participated in the KIRP progression. Finally, we identified two hub genes in tumor tissues (*IL6* and *CASP9*), which were validated *in vitro.* In conclusion, we conducted a comprehensive analysis of PRGs in KIRP and tried to provide a pyroptosis-related signature for predicting the prognosis.

Keywords: pyroptosis, kidney renal papillary cell carcinoma, signature, prognosis, gene

OPEN ACCESS

Edited by:
Alaguraj Veluchamy,
St. Jude Children's Research Hospital, United States

Reviewed by:
Kesavan Babu,
UT Southwestern Medical Center, United States
Atrayee Bhattacharya,
Dana–Farber Cancer Institute, United States

****Correspondence:***
Peihe Liang
302478@cqmu.edu.cn

[†]These authors have contributed equally to this work and share first authorship

Specialty section:
This article was submitted to Epigenomics and Epigenetics, a section of the journal Frontiers in Genetics

Received: *10 January 2022*
Accepted: *28 February 2022*
Published: *23 March 2022*

Citation:
Hu J, Chen Y, Gao L, Ge C, Xie X, Lei P, Zhang Y and Liang P (2022) A Novel Pyroptosis-Related Gene Signature for Predicting Prognosis in Kidney Renal Papillary Cell Carcinoma. Front. Genet. 13:851384. doi: 10.3389/fgene.2022.851384

INTRODUCTION

Renal cell carcinoma (RCC) is one of the most common tumors in the genitourinary system, accounting for 3.7% of all malignancies globally (Sung et al., 2021). Kidney renal papillary cell carcinoma (KIRP) refers to a subtype of RCC, with a relatively lower invasiveness and better prognosis than other types of RCC. However, approximately 25–35% of RCC patients had distant metastasis at the time of initial diagnosis, and the five-year survival rate of metastatic RCC was found to be only about 12% (Brozovich et al., 2021; Roberto et al., 2021). Accordingly, a novel risk model should be developed to identify potential high-risk KIRP patients, which may be conductive to clinical decision-making or exploring novel therapeutic biomarkers.

Pyroptosis has been reported as an inflammatory type of programmed cell death mediated by gasdermin proteins (Xia et al., 2019). The members of gasdermin families consist of GSDMA,

GSDMB, GSDMC, GSDMD, GSDME (or DFNA5), and PJVK (or DFNB59) (Broz et al., 2020). Pyroptosis is characterized by pore formation in the plasma membrane, which can lead to the formation of inflammasomes and the release of pro-inflammatory factors, thus resulting in cell death. Pyroptosis was firstly discovered in the inflammatory response to infection (Zychlinsky et al., 1992). According to further research studies, more functions relating to pyroptosis in neurological, infectious, autoimmune, cardiovascular, and oncologic disorders have been found (Yu et al., 2021). Over the past few years, increasing studies have confirmed that pyroptosis might play a double-edged role since it could both promote and inhibit tumor cells. On the one hand, the activated pyroptosis can result in the release of inflammatory mediators, such as IL-1 and IL-8, which can form an inflammatory environment and facilitate the occurrence of cancer (Chavez-Dominguez et al., 2021). On the other hand, inducing pyroptosis of tumor cells showed a great potential in inhibiting tumor proliferation, migration, and invasion (Derangere et al., 2014; Wang et al., 2017). For example, iron-activated reactive oxygen species (ROS) could promote melanoma cell pyroptosis *via* a Tom20–Bax–caspase–GSDME pathway (Zhou et al., 2018). However, the effect of pyroptosis on the development and prognosis of KIRP remains unknown.

In this study, we performed a comprehensive analysis for the expression level of pyroptosis-related genes (PRGs) in KIRP and constructed a signature to predict the survival outcomes of KIRP patients. Subsequently, functional enrichment analysis and its interactions with cancer immunity of the signature were further explored. Furthermore, hub genes of the signature were validated.

MATERIALS AND METHODS

Dataset Acquisition

The normalized RNA sequencing (RNA-seq) expression data as transcripts per million (TPM) and corresponding clinical information of 321 KIRP samples were acquired from TCGA database (https://xenabrowser.net/datapages/, until December 01, 2021). After screening, the 72 samples were rejected based on the merged sample quality annotations (https://gdc.cancer.gov/about-data/publications/pancanatlas). Additionally, 28 normal kidney samples were collected from the Genotype-Tissue Expression (GTEx) database (https://xenabrowser.net/datapages/, until December 01, 2021). All RNA-seq data were $\log_2$-transformed for further analysis.

Identification of Differentially Expressed PRGs

As shown in **Supplementary Table S1**, the 52 PRGs were retrieved from GSEA (http://www.gsea-msigdb.org/gsea/index.jsp) and previous research (**Supplementary Table S1**) (Qi et al., 2021). The "limma" R package was utilized to determine differentially expressed genes (DEGs) between 28 normal kidney samples and 249 KIRP samples, with $|\text{Log}_2\text{FC}|>1$ and $p < 0.05$. The differentially expressed PRGs were selected through the "VennDiagram" package, and their protein–protein interaction (PPI) network was acquired from the STRING database (https://www.string-db.org/, version 11.5).

Consensus Clustering Analysis

To investigate the biological characteristics of differentially expressed PRGs in KIRP patients, we classified the patients into different subtypes using the "ConsensusClusterPlus" R package with a resampling rate of 80% and 500 iterations. The differential clinical information and expression of different subtypes were shown in the heat-map. The survival differences among clusters were visualized with the Kaplan–Meier curve using the "survival" R package.

Establishment of a Pyroptosis-Based Prognostic Model

Univariate Cox proportional hazards regression analysis determined the prognostic value of PRGs in KIRP patients, and genes with $p < 0.2$ were selected for subsequent analysis. The candidate PRGs were selected using 10-fold cross-validation of the least absolute shrinkage and selection operator (LASSO)-penalized Cox regression analysis in the "glmnet" R package. Then, the prognostic model was built based on the six genes (*CASP8*, *CASP9*, *CHMP2A*, *GPX4*, *IL6*, and *IRF1*) and their coefficients, and the penalty parameter (λ) was decided by the minimum criteria. The risk score of each patient was calculated according to regression coefficients derived from the LASSO-Cox regression model multiplied with its gene expression level, as follows: Risk score = $\sum_i^6 \text{Xi}^*\text{Yi}$ (X: coefficients, Y: gene expression level). Next, 249 patients were separated into the low-risk group and the high-risk group based on the median risk score, and Kaplan–Meier survival analysis and a log-rank test were performed to compare the survival outcomes between two risk groups. The area under the curve (AUC) of the receiver-operating characteristic (ROC) curve based on the "survival," "survminer," and "time-ROC" R packages was used to evaluate the predictive performance of the prognostic model.

Independent Prognostic Analysis of Risk Scores

To identify independent prognostic factors and validate the independent prognostic value of risk score, the risk score and clinical characteristics including age, gender, and T-stage, N-stage, M-stage, and tumor stage in TCGA dataset were analyzed *via* univariate and multivariate Cox regression models, respectively. These multivariate prognostic analysis results were calculated and then visualized by the "forestplot" R package.

Functional Enrichment Analysis of DEGs and Evaluation of Tumor Immune Microenvironment

The DEGs between the low-risk group and the high-risk group were identified *via* the "limma" R package. $|\text{Log}_2\text{FC}|>1$ and $p < 0.05$

were considered to be statistically significant. The Gene Ontology (GO) and Kyoto Encyclopedia of Genes and Genomes (KEGG) enrichment analyses of those DEGs were performed *via* the "clusterProfiler" R package. The "CIBERSORT" package was used to explore the landscape of 22 tumor-infiltrating immune cells and their connection with the signature.

Ethics Statement and Tissue Sample Collection

A total of three pairs of tissues from KIRP patients and their paired normal tissues were collected from the Department of Pathology of The Second Affiliated Hospital of Chongqing Medical University, which was approved by the Human Research Ethics Committee.

Immuno-Histochemical Staining

Paraffin sections were placed in a 60°C oven to melt the paraffin and soaked in xylene and ethanol at different concentrations to elute the paraffin. Then, the sections were incubated with 3% H_2O_2 at room temperature for 10 min to eliminate endogenous peroxidase activity. The sections were immersed in boiling EDTA repair solution for 10 min and allowed to cool naturally. Then, the sections were incubated with 5% BSA blocking solution at 37°C for 30 min. The sections were incubated with appropriately IL-6 primary antibody (1:50, Proteintech, 21865-1-AP) and CASP9 primary antibody (1:200, Abcam, ab202068) at 4°C overnight. The next day, the sections were washed three times with PBS for 10 min. The sections were incubated with secondary antibody at room temperature for 60 min. After washing three times with PBS for 10 min, the tissues were stained with DAB and hematoxylin. Then, the sections were sequentially immersed in 60, 75, 80, 95, and 100% ethanol for dehydration. Finally, the sections were sealed with neutral gum and observed with a light microscope.

Statistical Analysis

The DEGs between the normal and KIRP tissues were analyzed with one-way analysis of variance. The Kaplan–Meier curve with a two-sided log-rank test was utilized to assess the survival difference. Cox regression models were applied to identify prognostic factors, with hazard ratios (HRs) and 95% confidence intervals (CIs). All statistical analyses were completed by R software (v4.1.0), and $p < 0.05$ was considered statistically significant.

RESULTS

Identification of Differentially Expressed PRGs Between KIRP and Normal Tissues

The mRNA expression of 52 PRGs from 249 tumor and 28 normal tissues was examined on the basis of TCGA data. 20 genes were considered differentially expressed PRGs with $|\text{Log2FC}|>1$ and $p < 0.05$. As shown in **Figure 1A**, 13 genes (*GRX4*, *BAX*, *CHMP2A*, *PYCARD*, *CHMP48*, *IL18*, *CASP4*, *PLCG1*, *TP53*, *CASP1*, *CHMP6*, *CASP8*, and *CASP3*) of the above genes were upregulated, and 7 genes (*TIRAP*, *CHMP7*, *IL6*, *IRF1*, *CASP9*, *PRKACA*, and *CHMP3*) were downregulated in the tumor group. To further explore the interactions of these 20 differentially expressed PRGs, PPI network analysis was conducted, and the results are shown in **Figure 1B**. And the correlation network of these genes is shown in **Figure 1C**.

Consensus Clustering Analysis Based on Differentially Expressed PRGs

To investigate whether differentially expressed PRGs had an impact on survival outcomes, we carried out the consensus clustering analysis of 249 KIRP patients. Based on the above PRGs, the results showed that the clustering variable (k) = 2 was considered to have the optimal stability from k = 2 to 9, implying that KIRP patients could be divided into two clusters (cluster 1 and cluster 2) with the highest intragroup correlations and the lowest intergroup correlations (**Figures 2A–D**). Notably, compared with those in cluster 1, KIRP patients in cluster 2 had a significantly longer survival (**Figure 2E**, $p = 0.0041$), indicating a significant prognostic value of these PRGs. Moreover, clinical characteristics including gender, age, and tumor TNM stage were presented in two clusters without significant differences (**Figure 2F**).

Construction of a Prognostic Six-Gene Signature in KIRP Patients

The clinical implication of PRGs was further assessed in KIRP patients. As shown in univariate Cox regression analysis (**Figure 3A**), 11 (*IL6*, *CHMP2A*, *GPX4*, *CASP3*, *CASP4*, *CASP8*, *CASP9*, *CHMP7*, *PRKACA*, *TP53*, and *IRF1*) of PRGs were survival-related with $p < 0.2$. And then, LASSO-Cox regression analysis was performed using 11 prognostic genes, and a signature consisting of *CASP9*, *CHMP2A*, *GPX4*, *IL6*, *IRF1*, and *CASP8* was constructed based on the optimal λ score (**Figures 3B,C**). The risk score was calculated by the following formula: Risk score = (0.067**IL6* exp.) + (0.01011**CASP8* exp.) + (0.5066**IRF1* exp.) + (−0.4791**CASP9* exp.) + (−0.0988**CHMP2A* exp.) + (−0.119**GPX4* exp.). 249 KIRP patients were approximately divided into the low-risk group and the high-risk group according to the median risk score (**Figure 3D**). As shown in **Figure 3E**, the result of principal component analysis (PCA) indicated patients of two risk groups could be distributed into two directions. **Figure 3F** shows that patients of the low-risk group tended to have a low probability of mortality compared to those of the high-risk group. Consistently, Kaplan–Meier analysis showed that the high-risk group had a significantly shorter survival time (**Figure 3G**, $p < 0.001$). A time-dependent ROC curve was performed to evaluate the predictive performance. And the AUC was 0.85 at 1 year, 0.785 at 2 years, and 0.707 at 3 years (**Figure 3H**), showing that this risk model exhibited high accuracy and sensitivity in predicting the prognosis of KIRP patients.

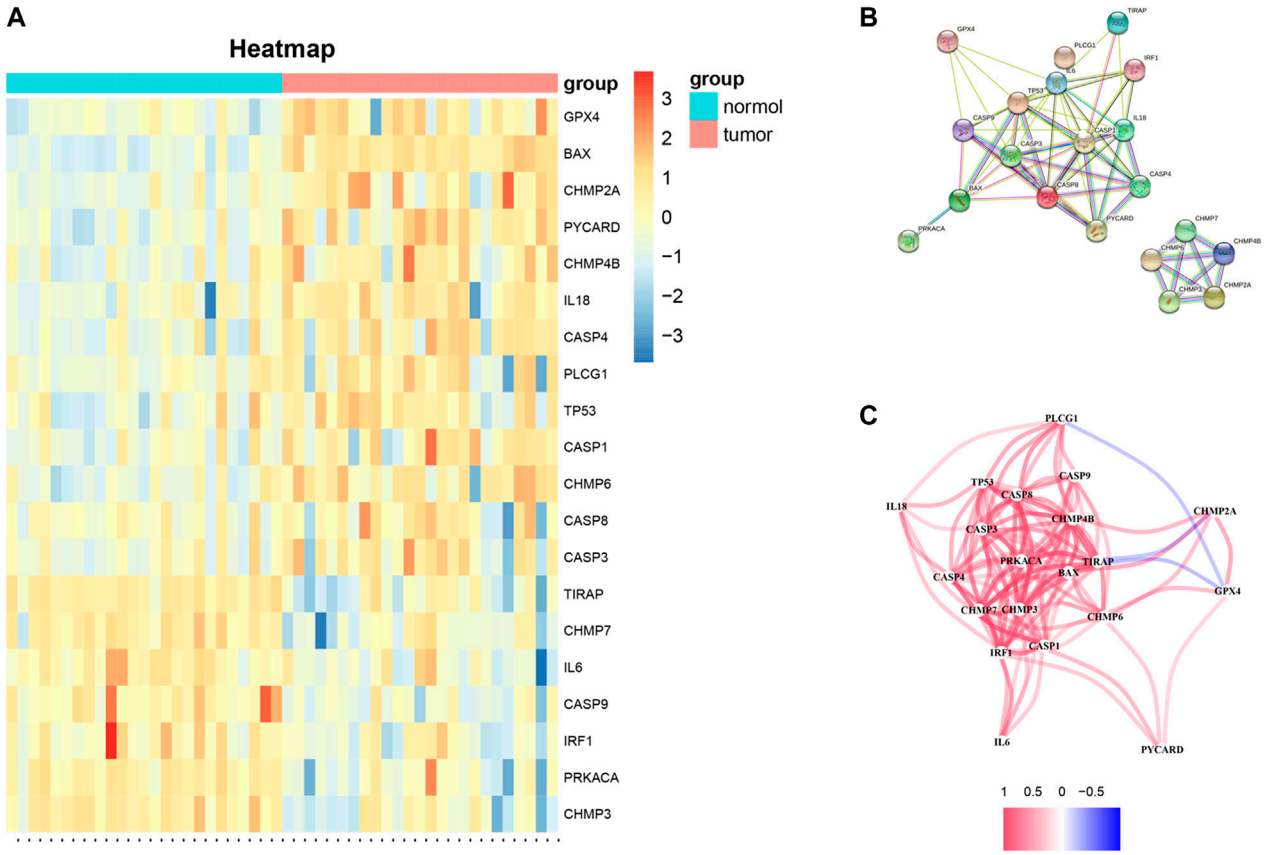

FIGURE 1 | (A) Heat-map of differentially expressed PRGs between the tumor and normal tissues (red color: higher expression; blue color: lower expression, all $p <$ 0.05). **(B)** PPI network of 20 differentially expressed PRGs obtained from the STRING database. **(C)** Correlation network of 20 differentially expressed PRGs (the correlation coefficients are presented by different colors: red line, positive correlation; blue line, negative correlation).

Independent Prognostic Value of the Signature

Univariate Cox regression analysis and multivariable Cox regression analysis were carried out to determine whether the risk score could serve as the independent prognostic predictor for survival in KIRP. The univariate Cox regression analysis showed that the risk score was significantly associated with poor survival (HR: 3.276, 95% CI 1.528–7.025, p = 0.002, **Figure 4A**). Moreover, other clinical characteristics including tumor stage and N-stage were found as the risk factors as well. After the adjustment of confounding factors, the result of multivariable Cox regression analysis suggested that the risk score was still a risk prognostic factor (HR: 2.655, 95% CI 1.192–5.911, p = 0.016, **Figure 4B**). As shown in **Figure 4C**, the patients suffering from advanced tumor stage had a higher probability of high risk score.

Functional Enrichment Based on the Signature

To further investigate the differences in biological function and pathway between the low-risk group and the high-risk group, DEGs were generated using the "limma" R package. Then, these DEGs were further analyzed with the GO term and KEGG pathway enrichment analysis. As presented in **Figure 5A**, the top-rank biological processes were lymphocyte mediated immunity, complement activation pathway, and humoral immune response mediated by circulating immunoglobulin. Moreover, the most highly enriched cellular components associated with DEGs were immunoglobulin complex, external side of plasma membrane, and T cell receptor complex (**Figure 5B**). As for the molecular functions, antigen binding, immunoglobulin receptor binding, and immune receptor activity were on the top list (**Figure 5C**). Furthermore, the KEGG pathway analysis is shown in **Figure 5D**, and the cytokine-cytokine receptor interaction pathway and the viral protein interaction with cytokine and cytokine receptor signaling pathway were mostly associated with these DEGs. These results showed that these DEGs were significantly enriched in immune-related functions or pathways.

Immune Characteristic Analysis Based on Pyroptosis-Related Risk Score

Based on functional enrichment, we speculated that tumor immune status of KIRP played an important role in the

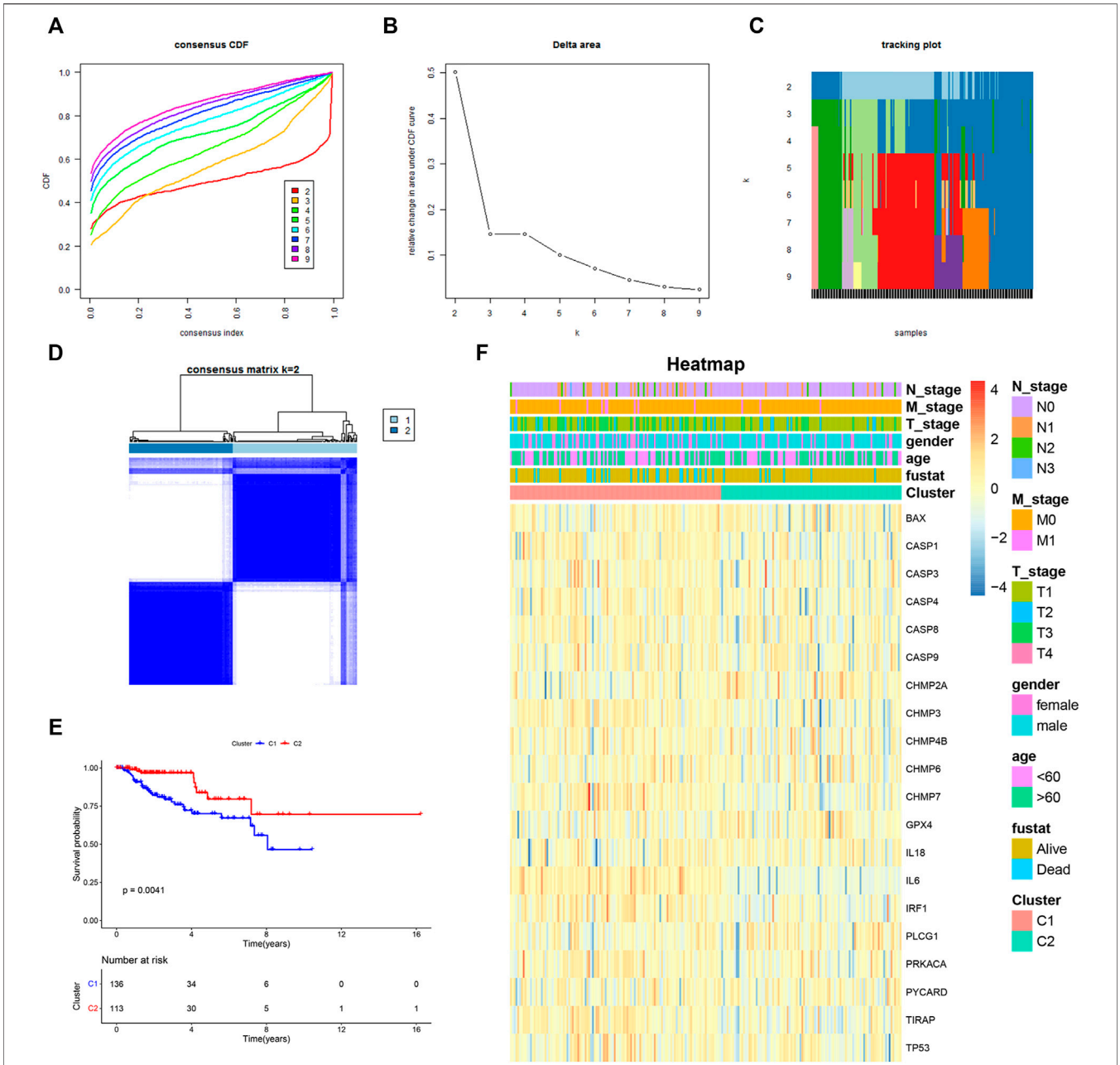

FIGURE 2 | Two KIRP clusters obtained by consensus clustering analysis based on differentially expressed PRGs. **(A)** Area under the cumulative distribution function (CDF) curve for k = 2–9. **(B)** CDF delta area for k = 2–9. **(C)** Tracking plot for k = 2–9. **(D)** Consensus clustering matrix for k = 2. **(E)** Kaplan–Meier survival analysis of two subgroups. **(F)** Heat-map of PRGs and the clinical characteristics between the two clusters.

development of cancer. Therefore, the tumor immune microenvironment (TIM) of KIRP was further explored. Firstly, the abundance of immune cell infiltration was investigated. The overview of tumor microenvironment immune cell compositions is shown in **Figure 6B**, in which 22 type cells had differential distributions in KIRP. To be specific, M2 macrophages were found with an especially high infiltration level. The infiltration levels of naïve B cells, $CD8^+$ T cells, regulatory T cells, and M1 macrophages in the high-risk group were significantly upregulated, while the infiltration levels of memory B cells, activated mast cells, and resting mast cells decreased (**Figures 6A,C**, $p < 0.05$).

Identification and Validation of the Hub Genes *In Vitro*

To further explore genetic interrelationships in the PRG signature, the PPI network of these genes was obtained

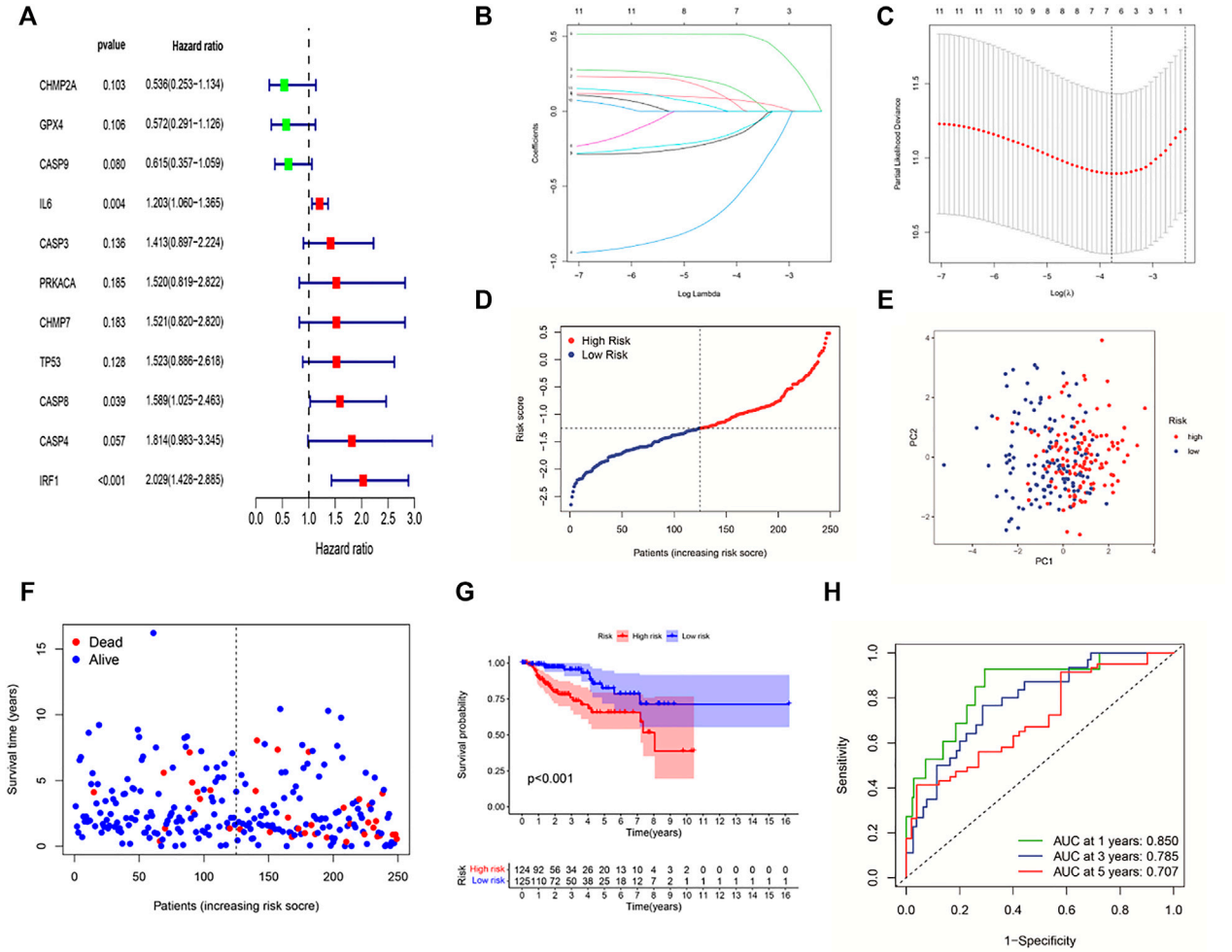

FIGURE 3 | Construction of a six-gene prognostic signature in KIRP patients. **(A)** Univariate cox regression analysis of 11 PRGs ($p < 0.2$). **(B,C)** LASSO regression of 11 PRGs and the tuning parameter (λ) selection cross-validation curve. **(D)** Distribution of risk scores for KIRP patients. **(E)** PCA plot based on the risk score. **(F)** Distribution of patient survival status according to the high-risk group and the low-risk group. **(G)** Kaplan–Meier curves for OS in the low- and high-risk groups. **(H)** ROC curves to evaluate the predictive efficiency of the risk model.

using the STRING database (**Figure 7A**). *IL6* was the hub node in the obtained interactive network. Next, the CytoHubba plugin in Cytoscape was used, and the genes with the top three MCC values (*IL6*, *CASP8*, and *CASP9*) were identified as candidate hub genes (**Figure 7B**). Meanwhile, we assessed the prognostic role of these PRGs in the signature, and three genes (*CASP9*, *IL6*, and *IRF1*) were survival-related ($p < 0.05$). High expression of *CASP9* was significantly correlated with longer overall survival in KIRP patients ($p = 0.031$), while high *IL6* ($p = 0.004$) and *IRF1* ($p < 0.001$) expressions had a shorter survival time (**Figures 7C–E**). The intersections of the above genes were selected as hub genes. Finally, two hub genes (*IL6* and *CASP9*) were identified and further validated through protein expression levels *in vitro*. As depicted in immuno-histochemical staining, the protein expression levels of *IL6* and *CASP9* were significantly downregulated in KIRP tissues compared with normal renal tissues (**Figures 7F,G**).

DISCUSSION

Pyroptosis has been defined as an inflammasome-induced programmed cell death, and it was initially observed in immune defense and anti-infection for eliminating viral and bacterial infections (Zychlinsky et al., 1992). Recently, increasing studies have demonstrated that pyroptosis played a vital role in carcinogenesis, and inducing tumor cell pyroptosis might be a potential treatment strategy for cancers (Wang et al., 2019). However, the role of pyroptosis in KIRP patients remains unclear.

In the present study, we comprehensively evaluated the mRNA expression levels of 52 PRGs in KIRP and normal tissues, from which 20 genes were differentially expressed. These patients were categorized into two groups based on consensus clustering analysis. Patients in cluster 2 had a longer survival time than those in cluster 1, implying that these PRGs might be important for predicting the prognosis of

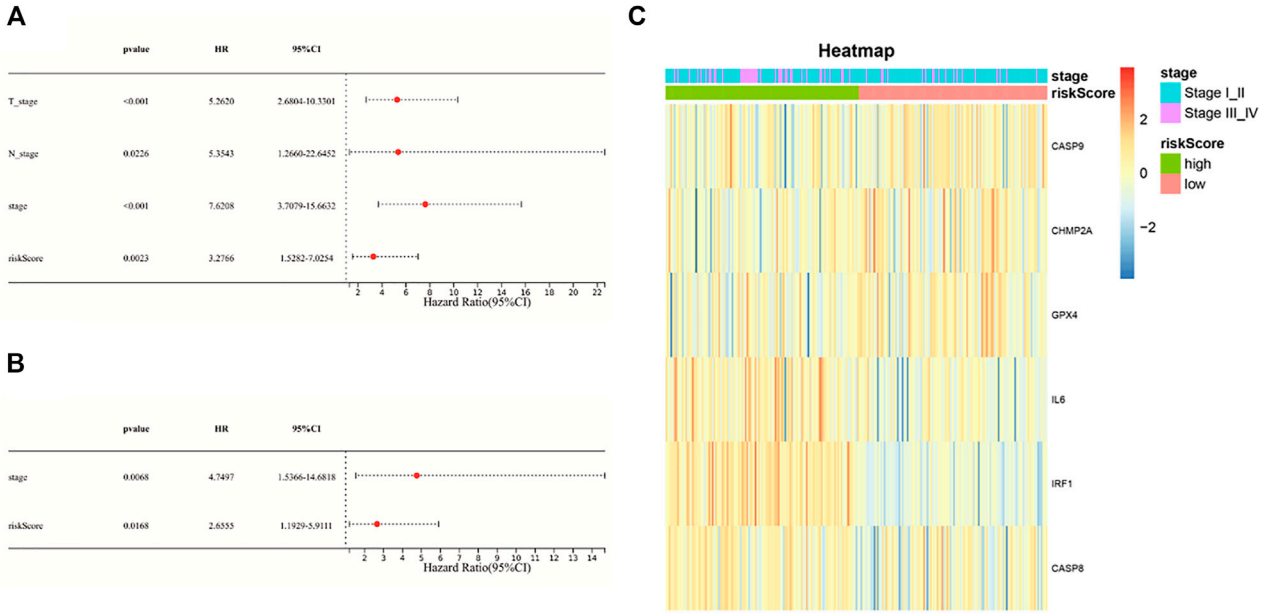

FIGURE 4 | (A) Univariate Cox regression analysis of the risk score and other clinical characteristics associated with overall survival; **(B)** multivariate Cox regression analysis of the risk score and other clinical characteristics; **(C)** heat-map showing the relationship of the risk groups and tumor stage.

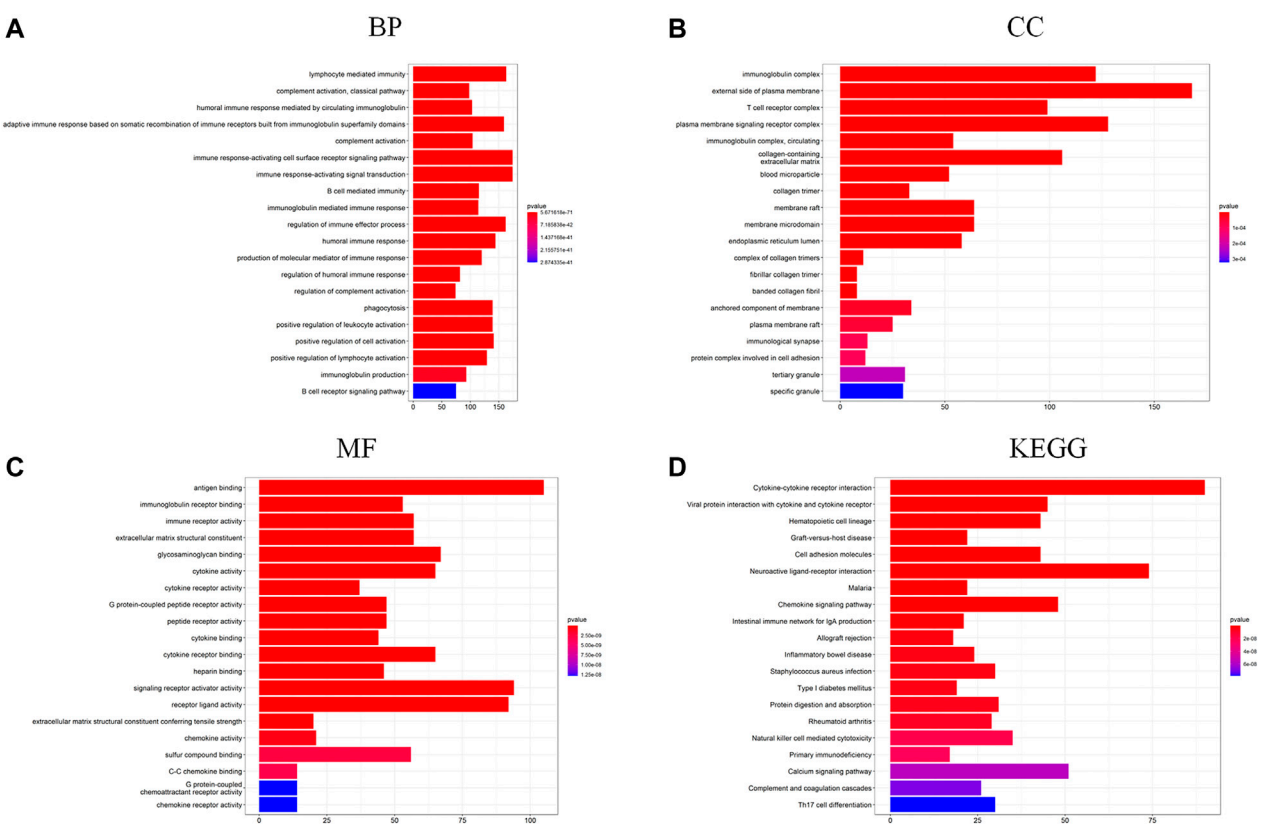

FIGURE 5 | (A–C) GO functional enrichment analysis of DEGs in the two risk groups (BP, biological process; CC, cellular component; MF, molecular function); **(D)** KEGG pathway analysis of DEGs in the two risk groups.

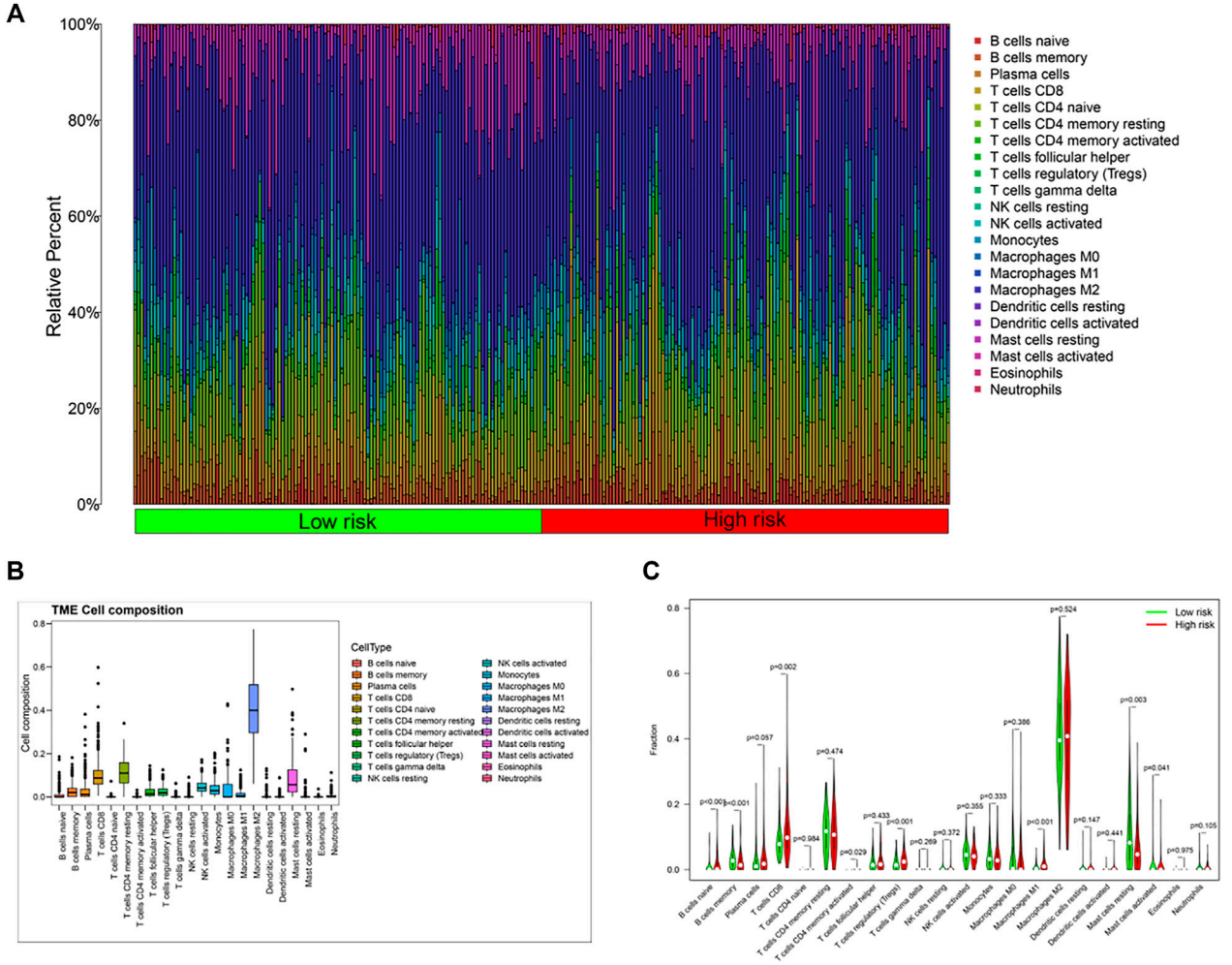

FIGURE 6 | (A,C) Differences in immune cell composition between the high-risk group and the low-risk group; **(B)** tumor microenvironment immune cell composition in KIRP patients.

KIRP patients. Subsequently, using univariate Cox regression analysis and LASSO-Cox regression analysis, we had constructed a six-gene risk model with good prediction performance in the survival of KIRP. The results showed that patients in the high-risk group had a poor survival outcome and the risk score was an independent prognostic factor. Functional analysis using GO/KEGG analysis indicated that DEGs between the high-risk group and the low-risk group were closely associated with immune functions or pathways. Following that, we further explored the TIM of KIRP, showing a high infiltration level of M2 macrophages and differential distributions of immune cells between two risk groups. Finally, we identified two hub genes (*IL6* and *CASP9*), which were validated *via* protein expression levels *in vitro*.

For genes within the constructed signature, caspase-9 encoded by *CASP9* is a caspase trigger point, which plays an important role in the GSDME-mediated pyroptosis pathway. Caspase-9 activation can trigger caspase-3, inducing GSDME-mediated pyroptosis. Recent studies demonstrated that caspase-9 could be activated by the Tom20/Bax/Cytochrome c pathway in melanoma or by lobaplatin/ROS and JNK phosphorylation/Bax/Cytochrome c pathways in colon cancer, showing a great potential value of clinical application (Zhou et al., 2018; Yu et al., 2019). In this study, we found that the mRNA expression of *CASP9* was significantly decreased in KIRP tissues, and patients with high *CASP9* expression levels were correlated with longer overall survival. Further research studies observed that the methylation level of *CASP9* promoter was significantly elevated in KIRP (**Supplementary Figure S1**, $p < 0.001$) and thus reduced the expression of the gene. Therefore, *CASP9* was a protective gene and might be a potential therapeutic target for KIRP. *IL6* is a cytokine involved in numerous biological processes including immune response, inflammation, and embryonic development, and it is also a key factor in tumor development and progression (Hirano, 2021). For example, *IL6* could promote the development and proliferation of pancreatic cancer cells through the STAT3–Pim kinase axis (Block et al., 2012). Lippitz et al. reported that serum *IL6* was positively correlated with tumor stage or metastases, and increased *IL6* meant poor survival outcomes (Lippitz and Harris, 2016). We also obtained a

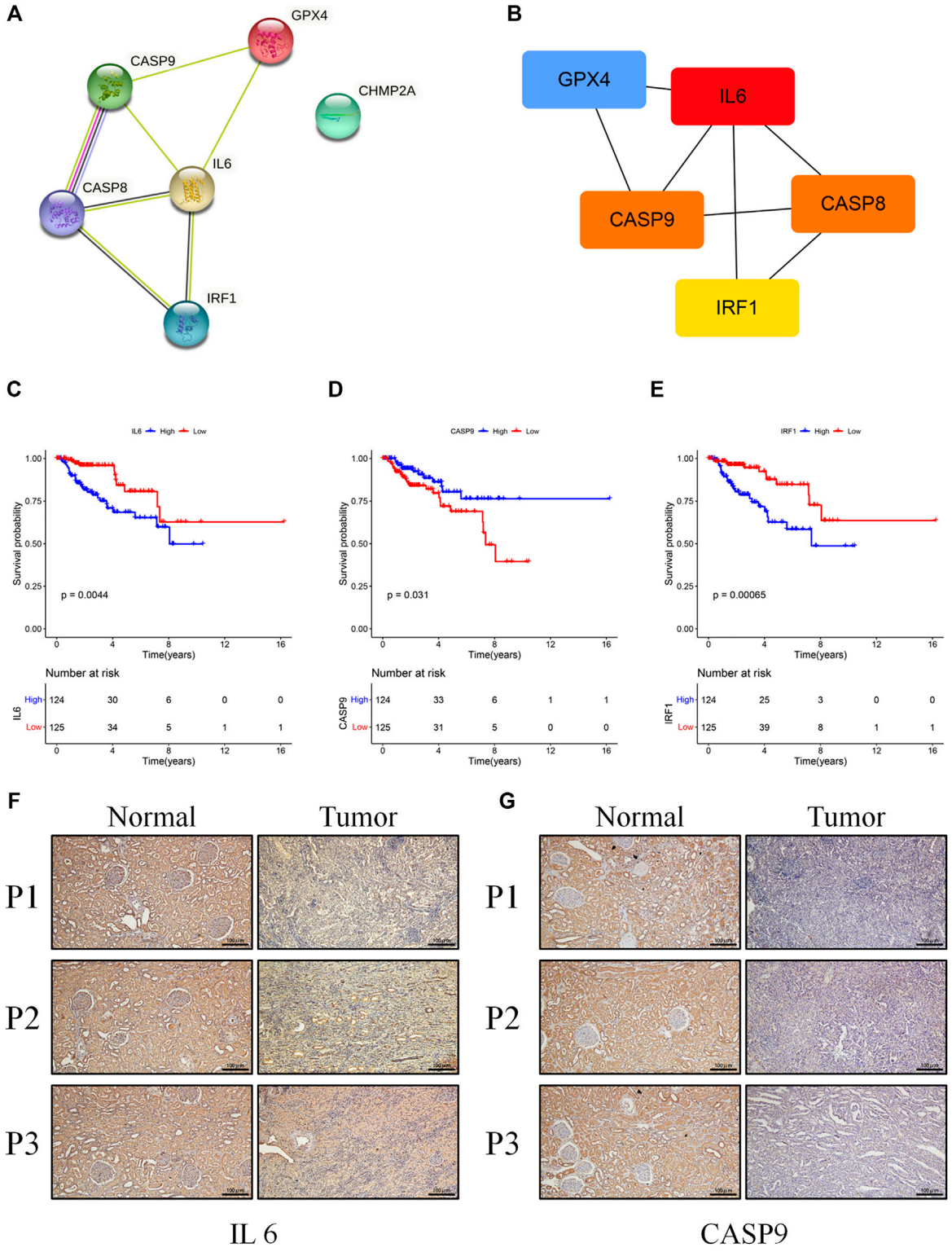

FIGURE 7 | (A) The PPI network was constructed containing six genes of the signature. **(B)** Screening hub genes from the PPI network (red node: genes with a high MCC score; blue node: genes with a low MCC score). **(C–E)** The cohort was divided into two groups (high and low) according to their median expression value separately, and the expressions of *IL6*, *RAF1*, and *CASP9* were associated with overall survival ($p < 0.05$). **(F,G)** Results of *IL6* and *CASP9* in immuno-histochemical staining between KIRP and normal tissues (scale bar values: 100 μm).

similar result ($p = 0.031$), showing that it was a prognostic risk factor. Notably, the mRNA expression of *IL6* was downregulated in KIRP. Caspase8, encoded by *CASP8*, was proved to activate caspase-1 and *GSDMD* cleavage, thus resulting in pyroptosis (Orning et al., 2018; Han et al., 2021). Additionally, *IRF1* was considered a transcription factor regulating pyroptosis. Recent studies had proved that *IRF1* could transcriptionally induce *GSDMD* expression for pyroptotic cell death (Karki et al., 2020). In our study, *IRF1* was also downregulated in KIRP. Kang et al. demonstrated that conditional *GPX4* knockout could trigger lipid peroxidation–dependent caspase-11 and *GSDMD* cleavage, leading to pyroptosis (Kang et al., 2018). Additionally, SU et al. observed that high expression of *GPX4* in ccRCC promoted cancer cell proliferation and metastasis *in vitro* (Su et al., 2019). Here, *GPX4* was found with high expression in KIRP tissues and increased significantly in the high-risk group. Given the role of *GPX4*, it could also serve as a therapeutic target. However, the role of *CHMP2A* in pyroptosis is largely unclear and deserves further exploration.

According to DEGs between the high-risk group and the low-risk group, functional enrichment analysis in GO/KEGG showed that immune functions or immune-related pathways were highly frequent, such as activation of immune response and adaptive immune response, which meant that the TIM might be the key to the KIRP progression. Then, a high infiltration level of M2 macrophages was observed in the tumor microenvironment of KIRP, which was related to the immunosuppression state. Existing studies have demonstrated tumor-associated M2 macrophages could promote cell proliferation and angiogenesis and accelerate tumor progression (Fan et al., 2021; Xie et al., 2021). This might be a part of reasons that KIRP patients obtained poor therapeutic effect from immune checkpoint inhibitors. The activated M1 macrophages could produce inflammatory cytokines, for example, TNF-α, IL-1, and IL-12, enhance T cell function, and then exert antitumor functions (Yang et al., 2021). Moreover, activated T cells and B cells play protective roles in tumor immunity (Lin et al., 2013). Conversely, regulatory T cells and mast cells exert negative effects in antitumor (Maciel et al., 2015; Hirano, 2021). However, compared with the low-risk group, the tumor-protective immune cells, such as M1 macrophages and CD8 + T cells, were increased in the high-risk group. The TIM is a complex and disordered process in the development of tumor, which needs further research.

To our knowledge, this is the first time to systemically explore the relationship of PRGs and KIRP. The above results might provide novel insights into predicting prognostic, clinical decision-making and future research studies of KIRP. However, some limitations exist in this study. Firstly, the pyroptosis-related risk model in KIRP was constructed based on TCGA database. Due to the lack of appropriate datasets, this risk prognostic model could not be verified by other databases. However, its prognostic value and robustness were proved *via* different methods. Secondly, in the process of constructing this model, we might have excluded other prognostic genes which were not associated with pyroptosis. Finally, although immuno-histochemical staining was performed to validate some differentially expressed PRGs, more fundamental experiments to elucidate the role of these genes were encouraged.

CONCLUSION

In conclusion, a prognostic model based on six PRGs was constructed, which could serve as an independent prognostic factor for KIRP patients. And the level of tumor immune cell infiltration was significantly different between the low-risk group and the high-risk group. Finally, two hub genes were identified and validated *in vitro*. These primary results might provide some useful value for the clinical prognosis and future research studies of KIRP.

DATA AVAILABILITY STATEMENT

The datasets presented in this study can be found in online repositories. The names of the repository/repositories and accession number(s) can be found in the article/ **Supplementary Material**.

ETHICS STATEMENT

Written informed consent was obtained from the individual(s) for the publication of any potentially identifiable images or data included in this article.

AUTHOR CONTRIBUTIONS

JH conceived the study. YC performed bioinformatics analysis and immuno-histochemical staining. JH, PL, and LG wrote this manuscript. PL and XX collected samples. YZ and CG performed quality control. All authors read and approved the final version of this manuscript.

FUNDING

This work was supported by the Innovation Program for Chongqing's Overseas Returnees (2019), High-Level Medical Reserved Personnel Training Project of Chongqing (the 4th batch), and Research Program of Basic Science and Frontier Technology in Chongqing (cstc2017jcyjAX0435).

ACKNOWLEDGMENTS

We appreciate the valuable cooperation of the Department of Pathology of The Second Affiliated Hospital of Chongqing Medical University in acquiring the samples of KIRP.

SUPPLEMENTARY MATERIAL

The Supplementary Material for this article can be found online at: https://www.frontiersin.org/articles/10.3389/fgene.2022.851384/full#supplementary-material

REFERENCES

Block, K. M., Hanke, N. T., Maine, E. A., and Baker, A. F. (2012). IL-6 Stimulates STAT3 and Pim-1 Kinase in Pancreatic Cancer Cell Lines. *Pancreas* 41 (5), 773–781. doi:10.1097/MPA.0b013e31823cdd10

Broz, P., Pelegrín, P., and Shao, F. (2020). The Gasdermins, a Protein Family Executing Cell Death and Inflammation. *Nat. Rev. Immunol.* 20 (3), 143–157. doi:10.1038/s41577-019-0228-2

Brozovich, A., Garmezy, B., Pan, T., Wang, L., Farach-Carson, M. C., and Satcher, R. L. (2021). All Bone Metastases Are Not Created Equal: Revisiting Treatment Resistance in Renal Cell Carcinoma. *J. Bone Oncol.* 31, 100399. doi:10.1016/j.jbo.2021.100399

Chavez-Dominguez, R., Perez-Medina, M., Aguilar-Cazares, D., Galicia-Velasco, M., Meneses-Flores, M., Islas-Vazquez, L., et al. (2021). Old and New Players of Inflammation and Their Relationship with Cancer Development. *Front. Oncol.* 11, 722999. doi:10.3389/fonc.2021.722999

Derangère, V., Chevriaux, A., Courtaut, F., Bruchard, M., Berger, H., Chalmin, F., et al. (2014). Liver X Receptor β Activation Induces Pyroptosis of Human and Murine colon Cancer Cells. *Cell Death Differ* 21 (12), 1914–1924. doi:10.1038/cdd.2014.117

Fan, Y., Dai, F., Yuan, M., Wang, F., Wu, N., Xu, M., et al. (2021). A Construction and Comprehensive Analysis of ceRNA Networks and Infiltrating Immune Cells in Papillary Renal Cell Carcinoma. *Cancer Med.* 10 (22), 8192–8209. doi:10.1002/cam4.4309

Han, J.-H., Park, J., Kang, T.-B., and Lee, K.-H. (2021). Regulation of Caspase-8 Activity at the Crossroads of Pro-inflammation and Anti-inflammation. *Int. J. Mol. Sci.* 22 (7), 3318. doi:10.3390/ijms22073318

Hirano, T. (2021). IL-6 in Inflammation, Autoimmunity and Cancer. *Int. Immunol.* 33 (3), 127–148. doi:10.1093/intimm/dxaa078

Kang, R., Zeng, L., Zhu, S., Xie, Y., Liu, J., Wen, Q., et al. (2018). Lipid Peroxidation Drives Gasdermin D-Mediated Pyroptosis in Lethal Polymicrobial Sepsis. *Cell Host & Microbe* 24 (1), 97–108. e104. doi:10.1016/j.chom.2018.05.009

Karki, R., Sharma, B. R., Lee, E., Banoth, B., Malireddi, R. K. S., Samir, P., et al. (2020). Interferon Regulatory Factor 1 Regulates PANoptosis to Prevent Colorectal Cancer. *JCI Insight* 5 (12), e136720. doi:10.1172/jci.insight.136720

Lin, Y.-C., Mahalingam, J., Chiang, J.-M., Su, P.-J., Chu, Y.-Y., Lai, H.-Y., et al. (2013). Activated but Not Resting Regulatory T Cells Accumulated in Tumor Microenvironment and Correlated with Tumor Progression in Patients with Colorectal Cancer. *Int. J. Cancer* 132 (6), 1341–1350. doi:10.1002/ijc.27784

Lippitz, B. E., and Harris, R. A. (2016). Cytokine Patterns in Cancer Patients: A Review of the Correlation between Interleukin 6 and Prognosis. *Oncoimmunology* 5 (5), e1093722. doi:10.1080/2162402X.2015.1093722

Maciel, T. T., Moura, I. C., and Hermine, O. (2015). The Role of Mast Cells in Cancers. *F1000prime Rep.* 7, 09. doi:10.12703/P7-09

Orning, P., Weng, D., Starheim, K., Ratner, D., Best, Z., Lee, B., et al. (2018). Pathogen Blockade of TAK1 Triggers Caspase-8-dependent Cleavage of Gasdermin D and Cell Death. *Science* 362 (6418), 1064–1069. doi:10.1126/science.aau2818

Qi, L., Xu, R., Wan, L., Ren, X., Zhang, W., Zhang, K., et al. (2021). Identification and Validation of a Novel Pyroptosis-Related Gene Signature for Prognosis Prediction in Soft Tissue Sarcoma. *Front. Genet.* 12, 773373. doi:10.3389/fgene.2021.773373

Roberto, M., Botticelli, A., Panebianco, M., Aschelter, A. M., Gelibter, A., Ciccarese, C., et al. (2021). Metastatic Renal Cell Carcinoma Management: From Molecular Mechanism to Clinical Practice. *Front. Oncol.* 11, 657639. doi:10.3389/fonc.2021.657639

Su, Y., Zhao, A., Chen, A. P., Liu, X. Z., Tian, Y. P., and Jin, J. Y. (2019). Effect of GPX4 on Proliferation and Metastasis of Renal clear Cell Carcinoma and its Relationship with Expression of IGF-1R and COX-2. *Zhonghua Bing Li Xue Za Zhi* 48 (12), 955–960. doi:10.3760/cma.j.issn.0529-5807.2019.12.008

Sung, H., Ferlay, J., Siegel, R. L., Laversanne, M., Soerjomataram, I., Jemal, A., et al. (2021). Global Cancer Statistics 2020: GLOBOCAN Estimates of Incidence and Mortality Worldwide for 36 Cancers in 185 Countries. *CA A. Cancer J. Clin.* 71 (3), 209–249. doi:10.3322/caac.21660

Wang, Y.-Y., Liu, X.-L., and Zhao, R. (2019). Induction of Pyroptosis and its Implications in Cancer Management. *Front. Oncol.* 9, 971. doi:10.3389/fonc.2019.00971

Wang, Y., Gao, W., Shi, X., Ding, J., Liu, W., He, H., et al. (2017). Chemotherapy Drugs Induce Pyroptosis through Caspase-3 Cleavage of a Gasdermin. *Nature* 547 (7661), 99–103. doi:10.1038/nature22393

Xia, X., Wang, X., Cheng, Z., Qin, W., Lei, L., Jiang, J., et al. (2019). The Role of Pyroptosis in Cancer: Pro-cancer or Pro-"host"? *Cell Death Dis* 10 (9), 650. doi:10.1038/s41419-019-1883-8

Xie, X., He, J., Wang, Q., Liu, Y., Chen, W., and Shi, K. (2021). FPR2 Participates in Epithelial Ovarian Cancer (EOC) Progression through RhoA-Mediated M2 Macrophage Polarization. *J. Ovarian Res.* 14 (1), 177. doi:10.1186/s13048-021-00932-8

Yang, G., Lu, S.-B., Li, C., Chen, F., Ni, J.-S., Zha, M., et al. (2021). Type I Macrophage Activator Photosensitizer against Hypoxic Tumors. *Chem. Sci.* 12 (44), 14773–14780. doi:10.1039/d1sc04124j

Yu, J., Li, S., Qi, J., Chen, Z., Wu, Y., Guo, J., et al. (2019). Cleavage of GSDME by Caspase-3 Determines Lobaplatin-Induced Pyroptosis in colon Cancer Cells. *Cel Death Dis* 10 (3), 193. doi:10.1038/s41419-019-1441-4

Yu, P., Zhang, X., Liu, N., Tang, L., Peng, C., and Chen, X. (2021). Pyroptosis: Mechanisms and Diseases. *Sig Transduct Target. Ther.* 6 (1), 128. doi:10.1038/s41392-021-00507-5

Zhou, B., Zhang, J.-y., Liu, X.-s., Chen, H.-z., Ai, Y.-l., Cheng, K., et al. (2018). Tom20 Senses Iron-Activated ROS Signaling to Promote Melanoma Cell Pyroptosis. *Cell Res* 28 (12), 1171–1185. doi:10.1038/s41422-018-0090-y

Zychlinsky, A., Prevost, M. C., and Sansonetti, P. J. (1992). Shigella Flexneri Induces Apoptosis in Infected Macrophages. *Nature* 358 (6382), 167–169. doi:10.1038/358167a0

Conflict of Interest: The authors declare that the research was conducted in the absence of any commercial or financial relationships that could be construed as a potential conflict of interest.

Publisher's Note: All claims expressed in this article are solely those of the authors and do not necessarily represent those of their affiliated organizations, or those of the publisher, the editors, and the reviewers. Any product that may be evaluated in this article, or claim that may be made by its manufacturer, is not guaranteed or endorsed by the publisher.

frontiers | Frontiers in Cell and Developmental Biology

ORIGINAL RESEARCH
published: 13 April 2022
doi: 10.3389/fcell.2022.887385

Expression, Prognostic Value, and Functional Mechanism of the KDM5 Family in Pancreatic Cancer

Yunjie Duan[†], *Yongxing Du*[†], *Zongting Gu, Xiaohao Zheng and Chengfeng Wang**

State Key Lab of Molecular Oncology and Department of Pancreatic and Gastric Surgery, National Cancer Center/National Clinical Research Center for Cancer/Cancer Hospital, Chinese Academy of Medical Sciences and Peking Union Medical College, Beijing, China

Background: The histone lysine demethylase KDM5 family is an important epigenetic state-modifying enzyme family. Increasing evidence supports that epigenetic abnormalities in the KDM5 family are related to multiple cancers in humans. However, the role of the KDM5 family in pancreatic cancer is not clear, and related research is very scarce.

Methods: R software, Kaplan–Meier Plotter, cBioPortal, TIMER, LinkedOmics, STRING, Metascape, TISIDB, and the GSCA Lite online tool were utilized for bioinformatics analysis.

Results: KDM5A/B/C was significantly overexpressed in many kinds of tumor tissues, including pancreatic adenocarcinoma (PAAD), while the expression of KDM5D was significantly downregulated. The high expression of KDM5A/B/C was related to poor clinical features, such as worse treatment efficacy, higher tumor grade, and more advanced clinical stage. Patients with a family history of breast cancer and melanoma, history of drinking or history chronic pancreatitis were more likely to have KDM5A/B/C gene abnormalities, which were related to a variety of adverse clinical features. The results of gene ontology (GO) and kyoto encyclopedia of genes and genomes (KEGG) pathway analyses of the KDM5 family and its 800 co-expressed genes showed that many gene terms related to cell proliferation, migration and many carcinogenic pathways. Notably, we found that the expression level of KDM5A/B/C was positively correlated with the expression of multiple key driver genes such as KRAS, BRCA1, and BRCA2 etc. In addition, PPI network analysis showed KDM5 family proteins have strong interactions with histone deacetylase family 1 (HDAC1), which could modify the lysines of histone H3, and co-act on many pathways, including the "longevity-regulating pathway" and "Notch signaling pathway". Moreover, the upregulation of KDM5A/B/C expression was associated with an increase in the infiltration of B cells, $CD8^+$ T cells and other infiltrating immune lymphocytes and the expression levels of immune molecules such

OPEN ACCESS

Edited by:
Xiao Zhu,
Guangdong Medical University, China

Reviewed by:
Chengcheng Wang,
Peking Union Medical College Hospital (CAMS), China
Juntao Gao,
Tsinghua University, China

***Correspondence:**
Chengfeng Wang
wangchengfeng62@163.com

[†]*These authors have contributed equally to this work*

Specialty section:
This article was submitted to Epigenomics and Epigenetics, a section of the journal Frontiers in Cell and Developmental Biology

Received: *01 March 2022*
Accepted: *24 March 2022*
Published: *13 April 2022*

Citation:
Duan Y, Du Y, Gu Z, Zheng X and Wang C (2022) Expression, Prognostic Value, and Functional Mechanism of the KDM5 Family in Pancreatic Cancer. Front. Cell Dev. Biol. 10:887385. doi: 10.3389/fcell.2022.887385

Abbreviations: PAAD, Pancreatic adenocarcinoma; FOLFIRINOX:5-fluorouracil, leucovorin, irinotecan, and oxaliplatin; GNP, Gemcitabine and naphthaclitaxel; TCGA, The cancer genome atlas; GTEx, Genotype-tissue expression; OS, Overall survival; RFS, Relapse free survival; DFS, Disease-free survival; GO, Gene ontology; KEGG, Kyoto encyclopedia of genes and genomes; DNA, Deoxyribonucleic acid; RNA, Ribonucleic acid; NSCLC, Non-small cell lung cancer; EMT, Epithelial-mesenchymal transformation; HDAC, Histone deacetylase family; PPI, Protein-protein interaction; BP, Biological process; CC, Cellular composition; MF, Molecular function; BRCA, Breast invasive carcinoma; STAD, Stomach adenocarcinoma; ACC, Adrenocortical carcinoma; SKCM, Skin cutaneous melanoma; PRAD, Prostate adenocarcinoma; Bak1, BCL2-antagonist/killer 1.

as NT5E and CD274. Interestingly, the overexpression of KDM5A/C was also corelated with reduced sensitivity of pancreatic cancer cells to many kinds of pancreatic cancer-targeting or chemotherapeutic drugs, including axitinib and gemcitabine.

Conclusion: KDM5 family members may be prognostic markers and new therapeutic targets for patients with pancreatic cancer.

Keywords: pancreatic cancer, prognostic markers, KDM5 family, bioinformatics analysis, pathogenesis introduction

INTRODUCTION

Pancreatic cancer has attracted wide attention because of its unusually high mortality rate, and pancreatic cancer ranks fourth or fifth among causes of cancer-related death in most developed countries. At the beginning of the 21st century, the estimated number of pancreatic cancer cases in the world was 1,10,000, and the global mortality rate was estimated at 98% (Parkin et al., 2001). In 2021, an estimated 60,430 people will be diagnosed with pancreatic cancer in the United States alone, and approximately 48,220 are expected to die from the disease (Siegel et al., 2021). Currently, pancreatic cancer is the fourth most common cause of cancer-related death in men (after lung, prostate and colorectal cancer) and women (after lung, breast and colorectal cancer) in the United States (Siegel et al., 2021). Surgery and adjuvant therapy are cornerstones of the treatment of pancreatic cancer. Resection does lead to a 5-years survival rate of approximately 20%, but only 10% of patients can undergo pancreatic cancer resection due to the presence of widespread locally advanced lesions or metastases (Raimondi et al., 2009). However, even after radical resection, most patients experience relapse. Multimodal therapy based on a combination of neoadjuvant therapy, chemotherapy, radiotherapy, immunotherapy, and surgery seems to be an important strategy for improving prognosis (Neoptolemos et al., 2018), but the vast majority of pancreatic cancer patients are treated with current systemic chemotherapy regimens (FOLFIRINOX: 5-fluorouracil, leucovorin, irinotecan, and oxaliplatin; GNP: gemcitabine and nab paclitaxel). Chemotherapy resistance is an important factor affecting the efficacy of multidisciplinary therapy (Von Hoff et al., 2013), and thus, the prognosis of pancreatic cancer remains poor. Therefore, there is an urgent need to clarify the specific mechanisms of the occurrence and development of pancreatic cancer and chemotherapy resistance, develop new targeted drugs and prognostic markers, improve the efficacy of multidisciplinary comprehensive treatment, and prolong the survival time of patients with pancreatic cancer.

Stable inheritance of epigenetic state is essential for maintaining the specific functions of tissue and cell types. Previous studies have shown that epigenetic aberrations play an important role in the occurrence and development of tumors (Feinberg et al., 2006). Research on the function of epigenetic state-modifying enzymes has become a hot topic in tumor therapy. In eukaryotes, deoxyribonucleic acid (DNA) is packaged in the form of chromatin (Kornberg, 1974). The basic component of chromatin is the nucleosome, which consists of 146 bp of DNA wrapped on octamers of the four core histones (H2A, H2B, H3, and H4) (Luger et al., 1997). Histone tails are subjected to a variety of posttranslational modifications, including acetylation, methylation, phosphorylation, ubiquitin and SUMOylation (Shilatifard, 2006) which affect chromatin structure, thus affecting gene expression and DNA repair. Abnormal histone demethylation can lead to excessive cell proliferation, which leads to tumorigenesis and has been shown to be associated with many cancers (Cao et al., 2002; Milne et al., 2002; Nakamura et al., 2002; Yokoyama et al., 2004). The KDM5 family of histone lysine demethylases is an important family of epigenetic state-modifying enzymes that contain five conserved domains: JmjN, ARID, JmjC, PhD, and a C5HC2 zinc finger (Blair et al., 2011) and can specifically catalyze the trimethylation, dimethylation and monomethylated lysine 4 demethylation of histone H3, thus playing a central role in histone coding (Zhang et al., 2014; Johansson et al., 2016; Tumber et al., 2017). The family includes lysine demethylase 5A (KDM5A), lysine demethylase 5B (KDM5B), lysine demethylase 5C (KDM5C), and lysine demethylase 5D (KDM5D). Many studies have reported the role of the KDM5 family in the occurrence and development of many cancers. KDM5A is closely related to breast cancer, prostate cancer, ovarian cancer and small-cell lung cancer (Hou et al., 2012; Feng et al., 2017; Oser et al., 2019; Du et al., 2020). The expression of KDM5B promotes the invasiveness of non-small-cell lung cancer (NSCLC) (Kuo et al., 2018). Furthermore, increased expression of KDM5B promotes the growth of liver cancer cells and maintains chronic myeloid leukemia through multiple epigenetic effects (Gong et al., 2018; Xue et al., 2020). KDM5C is overexpressed in prostate cancer. It is a prognostic marker of prostate-specific antigen recurrence after radical prostatectomy (Stein et al., 2014). In contrast, KDM5D inhibits the invasion and metastasis of prostate cancer, and its overexpression can reduce the invasive ability of gastric cancer (Li et al., 2016; Gu and Chu, 2021). However, the role of the KDM5 family in pancreatic cancer is not clear, and related research is very scarce.

As such, this study analyzed data related to KDM5 family members in pancreatic cancer. First, we compared KDM5 family member expression and prognosis between pancreatic cancer samples and matched normal pancreatic tissues with The Cancer Genome Atlas (TCGA) and Genotype-Tissue Expression (GTEx) databases and further studied the possible mechanism by which the family members participate in the occurrence and development of

pancreatic cancer through gene mutation, protein interaction, functional enrichment, and immune infiltration analyses. In addition, we used different databases to verify the results. The findings of this study will help to identify potential diagnostic markers and new treatment targets and ultimately improve the efficacy of multimodal comprehensive treatment of pancreatic cancer.

MATERIALS AND METHODS

Ethical Statement

This study was approved by the Academic Committee of Cancer Hospital of Chinese Academy of Medical Sciences and carried out in strict accordance with the principles of the Helsinki Declaration. The data in this study were retrieved from online databases, all necessary written informed consent forms were obtained, and no human or animal experiments were performed.

Expression Analysis

In this study, R (version3.6.3) was used to analyze the expression level (https://xenabrowser.net/datapages/) of the KDM5 family in tumor and paracancerous tissues in the PAAD TCGA cohort and normal pancreatic tissue in the GTEx database, and visualized with ggplot2 (3.3.3). The statistical significance of the differential expression was evaluated by the Wilcoxon test. To analyze the correlation between the gene expression levels of KDM5 family members and clinical variables, we used the R (version 3.6.3) to analyze PAAD samples from the TCGA database (https://portal.gdc.cancer.gov/). The statistical significance of the differential expression was evaluated by Fisher's test.

Gene Mutation Analysis

We used cBioPortal (https://www.cbioportal.org/) (Gao et al., 2013) to analyze the gene mutation of KDM5 family members in pancreatic cancer and further determined the correlation of these mutations with important clinicopathological factors. The statistical significance of the difference was evaluated by the chi-squared test. Furthermore, the log-rank test was used to evaluate the relationship between KDM5 family gene mutations and overall survival (OS) and disease-free survival (DFS) in patients with pancreatic cancer.

Survival Analysis

We used Kaplan–Meier Plotter (http://kmplot.com/analysis/) (Győrffy et al., 2013) to analyze the correlation between the expression of KDM5 family genes and OS and relapse-free survival (RFS) in pancreatic cancer. The cutoff for low expression versus high expression was set as the value automatically selected by the best cutoff model, and the array with deviation was excluded. The log rank test was used to calculate the p value ($p < 0.05$).

Correlation and Interaction Analyses

We used TIMER (http://timer.cistrome.org/) (Li et al., 2017) to analyze the correlations of KDM5 family gene expression in pancreatic cancer, and the statistical significance was evaluated by Spearman's test. LinkedOmics (http://www.linkedomics.org/) (Vasaikar et al., 2018) was used to assess and draw a volcano plot of the correlations between KDM5 family members and 800 coexpressed genes in pancreatic cancer and a heatmap of the top 50 positively/negatively related genes. The genes with the strongest interaction with KDM5 family proteins were determined by combined score analysis via STRING (https://string-db.org/) (Szklarczyk et al., 2015), and the corresponding protein-protein interaction (PPI) network was constructed by STRING.

Gene Annotation

The first 10 motifs with positive and negative correlations with the expression of each member of the KDM5 family were functionally annotated (https://www.genecards.org/) by GeneCards.

Functional Enrichment Analysis

We used Metascape (https://metascape.org) (Zhou et al., 2019) to visualize the enriched biological process (BP), cellular composition (CC), molecular function (MF) and KEGG pathway terms of the KDM5 family and its coexpressed genes. Furthermore, the R (version 3.6.3) and clusterProfiler package (version 3.14.3) were used to visualize the enriched BP, CC, MF, and KEGG pathway terms of the 9 genes with the strongest interaction with KDM5 family proteins.

Immune Infiltration Analysis

We used TIMER to analyze the correlation between the expression level of the KDM5 family and the degree of lymphocyte infiltration. The statistical significance of the difference was evaluated by Spearman's test. In addition, TISIDB (http://cis.hku.hk/TISIDB/) (Ru et al., 2019) was also used to analyze the correlation between KDM5 family expression and the expression of immune molecules in pancreatic cancer. The difference was evaluated by Spearman's test. We used the GSCA Lite online tool (http://bioinfo.life.hust.edu.cn/web/GSCALite/) (Liu et al., 2018) to analyze the correlation between KDM5 family expression and sensitivity to current chemotherapeutic or targeted drugs for pancreatic cancer. The difference was evaluated by Spearman's test.

RESULTS

Abnormal Expression of the KDM5 Family in Pancancer and PAAD Patients

We used the R (version 3.6.3) to analyze the expression level of the KDM5 family in tumor and paracancerous tissues in TCGA and normal tissues in GTEx. The analysis of gene expression levels showed that KDM5 family genes were upregulated or downregulated in tumors compared with normal or paracancerous tissues in each type of cancer. Compared with that in paracancerous tissues or normal tissues, the expression of KDM5A/B/C was significantly increased in 12 kinds of

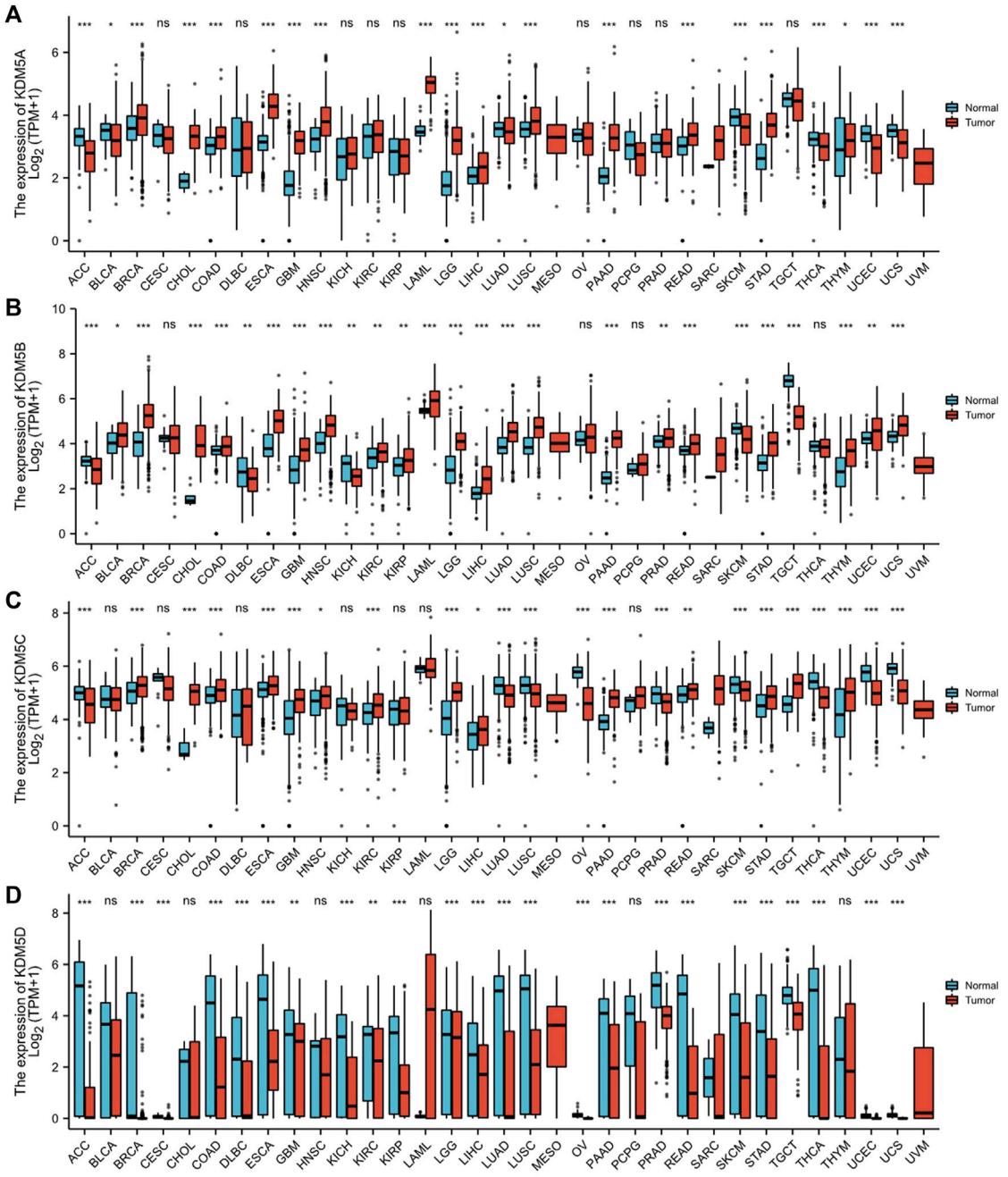

FIGURE 1 | The expression level of the KDM5 family in different tumor tissues and paracancerous tissues in the TCGA database and normal tissues in the GTEx database. **(A)** The expression level of KDM5A; **(B)** The expression level of KDM5B; **(C)** The expression level of KDM5C; **(D)**The expression level of KDM5D. ns, $p \geq 0.05$; *, $p < 0.05$; **, $p < 0.01$; ***, $p < 0.001$.

tumor tissues, such as PAAD, breast invasive carcinoma (BRCA) and stomach adenocarcinoma (STAD), but significantly downregulated in only adrenocortical carcinoma (ACC) and skin cutaneous melanoma (SKCM) (**Figures 1A–C**). In contrast, the expression of KDM5D was significantly decreased in 24 kinds of tumor tissues, such as PAAD, BRCA, and prostate adenocarcinoma (PRAD) (**Figure 1D**). In summary, our results show that KDM5A/B/C is significantly overexpressed in a variety of tumor tissues, including PAAD, while the expression of KDM5D is significantly downregulated, indicating that the expression of KDM5 family members is closely related to the occurrence and

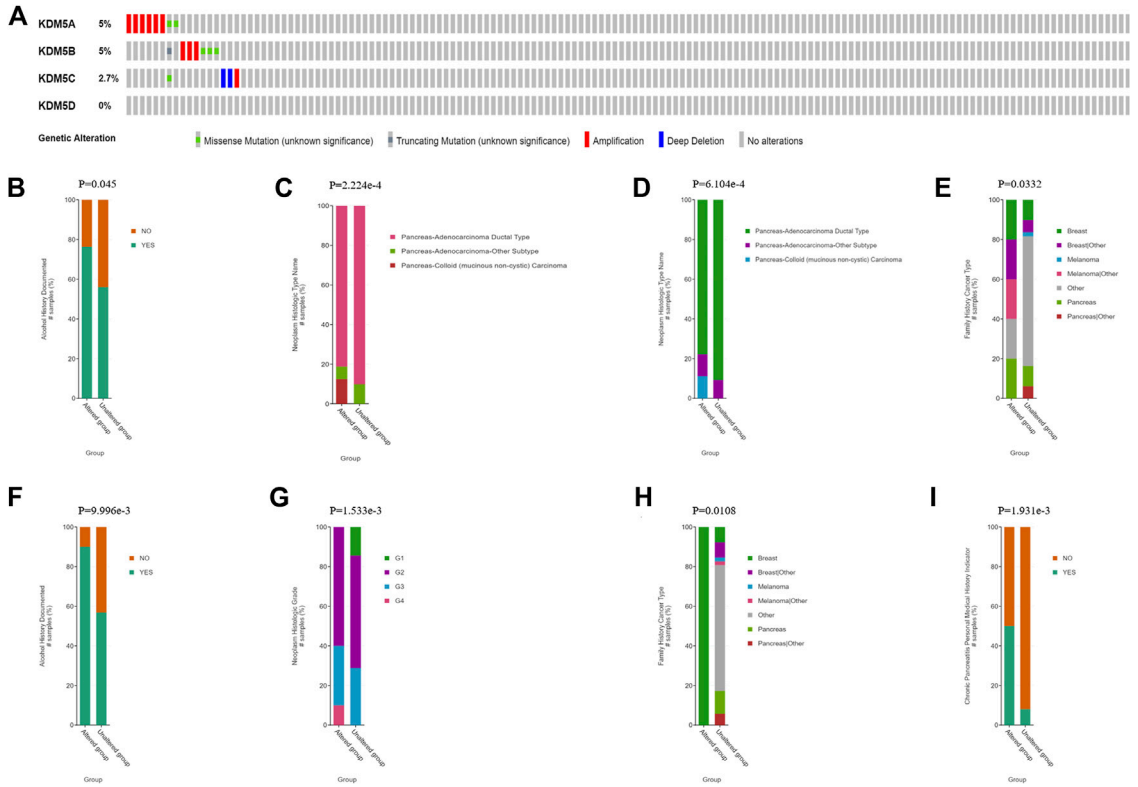

FIGURE 2 | KDM5 family gene mutations and clinical and prognostic characteristics in patients with PAAD. **(A)** KDM5 family mutations in pancreatic cancer; **(B)** Pancreatic cancer patients with a history of drinking are more likely to undergo KDM5 family gene mutation; **(C)** Pancreatic mucinous adenocarcinoma patients are more likely to undergo KDM5 family genes mutation; **(D)** Pancreatic cancer patients with a family history of breast cancer and melanoma are more likely to undergo KDM5A gene mutation; **(E)** Pancreatic mucinous adenocarcinoma patients are more likely to undergo KDM5A gene mutation; **(F)** Pancreatic cancer patients with a history of drinking are more likely to undergo KDM5B gene mutation; **(G)** Pancreatic cancer patients with a family history of breast cancer are more likely to undergo KDM5C gene mutation; **(H)** Pancreatic cancer patients with a history of chronic pancreatitis are more likely to undergo KDM5C gene mutation; **(I)** Pancreatic cancer patients with a higher pancreatic cancer tumor grade are more likely to undergo KDM5C gene mutation.

development of many kinds of human malignant tumors, including pancreatic cancer.

KDM5 Family Mutations and Their Correlation With Clinicopathological and Prognostic Features in Patients With PAAD

To further explore the mechanism of differential expression of the KDM5 family in pancreatic cancer, we used the cBioPortal online tool to analyze the gene mutations of the KD

M5 family. The KDM5 family had two or more types of gene variants in 17 samples (11%) from pancreatic cancer patients (**Figure 2A**). The most common variant was in the KDM5A/B gene (5%). The main types of variants were amplification and missense mutations. In addition, 2.7% of the variants occurred in KDM5C, and the most common type of variant was deep deletion, while no related mutations were detected in the KDM5D gene. Then, we comprehensively analyzed the clinical and pathological features of patients with KDM5 family gene mutations and those without mutations. The results showed that patients with a history of drinking and pancreatic cancer with mucinous adenocarcinoma were more likely to develop KDM5 family gene mutation (**Figures 2B,C**). Next, we analyzed the independent relationship between KDM5A/B/C gene mutation and clinicopathological features. The results showed that most of the patients with KDM5A gene mutation had a family history of breast cancer and melanoma or a pathological pancreatic cancer subtype of pancreatic mucinous adenocarcinoma (**Figures 2D,E**). Most of the patients with KDM5B gene mutation had a history of drinking (**Figure 2F**), and most of the patients with KDM5C gene mutation had a family history of breast cancer, a history of chronic pancreatitis and a higher pancreatic cancer tumor grade (**Figures 2G–I**). In the analysis of the prognostic characteristics of patients with KDM5 family gene mutation and those without mutation, it was not found that KDM5 family gene mutation had a significant effect on OS (**Supplementary Figure S1A**) and DFS (**Supplementary Figure S1B**) in patients with pancreatic cancer, which may have been related to the small sample size of patients. In summary, the frequency of KDM5A/B/C gene mutations was higher in patients with pancreatic cancer, while patients with a history of drinking, a family history of breast cancer, and a family history of melanoma or a history of chronic pancreatitis were more likely to develop KDM5A/B/C mutations. These mutations

TABLE 1 | Relationship Between KDM5 family member expression and clinicopathological features in the PAAD cohort.

Variable	Number (%) (*n* = 178)	KDM5A expression		*p*-value	KDM5B expression		*p*-value	KDM5C expression		*p*-value	KDM5D expression		*p*-value
		High (%) (*n* = 89)	Low (%) (*n* = 89)		High (%) (*n* = 89)	Low (%) (*n* = 89)		High (%) (*n* = 89)	Low (%) (*n* = 89)		High (%) (*n* = 89)	Low (%) (*n* = 89)	
Age (years) ≤65 > 65	93 (52.25)	51 (57.30)	42 (47.19)	0.230	54 (60.67)	39 (43.82)	0.036*	53 (59.55)	40 (44.94)	0.072	43 (48.31)	50 (56.18)	0.368
	85 (47.75)	38 (42.70)	47 (52.81)		35 (39.33)	50 (56.18)		36 (40.45)	49 (55.06)		46 (51.69)	39 (43.82)	
Gender	80 (44.94)	35 (39.33)	45 (50.56)	0.175	34 (38.20)	46 (51.69)	0.097	61 (68.54)	19 (21.35)	<0.001*	0 (0.00)	80 (89.89)	<0.001*
Female													
Male	98 (55.06)	54 (60.67)	44 (49.44)		55 (61.80)	43 (48.31)		28 (31.46)	70 (78.65)		89 (1.00)	9 (10.11)	
Race	11 (6.18)	6 (6.74)	8 (8.99)	0.685	9 (10.11)	3 (3.37)	0.057	8 (8.99)	4 (4.49)	0.412	4 (4.49)	8 (8.99)	0.580
Asian	6 (3.37)	4 (4.49)	3 (3.37)		6 (6.74)	1 (1.12)		5 (5.62)	2 (2.25)		3 (3.37)	4 (4.49)	
Black or African American	161 (90.45)	79 (88.76)	78 (87.64)		74 (83.15)	85 (95.51)		76 (85.39)	83 (93.26)		82 (92.13)	77 (86.52)	
White													
Smoker	82 (46.07)	36 (40.45)	46 (51.69)	0.149	35 (39.33)	47 (52.81)	0.088	43 (48.31)	39 (43.82)	0.627	34 (38.20)	48 (53.93)	0.041*
No													
Yes	96 (53.93)	53 (59.55)	43 (48.31)		54 (60.67)	42 (47.19)		46 (51.69)	50 (56.18)		55 (61.80)	41 (46.07)	
Alcohol history													
No	71 (39.89)	39 (43.82)	32 (35.96)	0.376	36 (40.45)	35 (39.33)	1.000	36 (40.45)	35 (39.33)	1.000	37 (41.57)	34 (38.20)	0.750
Yes	107 (60.11)	50 (56.18)	57 (64.04)		53 (59.55)	54 (60.67)		53 (59.55)	54 (60.67)		52 (58.43)	55 (61.80)	
History of diabetes	124 (69.66)	59 (66.29)	65 (73.03)	0.688	68 (76.40)	56 (62.92)	0.038*	67 (75.28)	58 (65.17)	0.075	59 (66.29)	65 (73.03)	0.346
No													
Yes	54 (30.34)	30 (33.71)	24 (26.97)		21 (23.60)	33 (37.08)		22 (24.72)	31 (34.83)		30 (33.71)	24 (26.97)	
History of chronic pancreatitis	150 (84.27)	72 (80.90)	74 (83.15)	1.000	70 (78.65)	77 (86.52)	0.076	72 (80.90)	75 (84.27)	0.893	76 (85.39)	71 (79.78)	0.507
No													
Yes	28 (15.73)	17 (19.10)	15 (16.85)		19 (21.35)	12 (13.48)		17 (19.10)	14 (15.73)		13 (14.61)	18 (20.22)	
Family history of cancer	81 (45.51)	43 (48.31)	37 (41.57)	0.408	43 (48.31)	37 (41.57)	0.408	38 (42.70)	42 (47.19)	0.544	42 (47.19)	38 (42.70)	0.621
No													
Yes	97 (54.49)	46 (51.59)	52 (58.43)		46 (51.69)	52 (59.43)		51 (57.30)	47 (52.81)		47 (52.81)	51 (57.30)	
Anatomic neoplasm subdivision	138 (77.53)	73 (82.02)	65 (73.03)	0.209	66 (74.16)	72 (80.90)	0.369	67 (75.28)	71 (79.78)	0.590	71 (79.78)	67 (75.28)	0.590
Head of Pancreas	40 (22.47)	16 (17.98)	24 (26.97)		23 (25.84)	17 (19.10)		22 (24.72)	18 (20.22)		18 (20.22)	22 (24.72)	
Other													
Primary therapy outcome	58 (32.58)	34 (38.2)	25 (28.09)	0.037*	34 (38.20)	25 (28.09)	0.371	29 (32.58)	30 (33.71)	0.200	33 (37.08)	26 (29.21)	0.548
PD													
SD	19 (10.67)	5 (5.62)	14 (15.73)		9 (10.11)	9 (10.11)		11 (12.36)	7 (7.87)		6 (6.74)	12 (13.48)	
PR	20 (11.24)	8 (8.99)	11 (12.36)		9 (10.11)	10 (11.24)		7 (7.87)	13 (14.61)		9 (10.11)	11 (12.36)	
CR	81 (45.51)	42 (47.19)	39 (43.82)		37 (41.57)	45 (50.56)		42 (47.19)	39 (43.82)		41 (46.07)	40 (44.94)	
Radiation therapy	126 (70.79)	68 (76.40)	58 (65.17)	0.108	66 (74.16)	60 (67.42)	0.365	59 (66.29)	67 (75.28)	0.298	65 (73.03)	61 (68.54)	0.620
No													
Yes	52 (29.21)	21 (23.60)	31 (34.83)		23 (25.84)	29 (32.58)		30 (33.71)	22 (24.72)		24 (26.97)	28 (31.46)	
Residual tumor	112 (62.92)	55 (61.80)	58 (65.17)	0.265	55 (61.80)	58 (65.17)	0.914	51 (57.30)	61 (68.54)	0.378	56 (62.92)	57 (64.04)	0.915
R0													
R1	57 (32.02)	32 (35.96)	25 (28.09)		28 (31.46)	28 (31.46)		32 (35.96)	25 (28.09)		30 (33.71)	28 (31.46)	
R2	9 (5.06)	2 (2.25)	6 (6.74)		6 (6.74)	3 (3.37)		6 (6.74)	3 (3.37)		3 (3.37)	4 (4.49)	
Histologic grade	31 (17.42)	12 (13.48)	19 (21.35)	0.019*	11 (12.36)	21 (23.60)	0.048*	14 (15.73)	17 (19.10)	0.938	12 (13.48)	20 (22.47)	0.080
G1													
G2	96 (53.93)	45 (50.56)	52 (58.43)		48 (53.93)	48 (53.93)		49 (55.06)	48 (53.93)		47 (52.81)	49 (55.06)	
G3	49 (27.53)	32 (35.96)	16 (17.98)		30 (33.71)	18 (20.22)		25 (28.09)	23 (25.84)		30 (33.71)	18 (20.22)	
G4	2 (1.12)	0 (0.00)	2 (2.25)		0 (0.00)	2 (2.25)		1 (1.12)	1 (1.12)		0 (0.00)	2 (2.25)	
Pathologic stage	22 (12.36)	9 (10.11)	13 (14.61)	0.171	5 (5.62)	17 (19.10)	0.004*	13 (14.61)	9 (10.11)	0.252	8 (8.99)	14 (15.73)	0.261
Stage I													

(Continued on following page)

TABLE 1 | (*Continued*) Relationship Between KDM5 family member expression and clinicopathological features in the PAAD cohort.

Variable	Number (%) (*n* = 178)	KDM5A expression		*p*-value	KDM5B expression		*p*-value	KDM5C expression		*p*-value	KDM5D expression		*p*-value
		High (%) (*n* = 89)	Low (%) (*n* = 89)		High (%) (*n* = 89)	Low (%) (*n* = 89)		High (%) (*n* = 89)	Low (%) (*n* = 89)		High (%) (*n* = 89)	Low (%) (*n* = 89)	
Stage II	147 (82.58)	76 (85.39)	72 (80.90)		80 (89.89)	68 (76.40)		73 (82.02)	75 (84.27)		79 (88.76)	69 (77.53)	
Stage III	3 (1.69)	0 (0.00)	3 (3.37)		0 (0.00)	3 (3.37)		0 (0.00)	3 (3.37)		1 (1.12)	2 (2.25)	
Stage IV	6 (3.37)	4 (4.49)	1 (1.12)		4 (4.49)	1 (1.12)		3 (3.37)	2 (2.25)		1 (1.12)	4 (4.49)	
T stage	7 (3.93)	4 (4.49)	3 (3.37)	0.143	3 (3.37)	4 (4.49)	0.020*	3 (3.37)	4 (4.49)	0.343	4 (4.49)	3 (3.37)	0.893
T1	25 (14.04)	9 (10.11)	16 (17.98)		7 (7.87)	18 (20.22)		14 (15.73)	11 (12.36)		11 (12.36)	13 (14.61)	
T2	143 (80.34)	76 (85.39)	67 (75.28)		79 (88.76)	64 (71.91)		72 (80.90)	71 (79.78)		73 (82.02)	71 (79.78)	
T3	3 (1.69)	0 (0.00)	3 (3.37)		0 (0.00)	3 (3.37)		0 (0.00)	3 (3.37)		1 (1.12)	2 (2.25)	
T4	52 (29.21)	26 (29.21)	26 (29.21)	1.000	26 (29.21)	27 (30.34)	1.000	23 (25.84)	29 (32.58)	0.429	26 (29.21)	26 (29.21)	1.000
N stage													
N0	126 (70.79)	63 (70.79)	63 (70.79)		63 (70.79)	62 (69.66)		66 (74.16)	60 (67.42)		63 (70.79)	63 (70.79)	
N1	126 (70.79)	65 (73.03)	61 (68.54)	0.396	65 (73.03)	62 (69.66)	0.386	63 (70.79)	64 (71.91)	1.000	63 (70.79)	63 (70.79)	0.366
M stage													
M0	52 (29.21)	24 (26.97)	28 (31.46)		24 (26.97)	27 (30.34)		26 (29.21)	25 (28.09)		26 (29.21)	26 (29.21)	
M1													

may lead to more malignant and higher-grade tumors. However, the effect of KDM5A/B/C gene mutation on the prognosis of patients with pancreatic cancer needs to be further clarified in studies with a large sample size.

Correlation Between KDM5 Family Gene Expression and Clinical and Prognostic Characteristics in Patients With PAAD

To analyze the correlation between the gene expression levels of KDM5 family members and clinical variables, we used the basic R package (version 3.6.3) to analyze the samples of the PAAD cohort in the TCGA database. As shown in **Table 1**, high expression of KDM5A was significantly associated with poorer treatment efficacy ($p = 0.037$) and higher tumor grade ($p = 0.019$). High expression of KDM5B was significantly correlated with age ≤65 years old ($p = 0.036$), no history of diabetes ($p = 0.038$), higher tumor grade ($p = 0.048$), more advanced clinical stage ($p = 0.004$), and more advanced T stage ($p = 0.020$). High expression of KDM5C was significantly correlated with female sex ($p < 0.001$). High expression of KDM5D was significantly correlated with male sex ($p < 0.001$) and smoking history ($p = 0.041$). The results of this study suggest that the high expression levels of KDM5A and KDM5B can increase the degree of malignancy of PAAD and lead to a worse prognosis of patients, further confirming that members of KDM5 family may be oncogenes of PAAD. Next, we analyzed the correlation between the expression levels of KDM5 family genes and prognosis in patients with pancreatic cancer via Kaplan–-Meier Plotter. The results showed that upregulated expression of KDM5A was associated with shorter OS and RFS (**Figures 3A,B**). Downregulation of KDM5D expression was significantly correlated with shorter OS and RFS (**Figures 3A,B**). In addition, although there was a lack of consistent significance in the associations with OS and RFS, overexpression of KDM5B and KDM5C was significantly associated with shorter OS and shorter RFS, respectively (**Figures 3A,B**). The above data show that abnormal expression of the KDM5 family can be used as a biomarker to predict the prognosis of patients with pancreatic cancer, which is worthy of further experimental data verification.

Enrichment Analysis of the KDM5 Family and 800 Co-Expressed Genes in Patients With PAAD

To explore the interaction between KDM5 family genes and their co-expressed genes in pancreatic cancer, 800 co-expressed genes of the KDM5 family in pancreatic cancer were obtained from the LinkedOmics database (**Supplementary Material S1**), and a volcano plot of the KDM5 family and co-expressed genes in pancreatic cancer was drawn (**Figure 4A**). Then, we analyzed the GO and KEGG pathway terms of these 800 genes using the Metascape database. To study the functional mechanism of the KDM5 family in the occurrence and development of pancreatic cancer, GO analysis was performed. The results showed significant enrichment of the BP terms “peptide metabolic process”, “chromatin organization”, and “cellular response to

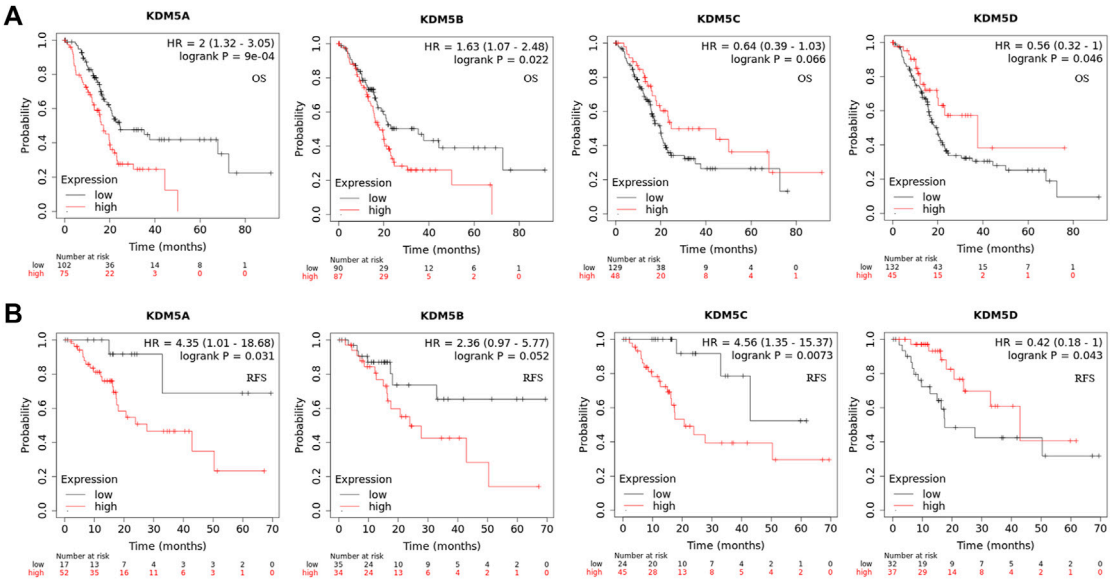

FIGURE 3 | Gene expression level of and prognostic characteristics associated with the KDM5 family in patients with PAAD. **(A)** Upregulated expression of KDM5A is associated with shorter OS/Downregulation of KDM5D expression is significantly correlated with shorter OS; **(B)** Upregulated expression of KDM5A is associated with shorter RFS/Downregulation of KDM5D expression is significantly correlated with shorter RFS.

DNA damage stimulus" (**Figure 4B**). The enriched CC terms mainly included "cytosolic ribosome", "transferase complex" and "mitochondrial envelope" (**Figure 4C**). The enriched MF terms mainly included "structural constituent of ribosome", "chromatin binding", and "transcription factor binding" (**Figure 4D**). The KEGG pathway analysis showed that the target genes were mainly associated with the terms "ribosome", "chemical carcinogenesis—reactive oxygen species", and "transcriptional misregulation in cancer" (**Figure 4E**). To further analyze the mechanisms of the KDM5 family and its coexpressed genes, the top 50 genes with a positive correlation (**Figure 5A**) and the top 50 genes with a negative correlation (**Figure 5B**) with KDM5 family genes were visualized in a heatmap. GeneCards was used to annotate the top 10 genes positively related to the expression of KDM5A/B/C and the first 10 genes negatively related to the expression of KDM5D. The results showed that the functions of related genes included transcriptional regulation (DDI2, ASXL2, CCNT1, CNOT1, REST, TRIM44, IRF6, KDM6A, EIF1AX, DDX3X, TSIX, ZFX, TXLNG, KRAS, GPATCH2, and ZRSR2), protein modification (WNK1, UBXN7, RAPGEF6, CHML, WDR26, and SYAP1), DNA damage repair (SMC1A), cell cycle regulation (TP53BP2), and cell migration regulation (F11R). Then, the top 10 genes negatively related to the expression of KDM5A/B/C and the top 10 genes positively related to the expression of KDM5D were functionally annotated. The results showed that the functions of the genes included transcriptional regulation (DDX3Y, ZFY, and RPS4Y1), protein modification (USP9Y and UTY), translation regulation (EIF1AY and RPS4Y1), cell cycle regulation (GADD45GIP1), cell migration regulation (NLGN4Y), cell proliferation regulation (TMSB4Y, TP53I13, EGFL7, and TSPAN33) and apoptosis regulation (DPP7). Notably, our analysis showed that the KRAS gene was positively related to the expression of KDM5B (**Figure 5A**). KRAS can induce transcriptional silencing of tumor suppressor genes, and its mutations produce modified proteins that drive the occurrence and development of pancreatic cancer (Asimgil et al., 2022). This correlation further suggested that the KDM5 family plays a unique role in malignant tumors driven by KRAS mutations, including pancreatic cancer. At the same time, this important finding inspired us to analyze the correlation between the expression of KDM5 family genes and other pathogenic genes in pancreatic cancer. We used the R (version 3.6.3) to analyze the TCGA PAAD data. The results showed that the expression level of KDM5A/B/C was positively correlated with the expression of KRAS, BRCA1, BRCA2, ATM, SLC16A4, and RABL3. We speculated that although some of the genes known to be pathogenic in pancreatic cancer were not in the top 50 genes positively correlated with the expression of KDM5 family genes, they may still have a co-expression relationship with the KDM5 family. Furthermore, it is suggested that the KDM5 family may play an important role in the pathogenesis of pancreatic cancer. Finally, we used the TIMER database to analyze the relationships among the members of the KDM5 family, and the results showed that the expression of each member was significantly positively correlated: the correlation between KDM5A and KDM5B was the strongest (cor = 0.594) (**Figure 5D**). According to the above results, we speculated that members of the KDM5 family can cooperate with a variety of pathogenic genes, transcriptional regulatory factors, protein-modifying factors, DNA damage repair factors, cell cycle regulatory factors, and cell migration regulatory factors in pancreatic cancer, including factors related to the terms

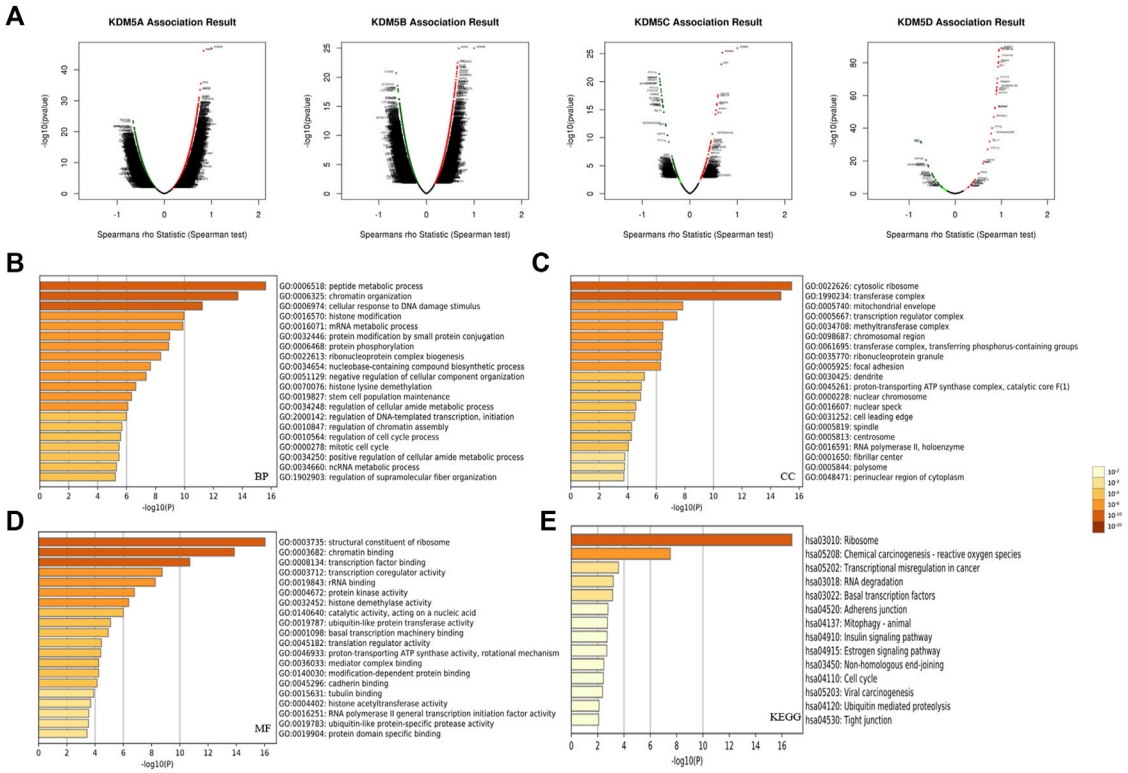

FIGURE 4 | Functional enrichment analysis of the KDM5 family and its 800 co-expressed genes in patients with PAAD. **(A)** A volcano plot of the KDM5 family and its co-expressed genes in pancreatic cancer; **(B)** The GO enrichment of the BP terms of 800 co-expressed genes; **(C)** The GO enrichment of the CC terms of 800 co-expressed genes; **(D)** The GO enrichment of the MF terms of 800 co-expressed genes; **(E)** The KEGG enrichment of the 800 co-expressed genes.

"chemical carcinogenesis—reactive oxygen species", and "transcriptional misregulation in cancer", to participate in the occurrence and development of pancreatic cancer.

Gene Enrichment Analysis of KDM5 Family Genes and PPI Network Members in PAAD

To explore the PPIs between KDM5 family genes and related genes in pancreatic cancer, we analyzed the protein expression of members of the KDM5 family and related genes using the STRING database (**Supplementary Material S2**). The nine genes with the strongest protein-protein interaction (PPI) with KDM5 family members were determined. We analyzed the PPI network related to the KDM5 family expression in pancreatic cancer. The PPI network included 9 gene nodes and 24 edges (**Figure 6A**). The results showed that the protein expression of KDM5A/B/C was closely related to that of HDAC1. The protein encoded by HDAC1 can deacetylate part of the lysine residue of histone H3 and plays an important role in transcriptional regulation and cell proliferation (Cai et al., 2000). The proteins encoded by the KDM5 family play a role in the regulation of gene expression through the specific demethylation of histone H3 lysine 4 (Zhang et al., 2014). Both proteins act on histone H3 lysines, suggesting that they may have a synergistic effect in the regulation of gene expression. Next, we used the R (version 3.6.3) to analyze the GO and KEGG pathway terms of the 9 genes with the strongest interaction with KDM5 family proteins (**Figure 6B**). The results of the GO analysis showed significant enrichment of the BP terms "histone lysine demethylation", "histone demethylation", and "protein demethylation". The significantly enriched CC terms mainly included "histone methyltransferase complex", "methyltransferase complex", and "Sin3 complex". The significantly enriched MF terms mainly included "histone demethylase activity", "demethylase activity", and "transcription corepressor activity". The KEGG pathway analysis showed that the target genes were mainly associated with the terms "longevity-regulating pathway", "Notch signaling pathway", and "amphetamine addiction". The above results show that KDM5 family proteins may have strong interactions with HDAC1 and other proteins, modify the lysines of histone H3, and act on many pathways, including the "longevity-regulating pathway" and "Notch signaling pathway", which play a regulatory role in the proliferation of pancreatic cancer cells.

Relationship Between the KDM5 Family and Tumor-Infiltrating Immune Cells and Immune Molecules in Patients With PAAD

The immune system is a complex system in which immune cells both act as the first line of defense against a variety of pathogens and provide surveillance by identifying and destroying latent cancer cells. However, in some cases, the immune system can help

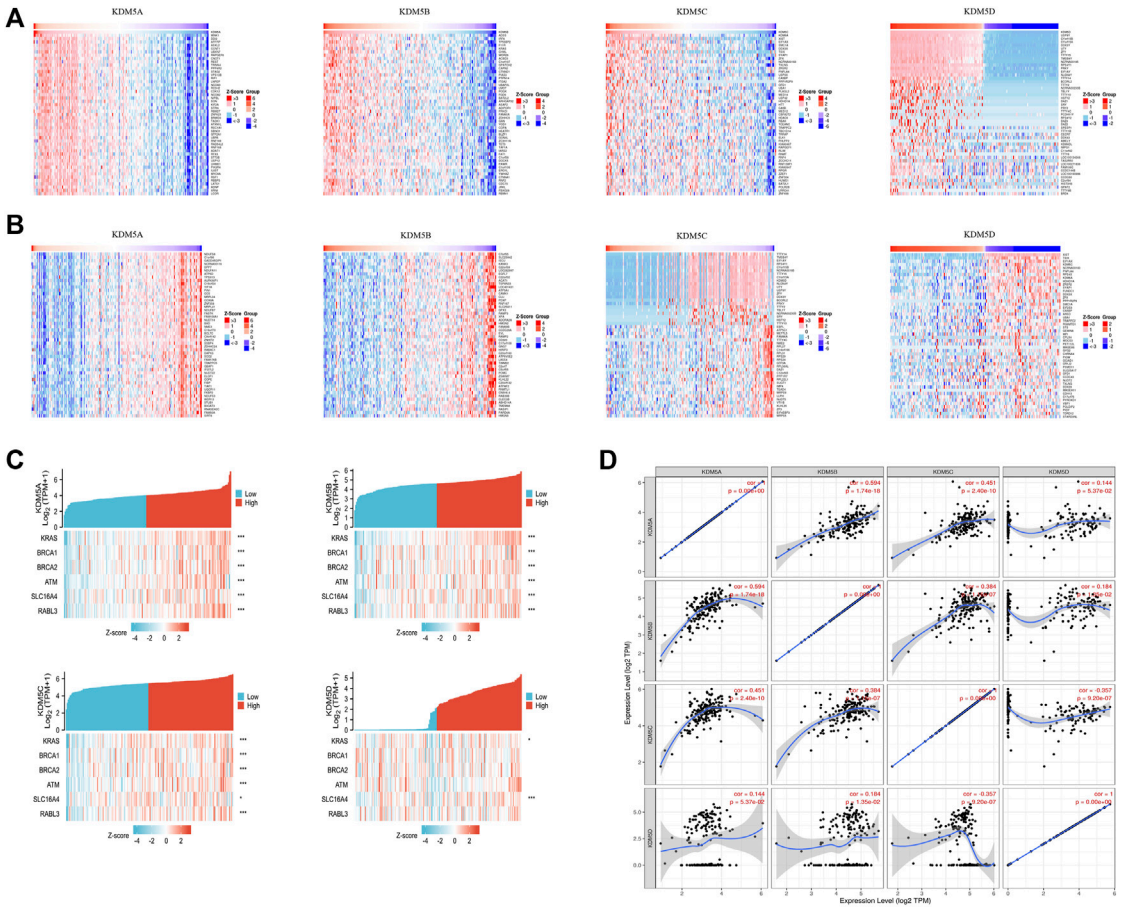

FIGURE 5 | The top 50 positively correlated genes and top 50 negatively correlated genes of the KDM5 family genes in patients with PAAD; Co-expression correlations of KDM5 family members and pathogenic genes of PAAD. **(A)** The top 50 genes with a positive correlation with KDM5 family genes are visualized in a heatmap; **(B)** The top 50 genes with a negative correlation with KDM5 family genes are visualized in a heatmap; **(C)** The expression of KDM5A/B/C is positively correlated with the expression of KRAS, BRCA1, BRCA2, ATM, SLC16A4 and RABL3. *, $p < 0.05$; **, $p < 0.01$; ***, $p < 0.001$; **(D)** The expression of each KDM5 family member is significantly positively correlated.

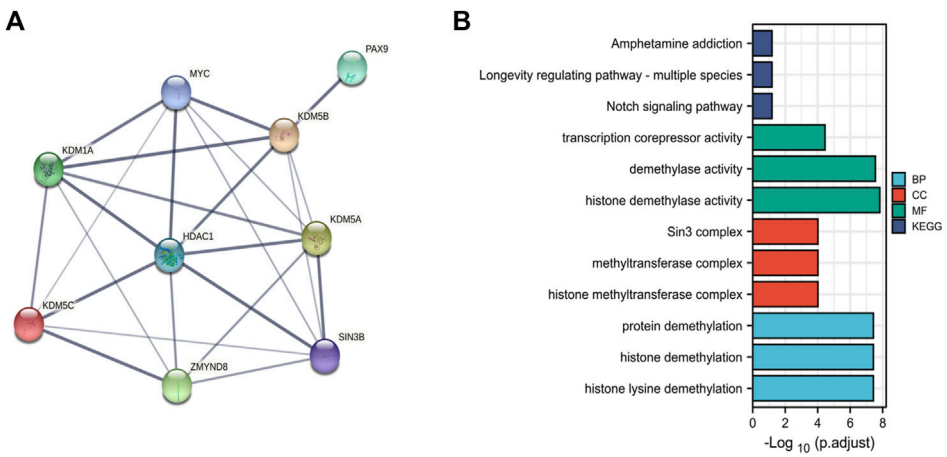

FIGURE 6 | PPI and functional enrichment analysis of the KDM5 family and related genes in patients with PAAD. **(A)** The PPI network associated with the KDM5 family in pancreatic cancer; **(B)** The GO and KEGG pathway terms of the 9 genes with the strongest interaction with KDM5 family proteins.).

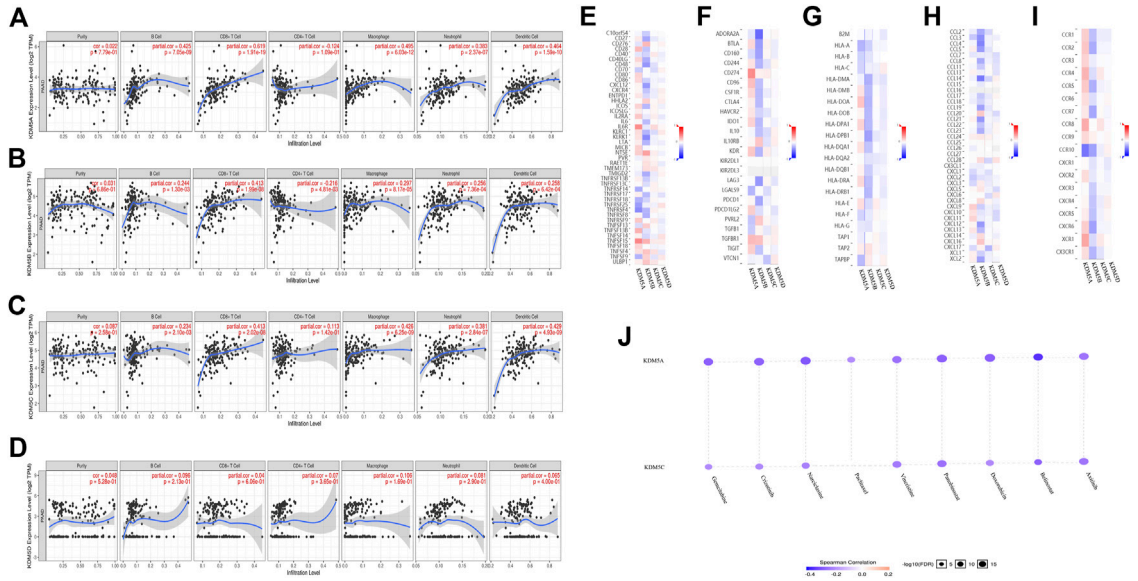

FIGURE 7 | Relationships between the expression levels of KDM5 family members and tumor-infiltrating immune cells, immune molecules, and sensitivity to pancreatic cancer-targeting and chemotherapeutic drugs. **(A–C)** Upregulation of KDM5A/B/C expression is associated with increased infiltration of B cells, $CD8^+$ T cells, macrophages, neutrophils, dendritic cells, and other infiltrating lymphocytes; **(D)** Upregulation of KDM5D expression is not associated with increased infiltration of B cells, $CD8^+$ T cells, macrophages, neutrophils, dendritic cells and other infiltrating lymphocytes; **(E–I)** The correlation between KDM5 family expression and immunostimulatory molecules, immunosuppressive molecules, MHC molecule, chemokines, and chemokine receptors in pancreatic cancer; **(J)** The expression levels of KDM5A and KDM5C are negatively correlated with sensitivity to many pancreatic cancer-targeting and chemotherapeutic drugs, including axitinib, and gemcitabine.

tumor cells escape immune control (Shalapour and Karin, 2015). Tumor-infiltrating lymphocytes are a unique kind of lymphocytes that infiltrate the tumor microenvironment by detecting cancer antigens and releasing proinflammatory cells. We used the TIMER database to further explore the relationship between the expression of KDM5 family genes and the level of infiltrating lymphocytes. The results showed that upregulation of KDM5A/B/C expression was associated with increased infiltration of B cells, $CD8^+$ T cells, macrophages, neutrophils, dendritic cells and other infiltrating lymphocytes (**Figures 7A–C**) and the upregulation of KDM5D expression was not associated with increased infiltration of B cells, $CD8^+$ T cells, macrophages, neutrophils, dendritic cells and other infiltrating lymphocytes (**Figure 7D**). Next, we analyzed the correlation between KDM5 family expression and immunostimulatory molecules (**Figure 7E**), immunosuppressive molecules (**Figure 7F**), MHC molecules (**Figure 7G**), chemokines (**Figure 7H**), and chemokine receptors (**Figure 7I**) in pancreatic cancer using the TISIDB database. The results showed that upregulated expression of KDM5A/B/C was associated with an increase in the expression of immunostimulatory molecules such as NT5E, TNFSF4, and TNFSF15, immunosuppressive molecules such as CD274 and TGFBR1, MHC molecules such as TAP2, chemokines such as CCL24, and chemokine receptors such as CCR8 and CCR9 (**Figures 7E–I**), which provides important information for predicting potential therapeutic targets. Finally, we used GSCALiteonlinetool to analyze the relationship between the expression of KDM5 family genes and sensitivity to current immune or targeted therapies for pancreatic cancer (**Figure 7J**). The results showed that the expression levels of KDM5A and KDM5C were negatively correlated with sensitivity to many pancreatic cancer-targeting or chemotherapeutic drugs, including axitinib and gemcitabine. Thus, the KDM5 family might represent a new target for predicting drug sensitivity and for developing multitarget combined therapy for pancreatic cancer.

DISCUSSION

Unlike other histone-modifying enzymes, members of the KDM5 family of histone lysine demethylases contain an ARID domain and thus can recognize the specific DNA sequence in targets; this feature is also an important marker to distinguish the KDM5 family from other histone lysine demethylase families (Blair et al., 2011). In recent years, an increased understanding of the carcinogenic role of the KDM5 family has been gained, and related experimental studies have found a potential cancer-promoting role of the KDM5 family in a variety of malignant tumors, including breast cancer, lung cancer, and prostate cancer (Hou et al., 2012; Stein et al., 2014; Li et al., 2016; Feng et al., 2017; Gong et al., 2018; Kuo et al., 2018; Oser et al., 2019; Du et al., 2020; Xue et al., 2020; Gu and Chu, 2021). However, research on the role and mechanism of the KDM5 family in the occurrence and development of pancreatic cancer is still lacking, and specific bioinformatics analyses have not been carried out. This study is the first to analyze the expression, gene mutation, relationship with immune cell infiltration and prognostic role of the KDM5

family in pancreatic cancer. We employed multiple public databases to reveal that the expression of KDM5A, KDM5B, and KDM5C (all members of the KDM5 family) is significantly increased in pancreatic cancer. In contrast, the expression of KDM5D was significantly decreased, and the expression level KDM5 family members was closely related to tumor stage, tumor grade, treatment efficacy, and other clinicopathological factors, suggesting that KDM5 family members have significant prognostic and diagnostic value and can be used as potential biomarkers for the diagnosis and prognostication of pancreatic cancer. In addition, we revealed a possible mechanism by which the KDM5 family participates in the occurrence and development of pancreatic cancer and its relationship with the tumor immune response, providing potential targets for multitarget combined therapy of pancreatic cancer, and important clinical significance.

Studies have shown that KDM5A promotes the resistance of breast cancer cells to clinical drugs such as trastuzumab and erlotinib by blocking the regulation of p21 and BCL2-antagonist/killer 1 (Bak1) (Hou et al., 2012; Choi et al., 2018). Similarly, our study revealed that the expression of KDM5A can also reduce the sensitivity of pancreatic cancer cells to a variety of targeted and chemotherapeutic drugs (such as gemcitabine and paclitaxel). Because KDM5A can lead to tumor cell chemotherapy resistance in a variety of cancers, we urgently need to further study the mechanism of drug resistance to develop new therapeutic targets for pancreatic cancer. In addition, compared with that in normal prostate tissue, the expression of KDM5A in prostate cancer tissue was upregulated (Vieira et al., 2013). This overexpression significantly reduced the methylation level of H3K4, which in turn reduced the expression level of the KLF4 and E-cadherin genes, which suppress tumor cell proliferation, and made prostate cancer more invasive (Huang et al., 2011). KDM5A can also promote the progression of prostate cancer through the KDM5A/miRNA-495/YTHDF2/m6A-MOB3B axis (Du et al., 2020). This study revealed a possible synergistic effect of KDM5A and m6A regulators in the pathogenesis of prostate cancer. In addition, KDM5A can also promote the occurrence of small-cell lung cancer by inhibiting the target genes NOTCH1 and NOTCH2 (Oser et al., 2019). The results of KEGG pathway analysis of the genes with the strongest interaction with KDM5 family proteins in this study also suggest that the family may promote the occurrence and development of pancreatic cancer through the NOTCH pathway. Intriguingly, the GO and KEGG analyses of the KDM5 family and its 800 coexpressed genes in this study suggest that they play a role in many biological processes, such as "cell cycle regulation", "chromatin binding", "transcription factor binding" and "transcriptional disorders in cancer", which is consistent with the finding that overexpression of KDM5A promotes the proliferation, invasion, and metastasis of many kinds of tumors. The KDM5A family likely plays a key role in regulating the proliferation of pancreatic cancer cells and inducing chemotherapy resistance.

KDM5B is a transcriptional inhibitor that specifically demethylates histone H3 lysine 4 (H3K4), putting it in a state of transcriptional inactivity (Benevolenskaya, 2007). Related studies have shown that KDM5B inhibits the expression of PTEN at the transcriptional level through H3K4 demethylation, thus inhibiting phosphorylated PI3K and AKT and increasing the proliferation, migration and invasion of hepatocellular carcinoma cells *in vivo* and *in vitro* (Tang et al., 2015). In addition, in syngeneic mouse breast tumor models and xenotransplantation models, KDM5B knockout leads to upregulation of tumor suppressor genes such as BRCA1, CAV1, and HOXA5 (Yamane et al., 2007) and increased H3K4 methylation in the chromatin regions of these target genes (Rasmussen and Staller, 2014). KDM5B is also related to chemotherapeutic drug resistance in NSCLC. Related experiments have shown that knockout of the KDM5B gene enhances the death of NSCLC cells induced by cisplatin and doxorubicin, suggesting that KDM5B may promote the invasiveness of NSCLC cells through epigenetic regulation of epithelial-mesenchymal transformation (EMT) regulatory factors such as vimentin, snail, and E-cadherin and upregulation of multipotent transcription factors such as OCT4, SOX2, KLF4, and c-Myc (Kristensen et al., 2012; Rasmussen and Staller, 2014; Yamamoto et al., 2014). These studies have revealed that KDM5B may be a marker of malignant tumor progression and a potential therapeutic target.

There is an interaction between KDM5C and histone deacetylases (HDACs), which have been successfully targeted in cancer therapy (Huang et al., 2011), consistent with the results of our protein interaction analysis. In addition, some studies have shown that the success of HDAC inhibitors is closely related to their interaction with KDM5C. HDACs usually act on many different histone residues, while the catalytic activity of KDM5C is limited to specific histone residues (Huang et al., 2011). This suggests that KDM5C inhibitors may have more specific biological effects and are more specific anticancer drugs than HDAC inhibitors. In addition, Johannes Stein et al. found that KDM5C gene knockout leads to growth retardation of prostate cancer cells *in vitro* and induces the regulation of several proliferation-related genes. This finding implies that KDM5C is an ideal drug target for prostate cancer (Stein et al., 2014). Recent studies have found that KDM5C is also highly expressed in ER-positive primary gastric cancer, regulated by ER and HIF1, and can significantly promote the proliferation, migration and invasion of gastric cancer cells (Xu et al., 2017). This study provides additional strong evidence for the role of KDM5C in promoting cancer. Therefore, we speculate that KDM5C may also play the role of an oncogene in pancreatic cancer and expect it to become a new target for tumor therapy.

KDM5D is a male-specific protein that inhibits the expression of genes associated with cell invasion (Li et al., 2016). There is growing evidence that EMT is necessary for tumor metastasis, and KDM5D gene knockout increases the expression of key EMT regulators (such as N-cadherin and Slug) (Li et al., 2016). In addition, related studies have shown that the expression of ETV4 is significantly increased in the process of gastric cancer cell proliferation and is closely related to lymph node metastasis, distant metastasis, and poor prognosis of gastric cancer patients, while KDM5D can downregulate the expression of ETV4 (Cai et al., 2020). In addition, overexpression of KDM5D can increase the sensitivity of cancer patients to ATR inhibitors or cell cycle inhibitors (Schäfer et al., 2021). These studies suggest that

decreased expression of KDM5D may be an important reason for the occurrence of many kinds of cancers and tumor drug resistance.

Another key finding of this study is that the expression levels of KDM5 family members are related to the infiltration of many kinds of infiltrating lymphocytes and the expression level of immune molecules in pancreatic cancer. The immune system is a complex system (Saab et al., 2020). In addition to acting as the first line of defense against a variety of pathogens, immune cells can also provide surveillance by identifying and destroying latent cancer cells. However, in some cases, the immune system can help tumor cells escape immune control (Shalapour and Karin, 2015). Tumor-infiltrating lymphocytes are a unique kind of lymphocytes that infiltrate the tumor microenvironment by detecting cancer antigens and releasing proinflammatory and immune molecules that are important substances that regulate the immune function of the body (Lee et al., 2016). Upregulation of KDM5A/B/C expression was associated with increased infiltration of B cells, $CD8^+$ T cells, macrophages, neutrophils, dendritic cells, and other infiltrating lymphocytes and increased expression of immunostimulatory molecules such as NT5E, TNFSF4, and TNFSF15, immunosuppressive molecules such as CD274 and TGFBR1, MHC molecules such as TAP2, and chemokine receptors such as CCL24, CCR8, and CCR9. These findings prove that the KDM5 family is closely related to immune function in pancreatic cancer, which provides important information for predicting potential therapeutic targets. Intriguingly, we found that overexpression of KDM5A/C was associated with reduced sensitivity of pancreatic cancer cells to a variety of pancreatic cancer-targeting and chemotherapeutic drugs, such as axitinib and gemcitabine. This discovery provides strong evidence for the study of KDM5A and KDM5C as targets for new pancreatic cancer-targeting and chemotherapeutic drugs. However, this study has some limitations. For example, the number of databases included in this study is somewhat inadequate. In addition, this study is only a bioinformatics analysis of the function of KDM5 family in PAAD. Future basic research may further confirm the tumor-promoting or tumor-suppressing role of the KDM5 family in PAAD.

CONCLUSION

In summary, our bioinformatics analysis of the KDM5 family and the pathogenesis of pancreatic cancer found that KDM5 family members can be used as prognostic markers and new therapeutic targets for patients with pancreatic cancer. However, relevant experimental studies *in vivo* and *in vitro* are urgently needed. Importantly, the increased understanding of the pathogenic mechanism by which this family participates in pancreatic cancer is expected to significantly improve the efficacy of multimodal comprehensive treatment of pancreatic cancer.

DATA AVAILABILITY STATEMENT

The original contributions presented in the study are included in the article/**Supplementary Material**, further inquiries can be directed to the corresponding author.

AUTHOR CONTRIBUTIONS

YuD and YoD conceived and designed the study. YuD, ZG and XZ performed the analyses. YuD and YoD wrote the manuscript. CW supervised the study. All authors contributed to the article and approved the submitted version.

FUNDING

This work was supported by CAMS Innovation Fund for Medical Sciences (CIFMS No. 2016-I2M-1-001) and National Natural Science Foundation of China (81972314 and 81802463).

ACKNOWLEDGMENTS

We thank ZG, XZ, YoD and CW from the department of Pancreatic and Gastric Surgery, National Cancer Center/ Cancer Hospital, Chinese Academy of Medical Sciences and Peking Union Medical College for their kind technical assistance.

SUPPLEMENTARY MATERIAL

The Supplementary Material for this article can be found online at: https://www.frontiersin.org/articles/10.3389/fcell.2022.887385/full#supplementary-material

Supplementary Figure S1 | Prognostic characteristics of patients with and without gene mutations of the KDM5 family. (A)OS; B(FPS).

Supplementary Table S1 | 800 coexpressed genes of the KDM5 family in PAAD.

Supplementary Table S2 | Protein expression of KDM5 family members and related genes.

REFERENCES

Asimgil, H., Ertetik, U., Çevik, N. C., Ekizce, M., Doğruöz, A., Gökalp, M., et al. (2022). Targeting the Undruggable Oncogenic KRAS: the Dawn of hope. *JCI insight* 7 (1), e153688. doi:10.1172/jci.insight.153688

Benevolenskaya, E. V. (2007). Histone H3K4 Demethylases Are Essential in Development and differentiationThis Paper Is One of a Selection of Papers Published in This Special Issue, Entitled 28th International West Coast Chromatin and Chromosome Conference, and Has Undergone the Journal's Usual Peer Review Process. *Biochem. Cel Biol.* 85 (4), 435–443. doi:10.1139/O07-057

Blair, L. P., Cao, J., Zou, M. R., Sayegh, J., and Yan, Q. (2011). Epigenetic Regulation by Lysine Demethylase 5 (KDM5) Enzymes in Cancer. *Cancers* 3 (1), 1383–1404. doi:10.3390/cancers3011383

Cai, L. S., Chen, Q. X., Fang, S. Y., Lian, M. Q., Lian, M. J., and Cai, M. Z. (2020). ETV4 Promotes the Progression of Gastric Cancer through Regulating

KDM5D. *Eur. Rev. Med. Pharmacol. Sci.* 24 (5), 2442–2451. doi:10.26355/eurrev_202003_20511

Cai, R. L., Yan-Neale, Y., Cueto, M. A., Xu, H., and Cohen, D. (2000). HDAC1, a Histone Deacetylase, Forms a Complex with Hus1 and Rad9, Two G2/M Checkpoint Rad Proteins. *J. Biol. Chem.* 275 (36), 27909–27916. doi:10.1074/jbc.M000168200

Cao, R., Wang, L., Wang, H., Xia, L., Erdjument-Bromage, H., Tempst, P., et al. (2002). Role of Histone H3 Lysine 27 Methylation in Polycomb-Group Silencing. *Science* 298 (5595), 1039–1043. doi:10.1126/science.1076997

Choi, H. J., Joo, H. S., Won, H. Y., Min, K. W., Kim, H. Y., Son, T., et al. (2018). Role of RBP2-Induced ER and IGF1R-ErbB Signaling in Tamoxifen Resistance in Breast Cancer. *J. Natl. Cancer Inst.* 110 (4), 10–1093. doi:10.1093/jnci/djx207

Du, C., Lv, C., Feng, Y., and Yu, S. (2020). Activation of the KDM5A/miRNA-495/YTHDF2/m6A-Mob3b axis Facilitates Prostate Cancer Progression. *J. Exp. Clin. Cancer Res.* 39 (1), 223. doi:10.1186/s13046-020-01735-3

Feinberg, A. P., Ohlsson, R., and Henikoff, S. (2006). The Epigenetic Progenitor Origin of Human Cancer. *Nat. Rev. Genet.* 7 (1), 21–33. doi:10.1038/nrg1748

Feng, T., Wang, Y., Lang, Y., and Zhang, Y. (2017). KDM5A Promotes Proliferation and EMT in Ovarian Cancer and Closely Correlates with PTX Resistance. *Mol. Med. Rep.* 16 (3), 3573–3580. doi:10.3892/mmr.2017.6960

Gao, J., Aksoy, B. A., Dogrusoz, U., Dresdner, G., Gross, B., Sumer, S. O., et al. (2013). Integrative Analysis of Complex Cancer Genomics and Clinical Profiles Using the cBioPortal. *Sci. Signal.* 6 (269), pl1. doi:10.1126/scisignal.2004088

Gong, J., Yan, S., Yu, H., Zhang, W., and Zhang, D. (2018). Increased Expression of Lysine-specific Demethylase 5B (KDM5B) Promotes Tumor Cell Growth in Hep3B Cells and Is an Independent Prognostic Factor in Patients with Hepatocellular Carcinoma. *Med. Sci. Monit.* 24, 7586–7594. doi:10.12659/msm.910844

Gu, J., and Chu, K. (2021). Increased Mars2 Expression upon microRNA-4661-5p-mediated KDM5D Downregulation Is Correlated with Malignant Degree of Gastric Cancer Cells. *Cell Biol Int* 45 (10), 2118–2128. doi:10.1002/cbin.11661

Győrffy, B., Surowiak, P., Budczies, J., and Lánczky, A. (2013). Online Survival Analysis Software to Assess the Prognostic Value of Biomarkers Using Transcriptomic Data in Non-small-cell Lung Cancer. *PloS one* 8 (12), e82241. doi:10.1371/journal.pone.0082241

Hou, J., Wu, J., Dombkowski, A., Zhang, K., Holowatyj, A., Boerner, J. L., et al. (2012). Genomic Amplification and a Role in Drug-Resistance for the KDM5A Histone Demethylase in Breast Cancer. *Am. J. Transl Res.* 4 (3), 247–256.

Huang, P.-H., Chen, C.-H., Chou, C.-C., Sargeant, A. M., Kulp, S. K., Teng, C.-M., et al. (2011). Histone Deacetylase Inhibitors Stimulate Histone H3 Lysine 4 Methylation in Part via Transcriptional Repression of Histone H3 Lysine 4 Demethylases. *Mol. Pharmacol.* 79 (1), 197–206. doi:10.1124/mol.110.067702

Johansson, C., Velupillai, S., Tumber, A., Szykowska, A., Hookway, E. S., Nowak, R. P., et al. (2016). Structural Analysis of Human KDM5B Guides Histone Demethylase Inhibitor Development. *Nat. Chem. Biol.* 12 (7), 539–545. doi:10.1038/nchembio.2087

Kornberg, R. D. (1974). Chromatin Structure: a Repeating Unit of Histones and DNA. *Science* 184 (4139), 868–871. doi:10.1126/science.184.4139.868

Kristensen, L. H., Nielsen, A. L., Helgstrand, C., Lees, M., Cloos, P., Kastrup, J. S., et al. (2012). Studies of H3K4me3 Demethylation by KDM5B/Jarid1B/PLU1 Reveals strong Substrate Recognition *In Vitro* and Identifies 2,4-Pyridine-Dicarboxylic Acid as an *In Vitro* and in Cell Inhibitor. *FEBS J.* 279 (11), 1905–1914. doi:10.1111/j.1742-4658.2012.08567.x

Kuo, K.-T., Huang, W.-C., Bamodu, O. A., Lee, W.-H., Wang, C.-H., Hsiao, M., et al. (2018). Histone Demethylase JARID1B/KDM5B Promotes Aggressiveness of Non-small Cell Lung Cancer and Serves as a Good Prognostic Predictor. *Clin. Epigenet* 10 (1), 107. doi:10.1186/s13148-018-0533-9

Lee, N., Zakka, L. R., Mihm, M. C., Jr, and Schatton, T. (2016). Tumour-infiltrating Lymphocytes in Melanoma Prognosis and Cancer Immunotherapy. *Pathology* 48 (2), 177–187. doi:10.1016/j.pathol.2015.12.006

Li, N., Dhar, S. S., Chen, T.-Y., Kan, P.-Y., Wei, Y., Kim, J.-H., et al. (2016). JARID1D Is a Suppressor and Prognostic Marker of Prostate Cancer Invasion and Metastasis. *Cancer Res.* 76 (4), 831–843. doi:10.1158/0008-5472.CAN-15-0906

Li, T., Fan, J., Wang, B., Traugh, N., Chen, Q., Liu, J. S., et al. (2017). TIMER: A Web Server for Comprehensive Analysis of Tumor-Infiltrating Immune Cells. *Cancer Res.* 77 (21), e108–e110. doi:10.1158/0008-5472.CAN-17-0307

Liu, C.-J., Hu, F.-F., Xia, M.-X., Han, L., Zhang, Q., and Guo, A.-Y. (2018). GSCALite: a Web Server for Gene Set Cancer Analysis. *Bioinformatics (Oxford, England)* 34 (21), 3771–3772. doi:10.1093/bioinformatics/bty411

Luger, K., Mäder, A. W., Richmond, R. K., Sargent, D. F., and Richmond, T. J. (1997). Crystal Structure of the Nucleosome Core Particle at 2.8 Å Resolution. *Nature* 389 (6648), 251–260. doi:10.1038/38444

Milne, T. A., Briggs, S. D., Brock, H. W., Martin, M. E., Gibbs, D., Allis, C. D., et al. (2002). MLL Targets SET Domain Methyltransferase Activity to Hox Gene Promoters. *Mol. Cel.* 10 (5), 1107–1117. doi:10.1016/s1097-2765(02)00741-4

Nakamura, T., Mori, T., Tada, S., Krajewski, W., Rozovskaia, T., Wassell, R., et al. (2002). ALL-1 Is a Histone Methyltransferase that Assembles a Supercomplex of Proteins Involved in Transcriptional Regulation. *Mol. Cel.* 10 (5), 1119–1128. doi:10.1016/s1097-2765(02)00740-2

Neoptolemos, J. P., Kleeff, J., Michl, P., Costello, E., Greenhalf, W., and Palmer, D. H. (2018). Therapeutic Developments in Pancreatic Cancer: Current and Future Perspectives. *Nat. Rev. Gastroenterol. Hepatolgastroenterology Hepatology* 15 (6), 333–348. doi:10.1038/s41575-018-0005-x

Oser, M. G., Sabet, A. H., Gao, W., Chakraborty, A. A., Schinzel, A. C., Jennings, R. B., et al. (2019). The KDM5A/RBP2 Histone Demethylase Represses NOTCH Signaling to Sustain Neuroendocrine Differentiation and Promote Small Cell Lung Cancer Tumorigenesis. *Genes Dev.* 33 (23-24), 1718–1738. doi:10.1101/gad.328336.119

Parkin, D. M., Bray, F., Ferlay, J., and Pisani, P. (2001). Estimating the World Cancer burden: Globocan 2000. *Int. J. Cancer* 94 (2), 153–156. doi:10.1002/ijc.1440

Raimondi, S., Maisonneuve, P., and Lowenfels, A. B. (2009). Epidemiology of Pancreatic Cancer: an Overview. *Nat. Rev. Gastroenterol. Hepatolgastroenterology Hepatology* 6 (12), 699–708. doi:10.1038/nrgastro.2009.177

Rasmussen, P. B., and Staller, P. (2014). The KDM5 Family of Histone Demethylases as Targets in Oncology Drug Discovery. *Epigenomics* 6 (3), 277–286. doi:10.2217/epi.14.14

Ru, B., Wong, C. N., Tong, Y., Zhong, J. Y., Zhong, S. S. W., Wu, W. C., et al. (2019). TISIDB: an Integrated Repository portal for Tumor-Immune System Interactions. *Bioinformatics (Oxford, England)* 35 (20), 4200–4202. doi:10.1093/bioinformatics/btz210

Saab, S., Zalzale, H., Rahal, Z., Khalifeh, Y., Sinjab, A., and Kadara, H. (2020). Insights into Lung Cancer Immune-Based Biology, Prevention, and Treatment. *Front. Immunol.* 11, 159. doi:10.3389/fimmu.2020.00159

Schäfer, G., Bednarova, N., Heidenreich, A., Klocker, H., and Heidegger, I. (2021). KDM5D Predicts Response to Docetaxel Chemotherapy in Metastatic Castration Resistant Prostate Cancer Patients. *Transl Androl. Urol.* 10 (10), 3946–3952. doi:10.21037/tau-20-1084

Shalapour, S., and Karin, M. (2015). Immunity, Inflammation, and Cancer: an Eternal Fight between Good and Evil. *J. Clin. Invest.* 125 (9), 3347–3355. doi:10.1172/JCI80007

Shilatifard, A. (2006). Chromatin Modifications by Methylation and Ubiquitination: Implications in the Regulation of Gene Expression. *Annu. Rev. Biochem.* 75, 243–269. doi:10.1146/annurev.biochem.75.103004.142422

Siegel, R. L., Miller, K. D., Fuchs, H. E., and Jemal, A. (2021). Cancer Statistics, 2021. *CA A. Cancer J. Clin.* 71 (1), 7–33. doi:10.3322/caac.21654

Stein, J., Majores, M., Rohde, M., Lim, S., Schneider, S., Krappe, E., et al. (2014). KDM5C Is Overexpressed in Prostate Cancer and Is a Prognostic Marker for Prostate-specific Antigen-Relapse Following Radical Prostatectomy. *Am. J. Pathol.* 184 (9), 2430–2437. doi:10.1016/j.ajpath.2014.05.022

Szklarczyk, D., Franceschini, A., Wyder, S., Forslund, K., Heller, D., Huerta-Cepas, J., et al. (2015). STRING V10: Protein-Protein Interaction Networks, Integrated over the Tree of Life. *Nucleic Acids Res.* 43 (Database issue), D447–D452. doi:10.1093/nar/gku1003

Tang, B., Qi, G., Tang, F., Yuan, S., Wang, Z., Liang, X., et al. (2015). JARID1B Promotes Metastasis and Epithelial-Mesenchymal Transition via PTEN/AKT Signaling in Hepatocellular Carcinoma Cells. *Oncotarget* 6 (14), 12723–12739. doi:10.18632/oncotarget.3713

Tumber, A., Nuzzi, A., Hookway, E. S., Hatch, S. B., Velupillai, S., Johansson, C., et al. (2017). Potent and Selective KDM5 Inhibitor Stops Cellular Demethylation of H3K4me3 at Transcription Start Sites and Proliferation of MM1S Myeloma Cells. *Cel Chem. Biol.* 24 (3), 371–380. doi:10.1016/j.chembiol.2017.02.006

Vasaikar, S. V., Straub, P., Wang, J., and Zhang, B. (2018). LinkedOmics: Analyzing Multi-Omics Data within and across 32 Cancer Types. *Nucleic Acids Res.* 46 (D1), D956–D963. doi:10.1093/nar/gkx1090

Vieira, F. Q., Costa-Pinheiro, P., Ramalho-Carvalho, J., Pereira, A., Menezes, F. D., Antunes, L., et al. (2013). Deregulated Expression of Selected Histone Methylases and Demethylases in Prostate Carcinoma. *Endocr. Relat. Cancer* 21 (1), 51–61. doi:10.1530/ERC-13-0375

Von Hoff, D. D., Ervin, T., Arena, F. P., Chiorean, E. G., Infante, J., Moore, M., et al. (2013). Increased Survival in Pancreatic Cancer with Nab-Paclitaxel Plus Gemcitabine. *N. Engl. J. Med.* 369 (18), 1691–1703. doi:10.1056/NEJMoa1304369

Xu, L., Wu, W., Cheng, G., Qian, M., Hu, K., Yin, G., et al. (2017). Enhancement of Proliferation and Invasion of Gastric Cancer Cell by KDM5C via Decrease in P53 Expression. *Technol. Cancer Res. Treat.* 16 (2), 141–149. doi:10.1177/1533034616629261

Xue, S., Lam, Y. M., He, Z., Zheng, Y., Li, L., Zhang, Y., et al. (2020). Histone Lysine Demethylase KDM5B Maintains Chronic Myeloid Leukemia via Multiple Epigenetic Actions. *Exp. Hematol.* 82, 53–65. doi:10.1016/j.exphem.2020.01.006

Yamamoto, S., Wu, Z., Russnes, H. G., Takagi, S., Peluffo, G., Vaske, C., et al. (2014). JARID1B Is a Luminal Lineage-Driving Oncogene in Breast Cancer. *Cancer cell* 25 (6), 762–777. doi:10.1016/j.ccr.2014.04.024

Yamane, K., Tateishi, K., Klose, R. J., Fang, J., Fabrizio, L. A., Erdjument-Bromage, H., et al. (2007). PLU-1 Is an H3K4 Demethylase Involved in Transcriptional Repression and Breast Cancer Cell Proliferation. *Mol. Cel.* 25 (6), 801–812. doi:10.1016/j.molcel.2007.03.001

Yokoyama, A., Wang, Z., Wysocka, J., Sanyal, M., Aufiero, D. J., Kitabayashi, I., et al. (2004). Leukemia Proto-Oncoprotein MLL Forms a SET1-like Histone Methyltransferase Complex with Menin to Regulate Hox Gene Expression. *Mol. Cel Biol* 24 (13), 5639–5649. doi:10.1128/mcb.24.13.5639-5649.2004

Zhang, Y., Yang, H., Guo, X., Rong, N., Song, Y., Xu, Y., et al. (2014). The PHD1 finger of KDM5B Recognizes Unmodified H3K4 during the Demethylation of Histone H3K4me2/3 by KDM5B. *Protein Cell* 5 (11), 837–850. doi:10.1007/s13238-014-0078-4

Zhou, Y., Zhou, B., Pache, L., Chang, M., Khodabakhshi, A. H., Tanaseichuk, O., et al. (2019). Metascape Provides a Biologist-Oriented Resource for the Analysis of Systems-Level Datasets. *Nat. Commun.* 10 (1), 1523. doi:10.1038/s41467-019-09234-6

Conflict of Interest: The authors declare that the research was conducted in the absence of any commercial or financial relationships that could be construed as a potential conflict of interest.

Publisher's Note: All claims expressed in this article are solely those of the authors and do not necessarily represent those of their affiliated organizations, or those of the publisher, the editors and the reviewers. Any product that may be evaluated in this article, or claim that may be made by its manufacturer, is not guaranteed or endorsed by the publisher.

frontiers | Frontiers in Genetics

ORIGINAL RESEARCH
published: 20 June 2022
doi: 10.3389/fgene.2022.805960

Tumor Suppressor 4.1N/*EPB41L1* is Epigenetic Silenced by Promoter Methylation and MiR-454-3p in NSCLC

Qin Yang[1,2†], Lin Zhu[1†], Mao Ye[3,4], Bin Zhang[5], Peihe Zhan[5], Hui Li[1,3,4], Wen Zou[6*] and Jing Liu[1*]*

[1]Molecular Biology Research Center and Center for Medical Genetics, School of Life Sciences, Central South University, Changsha, China, [2]School of Medical Laboratory, Shao Yang University, Shaoyang, China, [3]Molecular Science and Biomedicine Laboratory, College of Biology, College of Chemistry and Chemical Engineering, Collaborative Innovation Center for Chemistry and Molecular Medicine, Hunan University, Changsha, China, [4]State Key Laboratory for Chemo/Biosensing and Chemometrics, College of Biology, College of Chemistry and Chemical Engineering, Collaborative Innovation Center for Chemistry and Molecular Medicine, Hunan Univers ity, Changsha, China, [5]Department of Histology and Embryology, Xiangya School of Medicine, Central South University, Changsha, China, [6]Department of Oncology, The Second Xiangya Hospital of Central South University, Central South University, Changsha, China

OPEN ACCESS

Edited by:
Biaoru Li,
Augusta University, United States

Reviewed by:
Fei Han,
Army Medical University, China
Hongde Liu,
Southeast University, China

***Correspondence:**
Jing Liu
jingliucsu@hotmail.com
Wen Zou
zouwen29w@csu.edu.cn
Hui Li
lihuiscience@163.com

[†]These authors contributed equally to this work

Specialty section:
This article was submitted to Epigenomics and Epigenetics, a section of the journal Frontiers in Genetics

Received: *31 October 2021*
Accepted: *08 April 2022*
Published: *20 June 2022*

Citation:
Yang Q, Zhu L, Ye M, Zhang B, Zhan P, Li H, Zou W and Liu J (2022) Tumor Suppressor 4.1N/EPB41L1 is Epigenetic Silenced by Promoter Methylation and MiR-454-3p in NSCLC. Front. Genet. 13:805960. doi: 10.3389/fgene.2022.805960

Non–small-cell lung cancer (NSCLC) is divided into three major histological types, namely, lung adenocarcinoma (LUAD), lung squamous cell carcinoma (LUSC), and large-cell lung carcinoma (LCLC). We previously identified that 4.1N/*EPB41L1* acts as a tumor suppressor and is reduced in NSCLC patients. In the current study, we explored the underlying epigenetic mechanisms of 4.1N/*EPB41L1* reduction in NSCLC. The 4.1N/*EPB41L1* gene promoter region was highly methylated in LUAD and LUSC patients. LUAD patients with higher methylation level in the 4.1N/*EPB41L1* gene promoter (TSS1500, cg13399773 or TSS200, cg20993403) had a shorter overall survival time (Log-rank $p = 0.02$ HR = 1.509 or Log-rank $p = 0.016$ HR = 1.509), whereas LUSC patients with higher methylation level in the 4.1N/*EPB41L1* gene promoter (TSS1500 cg13399773, TSS1500 cg07030373 or TSS200 cg20993403) had a longer overall survival time (Log-rank $p = 0.045$ HR = 0.5709, Log-rank $p = 0.018$ HR = 0.68 or Log-rank $p = 0.014$ HR = 0.639, respectively). High methylation of the 4.1N/*EPB41L1* gene promoter appeared to be a relatively early event in LUAD and LUSC. DNA methyltransferase inhibitor 5-Aza-2′-deoxycytidine restored the 4.1N/*EPB41L1* expression at both the mRNA and protein levels. MiR-454-3p was abnormally highly expressed in NSCLC and directly targeted 4.1N/*EPB41L1* mRNA. MiR-454-3p expression was significantly correlated with 4.1N/*EPB41L1* expression in NSCLC patients ($r = -0.63$, $p < 0.0001$). Therefore, we concluded that promoter hypermethylation of the 4.1N/*EPB41L1* gene and abnormally high expressed miR-454-3p work at different regulation levels but in concert to restrict 4.1N/*EPB41L1* expression in NSCLC. Taken together, this work contributes to elucidate the underlying epigenetic disruptions of 4.1N/*EPB41L1* deficiency in NSCLC.

Keywords: 4.1N/EPB41L1, lung adenocarcinoma (LUAD), methylation, miR-454-3P, non–small-cell lung cancer (NSCLC), lung squamous cell carcinoma (LUSC)

Abbreviations: 3′UTRs, 3′-untranslated regions; 5-Aza-CdR, 5-Aza-2′-deoxycytidine; HR, hazard ratio; LCLC, large-cell lung carcinoma; LR, log-likelihood ratio; LUAD, lung adenocarcinoma; LUSC, lung squamous cell carcinoma; NSCLC, non–small-cell lung cancer; SD, standard deviation; TBS-seq, targeted bisulfite sequencing; TSS, transcription start site.

INTRODUCTION

Lung cancer is the most commonly diagnosed cancer and the most lethal cause of cancer mortality worldwide (Bray et al., 2018). Non–small-cell lung cancer (NSCLC), consisting of lung adenocarcinoma (LUAD), lung squamous cell carcinoma (LUSC), and large-cell lung carcinoma (LCLC) (Rodriguez-Canales et al., 2016), represents major types of lung cancers (80–85%) (D'Addario et al., 2010). Owing to a lack of obvious early symptoms and early-stage diagnosis, most patients with NSCLC are diagnosed in the advanced clinical stage—that is—III or IV (Norouzi and Hardy, 2021). Despite recent advances in NSCLC treatment, less than 15% of the patients eventually survived (Quintanal-Villalonga and Molina-Pinelo, 2019; Norouzi and Hardy, 2021).

Gene promoter methylation and miRNA dysregulation are typical markers of cancer epigenetics (Nebbioso et al., 2018). Gene promoter methylation most commonly occurs at the CpG islands and regulates the gene expression at the transcriptional level (Yang et al., 2014; Zhou et al., 2017; Arechederra et al., 2018). 5–10% of CpG islands in the promoter of genes have been identified as cancer-specifically methylated, which should not be methylated in normal cells (Heller et al., 2013; Olbromski et al., 2020). The methylations of certain genes are of clinical relevance for patients with NSCLC (Heller et al., 2013). MiRNAs are endogenous small non-coding RNAs, which directly bind to the 3′-untranslated regions (3′UTRs) of target mRNAs to regulate the gene expression at the posttranscriptional level. NSCLC patients have widespread dysregulation of miRNA expression (Du et al., 2018; Uddin and Chakraborty, 2018). It has been well-documented that 4.1 family members 4.1N/*EPB41L1* and its homologs (4.1B/*EPB41L3*, 4.1G/*EPB41L2*, and 4.1R/*EPB41*) are lost in various cancers (Yang et al., 2021). However, epigenetic silencing of 4.1 family members in cancers is still largely unknown. Loss of 4.1B/*EPB41L3* is the only case that has been linked to high promoter methylation in cancers (Kikuchi et al., 2005; Zhang et al., 2012). No miRNAs have been found to regulate 4.1 family members.

Our previous studies suggested that 4.1N/*EPB41L1* is abnormally low expressed and exerts anticancer effects in NSCLC (Wang et al., 2016; Yang et al., 2016; Yang et al., 2021). In the current study, for the first time, we focus on identifying the underlying epigenetic disruptions of 4.1N/*EPB41L1* deficiency in NSCLC. We report that promoter hypermethylation and aberrant miR-454-3p expression regulate 4.1N/*EPB41L1* expression at transcriptional and posttranscriptional levels, respectively, but work in concert to restrict its expression in NSCLC.

MATERIALS AND METHODS

Antibodies

Rabbit anti-4.1N antibody was purchased from ATLAS (Bromma, Sweden). Rabbit anti-GAPDH antibody was purchased from Santa Cruz (Santa Cruz Biotechnology, United States).

Cell Culture

MRC5, 95C, and 95D cells were grown in DMEM medium (Gibco, United States) and supplemented with 10% fetal bovine serum (Gibco, United States). H460 and A549 cells were grown in RPMI 1640 medium (Gibco, United States) and supplemented with 10% fetal bovine serum. All the cells were grown at 37°C in a humidified atmosphere containing 5% CO_2.

NSCLC Tissue Samples

Tumor tissues and tumor-adjacent tissues were obtained from the Second Xiangya Hospital of Central South University (Changsha, China). The tissue samples were subjected to qPCR experiments after approval by the Ethics Committee of the Second Xiangya Hospital. Informed consent was obtained from all participating subjects.

Methylation-Based Analysis

The MethSurv tool (https://biit.cs.ut.ee/methsurv/) (Modhukur et al., 2018) was used to perform the assessment of methylation-based analysis for the 4.1N/*EPB41L1* gene in LUAD and LUSC. The raw data for LUAD and LUSC could be downloaded from the website (https://biit.cs.ut.ee/methsurv/).

Cell Transfection and Western Blot

MiR-454-3p and the control mimics were purchased from RiboBio (Guangzhou, China) and transfected according to our previously published protocol (Li et al., 2016). Western blot was also performed according to our previous protocol (Yang et al., 2016).

Targeted Bisulfite Sequencing

The cells were sent to Biomarker Acegene Corporation, Shenzhen, China for targeted bisulfite sequencing (TBS-seq) analysis. 4.1N/*EPB41L1* promoter methylation was assessed according to the previously published method (Gao et al., 2014a; Gao et al., 2014b; Gao et al., 2015; Pan et al., 2018). Methylation levels are defined as the fraction of read counts of 'C' in the total read counts of both 'C' and 'T' for each covered C site. On the basis of such read fraction, methylated cytosine was called using a binomial distribution as in the method described by Lister et al. (2009), whereby a probability mass function is calculated for each methylation context (CpG). Two-tailed Fisher's exact test was used to identify cytosines that are differentially methylated between two samples or groups. Only those CGs covered by at least 200 reads in at least one sample were considered for testing.

5-Aza-2′-deoxycytidine(5-Aza-CdR) treatment

5-Aza-CdR (Merck, Germany) was diluted in PBS. The cells were seeded in a 6-well plate and treated with 0, 1, or 10 μM 5-Aza-CdR for 48 h. 5-Aza-CdR was replaced every 24 h.

RNA Extraction and qPCR

Total RNA was isolated using the RNeasy kit (QIAGEN, United States). cDNA was synthesized using the RevertAid H Minus First-Strand cDNA Synthesis Kit (Thermo Scientific,

United States). Stem-loop RT primers (RiboBio, China) were used in reverse transcription for miR-454-3p. qPCR was performed using the One-Step qRT-PCR SYBR® Green Kit (Vazyme Biotech, China). The sequences of primers targeting 4.1N/*EPB41L1* and miR-454-3p were used as described earlier (Wang et al., 2010) and designed by Vazyme Biotech (Nanjing, China). U6 small nuclear RNA was used as an internal control for miR-454-3p analysis.

Dual-Luciferase Reporter Gene Assay

The 3′UTR target sites of 4.1N/*EPB41L1* mRNA were amplified by PCR with genomic DNA from MRC5 cells. The PCR product was cloned in the psiCHECK2 vector (Promega, United States) to construct the wild-type plasmid (psiCHECK2-4.1N-wt). The corresponding mutant psiCHECK2-4.1N-mut was constructed by *in vitro* site-directed mutagenesis (Mut ExpressMultiS Fast Mutagenesis Kit, Vazyme Biotech, China). Bidirectional sequencing was applied to confirm the correct sequence of the two constructs. For the dual-luciferase reporter gene assay, A549 and H460 cells were cultured in a 24-well plate for 24 h and transfected with psiCHECK2-4.1N-wt or psiCHECK2-4.1N-mut plasmids and miR-454-3p mimics or miR-negative-control using the RiboFECT™CP transfection kit (Ribo Biotechnology, China) and Lipofectamine 2000 (Invitrogen, United States). 48 hours after the transfection, the Dual-Luciferase Reporter Assay System (Promega, Madison, WI, United States) was used to measure the luciferase activity according to the manufacturer's protocol.

Statistics

All the experiments were performed in triplicate, and statistical analyses were conducted using GraphPad Prism 5.0. The data were presented as the mean ± standard deviation (SD). Student's *t*-tests were used to calculate the results. A p-value < 0.05 was considered significant statistically. DNA methylation values were represented as beta values (range from 0 to 1). Any beta value equal to or greater than 0.6 was considered fully methylated. Any beta value equal to or less than 0.2 was considered to be fully unmethylated. Beta values between 0.2 and 0.6 were considered to be partially methylated. Differential methylation for individual CpG loci was assessed by comparing the beta values. The patients were classified into high-methylation and low-methylation levels based on maxstat (Modhukur et al., 2018). Cox proportional hazards models were used to perform the survival analysis based on methylation levels of the CpG sites. The methylation levels and overall survival time were used as explanatory variables and response variables, respectively, to perform overall survival analysis.

RESULTS

Hypermethylation of the 4.1N/*EPB41L1* Gene in NSCLC

Aberrant hypermethylations in the promoter region of genes are considered a major reason for gene silencing in cancer (Lamy et al., 2001). The CpG island methylation prediction using the CpGPNP program (http://forensicdna.kr/cpgpnp/) showed four CpG islands in the 4.1N/*EPB41L1* gene promoter (2,000 bp upstream to 1,000 bp downstream of the transcription start site, **Figure 1A**). NSCLC predominantly encompasses the LUAD (40% prevalence) and LUSC subtypes (25% prevalence). The MethSurv tool (https://biit.cs.ut.ee/methsurv/) (Modhukur et al., 2018) was used to perform the assessment of methylation-based analysis for the 4.1N/*EPB41L1* gene promoter region (TSS200 and TSS1500) in LUAD and LUSC. The heat map showed that high methylation of the 4.1N/*EPB41L1* gene was prevalent in both LUAD (**Figure 1B**) and LUSC (**Figure 1C**). Because the MethSurv tool (https://biit.cs.ut.ee/methsurv/) lacks LCLC data, we investigated the methylation of the 4.1N/*EPB41L1* gene in LCLC cells (95C, 95D, and H460) and normal lung fibroblast cells (MRC5). TBS-seq results showed that promoter methylation of 4.1N/*EPB41L1* was significantly higher in LCLC cells (95C, 95D, and H460) than in normal lung cells (MRC5) ($p < 0.001$) (**Figures 1D,E**). To further validate the role of methylation in 4.1N/*EPB41L1* gene repression, we treated the LCLC cells (95C and H460) and LUAD cells (A549) with DNA methyltransferase inhibitor 5-Aza-CdR. After demethylation treatment, the 4.1N/*EPB41L1* gene was restored both at mRNA (**Figures 2A–C**) and protein levels (**Figures 2D–F**). Taken together, these results indicated that 4.1N/*EPB41L1* gene methylation is a cause of decreased 4.1N/*EPB41L1* expression in NSCLC patients.

Prognostic Relevance of 4.1N/*EPB41L1* Hypermethylation in LUAD and LUSC

In most cases, evaluating DNA methylation signature in the promoter region is highly desirable and sensitive for cancer diagnosis and prognosis. The Kaplan–Meier survival curve showed that the higher methylation levels in the promoter (TSS1500, cg13399773 or TSS200, cg20993403) of the 4.1N/*EPB41L1* gene were significantly associated with a shorter overall survival time (Log-rank $p = 0.02$, HR = 1.509 or Log-rank $p = 0.016$, HR = 1.509, respectively) for LUAD patients (**Figures 3A,C**). Median methylation levels of the two CpG sites (cg13399773 and cg20993403) were high (beta>0.5) at stage I and did not essentially change in tumors of more advanced stages (**Figures 3B,D**). Unlike the LUAD, the Kaplan–Meier survival curve showed that the higher methylation levels in the promoter (TSS1500 cg13399773, TSS1500 cg07030373, or TSS200 cg20993403) of the 4.1N/*EPB41L1* gene were significantly associated with a shorter overall survival time (Log-rank $p = 0.045$ HR = 0.5709, Log-rank $p = 0.018$ HR = 0.68 or Log-rank $p = 0.014$ HR = 0.639 respectively) for LUSC patients (**Figures 4A,C,E**). Median methylation levels of the three CpG sites (TSS1500 cg13399773, TSS1500 cg07030373, or TSS200 cg20993403) were high (beta>0.5) from stage I to IV and tended to decline with tumor progression (**Figures 4B,D,F**). We did not further explore the contrasting prognostic relevance of 4.1N/*EPB41L1* hypermethylation between LUAD and LUSC. However, methylation of the 4.1N/*EPB41L1* gene might be an important mechanism for tumor formation in LUAD and LUSC because high 4.1N/*EPB41L1* gene methylations were observed at stage I. Because the MethSurv tool (https://biit.cs.ut.ee/methsurv/) lacks LCLC data, the prognostic relevance of 4.1N/*EPB41L1* hypermethylation in LCLC was unknown.

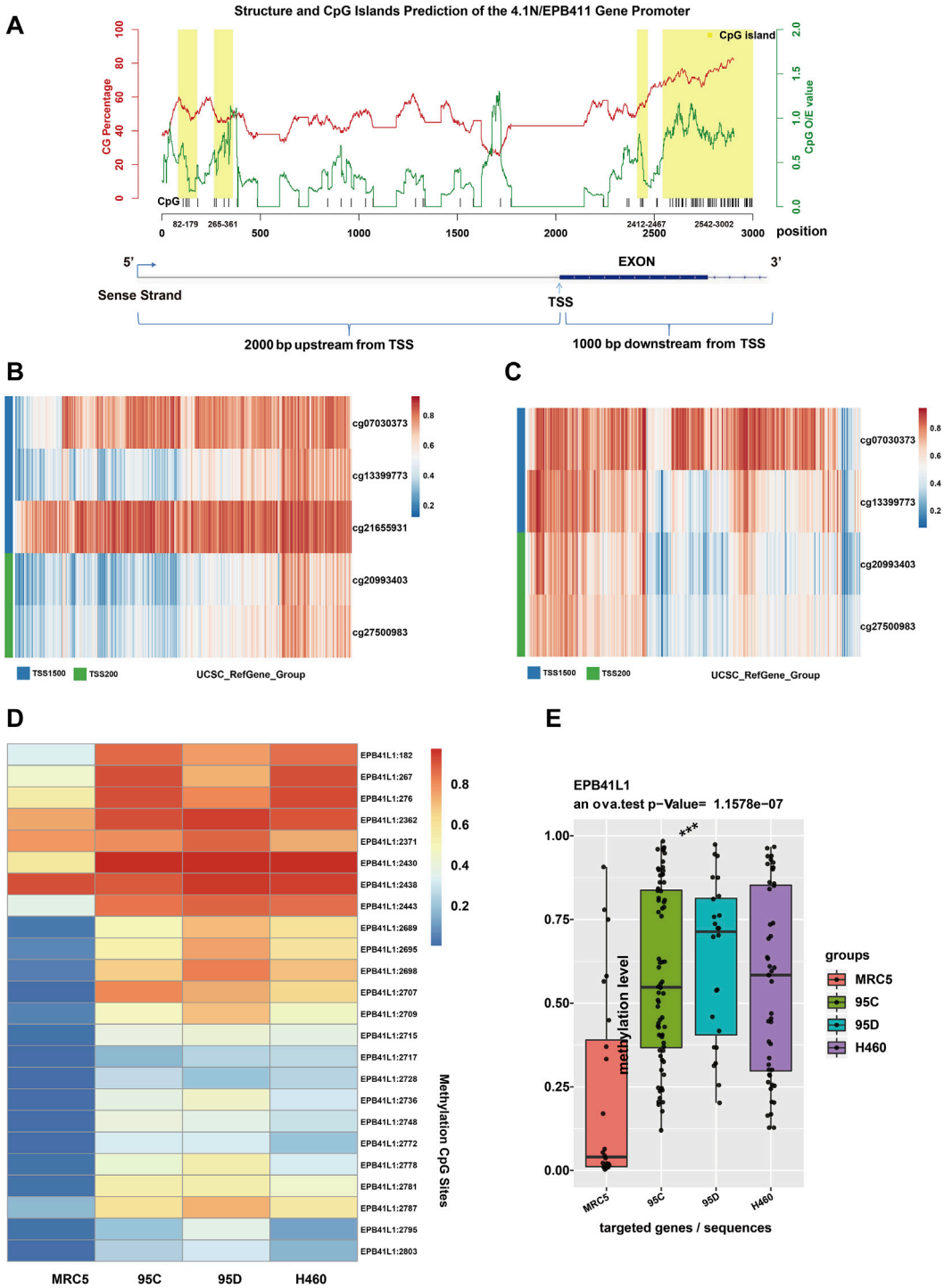

FIGURE 1 | Promoter methylation of the 4.1N/*EPB41L1* gene in NSCLC. **(A)** In the upper panel, CpG island prediction of the 4.1N/*EPB41L1* gene promoter was integrated using the CpGPNP program. The red line represented GC content, the green line represents CpG O/E value, and the yellow box represented four predicted locations of CpG island (range from 82 to 179, 265–361, 2412–2467, and 2542–3002, sequence length >100 bp, GC content >50%, O/E value >0.6). The lower panel represented the structure of the 4.1N/*EPB41L1* gene promoter (range from TSS -2000 to TSS 1000). Coordinate values of abscissas in the lower and upper panels were correlated. TSS -2000 in the lower panel corresponded to 0 in the upper panel. The TSS site in the lower panel corresponded to 2000 in the upper panel. TSS 1000 in the lower panel corresponded to 3000 in the upper panel. **(B,C)** Heatmap depicting the CpG methylation level of the 4.1N/*EPB41L1* gene promoter in LUAD and LUSC patients. Rows and columns represented the CpGs and the patients, respectively. **(D)** Heatmap depicting the methylation levels of the 4.1N/*EPB41L1* gene promoter in normal lung fibroblast cells MRC5 and LCLC cells (95C, 95D, and H460). The row label was the methylation site. The number of row labels corresponded to the coordinate value of abscissa in the upper panel of Panel 1A. Methylation levels were represented as beta values and shown as a continuous variable from blue to red. Any

(*Continued*)

FIGURE 1 | beta value equal to or greater than 0.6 was considered fully methylated. Any beta value equal to or less than 0.2 was considered to be fully unmethylated. Beta values between 0.2 and 0.6 were considered to be partially methylated. **(E)** Boxplots indicating the methylation differences between normal lung fibroblast cells MRC5 and LCLC cells (95C, 95D, and H460). Median methylation levels (show by a thick black line). ***$p < 0.001$.

4.1N/*EPB41L1* mRNA is a Direct Target of miR-454-3p

We previously described that the 95D cells had remarkably lower 4.1N/*EPB41L1* expression than the 95C cells (Yang et al., 2016). Unexpectedly, although the methylation level of the 95D promoter was higher than that of 95C, there was no significant difference between the two homologous NSCLC subclones 95C/95D (**Figure 5A**). Over half of all protein-encoding genes are regulated by miRNAs (Turchinovich et al., 2012). Aberrantly high-expressed oncomiRNA silencing cancer suppressing genes are frequently found in NSCLC. Therefore, we investigated the potential miRNAs regulating 4.1N/*EPB41L1* expression. The miRNA-target gene database TargetScan (miRBase:www.mirbase.org) was used to predict the potential miRNAs regulating 4.1N/*EPB41L1*, and miR-454-3p was suggested as a potential miRNA (**Figure 5B**). qPCR results showed that the miR-454-3p was expressed significantly lower in the 95D cells than in 95C cells (**Figure 5C**). After overexpressing the miR-454-3p in A549 cells (**Figure 5D**), the expression level of protein 4.1N/*EPB41L1* was downregulated (**Figure 5E**).

To further examine if 4.1N/*EPB41L1* was a target gene of miR-454-3p, the dual-luciferase activity assay was applied in A549 and H460 cells. The predicted binding sites of miR-454-3p and 4.1N/*EPB41L1* mRNA and mutant sequences containing four mutated nucleotides are shown in **Figure 5F**. MiR-454-3p significantly suppressed the luciferase activity, and this suppressive effect was abolished by the mutation in the miR-454-3p-binding region of the 4.1N/*EPB41L1* mRNA 3′UTR in H460 and A549 cells (**Figures 5G,H**). The abovementioned results signified that abnormally highly expressed miR-454-3p is another epigenetic cause of 4.1N/*EPB41L1* decreasing in NSCLC patients.

Abnormally High-Expressed miR-454-3p Decreases 4.1N/*EPB41L1* in NSCLC

TCGA data were used to extract RNA transcript levels of the miR-454-3p. We found that the miR-454-3p was significantly higher in the LUAD (**Figure 6A**) and LUSC (**Figure 6C**) tissues in comparison to the adjacent tissues, whereas the 4.1N/*EPB41L1* mRNA was significantly lower in LUAD (**Figure 6B**) and LUSC (**Figure 6D**) tissues than the corresponding adjacent tissues. Then, we used qPCR to measure the miR-454-3p and 4.1N/*EPB41L1* mRNA expressions in 37 NSCLC tissues and 31 tumor-adjacent tissues. We found that the expression patterns are consistent with TCGA data (**Figures 6E,F**). Moreover, the association between miR-454-3p and 4.1N/*EPB41L1* mRNA was validated by Spearman's coefficient analysis. The MiR-454-3p expression level showed a significantly negative correlation with 4.1N/*EPB41L1* mRNA ($r = -0.63$, $p < 0.0001$, **Figure 6G**). Expression patterns of miR-454-3p and 4.1N/*EPB41L1* mRNA showed that abnormally high expression of miR-454-3p negatively regulates 4.1N/*EPB41L1* in NSCLC.

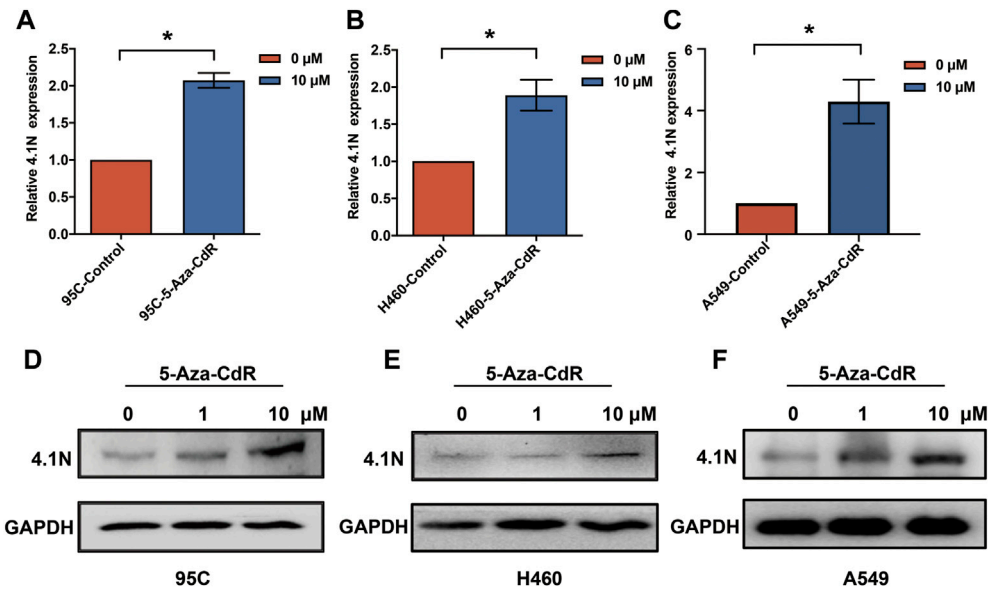

FIGURE 2 | 4.1N/*EPB41L1* was restored by methyltransferase inhibitor 5-Aza-CdR in NSCLC cells. **(A–C)** qPCR was performed to evaluate expressions of 4.1N/*EPB41L1* mRNA in 95C, H460, and A549 cells after 0 μM or 1 μM 5-Aza-CdR treatments for 48 h **(D–F)** 95C, H460, and A549 cells were treated with 0, 1 or 10 μM 5-Aza-CdR for 48 h, and then the protein was detected by Western blot. The data were presented as the mean ± SD, *$p < 0.05$.

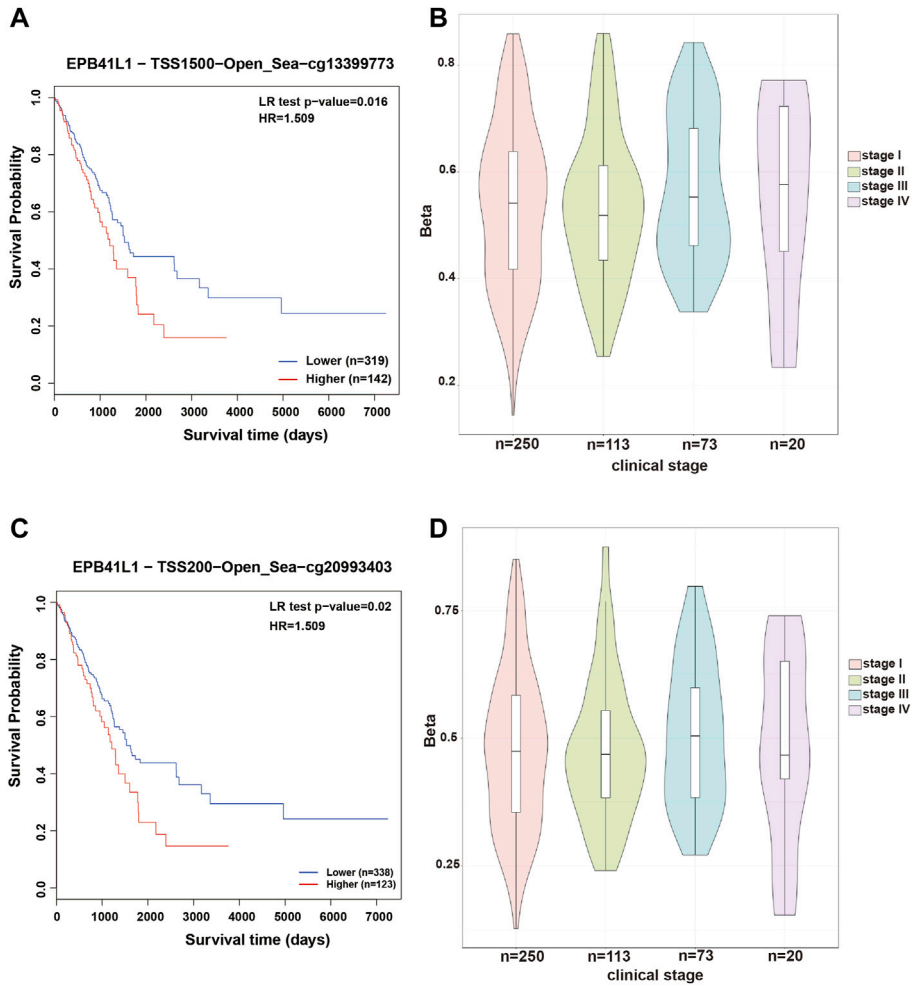

FIGURE 3 | Methylation levels and prognosis of the 4.1N/*EPB41L1* promoter in patients with LUAD. **(A)** Kaplan–Meier curves for cg13399773-4.1N showing survival in lower (beta <0.611, shown in blue) and higher methylation groups (beta > 0.611, shown in red) dichotomized by the maxstat method. **(C)** Kaplan–Meier curves for cg20993403-4.1N showing survival in lower (beta <0.59, shown in blue) and higher methylation groups (beta > 0.59, shown in red) dichotomized by the maxstat method. **(B,D)** Violin plots showing the methylation levels of cg13399773-4.1N and cg20993403-4.1N among stage I–IV LUAD patients. Median methylation levels (show by a thick black line) and interquartile range were summarized by the boxplot within each violin plot. HR: hazard ratio; LR: log-likelihood ratio; LUAD: lung adenocarcinoma. Methylation levels were represented as beta values. Any beta value equal to or greater than 0.6 was considered fully methylated. Any beta value equal to or less than 0.2 was considered to be fully unmethylated. Beta values between 0.2 and 0.6 were considered to be partially methylated.

DISCUSSIONS

DNA methylation in the promoter region results in gene repression, which is one of the most well-defined epigenetic hallmarks. We previously revealed that downregulated 4.1N/*EPB41L1* exerts antitumor effects by activating the classical Wnt pathway and C-MYC expression in NSCLC (Wang et al., 2016; Yang et al., 2016; Yang et al., 2021). The Wnt pathway disruption driven by methylation of promoter regions plays a key driving role in the high CpG island methylated phenotype LUAD subtype. This subtype is also significantly correlated with the overexpressed *MYC* gene (Cancer Genome Atlas Research, 2014; Duruisseaux and Esteller, 2018). 4.1N/*EPB41L1* has many similar biological characteristics to its homologous 4.1B/*EPB41L3*. High promoter methylation of the 4.1B/*EPB41L3* gene–induced gene-silencing frequently occurs in NSCLC (Kikuchi et al., 2005; Zhang et al., 2012), breast cancer (Heller et al., 2007), renal clear cell carcinoma (Yamada et al., 2006), and prostate cancer (Schulz et al., 2007; Schulz et al., 2010). Thus, we decided to explore the underlying epigenetic disruptions of 4.1N/*EPB41L1* deficiency in NSCLC. Similarly, we found that high 4.1N/*EPB41L1* gene methylation was prevalent in LUAD and LUSC. 4.1B/*EPB41L3* gene methylation is a potential indicator for poor prognosis in NSCLC patients, especially in LUAD patients (Kikuchi et al., 2005). We found that a higher methylation level of 4.1N/*EPB41L1* gene CpG sites (cg13399773 and cg20993403) was potential predictive markers of shorter overall survival in LUAD patients. It is acceptable that patients with higher promoter methylation within the 4.1N/*EPB41L1* gene have a shorter overall survival time because the methylation inhibits tumor suppressor 4.1N/*EPB41L1* expression at the transcriptional level. However, it is a different matter for LUSC, which remains to be

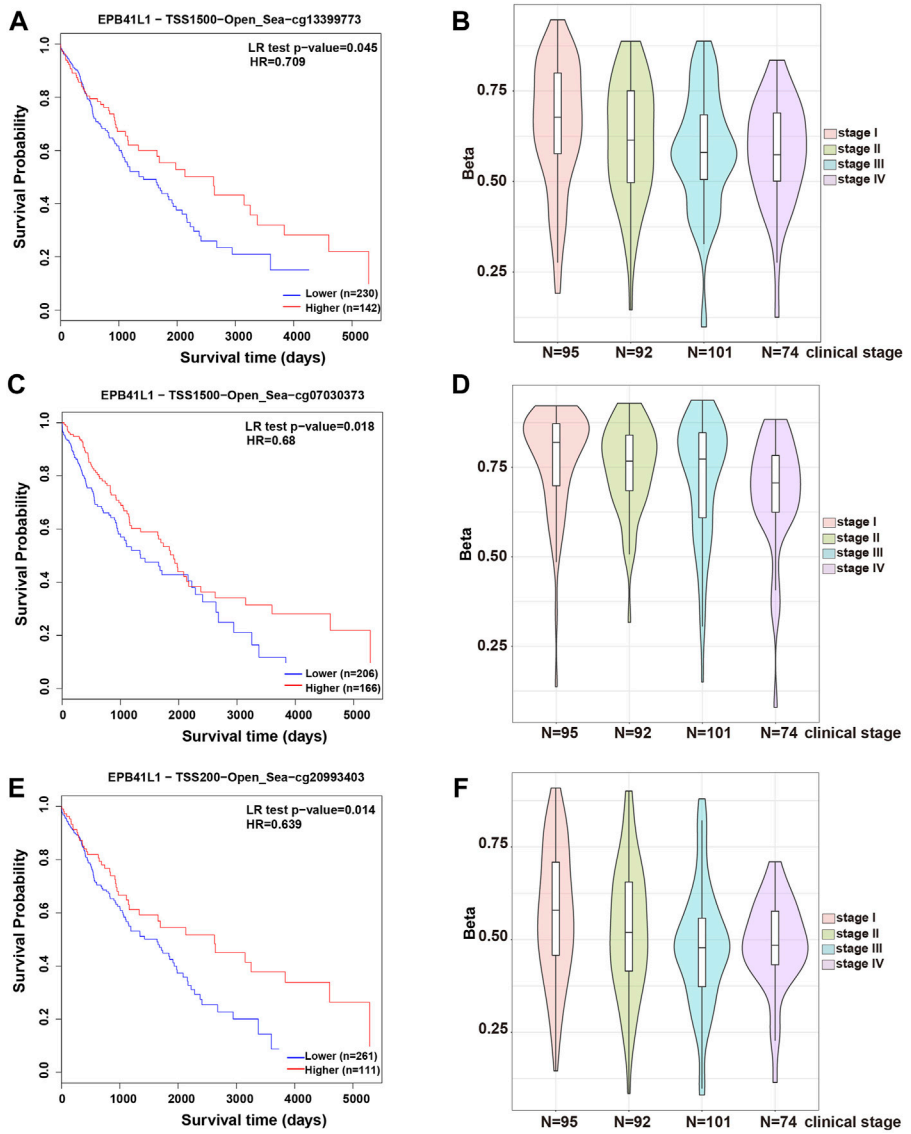

FIGURE 4 | Methylation levels and prognosis of the 4.1N/*EPB41L1* promoter in patients with LUSC. **(A)** Kaplan–Meier curves for cg13399773-4.1N showing survival in lower (beta <0.675, shown in blue) and higher methylation groups (beta > 0.675, shown in red) dichotomized by the maxstat method. **(C)** Kaplan–Meier curves for cg07030373-4.1N showing survival in lower (beta <0.796, shown in blue) and higher methylation groups (beta > 0.796, shown in red) dichotomized by the maxstat method. **(E)** Kaplan–Meier curves for cg20993403-4.1N showing survival in lower (beta <0.611, shown in blue) and higher methylation groups (beta > 0.611, shown in red) dichotomized by the maxstat method. **(B,D,F)** Violin plots showing the methylation levels of cg13399773-4.1N, cg07030373-4.1N, and cg20993403-4.1N among stage I–IV LUAD patients. Median methylation levels (show by a thick black line) and interquartile range were summarized by the boxplot within each violin plot. HR: hazard ratio; LR: log-likelihood ratio; LUSC: lung squamous cell carcinoma. Methylation levels were represented as beta values. Any beta value equal to or greater than 0.6 was considered fully methylated. Any beta value equal to or less than 0.2 was considered to be fully unmethylated. Beta values between 0.2 and 0.6 were considered to be partially methylated.

elucidated in the future. The 5-year survival rate is less than 15% for NSCLC patients, but the rate can increase to 63% with the early stage of initial diagnosis (van Rens et al., 2000; Geng et al., 2017), thus demonstrating the value of the early diagnosis of NSCLC. 4.1B/*EPB41L3* gene promoter methylation is regarded as an early event in renal clear cell carcinoma (Yamada et al., 2006). In this study, high 4.1N/*EPB41L1* gene methylation was also observed to be a relatively early event in LUAD and LUSC patients, indicating its valuable role in tumorigenesis and potential as an early detection marker.

qPCR results of our sample set and the TCGA database together showed that the miR-454-3p was upregulated in the NSCLC tumor tissue, which contrasted with the results from another independent study (Jin et al., 2019). Interestingly, tumor expression of miR-454-5p in NSCLC is reported as upregulated (Zhu et al., 2016), but another report suggests its expression to be downregulated (Liu et al., 2018). It is not rare when various clinical specimens are evaluated; the expression levels of some miRNAs are different. Because of the complexity of NSCLC

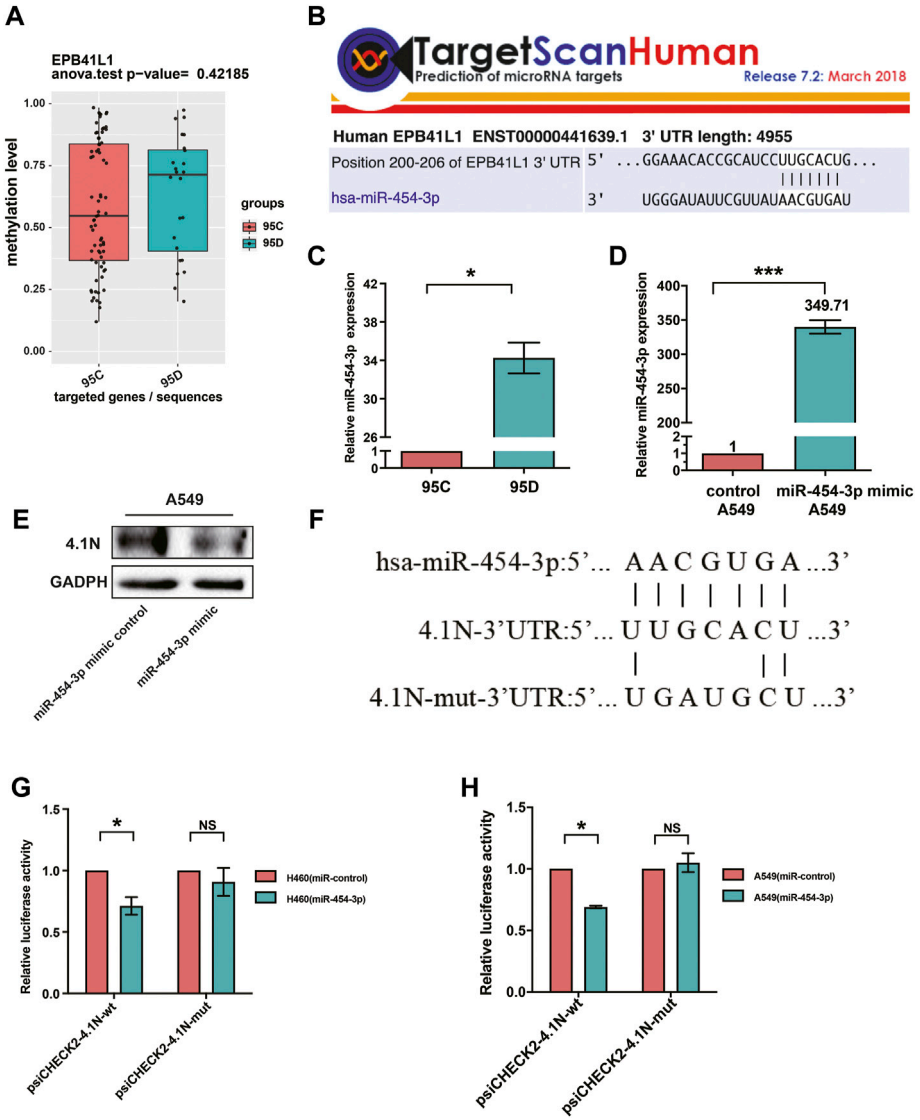

FIGURE 5 | MiR-454-3p directly bound to 3′UTR of 4.1N/*EPB41L1* mRNA. **(A)** There was no significant difference in methylation levels of the 4.1N/*EPB41L1* gene promoter between the two homologous NSCLC subclones 95C and 95D. **(B)** MiR-454-3p was a predicted binding partner of 4.1N/*EPB41L1*. **(C,D)** After transfecting A549 cells with miR-454-3p or negative control mimics, the expression levels of miR-454-3p and protein 4.1N/*EPB41L1* were detected using qPCR and Western blot, respectively. **(E)** miR-454-3p expression was significantly lower in 95C cells than 95D cells. **(F)** Schematic representation of the predicted binding sites of miR-454-3p and 4.1N/*EPB41L1* mRNA and the mutated sequences in potential binding sites. **(G,H)** A549 or H460 cells were co-transfected with miR-454-3p or control mimics and wild-type (psiCHECK2-4.1N-wt) or mutant-type (psiCHECK2-4.1N-mut) plasmids. 48 h later, dual-luciferase activity was measured. The data were presented as the mean ± SD. *$p < 0.05$ GADPH and U6 were used as loading control of 4.1N/*EPB41L1* mRNA and miR-454-3p, respectively.

development, for these miRNAs, the specimen integration of different NSCLC stages and histological types could impede their expressions together (Zhong et al., 2021). In NSCLC, our study showed aberrantly high-expressed miR-454-3p directly bound to 4.1N/*EPB41L1* mRNA 3′UTR and led to the depression of tumor suppressor 4.1N/*EPB41L1* at the posttranscriptional level, uncovering the known miRNAs regulating 4.1N/*EPB41L1*. It has been reported that the miR-454-3p also acts as oncomiRNA in oral squamous cell carcinoma (Shi et al., 2021), cervical cancer (Guo et al., 2018; Shukla et al., 2019; Song et al., 2019; Li et al., 2021), liver cancer (Li et al., 2019), breast cancer (Ren et al., 2019; Wang et al., 2020), and colon cancer (Li et al., 2018). Moreover, an integrative bioinformatics analysis indicates that miR-454-3p is a biomarker for diagnosing some cancers, including the LUAD (Botling et al., 2013), which needs further confirmation studies in the future.

Epigenetic alterations have been demonstrated to be highly orchestrated from the initiation step to therapy resistance step in lung cancer (Quintanal-Villalonga and Molina-Pinelo, 2019). Although many research studies have revealed the vital anticancer roles of 4.1 family members, the knowledge of the underlying epigenetic mechanism behind their loss in cancers is

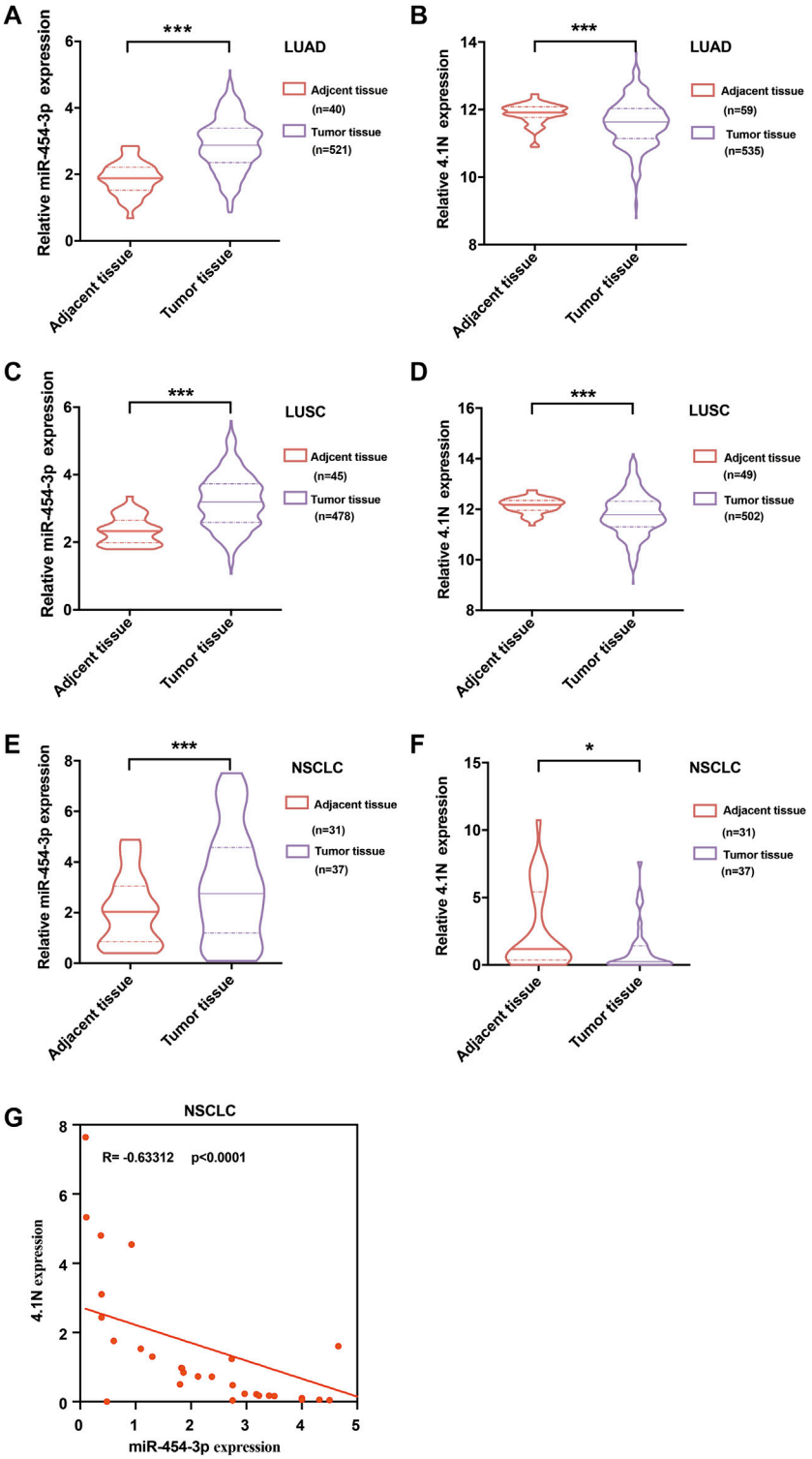

FIGURE 6 | Validation of expression patterns of miR-454-3p and 4.1N/*EPB41L1* mRNA in NSCLC. Relative expressions of miR-454-3p and 4.1N/*EPB41L1* mRNA in LUAD. **(A,B)** and LUSC **(C,D)** were analyzed using the data from the TCGA dataset. **(E-F)** Relative expression of miR-454-3p and 4.1N/*EPB41L1* mRNA in NSCLC and adjacent tissues was measured by qPCR. GADPH and U6 were used as loading control of 4.1N/*EPB41L1* mRNA and miR-454-3p, respectively. **(G)** Correlation between miR-454-3p and 4.1N/*EPB41L1* mRNA was determined using Spearman's coefficient analysis. The data were presented as the mean ± SD. $^{*}p < 0.05$ and $^{***}p < 0.001$.

nearly empty. This study showed that promoter methylation and miR-454-3p were implicated in the expression deregulation of the 4.1N/*EPB41L1* at transcriptional and posttranscriptional levels, respectively. The epigenetic abnormalities are reversible; the application of upregulating 4.1N/*EPB41L1* by targeting DNA methylation and miR-454-3p may represent a promising therapy for NSCLC treatment.

DATA AVAILABILITY STATEMENT

Publicly available datasets were analyzed in this study. These data can be found here: To investigate the 4.1N/EPB41L1 gene methylation and its relation to NSCLC patient prognosis, TCGA methylation data (https://cancergenome.nih.gov/) of the array features 450k CpG sites covering the 4.1N gene promoter region (TSS200 and TSS1500) were analyzed. The MethSurv tool (https://biit.cs.ut.ee/methsurv/) was used to perform the assessment of methylation-based analysis for the 4.1N/EPB41L1 gene in lung adenocarcinoma (LUAD) and lung squamous cell carcinoma (LUSC). TCGA data for LUAD and LUSC were used to extract RNA transcript levels of the miR-454-3p.

ETHICS STATEMENT

The studies involving human participants were reviewed and approved by the Ethics Committee of the Second Xiangya Hospital, Central South University. The patients/participants provided their written informed consent to participate in this study.

AUTHOR CONTRIBUTIONS

QY, LZ, HL, and JL contributed the central idea, performed the experiments, analyzed the data, and wrote the initial draft of the manuscript. The remaining authors discussed the results and finalized this manuscript. All authors read and approved the final manuscript.

FUNDING

This study was funded by the National Natural Science Foundation of China (Grant Nos 81770107 and 82003286); the Natural Science Foundation of Hunan Province (Grant No. 2020JJ4560); Scientific Research Foundation of Hunan Provincial Education Department (Grant No. 20B528); Guidance Science and Technology Program of Shaoyang City (Grant No. 2019ZD07); the Fellowship of China Postdoctoral Science Foundation (Grant Nos 2020M672474 and 2021T140195); and the Changsha Municipal Natural Science Foundation (Grant Number kq20140421); Postgraduate Innovation and Research Project of Central South University (Grant No. 2021zzts0569).

REFERENCES

Arechederra, M., Daian, F., Yim, A., Bazai, S. K., Richelme, S., Dono, R., et al. (2018). Hypermethylation of Gene Body CpG Islands Predicts High Dosage of Functional Oncogenes in Liver Cancer. *Nat. Commun.* 9 (1), 3164. doi:10.1038/s41467-018-05550-5

Botling, J., Edlund, K., Lohr, M., Hellwig, B., Holmberg, L., Lambe, M., et al. (2013). Biomarker Discovery in Non-small Cell Lung Cancer: Integrating Gene Expression Profiling, Meta-Analysis, and Tissue Microarray Validation. *Clin. Cancer Res.* 19 (1), 194–204. doi:10.1158/1078-0432.ccr-12-1139

Bray, F., Ferlay, J., Soerjomataram, I., Siegel, R. L., Torre, L. A., and Jemal, A. (2018). Global Cancer Statistics 2018: GLOBOCAN Estimates of Incidence and Mortality Worldwide for 36 Cancers in 185 Countries. *CA A Cancer J. Clin.* 68 (6), 394–424. doi:10.3322/caac.21492

Cancer Genome Atlas Research (2014). Comprehensive Molecular Profiling of Lung Adenocarcinoma. *Nature* 511 (7511), 543–550. doi:10.1038/nature13385

D'Addario, G., Früh, M., Reck, M., Baumann, P., Klepetko, W., and Felip, E. (2010). Metastatic Non-small-cell Lung Cancer: ESMO Clinical Practice Guidelines for Diagnosis, Treatment and Follow-Up. *Ann. Oncol.* 21 (Suppl. 5), v116–v119. doi:10.1093/annonc/mdq189

Du, X., Zhang, J., Wang, J., Lin, X., and Ding, F. (2018). Role of miRNA in Lung Cancer-Potential Biomarkers and Therapies. *Cpd* 23 (39), 5997–6010. doi:10.2174/1381612823666170714150111

Duruisseaux, M., and Esteller, M. (2018). Lung Cancer Epigenetics: From Knowledge to Applications. *Seminars cancer Biol.* 51, 116–128. doi:10.1016/j.semcancer.2017.09.005

Gao, F., Liang, H., Lu, H., Wang, J., Xia, M., Yuan, Z., et al. (2015). Global Analysis of DNA Methylation in Hepatocellular Carcinoma by a Liquid Hybridization Capture-Based Bisulfite Sequencing Approach. *Clin. Epigenet* 7, 86. doi:10.1186/s13148-015-0121-1

Gao, F., Xia, Y., Wang, J., Lin, Z., Ou, Y., Liu, X., et al. (2014). Integrated Analyses of DNA Methylation and Hydroxymethylation Reveal Tumor Suppressive Roles of ECM1, ATF5, and EOMESin Human Hepatocellular Carcinoma. *Genome Biol.* 15 (12), 533. doi:10.1186/s13059-014-0533-9

Gao, F., Zhang, J., Jiang, P., Gong, D., Wang, J.-W., Xia, Y., et al. (2014). Marked Methylation Changes in Intestinal Genes during the Perinatal Period of Preterm Neonates. *BMC Genomics* 2615, 716. doi:10.1186/1471-2164-15-716

Geng, X., Pu, W., Tan, Y., Lu, Z., Wang, A., Tan, L., et al. (2017). Quantitative Assessment of the Diagnostic Role of FHIT Promoter Methylation in Non-small Cell Lung Cancer. *Oncotarget* 8 (4), 6845–6856. doi:10.18632/oncotarget.14256

Guo, Y., Tao, M., and Jiang, M. (2018). MicroRNA-454-3p Inhibits Cervical Cancer Cell Invasion and Migration by Targeting C-Met. *Exp. Ther. Med.* 15 (3), 2301–2306. doi:10.3892/etm.2018.5714

Heller, G., Babinsky, V. N., Ziegler, B., Weinzierl, M., Noll, C., Altenberger, C., et al. (2013). Genome-wide CpG Island Methylation Analyses in Non-small Cell Lung Cancer Patients. *Carcinog. Mar.* 34 (3), 513–521. doi:10.1093/carcin/bgs363

Heller, G., Geradts, J., Ziegler, B., Newsham, I., Filipits, M., Markis-Ritzinger, E.-M., et al. (2007). Downregulation of TSLC1 and DAL-1 Expression Occurs Frequently in Breast Cancer. *Breast Cancer Res. Treat.* 103 (3), 283–291. doi:10.1007/s10549-006-9377-7

Jin, C., Lin, T., and Shan, L. (2019). Downregulation of Calbindin 1 by miR-454-3p Suppresses Cell Proliferation in Nonsmall Cell Lung Cancer *In Vitro*. *Cancer Biotherapy Radiopharm.* 34 (2), 119–127. doi:10.1089/cbr.2018.2598

Kikuchi, S., Yamada, D., Fukami, T., Masuda, M., Sakurai-Yageta, M., Williams, Y. N., et al. (2005). Promoter Methylation of DAL-1/4.1B Predicts Poor Prognosis in Non-small Cell Lung Cancer. *Clin. Cancer Res.* 11 (8), 2954–2961. doi:10.1158/1078-0432.ccr-04-2206

Lamy, A., Metayer, J., Thiberville, L., Frebourg, T., and Sesboue, R. (2001). Re: Promoter Methylation and Silencing of the Retinoic Acid Receptor- Gene in

Lung Carcinomas. *JNCI J. Natl. Cancer Inst.* 93 (1), 66–67. doi:10.1093/jnci/93.1.66

Li, H., Ouyang, R., Wang, Z., Zhou, W., Chen, H., Jiang, Y., et al. (2016). MiR-150 Promotes Cellular Metastasis in Non-small Cell Lung Cancer by Targeting FOXO4. *Sci. Rep.* 6, 39001. doi:10.1038/srep39001

Li, P., Wang, J., Zhi, L., and Cai, F. (2021). Linc00887 Suppresses Tumorigenesis of Cervical Cancer through Regulating the miR-454-3p/FRMD6-Hippo axis. *Cancer Cell Int.* 21 (1), 33. doi:10.1186/s12935-020-01730-w

Li, W., Feng, Y., Ma, Z., and Lu, L. (2018). Expression of miR-454-3p and its Effect on Proliferation, Invasion and Metastasis of Colon Cancer. *Nan Fang. Yi Ke Da Xue Xue Bao* 38 (12), 1421–1426. doi:10.12122/j.issn.1673-4254.2018.12.04

Li, Y., Jiao, Y., Fu, Z., Luo, Z., Su, J., and Li, Y. (2019). High miR-454-3p Expression Predicts Poor Prognosis in Hepatocellular Carcinoma. *Cmar* Vol. 11, 2795–2802. doi:10.2147/cmar.s196655

Lister, R., Pelizzola, M., Dowen, R. H., Hawkins, R. D., Hon, G., Tonti-Filippini, J., et al. (2009). Human DNA Methylomes at Base Resolution Show Widespread Epigenomic Differences. *Nature* 462 (7271), 315–322. doi:10.1038/nature08514

Liu, S., Ge, X., Su, L., Zhang, A., and Mou, X. (2018). MicroRNA-454 Inhibits Nonsmall Cell Lung Cancer Cells Growth and Metastasis via Targeting Signal Transducer and Activator of Transcription-3. *Mol. Med. Rep.* 17 (3), 3979–3986. doi:10.3892/mmr.2017.8350

Modhukur, V., Iljasenko, T., Metsalu, T., Lokk, K., Laisk-Podar, T., and Vilo, J. (2018). MethSurv: a Web Tool to Perform Multivariable Survival Analysis Using DNA Methylation Data. *Epigenomics* 10 (3), 277–288. doi:10.2217/epi-2017-0118

Nebbioso, A., Tambaro, F. P., Dell'Aversana, C., and Altucci, L. (2018). Cancer Epigenetics: Moving Forward. *PLoS Genet.* 14 (6), e1007362. doi:10.1371/journal.pgen.1007362

Norouzi, M., and Hardy, P. (2021). Clinical Applications of Nanomedicines in Lung Cancer Treatment. *Acta Biomater.* 121, 134–142. doi:10.1016/j.actbio.2020.12.009

Olbromski, M., Podhorska-Okołów, M., and Dzięgiel, P. (2020). Role of SOX Protein Groups F and H in Lung Cancer Progression. *Cancers (Basel)* 12 (11), 13235. doi:10.3390/cancers12113235

Pan, X., Gong, D., Nguyen, D. N., Zhang, X., Hu, Q., Lu, H., et al. (2018). Early Microbial Colonization Affects DNA Methylation of Genes Related to Intestinal Immunity and Metabolism in Preterm Pigs. *DNA Res. Int. J. rapid Publ. Rep. Genes Genomes* 25 (3), 287–296. doi:10.1093/dnares/dsy001

Quintanal-Villalonga, Á., and Molina-Pinelo, S. (2019). Epigenetics of Lung Cancer: a Translational Perspective. *Cell Oncol.* 42 (6), 739–756. doi:10.1007/s13402-019-00465-9

Ren, L., Chen, H., Song, J., Chen, X., Lin, C., Zhang, X., et al. (2019). MiR-454-3p-Mediated Wnt/β-Catenin Signaling Antagonists Suppression Promotes Breast Cancer Metastasis. *Theranostics* 9 (2), 449–465. doi:10.7150/thno.29055

Rodriguez-Canales, J., Parra-Cuentas, E., and Wistuba, II (2016). Diagnosis and Molecular Classification of Lung Cancer. *Cancer Treat. Res.* 170, 25–46. doi:10.1007/978-3-319-40389-2_2

Schulz, W. A., Alexa, A., Jung, V., Hader, C., Hoffmann, M. J., Yamanaka, M., et al. (2007). Factor Interaction Analysis for Chromosome 8 and DNA Methylation Alterations Highlights Innate Immune Response Suppression and Cytoskeletal Changes in Prostate Cancer. *Mol. Cancer* 6, 14. doi:10.1186/1476-4598-6-14

Schulz, W. A., Ingenwerth, M., Djuidje, C. E., Hader, C., Rahnenführer, J., and Engers, R. (2010). Changes in Cortical Cytoskeletal and Extracellular Matrix Gene Expression in Prostate Cancer Are Related to Oncogenic ERG Deregulation. *BMC Cancer* 10, 505. doi:10.1186/1471-2407-10-505

Shi, D., Li, H., Zhang, J., and Li, Y. (2021). CircGDI2 Regulates the Proliferation, Migration, Invasion and Apoptosis of OSCC via miR-454-3p/FOXF2 Axis. *Cancer. Manag. Res.* Vol. 13, 1371–1382. doi:10.2147/cmar.s277096

Shukla, V., Varghese, V. K., Kabekkodu, S. P., Mallya, S., Chakrabarty, S., Jayaram, P., et al. (2019). Enumeration of Deregulated miRNAs in Liquid and Tissue Biopsies of Cervical Cancer. *Gynecol. Oncol.* 155 (1), 135–143. doi:10.1016/j.ygyno.2019.08.012

Song, Y., Guo, Q., Gao, S., and Hua, K. (2019). miR-454-3p Promotes Proliferation and Induces Apoptosis in Human Cervical Cancer Cells by Targeting TRIM3. *Biochem. biophysical Res. Commun.* 516 (3), 872–879. doi:10.1016/j.bbrc.2019.06.126

Turchinovich, A., Weiz, L., and Burwinkel, B. (2012). Extracellular miRNAs: the Mystery of Their Origin and Function. *Trends Biochem. Sci.* 37 (11), 460–465. doi:10.1016/j.tibs.2012.08.00

Uddin, A., and Chakraborty, S. (2018). Role of miRNAs in Lung Cancer. *J. Cell Physiol.* 20, 1–10. doi:10.1002/jcp.26607

van Rens, M. T. M., van den Bosch, J. M. M., Brutel de la Rivière, A., and Elbers, H. R. J. (2000). Prognostic Assessment of 2,361 Patients Who Underwent Pulmonary Resection for Non-small Cell Lung Cancer, Stage I, II, and IIIA. *Chest* 117 (2), 374–379. doi:10.1378/chest.117.2.374

Wang, H., Liu, C., Debnath, G., Baines, A. J., Conboy, J. G., Mohandas, N., et al. (2010). Comprehensive Characterization of Expression Patterns of Protein 4.1 Family Members in Mouse Adrenal Gland: Implications for Functions. *Histochem Cell Biol.* 134 (4), 411–420. doi:10.1007/s00418-010-0749-z

Wang, L., He, M., Fu, L., and Jin, Y. (2020). Exosomal Release of microRNA-454 by Breast Cancer Cells Sustains Biological Properties of Cancer Stem Cells via the PRRT2/Wnt axis in Ovarian Cancer. *Life Sci.* 257, 118024. doi:10.1016/j.lfs.2020.118024

Wang, Z., Ma, B., Li, H., Xiao, X., Zhou, W., Liu, F., et al. (2016). Protein 4.1N Acts as a Potential Tumor Suppressor Linking PP1 to JNK-C-Jun Pathway Regulation in NSCLC. *Oncotarget* 7 (1), 509–523. doi:10.18632/oncotarget.6312

Yamada, D., Kikuchi, S., Williams, Y. N., Sakurai-Yageta, M., Masuda, M., Maruyama, T., et al. (2006). Promoter Hypermethylation of the Potential Tumor suppressorDAL-1/4.1Bgene in Renal Clear Cell Carcinoma. *Int. J. Cancer* 118 (4), 916–923. doi:10.1002/ijc.21450

Yang, Q., Liu, J., and Wang, Z. (2021). 4.1N-Mediated Interactions and Functions in Nerve System and Cancer. *Front. Mol. Biosci.* 8, 711302. doi:10.3389/fmolb.2021.711302

Yang, Q., Zhu, M., Wang, Z., Li, H., Zhou, W., Xiao, X., et al. (2016). 4.1N Is Involved in a Flotillin-1/β-catenin/Wnt Pathway and Suppresses Cell Proliferation and Migration in Non-small Cell Lung Cancer Cell Lines. *Tumor Biol.* 37 (9), 12713–12723. doi:10.1007/s13277-016-5146-3

Yang, X., Han, H., De Carvalho, D. D., Lay, F. D., Jones, P. A., and Liang, G. (2014). Gene Body Methylation Can Alter Gene Expression and Is a Therapeutic Target in Cancer. *Cancer Cell* 26 (4), 577–590. doi:10.1016/j.ccr.2014.07.028

Zhang, Y., Xu, R., Li, G., Xie, X., Long, J., and Wang, H. (2012). Loss of Expression of the Differentially Expressed in Adenocarcinoma of the Lung (DAL-1) Protein Is Associated with Metastasis of Non-small Cell Lung Carcinoma Cells. *Tumor Biol.* 33 (6), 1915–1925. doi:10.1007/s13277-012-0452-x

Zhong, S., Golpon, H., Zardo, P., and Borlak, J. (2021). miRNAs in Lung Cancer. A Systematic Review Identifies Predictive and Prognostic miRNA Candidates for Precision Medicine in Lung Cancer. *Transl. Res.* 230, 164–196. doi:10.1016/j.trsl.2020.11.012

Zhou, S., Shen, Y., Zheng, M., Wang, L., Che, R., Hu, W., et al. (2017). DNA Methylation of METTL7A Gene Body Regulates its Transcriptional Level in Thyroid Cancer. *Oncotarget* 8 (21), 34652–34660. doi:10.18632/oncotarget.16147

Zhu, D.-Y., Li, X.-N., Qi, Y., Liu, D.-L., Yang, Y., Zhao, J., et al. (2016). MiR-454 Promotes the Progression of Human Non-small Cell Lung Cancer and Directly Targets PTEN. *Biomed. Pharmacother.* 81, 79–85. doi:10.1016/j.biopha.2016.03.029

Conflict of Interest: The authors declare that the research was conducted in the absence of any commercial or financial relationships that could be construed as a potential conflict of interest.

Publisher's Note: All claims expressed in this article are solely those of the authors and do not necessarily represent those of their affiliated organizations, or those of the publisher, the editors, and the reviewers. Any product that may be evaluated in this article, or claim that may be made by its manufacturer, is not guaranteed or endorsed by the publisher.

Frontiers in
Cell and Developmental Biology

Explores the fundamental biological processes of life, covering intracellular and extracellular dynamics.

The world's most cited developmental biology journal, advancing our understanding of the fundamental processes of life. It explores a wide spectrum of cell and developmental biology, covering intracellular and extracellular dynamics.

Discover the latest Research Topics

See more →

Frontiers

Avenue du Tribunal-Fédéral 34
1005 Lausanne, Switzerland
frontiersin.org

Contact us

+41 (0)21 510 17 00
frontiersin.org/about/contact